Inactivation mechanisms and resistance properties of *Bacillus* spores during cold atmospheric pressure plasma treatment

---

vorgelegt von
Diplom-Ingenieur
Christian Hertwig
geboren in Nauen

Von der Fakultät III – Prozesswissenschaften
der Technischen Universität Berlin

zur Erlangung des akademischen Grades
Doktor der Ingenieurwissenschaften
- Dr.-Ing. -

genehmigte Dissertation

Promotionsausschuss:

Vorsitzender: Prof. Dr.-Ing. Frank-Jürgen Methner

1. Gutachter: Prof. Dr.-Ing. habil. Cornelia Rauh

2. Gutachter: Prof. Dr.-Ing. Alexander Mathys

3. Gutachter: Prof. Dr. Dipl.-Ing. Dietrich Knorr

Tag der wissenschaftlichen Aussprache: 21.04.2017

Berlin 2017

Preface

This thesis is based on reformatted work which has been published in the following peer reviewed publications:

1. Reineke, K., Langer, K., Hertwig, C., Ehlbeck, J., Schlüter, O., 2015. The impact of different process gas compositions on the inactivation effect of an atmospheric pressure plasma jet on *Bacillus* spores. Innovative Food Science & Emerging Technologies. 30: 112–118.

   doi: http://dx.doi.org/10.1016/j.ifset.2015.03.019

2. Hertwig, C., Steins, V., Reineke, K., Rademacher, A., Klocke, M., Rauh, C., Schlüter O., 2015. Impact of surface structure and feed gas composition on *Bacillus subtilis* endospore inactivation during direct plasma treatment. Front. Microbiol. 6:774.

   doi: https://doi.org/10.3389/fmicb.2015.00774

3. Hertwig, C., Reineke, K., Rauh, C., Schlüter, O., 2017. Factors involved in *Bacillus* spores' resistance to cold atmospheric pressure plasma. Innovative Food Science & Emerging Technologies. (submitted).

4. Hertwig, C., Reineke, K., Ehlbeck, J., Knorr, D., Schlüter, O., 2015. Decontamination of whole black pepper using different cold atmospheric pressure plasma applications. Food Control. 50: 221–229.

   doi: http://dx.doi.org/10.1016/j.foodcont.2015.03.003

Zusammenfassung

Kaltes Atmosphärendruckplasma (KADP) ist eine vielversprechende und innovative nichtthermische Technologie zur Inaktivierung von Mikroorganismen auf verschiedenen Oberflächen. Plasmaanwendungen werden in der Lebensmittelindustrie schon seit Jahrzehnten eingesetzt, z.B. zur Generierung von ultraviolettem (UV) Licht oder zur Erzeugung von Ozon. In den letzten Jahren fand die KADP Anwendung zur Inaktivierung von bakteriellen Sporen mehr Beachtung. Die Inaktivierungsmechanismen bakterieller Sporen sind komplex und bisher noch nicht vollständig verstanden. Sie hängen von den verschiedenen generierten Bestandteilen des Plasmas ab. Ziel dieser Arbeit war es, die Inaktivierungsmechanismen von *Bacillus* Sporen bei der Plasmabehandlung zu untersuchen. Des weiteren wurde der Einfluss bestimmter Prozessparameter, wie die Plasmaquelle, Prozessgase und deren Mischungen, sowie produktbezogene Parameter, wie die Struktur der Oberfläche und die Verteilung der Sporen auf dieser, auf den Inaktivierungsprozess untersucht.

Die verwendeten Plasmen wurden detailliert charakterisiert, durch die Verwendung von optischer Emissionsspektrometrie, faseroptischen Temperatursensoren und die Quantifizierung der generierten reaktiven Plasmakomponenten. Um den Einfluss verschiedener Prozessgase auf die Inaktivierung zu verstehen, wurde eine quantitative Polymerase-Kettenreaktion (qPCR) Analyse verwendet um den Effekt der Plasmabehandlung auf die DNA der Sporen zu untersuchen. Verschieden Oberflächen, von einer ebenen, glatten Glasoberfläche, zu einem runden, glatten Model bis zu einem reellen Lebensmittel (schwarze Pfefferkörner), wurden KADP behandelt, um den Einfluss der Oberfläche, auf welcher die Sporen vorliegen, auf den Inaktivierungsprozess zu untersuchen. Weiterhin wurde die Inaktivierung von isogen mutierten Sporenstämme untersucht, denen verschiedene Faktoren wie die äußere Sporenhülle und die kleinen säurelöslichen Proteine (SASP), sowie die Dipicolinsäure (DPA) im Sporenkern fehlen.

Durch diese Methoden konnte in dieser Arbeit ein umfangreicher Einblick in die Inaktivierung von *Bacillus* Sporen durch KADP gegeben werden. Es konnte gezeigt werden, dass die Prozess- und produktbezogenen Parameter den Inaktivierungsprozess beeinflussen. Die vom Plasma emittierten UV Photonen sind von wesentlicher Bedeutung für die Sporeninaktivierung. Durch die Verwendung bestimmter Prozessgase oder Mischungen, wie Stickstoff, kann die Menge der UV Emissionen optimiert werden. Weiterhin beeinflusst das Prozessgas

oder die Mischung, und dementsprechend auch die Zusammensetzung des Plasmas, den Prozess der Sporeninaktivierung. Die Verwendung von KADP mit einer hohen UV Emission verursacht einen hohen Grad an DNA-Schäden bei der Sporeninaktivierung. Die Oberfläche, auf der die Sporen vorliegen, hat ebenfalls einen großen Einfluss auf die Inaktivierung. Eine komplexe Oberflächenstruktur, wie bei schwarzen Pfefferkörnern, reduziert den antimikrobiellen Effekt der KADP-Behandlung wesentlich, vermutlich durch Schatteneffekte für die generierten Plasmakomponenten. Die Verteilung der Sporen auf der Oberfläche beeinflusst auch die Inaktivierung. Liegen die Sporen einzeln verteilt auf der Oberfläche vor, können sie schnell durch KADP mit einer hohen UV Emission inaktiviert werden. Wohingegen Sporenagglomerate die Inaktivierung erschweren, wahrscheinlich auf Grund der begrenzten Eindringtiefe der UV Photonen. Jedoch kann die Verwendung von einem KADP mit einem hohen Gehalt an reaktiven und metastabilen Partikeln die Inaktivierung durch die Zersetzung der Sporen fördern. Darüber hinaus wurden verschiedene Faktoren der Spore, die äußere Sporenhülle, die Sättigung der DNA mit SASPs und die DPA im Kern der Spore, identifiziert, die zur Resistenz der Spore gegenüber KADP beitragen.

Die in dieser Arbeit erhaltenen Daten ermöglichen ein erweitertes Verständnis der Sporeninaktivierung auf verschieden Oberflächen durch KADP und können zur Optimierung für zukünftige plasma-basierte Inaktivierungskonzepte in der Lebensmittelindustrie beitragen.

Abstract

Cold atmospheric pressure plasma (CAPP) is a promising and innovative emerging non-thermal technology for the inactivation of microorganisms on various surfaces. Plasma applications have already been used in the food industry at industrial scale for decades to generate e.g. ultraviolet (UV) light or ozone. In recent years, the inactivation of bacterial spores using CAPP has attracted more attention. The mechanisms leading to spore inactivation are complex, depending on the different generated components of the plasma and have not been fully understood yet. This study aimed to improve the understanding of the CAPP-based mechanisms responsible for *Bacillus* spore inactivation. Moreover, it was investigated how the different process parameters, such as plasma source, process gases and mixtures, and product related parameters, like the structure of the surface the spores are attached to and spore distribution on the surface, influence the inactivation process.

The different tested plasmas were characterized in detail using optical emission spectroscopy, fiber-optic temperature sensors and the quantification of the generated reactive components. To understand how the different process gases inactive the spores, a quantitative real-time polymerase chain reaction (qPCR) assay was used to detect the effect of the plasma treatment on the spore DNA. Different surfaces, from an even and smooth glass surface via a spherical and smooth model to a real food matrix (whole black peppercorns) were CAPP treated to investigate the effect of the surface, the spores are attached to, on the inactivation process. A detailed knowledge about the spore properties responsible for their resistance towards CAPP was obtained by using different isogenic mutant spore strains, which are lacking different factors, such as the outer spore coat, as well as the small acid soluble protein (SASP) and the dipicolinic acid (DPA) inside the spore coat.

Due to the various used methods, a comprehensive insight into the *Bacillus* spore inactivation by CAPP was given within this study. It was also shown how the process and product related parameters influence the inactivation process. Emitted UV photons of the plasma are of high importance for the spore inactivation. The amount of UV emissions can be optimized by the use of certain process gases or mixtures, such as N_2. Furthermore, the composition of the process gas, thus the composition of the generated plasma components, influence the process of spore inactivation. CAPP with a high UV emission caused a high degree of DNA damage during the spore inactivation. The surface, the spores are attached to, also affect the inactivation

efficiency tremendously. A complex surface structure, like on black peppercorns, lowers the antimicrobial effect of a CAPP treatment significantly, probably due to shadow effects for the generated plasma components. It was also shown, that the distribution of spores on the surface affects the inactivation. Spores present in a monolayer can be fast inactivated by CAPP with a high emission of UV photons. Spore agglomerates hamper the inactivation, probably due to the limited penetration depth of UV photons. However, using a CAPP with a high content of reactive and metastable species can support the inactivation by the decomposition of the spores. Moreover, it could be shown that different spore properties, such as the outer spore coat, saturation of the DNA with SASPs and the DPA inside the spore core, are responsible for the *Bacillus* spore resistance towards CAPP.

The obtained data from this work will lead to a better understanding of the CAPP-based spore inactivation on different surfaces and can aid to optimize future plasma-based inactivation concepts in the food industry.

Acknowledgments

This dissertation is based on the experimental work conducted at the Leibniz Institute for Agricultural Engineering and Bioeconomy (ATB) in collaboration with the Berlin University of Technology, Department of Food Biotechnology and Food Process Engineering. I'm grateful to Prof. Dr.-Ing. habil. Cornelia Rauh for the supervision of the thesis, her scientific advice, and especially, for the great independence she gave to me. I would like to thank Prof. Dr.-Ing. Alexander Mathys and Prof. Dr. Dietrich Knorr for their willingness to evaluate this thesis. I also want to express my gratitude to Prof. Dr. Frank-Jürgen Methner for being the chairman of the evaluation committee.

I acknowledge Dr.-Ing. Oliver Schlüter for his academic guidance, encouragement, support and independence throughout the course of this work. A very huge and special thanks goes to Dr.-Ing. Kai Reineke for introducing me to the "World of Spores", for his endless support, inspiration and the countless discussions over the years. Many thanks also go to Robert and to my colleagues from the Department of Horticultural Engineering and the team of the molecular biology lab, especially Susanne, Janett, Sara, Antje, Michael, Antje, Kerstin and Beate for discussions regarding professional and private topics.

This research was partly funded by the European Commission (project GreenFooDec, Development of novel and advanced decontamination sustainable technologies for the production of high quality dried herbs and spices, FP7-SME-2011-285838) and by the Federal Ministry of Food and Agriculture (BMEL) (^{3}Plas, Plasma decontamination of dry planted products to increase food safety, FKZ 2819102713).

Meinen Eltern, Ljudmila und Frank, möchte ich für ihre grenzenlose Unterstützung während des Studiums und der Promotion danken. Dir Ksuscha für das Korrekturlesen aller Paper und dieser Arbeit.

Моя самая большая благодарность принадлежит тебе, Даша, за твою бесконечную поддержку, понимание и, прежде всего, за твою любовь в это время.

Index

List of abbreviations

Abbreviation	Description
APPJ	Atmospheric pressure plasma jet
BC	Before Christ
CAPP	Cold atmospheric pressure plasma
CFU	Colony forming units
DBD	Dielectric barrier discharge
DC	Direct current
DCSBD	Diffuse coplanar surface barrier discharge
DNA	Desoxyribonucleic acid
DPA	Pyridine-2,6-dicarboxylic acid or Dipicolinic acid
DSM	German Collection of Microorganisms and Cell Cultures GmbH
D-value	Decimal reduction time
Eqn.	Equation
GBIF	Global Biodiversity Information Facility
HSA	Human serum albumin
KADP	Kaltes Atmosphärendruckplasma
PE	Polyethylene
PET	Polyethylene terephthalate
PP	Polypropylene
PPA	Plasma processed air
PTFE	Polytetrafluoroethylene
PVC	Polyvinyl chloride
qPCR	Quantitative real-time polymerase chain reaction
RF	Radio frequency
RNS	Reactive nitrogen species
ROS	Reactive oxygen species
SASP	Small acid soluble proteins
SDBD	Surface dielectric barrier discharge
SEM	Scanning electron microscopy

Abbreviation	Description
tRNA	Transfer ribonucleic acid
UV	Ultraviolet
VUV	Vacuum ultraviolet
WIS	Bundeswehr Research Institute for Protective Technologies and CBRN Protection

Symbol	Description	Unit
d	Gap	m
H_{kin}	Kinetic energy	J
k_B	Boltzmann constant	
m	Mass	kg
N	Number of particles in the system	
p	Pressure	Pa
T	Temperature	K
v	Velocity	$m*s^{-1}$
V_b	Breakdown voltage	V
σ	Sigma factor, protein subunit	

Abbreviations for Table 2-5	
stea	*Geobacillus stearothermophilus*
sub	*Bacillus subtilis*
atro	*Bacillus atrophaeus*
pum	*Bacillus pumilus*
cer	*Bacillus cereus*
an	*Bacillus anthracis*
mega	*Bacillus megaterium*
saf	*Bacillus safensis*
thu	*Bacillus thuringiensis*
bot	*Clostridium botulinum*
spo	*Clostridium sporogenes*
dif	*Clostridium difficile*

Abbreviations for Table 2-5

MA	Modified atmosphere
TT	Treatment temperature
RH	Relative humidity
lg	Log_{10}

List of figures

List of tables

1. Introduction

A typical plasma, which accompanied us in our daily life is the sun, another naturally occurring plasma is the *aurora borealis*. It is assumed that about 99 % of the universe consists of plasma, as for example solar winds, coronas and earth's ionosphere, not to forget the aurora borealis and most important the sun itself, a plasma which accompanies us in our daily life. Even though humans have been surrounded by it for thousands of years, the evolution of plasma processing itself just started in 1857, when Werner von Siemens investigated electric discharges and reported about the phenomena of dielectric barrier discharges (DBD) to ionize air and generate ozone. The DBD system was used by Siemens to construct the first industrial ozone generator to sanitize tap water. However, it took more than 70 years before it was Langmuir who defined "plasma" as an ionized gas, in which a significant and equal number of atoms and/or molecules are electrically charged or ionized (Langmuir 1928). The most well-known industrial application of plasma technology is probably found in plasma-based televisions. At industrial scale plasma processing has been used since the 1970s for the etching of semiconductor material (Manos & Flamm 1989) and continued in the 1980s with the fabrication of miniaturized circuits for the developing computer industry (Misra et al. 2016). Recently, the application of cold atmospheric pressure plasma (CAPP) gained importance for the decontamination of various surfaces of spacecraft (Shimizu et al. 2014), in the medical sector (Kong et al. 2009), food packaging material (Muranyi et al. 2010) and food products (Misra et al. 2011). The application of CAPP enables a microbial inactivation with temperatures below 70 °C (Schlüter et al. 2013). Consequently, CAPP technology offers a new approach for the gentle decontamination of temperature-sensitive materials and products, as for example fruits and vegetables. The application of CAPP is free of water or solvent. Furthermore many plasma systems require only a low energy input, therefore, CAPP technology is considered as environmentally friendly and energy efficient (Misra et al. 2016). Compared to other emerging nonthermal technologies, as the application of high pressure or pulsed electric field, the application of CAPP also allows the treatment of dry food products. Bacterial spores belonging to the class of *Bacilli* or *Clostridia* are extremely resistant to different environmentally stress conditions and are perfectly adapted to survive on surfaces of dry food products, hence, being the major vector causing food spoilage, foodborne diseases and other human illnesses (Logan 2012; Mallozzi et al. 2010). Current decontamination technologies for dry products, as herbs and spices, are chemical or thermal treat-

ments, like the application of steam, fumigation or γ-irradiation (Schweiggert et al. 2007). Irradiation with γ-rays can only be applied in authorized facilities and in controlled doses in order to be harmless and safe. Moreover, it has a poor consumer acceptance. The fumigation with ethylene oxide is a quite efficient process, however, the use of ethylene oxide can lead to carcinogenic byproducts and is banned by law in the European Union (Schweiggert et al. 2007; Tateo & Bononi 2006). In the European herbs and spices industry stream treatment is extensively used. But for spices with a high native microbial load, like black peppercorns, this method is not recommended due to its low reduction effects and the possible alteration in aroma and odor (Schweiggert et al. 2007; Tainter & Grenis 2001). The application of CAPP offers an emerging nonthermal technology, which enables a multi target inactivation on dry food surfaces.

The implementation of a new decontamination technology in the industry requires the understanding of the mechanisms involved in microbial inactivation and caused process-product interactions. The main object of this basic study was the investigation of bacterial spore inactivation under cold atmospheric pressure plasma, to clarify underlying mechanisms of CAPP-based spore inactivation and to understand how the different process and product related parameters influence the inactivation process. Different plasma systems, process gases and different treated matrices were evaluated regarding *Bacillus* spore inactivation. The different tested plasmas were characterized in detail using optical emission spectroscopy, fiber-optic temperatures sensors and quantification of the generated reactive components. A wide range of analytical methods were used, including innovative molecular biological tools, microscopic techniques and the use of genetically modified spore strains. The combination of these parameters allows a fundamental assessment of the CAPP-based spore inactivation and involved spore resistance properties. Furthermore, it is underlined how the process and product related parameters affect the inactivation process.

2. Theoretical background and literature review

2.1 Cold atmospheric pressure plasma

In general, plasma can be considered the 4th state of matter. With rising energy input to a system, phase transitions occur and various states of matter are recognized, from solid to liquid to gas and to an ionized state of plasma (Figure 2—1). Although the shift from the gas phase to a plasma is strictly not a real phase transition, plasma was recognized as a material state due to its unique properties, which significantly discriminates it from the gas phase. Plasma is, in a physical sense, a completely or partially ionized gas, which is composed of charged particles, such as electrons and ions, and neutral particles, like atoms, molecules and radicals, likewise of temperature and quanta of electromagnetic radiation (e.g. UV photons). Due to the presence of free electric charges (electrons and ions) plasma is electrically conductive, internally interactive and responses strongly to electromagnetic fields (Fridman 2008).

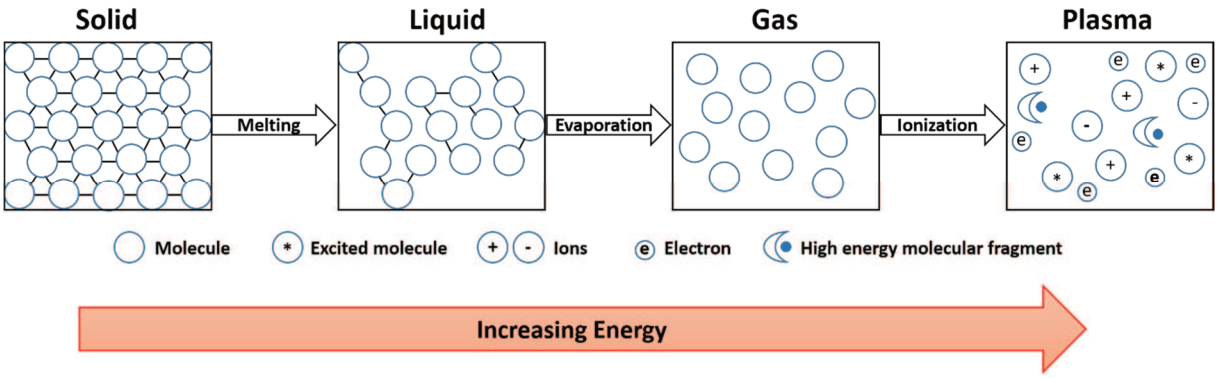

Figure 2—1: The four states of matter.

As previously mentioned, the term "plasma" was defined by Langmuir (1928). The way an ionized gas transports high-velocity electrons, molecules and ions of gas impurities reminded him of the transport process of red and white corpuscles and germs in blood plasma (Klämpfl 2014). According to their temperature, plasmas can be commonly categorized into thermal and nonthermal plasmas. As already mentioned, a plasma is a complex system of electrons, ions and neutral particles, whereby the temperature of those particles does not have to be equal. Referring to the kinetic theory of an ideal gas, the average kinetic energy $\langle H_{kin} \rangle$ of a particle depends on its mass *m* and velocity *v* can be described by the integral (Eqn. 1).

$$< H_{kin} >= \int_0^{+\infty} \left(\frac{1}{2} m v^2\right) f(v) dv \qquad \text{Eqn. 1}$$

Using the Maxwell-Boltzmann distribution (Eqn. 2), it can be shown that the average kinetic energy of the particles is proportional to their temperature (Eqn. 3).

$$f(v)dv = \frac{N(v)}{N} dv = \left(\frac{m}{2\pi k_B T}\right)^{3/2} 4\pi v^2 \, exp\left(-\frac{m v^2}{k_B T}\right) dv \qquad \text{Eqn. 2}$$

with: N number of particles in the system
N(v) fraction of particles with velocity between v and $v + dv$
k_B Boltzmann constant
T temperature

$$< H_{kin} >= \frac{3}{2} k_B T \qquad \text{Eqn. 3}$$

The mass of an electron is 1 m_e = 1/1860 Da (atomic mass) and equivalent to just 0.01 % of the mass of neutral particles (molecules and atoms) inside the plasma. Due to the large mass difference, the electron velocity is substantially higher as those of the heavy particles. The kinetic energy of the electrons is in the order of several eV, whereas 1 eV is about 1160 K. Consequently, the electron temperature is several orders of magnitude higher than the temperature of the heavy particles (atoms, molecules and ions). However, due to the low mass of the electrons compared to the heavy particles, the actual plasma temperature depends on the average kinetic energy of the heavy particles.

Thermal plasmas are (nearly) completely ionized. These plasmas have a high collision frequency, so that an efficient energy transfer in electron-ion collisions leads to a significant thermalization of the different particle species to the thermodynamic equilibrium temperature. In this case the temperature of all species is approximately equal, with temperatures typically reaching at least 15,000 K (Eliasson & Kogelschatz 1991). Nonthermal plasmas are just partially ionized, meaning the number of charged particles is much lower as the number of neutral particles. While the electron temperature is in the order of 10^4 K, the temperature of the ions and neutrals, which represent the main plasma compounds, can be close to ambient temperature. The hot electrons channel the electrical energy efficiently into the production of reactive radicals instead of heating the gas, thus the temperature of nonthermal plasmas can be close to the ambient temperature (Turner 2016). The plasma temperature depends on the pressure with which the plasma is generated, because the increase of the pressure resulted in an increase of

particle collisions, such as electron-ion or electron-neutral collisions (Eliasson & Kogelschatz 1991; Grzegorzewski 2010). In this respect, it is easier to generate a nonthermal plasma close to ambient temperature at reduced ($p < 1013$ mbar) or low pressure ($p < 10$ mbar) as at atmospheric pressure.

2.2 Cold atmospheric pressure plasma generation and sources

Plasma can be generated at atmospheric pressure or lower pressure. However, the focus of the food sector tends to plasma processes at atmospheric pressure, because atmospheric conditions allow continuous processing. Accordingly, this chapter will focus on plasma sources, which generate plasma at atmospheric conditions and have been used within this thesis. In general, plasma is generated by suppling energy to a neutral gas, whereby the nature of the energy source is irrelevant. Due to cosmic and radioactive rays each gas, which usually consists of neutral atoms and molecules, has a small density of charged ions and free electrons. The application of an electromagnetic field leads to an energy absorption and acceleration of the free electrons. The accelerated electrons collide with the neutral gas molecules. Depending on the kinetic energy of the electrons, different reactions like ionization, excitation, dissociation, attachment and elastic scattering are possible (Table 2-1). The collisions can be divided into elastic and inelastic collisions. Elastic collisions or scattering are characterized by a small energy transfer from the electrons to the neutral collision partner. All other collisions, such as ionization and excitation, are inelastic and of essential character for the plasma generation (Muranyi 2008).

Table 2-1: Main reaction in the gas involving electrons and their require kinetic energy, adapted from Scheubert (2001) and Muranyi (2008).

Description	Reaction	Kinetic energy
Ionization	$e^- + X \rightarrow X^+ + 2e^-$	> 15 eV
Excitation	$e^- + X \rightarrow X^* + e^-$	< 15 eV
Dissociation	$e^- + X_2 \rightarrow X\bullet + X\bullet + e^-$	> 2 eV
Attachment	$e^- + X \rightarrow X^-$	< 1 eV
Elastic scattering	$e^- + X \rightarrow X + e^-$	random

To obtain the plasma state the energy must be supplied continuously to the system, since the lifespan of plasma particles is quite small due to collision processes and this energy lost must be compensated continuously. Electric energy sources have been shown to be the most suitable ones to balance those energy losses. Whereby, the applied electric field must exceed a certain breakdown field strength to form a gas discharge, the plasma. The minimum voltage that must be applied between two electrodes with a gap *d* to initiate a breakdown is given by the Paschen's law (Eqn. 4).

$$V_b = \frac{A * p * d}{\ln(B * p * d) + C} \qquad \text{Eqn. 4}$$

V_B is the breakdown voltage, p the pressure in Pascal, d the gap in meters. A, B and C are gas and electrode specific coefficients (Turner 2016). The type of plasma sources and generation systems is diverse due to geometries, location and numbers of the used electrodes. Furthermore, plasma sources can be distinguished between their types of initiating and sustaining the electric and electromagnetic fields, as inductively and capacitively coupled plasmas, direct and alternating current plasmas, low- and high-frequency as well as microwave based discharges. Atmospheric pressure plasma jets (APPJ) have been used for more than 50 years now. The term "plasma jet" covers various kinds of configuration, which can realize the gas discharge operation in an "open" electrode configuration, whereby the generated reactive plasma components are projected in an open environment (Winter et al. 2015). One of the typical APPJ designs (Figure 2—2) consists of a dielectric, often ceramic, nozzle with an inner coaxial needle electrode mounted in the center and an outer grounded ring electrode at the nozzle outlet. An energy source, either radio frequency (RF) or direct current (DC) generator, is connected via a matching unit to the needle electrode. The matching unit adjusts the impedance of the generator to that of the plasma discharge to maximize the power transfer and minimize the reflected power.

The plasma is generated with a continuous process gas flow between the two electrodes at the tip of the needle electrode and expands outside the nozzle inside the ambient air. Plasma jets are usually generated using noble gases (e.g. argon), due to their lower breakdown field strength compared to air. However, noble gas plasma jets are not as reactive as air plasma jets. Therefore, noble gases are often mixed with small portions of molecule gases, e.g. nitrogen or oxygen. In dependence of the applied power and the composition and flow rate of the process gas the plasma jet can have a length up to several centimeters, whereas the radial size is limited by the inner diameter of the nozzle outlet. APPJ has been widely used in the biomedical field, for the inactivation of bacteria, wound healing or the treatment of cancer (Fridman & Friedman 2013;

Kong et al. 2009; Schlegel et al. 2013) and is a universal plasma source for a quick implementation of interdisciplinary studies. By reducing the diameter of the nozzle outlet the plasma jet can be reduced down to micrometer ranges to enable studies with a few biological cells, or even on single cell level (Lu et al. 2016). However, the application in the food sector requires the treatment of large areas or bulk treatment, therefore, APPJ must be operated in an array mode and/or must be moveable along the object surface. Besides the limitation of the treatment area, the operating costs of APPJ need also be to consider, since plasma jets are mostly operated with noble gas, which increases the plasma treatment costs.

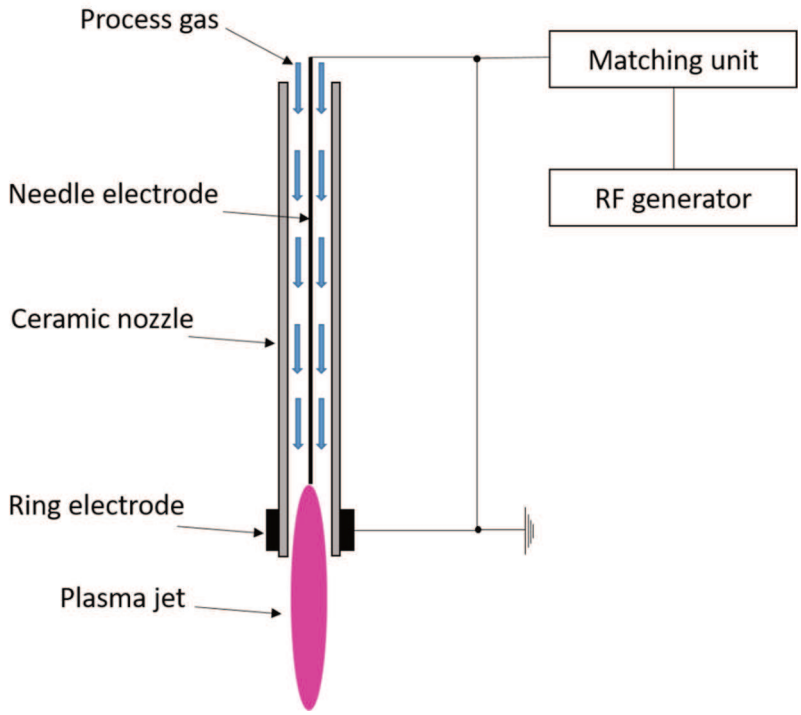

Figure 2—2: Scheme of a RF-driven plasma jet system.

A DBD system is defined by its configuration, in which the discharge is blocked by a dielectric barrier layer. The dielectric layer can cover one or both electrodes or can be suspended between them. The distance gap between the electrodes can vary between 0.1 mm to several centimeters. Materials such as glass, quartz, ceramics and polymer layers are usually used for the dielectric layer. The properties of the dielectric material, as insulation strength and dielectric constant, determine the stability and other parameters of the dielectric barrier discharge. A particular type of the DBD system is the diffuse coplanar surface barrier discharge (DCSBD) plasma source (CEPLANT, R&D Centre for Low-Cost Plasma and Nanotechnology Surface Modifications, Masaryk University, Brno, Czech Republic). The DCSBD plasma source (Figure 2—3) consists of two systems of parallel stripe-like silver electrodes on the bottom side of a Al_2O_3 ceramic. The electrodes have a width of 1.5 mm and a gap between them of 1 mm and are electrical

insulated by a circulating dielectric insulated oil. The diffuse homogeneous plasma is generated on the upper surface of the ceramic on an area of 200 x 80 mm with a thickness of approximately 0.3 mm. The plasma consists of a diffuse surface discharge developed of the single electrode stripes and of a filamentary streamer discharge between the electrodes. The plasma temperature of such a thin plasma layer depends strongly on the electrode system surface temperature, which is also effected by the ceramic dielectric heating (Černák et al. 2009). The circulating dielectric insulated oil works as a cooling system, maintaining plasma temperatures of below 70 °C, depending on the used process gas. As a process gas almost all gases and compositions can be used, like noble gases, ambient air or CO_2, O_2 and N_2. One main advantage, which the DCSBD system provides, is the treatment of larger areas. Various DCSBD plasma sources can be connected in a modular construction, to be employed at industrial scale, e.g. to increase felting properties of animal fibers in the textile industry (Cernak et al. 2014). In general, the DBD plasma system has various advantages, as the simple design and the stable and economical operation conditions. Due to these, those plasma systems are used in several applications, e.g. industrial ozone generation, surface modifications of polymers, as well as the treatment of biological matter in the medicine and food sector (Lu et al. 2016).

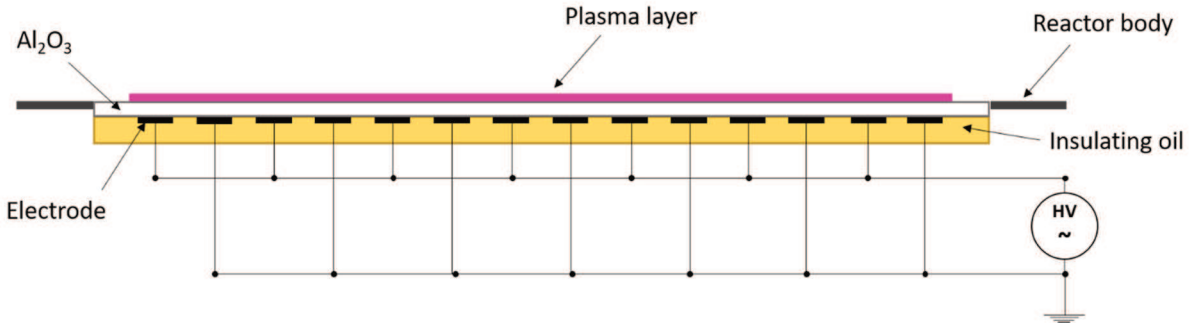

Figure 2—3: Scheme of the DCSBD setup.

Plasma at atmospheric pressure can be generated with either electrical energy or with microwaves. Compared to plasma jets and DBD plasma systems microwave-driven discharges are generated without electrodes, whereas the microwaves are generated by a magnetron. The electrons absorb the microwaves until they gain enough energy to ionize heavy particles. The generated microwaves are guided using wave guides or coaxial cable to a resonator or special discharge head, where the microwave plasma torch is ignited (Ehlbeck et al. 2011). Depending on the microwave power the plasma temperature can be close to room temperature or up to several thousand Kelvin (Uhm et al. 2006). The major advantages of microwave-driven plasma systems are the electrodeless setup and the easy handling of the torch-like discharges (Ehlbeck et al. 2011). These systems can be operated with ambient air or with special admixtures. As already

described for plasma jet systems, the microwave-driven discharge is also limited by its radial size. Accordingly, for the treatment of larger areas microwave-driven discharges must be operated in an array mode. Alternatively, these systems can be operated in a remote mode (Figure 2—4). Operating under this condition the plasma has no direct contact to the treated material, which means that the ionization of the process gas is spatially separated from the application area. In this case just the exhaust gas of the plasma torch, the "plasma processed air" (PPA) is used. The PPA is cooled down within a specific time and transported in a gas reservoir, where it is collected, humidified and further cooled to ambient temperature. From the gas reservoir, the PPA can be forwarded into certain treatment chambers, where the sample to be treated is placed. This remote microwave-driven discharge system allows the batch treatment for the decontamination of different dry plant products (Hertwig et al. 2015c).

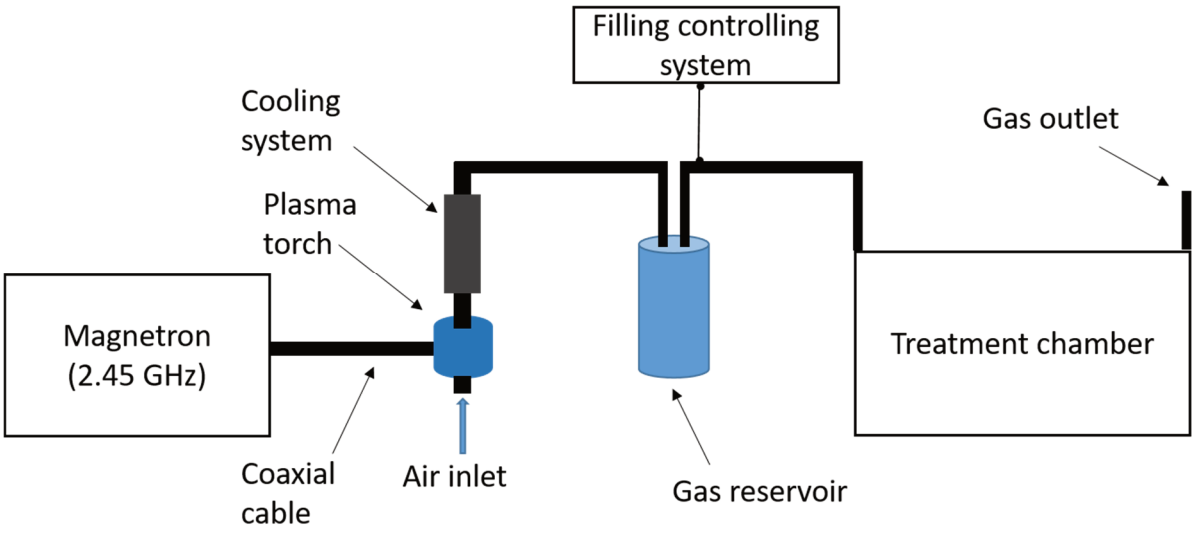

Figure 2—4: Scheme of a microwave-driven discharge system operating in a remote mode.

2.3 Application of cold atmospheric pressure plasma

Gas plasma is used in a broad range of industrial sectors. Application areas can be found in material processing, e.g. etching of semiconductor surfaces, and in surface modifications in textile industries (Misra et al. 2016). However, in the food sector cold plasma is a new technology, which offers different possible application areas at low temperatures (< 70°C) (Schlüter et al. 2013). In food processing CAPP can be applied in multiple ways (Table 2-2): direct, semi-direct or indirect. The type of application depends on the used plasma source, the properties of the treated material and the desired effects. The main point which needs to be considered regarding the application of CAPP in the food sector are the product-process interactions. The interaction of the CAPP with a food product can be diverse and depends strongly on the used CAPP system (e.g. source and process gas) and the properties of the treated product. Due to the plasma-product interactions during the treatment process, the generated plasma and the treated product cannot be considered as a static system. CAPP can be applied to solid/dry and liquid food products. The treatment of solid/dry food is normally limited to their surface. For the treatment of solid products, the penetration depth of the plasma and its generated reactive components is limited. It depends on various factors, as mainly the porosity, composition and water content of the treated surface (Surowsky et al. 2016), and on the generated plasma components. The penetration depth of UV photons can be above 1 µm, but depends on the material properties and the wavelength (Lerouge et al. 2000). Another factor limiting the penetration depth is the half-life of the generated reactive components, which can vary from 1 ms for hydrogen peroxide (H_2O_2) to 1 ns for hydroxyl radicals ($OH^{\bullet}$) (Møller et al. 2007). The low penetration depth of CAPP applications also minimizes unwanted effects on the nutrients inside the food product (Surowsky et al. 2016). Compared to solid/dry products liquid products have an opposite behavior. If CAPP is applied to a liquid, each volume element comes into contact with the generated components or their succeeding reaction products, which can result for instance in a pH change of the liquid media (Oehmigen et al. 2010). The two main application fields for the CAPP treatment of solid/dry material are:

- Surface modification
- Microbial inactivation.

Table 2-2: Overview of different types of cold plasma, adapted from Schlüter et al. 2013.

Type	Description	Examples
Direct	Plasma is in direct contact with the substrate	Plasma jet
	Interaction based on the irradiation (VUV, UV), charged molecules, radicals and reactive particles	DBD
Semi-direct	Distance between plasma and substrate much larger than the mean free particle path	SDBD with gap
	No interaction with charged particles	Sterrad process with plasma-activated hydrogen peroxide
	Antimicrobial effect based on irradiation, long-lived radicals, metastable and inhibitory substances	
Indirect	Irradiation with VUV, UV	UV lamps
	No reaction with plasma particles	
	Plasma is used to treat gas or liquids	Ozone generator
		Plasma-processed air (PPA)

2.3.1 Surface modification

CAPP induced surface modifications are induced and influenced by different plasma-induced fundamental processes (Table 2-3): etching, deposition, recombination, de-excitation and secondary emission from solid surfaces. These processes can alter the surface structure of the CAPP treated materials at the micro- to nanometer range (Pankaj et al. 2014a).

Table 2-3: Plasma-surface reactions, adapted from Braithwaite 2000.

Plasma-surface reactions	Reactions
Etching	$AB + C_{solid} \rightarrow A + BC_{vapour}$
Deposition	$AB \rightarrow A + B_{solid}$
Recombination	$e^- + A^+ \rightarrow A$
De-excitation	$A^* \rightarrow A$
Secondary emission	$A^* \rightarrow A + e^-$ (from surface)
	A^+ (fast) $\rightarrow A + e^-$ (from surface)

Etching processes, trigged by atomic oxygen, cause ablation of the first (atomic) layer, an extended plasma treatment results in further ablation due to UV photons and bombardment of energetic particles (electrons, ions, radicals, and excited atoms/molecules) on the surface (Surowsky et al. 2016). This plasma-induced interaction causes an increase of surface roughness (De Geyter et al. 2007). Further on, cold plasma can be used for the functionalization of

polymers, polymer degradation and cross-linking (Pankaj et al. 2014b). Responsible for the surface functionalization is the building of functional groups on the treated surface, due to oxidation and nitration processes occurring when hydrogen atoms on polymer chains form carbon radicals, resulting in oxygen- and nitrogen-containing functional groups (Surowsky et al. 2016). The functionalization can be used for instance to increase the wettability of plant seeds, resulting in a faster germination (Zahoranová et al. 2016). Bußler et al. (2015) reported, that CAPP treatment is able to modify protein and techno-functional properties of different flour fractions from grain pea. These researchers showed an increase of water and fat binding capacity in protein rich pea flour, probably due to structural changes of the contained protein. Besides these applications plasma treatment can also be used for the modification of packaging material. Hergelová et al. (2014) treated polylactic acid using the DCSBD plasma system resulting in an increased surface hydrophilicity, due to the formation of oxygen-containing functional groups, as hydroxyl-, carboxyl- or carbonyl-groups. The increased surface hydrophilicity of the polylactic acid depends on the treatment time. Furthermore, CAPP treatment can also be used in the textile industry to increase the felting properties of animal fibers instead of using chemicals (Cernak et al. 2014).

2.3.2 Microbial inactivation

The main investigated application of CAPP in the food sector is probably the inactivation of microorganisms. CAPP treatment enables the inactivation of various microorganisms and viruses, as bacterial spores, vegetative bacteria, as well as molds and yeasts, on different kinds of matrix (Zimmermann et al. 2011; Fröhling et al. 2012; Ziuzina et al. 2014; Baier et al. 2014; Hertwig et al. 2015c; Hertwig et al. 2016; Butscher et al. 2016). Responsible for the antimicrobial efficiency of CAPP are the reactive components, inter alia the vacuum ultraviolet (VUV) and UV photons, neutral and charged particles and free radicals, which can act individually and/or synergistically. These plasma-generated antimicrobial components attack various cellular targets, causing different involved inactivation mechanisms. Moreover, the plasma-based inactivation mechanisms can vary between microorganisms, e.g. bacterial spores and bacteria. Hereafter, the inactivation will be described based on bacteria. The mechanisms involved in plasma-based bacterial spore inactivation will be discussed in detail in chapter 2.5.3. Yet, the microbial inactivation by CAPP has not been fully understood. However, main involved mech-

anisms are, e.g. etching, DNA-damaging effect, photodesorption, membrane perforation, electrostatic disruption, oxidation effects, diffusion of reactive components and membrane perforation (Figure 2—5).

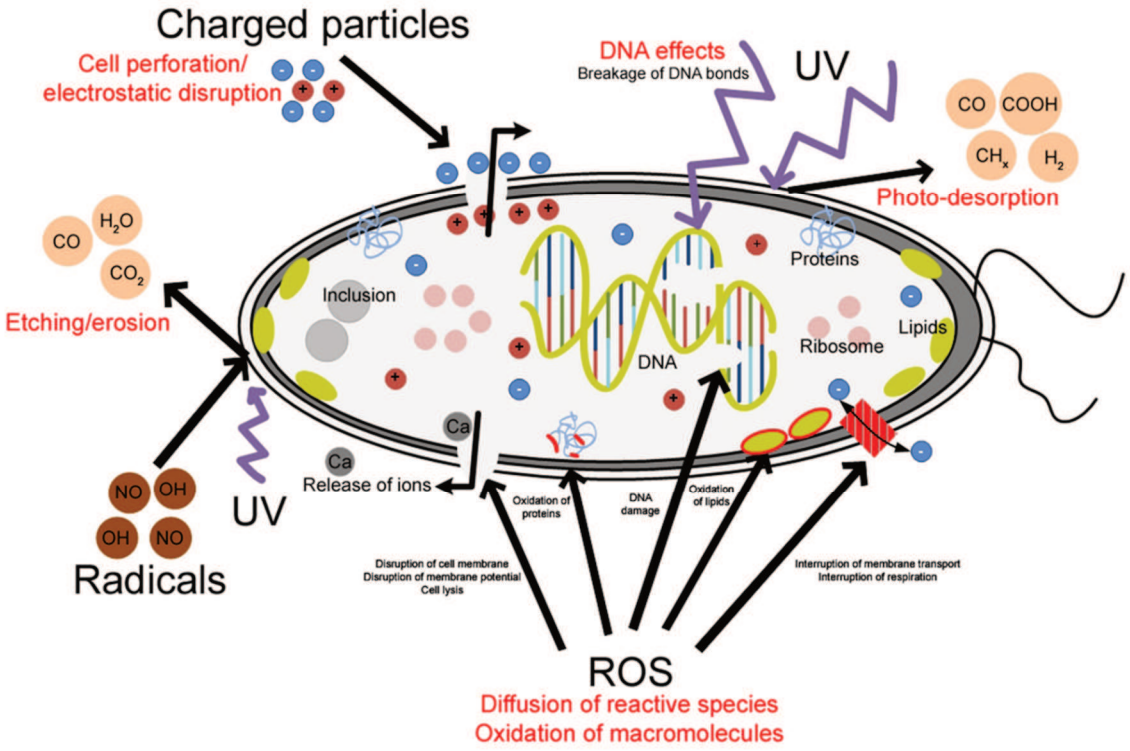

Figure 2—5: Schematic overview of plasma-based inactivation mechanisms (Schlüter & Fröhling 2014).

The CAPP treatment causes a continuous bombardment of the microorganisms with reactive components, as atomic and molecular radicals ($O^{\bullet}$,$OH^{\bullet}$ and $NO^{\bullet}$) and excited molecules, causing erosion of microorganisms atom by atom, through etching (Moisan et al. 2001). The etching process results from the adsorption of those reactive components on microorganisms' surface causing chemical reactions to form volatile compounds. Reactive oxygen, e.g. $O^{\bullet}$ and $OH^{\bullet}$, and nitrogen, e.g. $NO^{\bullet}$ and NO_x, species (ROS/RNS), can also affect cellular macromolecules, such as DNA, proteins and membrane lipids. The oxidation of membrane lipids compromises their function to act as a barrier against the transport of ions and polar compounds in and out of the cell (Laroussi & Leipold 2004). The oxidative DNA damage due to ROS can also be an important inactivation mechanism (Li et al. 2013). Reactive components can also diffuse into the cell causing for instance a decrease of the intracellular pH. If the pH homoeostasis cannot be maintained any longer, the bacterial cell will be inactivated (Booth 1985; Padan & Schuldiner 1987). The charged particles of the plasma can accumulate on the microorganisms' surface

causing a membrane rupture (Laroussi 2002), comparable to the effect of pulsed electric fields on membranes. Mendis et al. (2000) showed that the electrostatic forces caused by charge accumulation on an outer membrane surface could overcome the tensile strength of the membrane and cause its rupture. Emitted UV photons can induce the dimerization of thymine bases in bacterial DNA strands, which inhibits the bacteria ability to replicate (Laroussi 2002). Besides of causing DNA damage, UV photons are also able to break chemical bonds causing an erosion of the microorganisms atom by atom through intrinsic photodesorption (Moisan et al. 2001). Depending on the used plasma source, process gas and process parameters the composition of the reactive components within the plasma can vary tremendously, thus also mechanisms involved in the microbial inactivation process. The inactivation efficiency of a CAPP is likewise influenced by factors such as bacterial density on the treated material, bacterial species (gram positive or negative) (Fernández et al. 2012; Fröhling, Baier, et al. 2012) and properties of the treated material, as the structure (Smet et al. 2016) and the surface to volume ratio (Knorr et al. 2011). In the case of products with a high surface to volume ratio, like powdered products, it is more likely that the plasma interacts with the food surface itself than with the microorganisms on that surface (Hertwig et al. 2015c).

2.4 Bacterial Endospores

In 1876 both Cohn and Koch investigated bacterial endospores independently. Cohn (1876) described a “strongly refracting body”, which appeared in the homogeneous content of rods. This “strongly refracting body” did not germinate in the liquid in which they were formed, but they germinated in a fresh hay infusion. In 1888 Koch investigated the sporulation of *Bacillus anthracis* and other endospore-forming bacteria in microscopic cultures, being the first to describe the development cycle of spore formation.

Generally, endospore-forming bacteria belong generally to the phylum Firmicutes and can be divided into the aerobic class Bacilli and in the anaerobic class Clostridia. Bacterial spores are known to be the most durable cell type found in nature, which are still viable after extremely long time periods, e.g. hundreds millions of years (Cano & Borucki 1995; Vreeland et al. 2000). Consequently, bacterial spores are the perfect vehicle and the major vector causing food spoilage, foodborne diseases and other human illnesses (Logan 2012; Mallozzi et al. 2010). Furthermore, spores are monitoring their environmental conditions and if these conditions are in their favor, they start to germinate and potentially cause infections. The first diseases outbreaks

caused by spores is written down in Chapter 9 of the biblical book of Exodus (Torred et al. 2012). In Chapter 9 the fifth plague visiting upon Egypt is the death of livestock and the sixth plague is boils in humans. Some biblical scholars believe that the fifth plague was animal anthrax and the sixth one was cutaneous anthrax (Blane 1890; Hort 1958). Another disease known since antiquity and caused by spores of *Clostridium tetani* is tetanus. It was already described by Hippocrates in 380 BC (Torred et al. 2012). One foodborne disease, which occurred after mankind began to store and preserve food, is botulism caused by *Clostridium botulinum.* Botulism was named after the Latin word for sausage "botulus", because the first recorded case in Europe in 1735 was associated with the consumption of German sausage (Torred et al. 2012).

Endospores of *Bacillus subtilis* and isogenic mutant strains, as well as *Bacillus atrophaeus* were investigated in this study. At the moment the genus *Bacillus* includes in total 237 species (GBIF 2016), and is classified as:

Kingdom: Bacteria
Division: Firmicutes
Class: Bacilli
Order: Bacillales
Family: Bacillaceae
Genus: *Bacillus*

Out of the entire spore forming *Bacillus* genera, *Bacillus subtilis* is the best understood one in terms of its molecular and cell biology. *Bacillus atrophaeus* is used as the most common surrogate for the inactivation of pathogenic *B. anthracis* (Greenberg et al. 2010).

2.4.1 Sporulation

The endospore formation, the sporulation, is a well-characterized, complex and highly coordinated process, which takes place when the environmental conditions limit growing, e.g. lack of carbon and nitrogen (Phillips & Strauch 2002; Setlow 2007; Robleto et al. 2012). Bacteria avoid the sporulation under mild stress conditions, because the spore formation is an extremely energy-consuming process. The sporulation leads to the formation of two cell compartments; the fore spore and the mother cell. Whereby, the last stage of sporulation results in the lysis of the

mother cell and the release of the spore. The sporulation process for *Bacillus subtilis* is completed within eight to ten hours (Robleto et al. 2012) and can be divided into eight stages (0-VII), as shown in Figure 2—6.

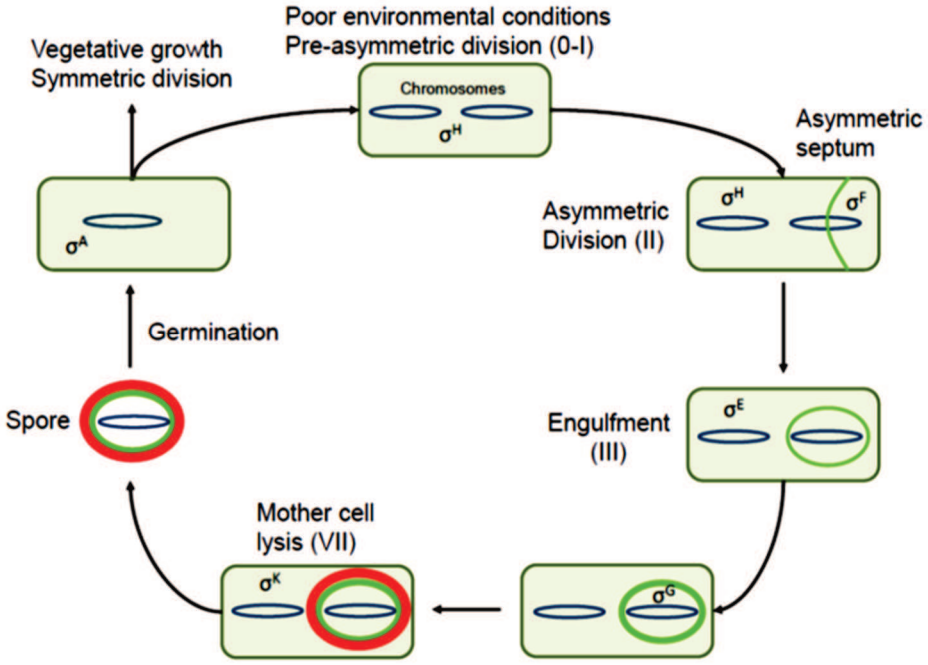

Figure 2—6: Scheme of Bacillus subtilis sporulation process, adapted from De Hoon et al. (2010).

It is controlled by five sigma (σ) factors (De Hoon et al. 2010). The sporulation is triggered by environmental cues and initiated by an enzyme-gene-cascade (mainly Spo0A and kinases), which directly affects the transcription of 121 genes (stage 0). After the initiation of the sporulation, the spore development starts (stage I), whereas the DNA coils along the central axis of the cell. Following the separation of the DNA into two asymmetric compartments (stage II), a small (forespore) and a large (mother cell) compartment are formed (Robleto et al. 2012). A certain sigma factor (σ^F) activates the transcription of 48 genes into the forespore, which are involved inter alia in DNA binding, the development of spore cortex components, detoxification and DNA repair. In stage III the forespore is engulfed by the mother cell membrane. Then the sigma factor σ^E from the mother cell controls the gene expression required for the cortex formation. In addition, regulates this factor about 260 genes and also the formation of the spore coat and the mother cell metabolism (Robleto et al. 2012). Afterwards, the mother cell membrane grows around the forspore, whereby the forespore is already surrounded by an intact membrane. The synthesis of a thick peptidoglycan cortex between the outer and inner forespore membranes initiates the formation of the cortex and the germ cell wall (stage IV). Concurrently to the cortex formation, the forespore loses water and ions, like potassium (K^+), prompting a

large decrease in volume and a simultaneous decrease in pH by approximately one unit. The uptake of significant quantities of divalent cations like Ca_{2+}, Mg^{2+}, or Mn^{2+} and pyridine-2,6-dicarboxylic acid (dipicolinic acid, DPA), which is synthesized in the mother cell, decreases the water content even further. After the final DPA concentration exceeds it saturation level, due the water removal from the spore, the formation of Ca^{2+}-DPA complexes is assumed. Within stage IV-V small acid-soluble proteins (SASPs) are synthesized, which remodel the forespore nucleotide into a ring. At stage V, the protoplast has an increased resistance to heat, radiation, high pressure, the action of enzyme and to chemical agents (Heinz & Knorr 2001). This resistance is mainly due to the spore´s high degree of compartmentalization. Within stage VI a complex proteinaceous coat, constructed with coat proteins from the mother cell, is layered on the outer surface of the spore and affects the specific hydrophobicity of bacterial spores. It is also responsible for the magnitude of adhesion forces to e.g. packaging material and other surfaces. This proteinaceous coat could cause a possible spore agglomeration (Mathys 2008). After the mother cell lyses, the spore is released (stage VII). The spores formed have no active metabolism and enable the microorganism to survive over long periods of time and under extreme environmental conditions (Gould 2006).

2.4.2 Structure of endospores and resistance mechanisms

The mature spore has a well-structured multilayer morphology, with several resistance mechanisms to withstand multiple environmental stress conditions, like wet and dry heat, irradiation, UV, high pressure and chemicals (Setlow 2014). The different spore layers consist, from the outside to the inside, of exosporium, coats, outer membrane, cortex, germ cell wall, inner membrane and the central spore core (Figure 2—7). The outermost exosporium surrounds the spore, but is not attached to the spore. It consists of specific glycoproteins and the thickness of this layer varies from microorganism to microorganism (Pedraza-Reyes et al. 2012). The exosporium is not present in spores of all species and absent in *Bacillus subtilis* spores (Setlow 2014). In spores of *Bacillus anthracis* the exosporium may act as a permeability barrier, which restricts the access of antibodies to antibodies to antigens in the spore coat (Henriques & Moran 2007). Next is the spore coat, which is a multilayered proteinaceous coat composed of more than 50 different proteins, consisting of the crust, the outer and inner coat and the basement (Setlow 2012). The coat acts as a permeability barrier restricting the access of large molecules and it acts as a chemical filter in protecting the spore against some chemicals, also against

enzymes, such as lysozyme that degrade peptidoglycan (Setlow 2014) and against predation by bacteriovores (Klobutcher et al. 2006). The spore coat contributes significantly to the absorption of UV-C and VUV photons, protecting the spore against radiation based damages (Fiebrandt et al. 2017). Additionally, it plays an important role in the germination process, since it is permeable to nutrients into the inner spore membrane (Pedraza-Reyes et al. 2012).

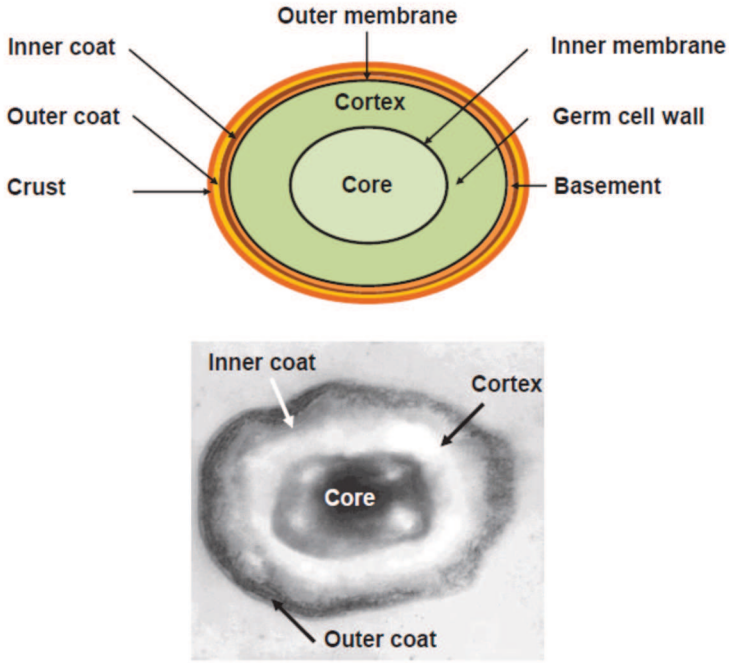

Figure 2—7: Schematic structure and transmission electron micrograph of Bacillus subtilis spore (Reineke 2012).

The outer membrane follows, which plays an essential role in the spore formation, but the specific role in dormant spore resistance remains an open question. Studies have even shown that the resistance of spores is not altered if the outer membrane is removed (Pedraza-Reyes et al. 2012). Underlying the outer membrane is a thick peptidoglycan layer, the cortex, and a thinner one, the germ cell wall. Both layers are essential for the spore viability, but it is not known that they are of relevance for the spore resistance. However, the cortex presumably serves as a retaining structure to withstand turgor pressures generated by high concentrated solutions and to keep the water content constant in the spore core (Popham 2002). Beneath the germ cell wall lays the inner spore membrane, which is analogue of the growing cell cytoplasmic membrane. The inner spore membrane has some novel properties: a much higher viscosity as cytoplasmic membrane, the lipids in the inner membrane are mainly immobile. In addition, the inner membrane is a strong permeability barrier, even for small molecules like water (Setlow 2014). Hence, is important in limiting the access of toxic chemicals and DNA damaging agents inside the spore core (Nicholson et al. 2000; Cortezzo & Setlow 2005). The final spore layer is the

central core, the analogue of the growing cell's protoplast. The core contains most spore enzymes as well as DNA, ribosomes and tRNAs. In almost all cases, the spore's enzymes and nucleic acids are identical to those in growing cells (Sevenich 2016). The spore core has some novel features, which are important for the spore resistance. These novel features are the low core water content, the high level of minerals and DPA inside, the decreased permeability of the spore core and the saturation of the DNA with SASPs (Pedraza-Reyes et al. 2012). Compared to growing cells with a water content between 75-80 %, the water in the spore core constitutes only 27-55 % of the spore's wet weight. Free water is also scarce, thus the movement of macromolecules is restricted inside the core. The low water content is important for the spore resistance against wet heat. The during the sporulation accumulated high DPA level inside the core makes up to 5-15 % of the dry matter content of the spore. The DPA is associated at a 1:1 ratio as a chelate with predominantly Ca^{2+} and protects the spore against some DNA damaging agents and also wet heat (Setlow 2014). The novel protein group SASP plays a significant role in the protection of the spore against different kinds of damages, especially the α/β-type SASP (Setlow & Setlow 1995). These proteins are highly concentrated in the core and constitute 3-6 % of the total spore protein. The α/β-type SASP binds to and saturates the DNA, causing structural changes in the DNA and altering their photochemistry. These proteins are significant for the protection against genotoxic chemicals, desiccation, dry and wet heat, as well as UV and γ-radiation (Fairheadt et al. 1993; Setlow & Setlow 1995; Pedraza-Reyes et al. 2012; Setlow 2014). Furthermore, the *Bacillus* spore is able to repair certain DNA damage during spore outgrowth, catalyzed in part by spore enzymes (Ramírez-Guadiana et al. 2012; Setlow 2006).

Table 2-4 gives an overview about certain inactivation technologies, such as dry and wet heat or high pressure, and the involved spores' resistance properties towards those treatments. For the application of cold atmospheric pressure plasma, the involved defense mechanisms and resistance properties of the spore have not yet been identified. However, similar defense mechanisms as for UV radiation and the treatment with oxidizing agents can probably be expected.

Table 2-4: Factors involved in endospore resistance towards different physical and chemical treatments, adapted from Reineke 2012.

Sporicidal treatment	Defense mechanism/ factor influencing the resistance	Reference
Wet heat	• Sporulation temperature	(Melly et al. 2002; Raso et al. 1995)
	• Core's level of DPA and Ca^{2+}	(Setlow et al. 2006)
	• α/β-type SASP	(Setlow 2007)
	• Core's low water content	(Gerhardt & Marquis 1989)
Dry heat	• DNA protection by α/β-type SASP	(Huesca Espitia et al. 2002; Setlow et al. 2006)
	• DNA repair enzymes ExoA and Nfo (active during germination)	(Salas-pacheco et al. 2005; Barraza-Salas et al. 2010)
Desiccation	• DNA protection by α/β-type SASP	(Setlow 1995)
Hydrogen peroxide	• DNA protection by α/β-type SASP	(Setlow 2006)
Ionizing radiation	• DNA repair enzymes ExoA and Nfo (active during germination)	(Salas-pacheco et al. 2005; Barraza-Salas et al. 2010)
	• Core's low water content	(Nicholson et al. 2000)
	• Sulphur-rich spore coat proteins and DPA	(Nicastro et al. 2002)
	• Increased levels of Mn2+ and other divalent cations	(Granger et al. 2011)
UV radiation	• UV-Photochemistry of DPA - DNA –formation of "spore photoproduct"	(Nicholson et al. 2000; Douki et al. 2005a)
	• Error free repair "spore photoproducts"	(Douki et al. 2005b)
	• DNA protection by α- and β- type SASP	(Setlow 2006)
	• DNA repair enzymes ExoA (active during germination)	(Nicholson et al. 2000)
	• Specific DNA repair system for "spore photoproduct"	(Nicholson et al. 2000)
High pressure	• Sporulation temperature	(Raso et al. 1998)
	• Demineralization of the core	(Igura et al. 2003)
	• Ability to retain DPA	(Margosch et al. 2004; Reineke et al. 2013)

2.5 Bacterial spore inactivation by cold atmospheric pressure plasma on solid surfaces – An overview of literature and discussed inactivation mechanisms

The first plasma experiments at atmospheric pressure with bacterial spores were performed by Menashi (1968). He used a pulsed RF field and argon as a process gas for the "plasma sterilization". The corona discharge plasma was generated inside a glass vial by a straight wire and a coil wrapped around the outside of the vial acting as the reference electrode to close the RF circuit. Using this CAPP system Menashi was able to sterilize the inner surface of the vials containing 10^6 bacterial spores within less than one second, whereas a direct contact of the generated plasma with the interior vial surface was required. The antimicrobial effect of this plasma application was attributed to an intense heating of the spores, in a time too short to obtain a noticeable heating of the glass vials. At the end of 1990 Kelly-Wintenberg et al. (1998) used "One Atmosphere Uniform Glow Discharge Plasma" to inactivate *Bacillus subtilis* and *Geobacillus stearothermophilus* spores inoculated on membrane filters and paper strips at ambient conditions, with a higher resistance of *Geobacillus stearothermophilus*. In 1999 Herrmann et al. treated *Bacillus atrophaeus* on glass coupons using a plasma jet with an $He/O_2/H_2O$ mixture and reported a D-value of 4.5 s.

Since the beginning of the 21st century extensive research have been conducted on the inactivation of bacterial spores on solid surfaces by cold atmospheric pressure plasma and a comprehensive overview of it is given in Table 2-5. It sums up briefly which plasma sources and process gases were used to inactivate various organisms and which results were obtained by the scientists.

Table 2-5: Bacterial spore inactivation on solid surfaces by cold atmospheric pressure plasma: An overview of literature.

Reference	Organism	Plasma source	Process gas	Surface	Comments
Menashi 1968	Bacterial spores	Corona-type discharge (pulsed RF field)	Ar	Glass slides $4*10^6$ spores per square inch	• Complete inactivation within 1/10 second
Kelly-Wintenberg et al. 1998	stea, sub	One atmosphere uniform glow discharge (RF 1-8 kHz, 2-6 kV, 10-150 W)	Air	Membrane filters $4*10^4$ stea Paper strips 10^6 sub	• Stea: ≥ 3 lg/7 min • Sub: ≥ 5 lg/5 min
Herrmann et al. 1999	atro	Plasma Jet (RF 13.56 MHz, 300 W)	He (92 slpm)/O_2 (0.72 slpm)/H_2O	Glass coupon ~10^7 CFU, spot with 5mm diameter	• D-value of 4.5 s, TT = 175°C • Hot gas $D_{175°C}$ of 45 s
Kelly-Wintenberg et al. 1999	atro, pum	One atmospheric uniform glow discharge (RF 1-20 kHz, up to 10 kV)	Air with maintained airflow	Paper stripes 10^6 CFU	• Pum: ≥ 5 lg/3 min, D_1 = 1.8 min, D_2 = 12 s • Atro: ≥ 5 lg/5.5 min, D_1 = 5.5 min, D_2 = 12 s • Biphasic inactivation curve
Trompeter et al. 2002	sub	Dielectric barrier discharge (300W)	Synthetic air, Ar, N_2; O_2	PET foils $2*10^4$ spores cm^{-1}	• Inactivation depended on used process gas, ≥ 4 lg/60 s for Ar and humid air • (V)UV emission seems to be important
Heise et al. 2004	sub	Dielectric barriers discharge Cascaded dielectric barrier discharge (20-50 kHz)	Synthetic air, N_2, Ar	PET foils	• Air 1 lg, N_2 4 lg/10 s, Ar 4 lg/5 s • faster reduction with cascaded plasma

continues…

Reference	Organism	Plasma source	Process gas	Surface	Comments
Laroussi & Leipold 2004	sub	Dielectric barrier discharge	Air, He, He/O_2 (97/3)	Biological sample	• He D-value ≥ 20 min, He/O_2 D-value of 10 min, Air D-value of 20 s • ROS/RNS important
Park et al. 2004	sub	Microwave induced jet (2.45 GHz)	Ar (100 lpm)	Filter paper	• 7 lg/10 s, 110°C • Etching effects
Pointu et al. 2005	stea	Corona discharge (10 kHz) flowing afterglow	N_2 (40slm)/O_2 (up to 50sccm)	Glass slides $2*10^4$ CFU cm^{-2}	• ≥ 2 lg/30 min
Rahul et al. 2005	atro	Microplasma afterglow plume (RF 13.56 MHz)	Ar	Strips	• 3 lg/10 min; ≤ 50°C
Akitsu et al. 2005	atro, stea	Dielectric barrier discharge (RF 100 kHz/13.56 MHz)	Water vapor/He/O_2	Cellulose and steel carrier ~10^6 CFU	• ≥ 6 lg/30 min 100 kHz • ≥ 3 lg/3 min 13.56 MHz stea
Boudam et al. 2006	sub	Dielectric barrier discharge	N_2-N_2O mixtures	Petri dish ~10^6 CFU	• Decreasing D-values with increasing UV emission • Partly biphasic inactivation
Lee et al. 2006	sub	Atmospheric pressure cold plasma (10 kHz, 6 kV)	He/O_2	Polypropylene carrier	• Biphasic inactivation • SEM showed shrunken morphology
Deng et al. 2006	sub	Plasma plume (29-37 kHz, 3-15 kV)	He (3 slm)/O_2 (max 2 sccm)	Polycarbonate membranes 3.5-7*10^6 CFU	• ~4 lg/10 min He, SEM ruptured spores with leakage • ROS important, other components play a minor role

continues…

Reference	Organism	Plasma source	Process gas	Surface	Comments
Morris et al. 2007	cer, stea	Dielectric barrier discharge (indirect, 60 Hz, 9 kV)	Air		• Stea: 50 % inactivation/15 min • Cer: 100 % inactivation/5 min
Lim et al. 2007	atro	Plasma jet (RF 13.56 MHz, 130 W)	Ar/O_2, He/O_2 (10 lpm/25 ccm)	Glass $2*10^7$ CFU	• TT 55-110°C, D-values 4.5-120 s depending on process gas and distance to jet outlet, SEM spore size reduction • ROS important
Muranyi et al. 2007	bot, spo pum, sub	Cascaded dielectric barrier discharge (130W)	Air	PET foils $6.25*10^4$ CFU cm^{-2}	• >5 lg/1 s for all spore strains
Weltmann et al. 2008	atro	Plasma jet (RF 27.12 MHz, 20 W)	Ar (20 slm)	Polyethylene strips $4*10^6$ CFU cm^{-2}	• 4 lg/7 min
Venezia et al. 2008	atro, stea	PlasmaSol (30 W)	$C_2H_4/O_2/N_2$ (1 %/50 %/49 %, 1 lpm)	Stainless steel disk ~10^6 CFU cm^{-2}	• Atro 5 lg/2 min, stea 5 lg/10 min
Pointu et al. 2008	stea	Corona discharge flowing afterglow (10 kHz)	N_2(40 slm)/O_2 (up to 50 sccm)	Glass slides $2*10^4$ CFU cm^{-2}	• N_2 ~3 lg/50 min, increasing inactivation due to O_2 addition
Ehlbeck et al. 2008	atro	Plasma jet (RF 27.12 MHz, 20 W)	Ar (20 slm)	PE strips	• 6 lg/10 min, inactivation due to reactive species assisted by (V)UV emission
		Magnetron (2.45 GHz, 1.7 kW)	Air	PET bottles	• ~2.5 lg/1.6 s and 5 min dwell of residue gas
Muranyi et al. 2008	sub	Cascaded dielectric barrier discharges (170 W)	Synth. air, 0-80 % humidity	PET foils $6.25*10^4$ CFU cm^{-2}	• Inactivation worsens with increasing humidity, more pronounces for short treatment times • Biphasic inactivation

continues…

Reference	Organism	Plasma source	Process gas	Surface	Comments
Brandenburg et al. 2009	atro	Plasma jet (RF 27.12 MHz, 20 W)	Ar (20 slm)	Polyethylene strips $3*10^6$ CFU cm^{-2}	• 5l lg/12 min, biphasic inactivation • (V)UV have lower effect
Hong et al. 2009	sub	Glow discharge (RF 13.56 MHz, 75 W)	He/O_2 (0-2 %) (4 lpm)	Glass $2*10^4$-$2*10^5$ CFU cm^{-2}	• 5 lg/120 s, D-value of 24 s for He/0.2 % O_2, TT of 70°C • ROS important, highest inactivation with maximum ROS
Dobrynin et al. 2010	an, cer	Dielectric barrier discharge (1.3 kHz, 30 kV)	Air	Plastic chamber or paper and plastic envelope ~10^4-10^6 CFU	• Complete inactivation after 45 s, independent of spore concentration, linear inactivation • SEM spores appear undamaged
Jung et al. 2010	sub	Glow discharge (RF 13.56 MHz, 75-100 W)	He, Ar (6 lpm)	Glass slide $2*10^6$ CFU	• He 100 W D-value of 435 s • Ar 75 W D-value of ~38 s • Ar 100 W D-value of 26 s
Muranyi et al. 2010	atro	Cascaded dielectricbarrier discharges (170-180 W)	Air	PET foils $6.25*10^4$ CFU cm^{-2}	• ~6 lg/7 s followed by tailing, effect on spores' DNA • SEM no obvious changes of outer spore shell
Ehlbeck et al. 2011	atro	Microwave torch (2.45 GHz, 1.2 kW)	Air, 20 % humidity	Glass bottles 10^7 CFU	• Indirect treatment with exhaust gas, dry air ~5 lg/30 min, with humidity 5 lg/2 min
Keener et al. 2012	atro	In-Package generation (P1: 60 Hz, 44 W, 13.4 kV, 1 cm gap; P2: 60 Hz, 150W, 80 kV, 4.5 cm gap)	Synthetic air: N_2/O_2 (78 %, 22 %), MA: $O_2/CO_2/N_2$ (65 %, 30 %, 5 %)	Strips $1.7*10^6$ CFU in low-densitiy polyethylene Ziploc bags	• P1: MA 6 lg/180 s indirect, 300 s direct; synthetic air 6 lg/300 s indirect 24 • P2: 6 lg/15 s for all 24 h after treatment

continues…

Reference	Organism	Plasma source	Process gas	Surface	Comments
Klämpfl et al. 2012	atro, pum, stea, sub	Surface microdischarge (1 kHz, 10 kV_{PP})	Air	Stainless steel, PTFE, PVC, glass $2*10^6$ CFU, wrapped with Tyvek	• ~5 lg/3 min sub, atro, pu • ~5 lg/5 min stea independent of surface • $D_{23°C}$-values of 0.9, 0.3, 0.6, 0.5 min for stea, sub, atro, pum
Polak et al. 2012	atro	In tube plasma (6.9 kHz, 21 kV_{pp})	Ar (1.5 slm); Ar/N_2 (20 sccm); $Ar/N_2/O_2$ (10/2 sccm); Ar/air (0.5 slm)	PTFE tube (2 mm diameter)	• 3.7 lg/10 min Ar with high (V)UV emission, increased UV emission increased inactivation 4.0 lg slightly • Highest inactivation with (V)UV, ROS and RNS
Schnabel et al. 2012a	atro	Microwave torch (2.45 GHz, 1.1 kW) remote application of exhaust gas	Air (16 slm)	Molecular sieve, seeds of: *Brassica napus, Raphanus sativus, Anethum graveolens, Daucus carota, Petroselinum crispum, Triticum aestivum and Piper nigrum* 10^6-10^7 CFU	• ≥ 5 lg/15 min for all seeds, except 1.7 lg/15 min *Piper nigrum* • Sieve: 1.3 lg/15 min, 2 lg/15 min loaded with oil, 2.3 lg/15 min loaded with tryptone, 3.5 lg/15 min loaded with volatile oil • RNS important
Schnabel et al. 2012b	atro	Microwave torch (2.45 GHz, 1.1 kW) remote application of exhaust gas	Air (20 slm)	*Brassica napus* seeds, molecular sieve, glass beads and helix 10^8 CFU ml^{-1}	• ≥ 5.2 lg/5 min glass beads • ≥ 5.2 lg/10 min glass helix • ≥ 5.2 lg15 min *Brassica napus* seeds • ≥ 0.9 lg/15 min molecular sieve • RNS important

continues…

Reference	Organism	Plasma source	Process gas	Surface	Comments
Shen et al. 2012	sub	Plasma jet (38 kHz, 20-40 kV)	Ar, Ar/5.8 % O_2 (750 l h^{-1})	PTFE sheet ~2*10^7 CFU cm^{-2}	• Ar: 40°C, D-value of 60 s, SEM no obvious damage, but protein leakage • Ar/O_2: ≤ 100°C, D-value of 10 s, SEM size and shape changed, charged particles • O_3 and ROS important
Koval'ová et al. 2013	cer	Corona discharge: positive streamer (20 kHz), negative Trichel pulses (1 MHz), pulsed corona (266 Hz)	Air	Polypropylene foil	• 2.2 lg/10 min, highest inactivation with negative pulsed discharge
Schnabel et al. 2013	atro	Microwave torch (2.45 GHz, 1.1 kW) remote application of exhaust gas	Air (18 slm) Addition of 5 slm O_2 or 2,000 ppm O_3 to 13/16 slm exhaust gas	Glass bottles 10^7 CFU 10^6 CFU with additional BSA loading	• ≥6 lg/30 min with exhaust gas • ≥5 lg/30 min with exhaust gas (with O_2) and BSA • RNS important
Sharma et al. 2013	sub	Plasma jet (30 kHz, 20 kV)	Ar/N_2 (10 slm/100 sccm)	Agar discs 3.4-6.8*10^4 CFU cm^{-2}	• Complete inactivation after 11 min, release of DPA • SEM showed collapsed spores
Cheng et al. 2014	sub	Plasma jet (38 kHz, 22 kV)	Ar, Ar/2.6 % H_2O (750 l h^{-1})	PTFE sheet ~2*10^7 CFU cm^{-2}	• Ar: 2 lg/5 min 40°C; Ar/H_2O 1.6 lg/5 min 40°C; SEM no obvious changes • OH radical and UV minor important
Schnabel et al. 2014	atro	Microwave torch (2.45 GHz, 1.1 kW) remote application of exhaust gas	Air (16 slm)	Lamb's lettuce, carrot, apple and strawberry 10^8 CFU ml^{-1}	• ~1 lg/15 min exposure to exhaust gas • RNS important

continues…

Reference	Organism	Plasma source	Process gas	Surface	Comments
Patil et al. 2014	atro	Dielectric barrier discharge in-package generation (50 Hz, 70 kV)	Air, N_2/O_2 (90 %/10 %), $O_2/CO_2/N_2$ (65 %/30 %/5 %)	Strips $2.3*10^6$ CFU	• Direct: ≥ 6 lg/60 s for all gases • Indirect: air ≥ 6 lg/120 s, $O_2/CO_2/N_2$ 1.7 lg/120 s, $O_2/CO_2/N_2$ ≥ 6 lg/30 s • TT always ~31°C
Jeon et al. 2014	stea	Surface microdischarge (0.1-100 kHz, 6.8 kV, 0.5-14 W)	Air/humidity (A 5.5, B 10.4 and C 17.9 g m^{-3})	Stainless steel substrates $1.5*10^6$ CFU	• A: 5 min almost no inactivation • B: 5 min/5 W 2.5 lg • C: 5 min/14 W > 3 lg • Linear inactivation, plasma activated water may important
Shimizu et al. 2014	atro, mega, saf, thu	Surface microdischarge (1-3 kHz, 14 kV) indirect exposure	Air	Aluminum disc 10^6 CFU cm^{-2}	• Atro: 3 lg/30 min, increased excitation frequency decreased O_3 concentration and increased inactivation • >6 lg/90 min saf, meg • ~3.5 lg/90 min atro, thu • TT ambient
Takemura et al. 2014	sub	Plasma jet (16-20 kHz, 280 V)	Ar (20 L min^{-1}), Ar/CO_2 (5/20 L min^{-1}), Ar/H_2O (20/0.5 L min^{-1})	Glass fiber filters	• ~1 lg/400 s Ar • 2 lg/400 s Ar/H_2O • ~3 lg/400 S Ar/CO_2
Hertwig et al. 2015a	atro, sub	Direct: plasma jet (RF 27.12 MHz, 30 W) Indirect: Microwave torch (2.45 GHz, 1.2 kW)	Ar (10 slm) Air (18 slm)	Black peppercorns ~10^7 CFU g^{-1}	• Direct: 0.8 lg/15 min sub, 1.3 lg/15 min atro • Atro: SEM damage of spore surface • Biphasic inactivation • Indirect: 2.4 lg/30 min sub, 2.8 lg/30 min atro • Atro: SEM no obvious damage

continues…

Reference	Organism	Plasma source	Process gas	Surface	Comments
Reineke et al. 2015	atro, sub	Plasma jet (RF 27.12 MHz, 30 W)	Ar, Ar/0.135 % vol. O_2, Ar/0.135 % vol. O_2,/0.2 % vol. N_2 (10 slm)	Glass petri dishes $1.4*10^6$-$4.4*10^5$ CFU cm^{-2}	• Ar: 3.1 lg/5 min atro, 2.4 lg/5 min sub • Ar/O2: 1.9 lg/5 min atro, 1.8 lg/5 min sub • Ar/O2/N2: 2.3 lg/5 min atro, 2.2 lg/5 min sub • Biphasic inactivation, extended initial phase with increasing UV emission • UV important, shown with UV sensitive spore mutants
Claro et al. 2015	dif	Single plasma jet (8 kHz, 2.5 kV, 25 W) Multi plasma jet (8 kHz, 1.5 kV, 15 W)	Air (12 or 13 slm)	Polyurethane coated mattress, stainless steel loaded with HSA $4*10^3$-$4*10^5$ CFU cm^{-2}	• Single-jet: negligible inactivation • Multi-jet: 2.7 lg/90 s on mattress, 1.8 lg/90 s on steel, HSA load no clear effect • TT ≤ 45°C
van Bokhorst-van de Veen et al. 2015	atro, cer, stea	Plasma jet (CP121 Plasma Demonstrator)	N_2 (15 slm)	GSWP filters $5.8*10^4$ CFU cm^{-2}	• Cer: 3.7 lg/20 min • Stea: 4.2 lg/20 min • Atro: 4.9 lg/20 min • Cer: SEM physical damage • No UV-C based inactivation
Matsui et al. 2015	stea	Plasma-excited neutral gas (12 kHz, 15 kV, 6.5 W) indirect	N_2, N_2/0.1 % O_2 (2 slm)	Stainless steel sheet $1.5*10^6$ CFU	• RH increase in source gas 30-90 % enhanced inactivation by the same degree, RH 60-90 % near sample highest inactivation after 20 min • RNS important

continues…

Reference	Organism	Plasma source	Process gas	Surface	Comments
Yoshino et al. 2015	atro, stea	Plasma sterilization system with circulating airflow (3 kHz, 16 kV) indirect	Air	Biological indicator	• Stea: 5 lg/25 min • Atro: 6 lg/35 min • SEM perforated spore coats, probably due to RNS • RNS important
Hertwig et al. 2015b	sub	Plasma jet (RF 27.12 MHz, 30 W)	Ar, Ar/0.135 % vol. O_2, Ar/0.135 % vol. O_2,/0.2 % vol. N_2 (10 slm)	Glass petri dishes and beads, whole black peppercorns $4*10^6$ CFU cm^{-2}	• Highest inactivation for Ar • Petri dishes: 2.7 lg/5 min • Beads 4.7 lg/10 min • Peppercorns < 1 lg/15 min • TT ≤ 90°C, biphasic inactivation, DNA damage, process gas composition influenced inactivation process
Butscher et al. 2016	stea	Dielectric barrier discharge (5-15 kHz, 6-10 kV)	Ar (2.8 nlm)	PP plate $5*10^5$, PP granules and wheat grains 10^7 CFU g^{-1}	• Plate: ~4 lg/10 min • Granules: ~5 lg/10 min • Grains: ~3 lg/60 min • Biphasic inactivation, increasing kV increased inactivation • SEM: erosion with strong perforation and reduction in spore size
Wang et al. 2016	cer, sub	Surface microdischarge (60 Hz, 14 kV)	Air	Glass coverslip $1.3*10^5$ CFU cm^{-2}	• ≥ 4.4 lg/3 min, ~2 lg/30 min placed inside an impermeable plastic bag • Inactivation probably by inner membrane and key germination protein damage • Charges particles and ROS important

continues…

Reference	Organism	Plasma source	Process gas	Surface	Comments
Hertwig et al. 2017	atro, sub	Diffuse coplanar surface barrier discharge (350 W, 15 kHz, 20 kV)	Air, N_2, O_2, CO_2	Glass beads $5*10^5$ to $6*10^6$ CFU cm^{-2}	• Sub: D-values : air 1.21 min, N_2 0.06 min, O_2 1.52 min. CO_2 1.10 min • Atro: D-values : air 1.22 min, N_2 0.05 min, O_2 1.80 min. CO_2 1.28 min • UV important • TT < 70°C • Spore resistance depends on SASP, DPA inside the core and the outer coat

Organism: stea, *Geobacillus stearothermophilus*; sub, *Bacillus subtilis*; atro, *Bacillus atrophaeus*; pum, *Bacillus pumi*lus; cer, *Bacillus cereus*; an, *Bacillus anthracis*; mega, *Bacillus megaterium*; saf, *Bacillus safensis*; thu, *Bacillus thuringiensis*; bot, *Clostridium botulinum*; spo, *Clostridium sporogenes*; dif, *Clostridium difficile*

Process gas: MA, modified atmosphere

Comments: lg = $\log_{10}$; TT, treatment temperature; RH, relative humidity

The literature review summarized in Table 2-5 shows the high diversity in plasma processing, regarding the used plasma source, process gas and kind of application. However, some milestones in bacterial spore inactivation on solid surfaces by cold atmospheric pressure plasma can be pointed out. Kelly-Wintenberg et al. (1999) reported a biphasic inactivation behavior, with an initial slower inactivation phase, followed by a second discrete phase exhibiting a more rapid inactivation. In 2002 Trompeter et al. showed, using a DBD plasma system, that the inactivation of *Bacillus subtilis* spores depends on the used process gas and that the UV emission of the plasma seems to be an important factor for spore inactivation. Whereas, Laroussi & Leipold (2004) stated that the generated reactive oxygen and nitrogen species of their used air plasma play the most important role in the inactivation process. The decomposition of spores by etching was shown by Park et al. (2004), they used a microwave driven plasma jet with argon as process gas and *Bacillus subtilis* spores inoculated on filter papers. In 2010 Muranyi et al. showed that a CAPP treatment of *Bacillus atrophaeus* spores has an effect on the spores' DNA. The first experiments with food matrices were carried out by Schnabel, Niquet & Krohmann (2012), they inoculated *Bacillus atrophaeus* spores on various plant seeds and exposed them to PPA. In these years, extensive studies were carried out investigating the inactivation process of bacterial spores by CAPP on different surfaces, as food packaging material (Muranyi et al. 2007; Muranyi et al. 2010), peppercorns (Hertwig et al. 2015a), wheat grains (Butscher et al. 2016), red pepper powder (Kim et al. 2014) or flat and spherical glass surfaces (Reineke et al. 2015; Hertwig et al. 2015b). Until now the mechanisms responsible for the bacterial spore inactivation have not been fully understood. Due to their well-structured multilayer morphology and various resistance properties, inactivation mechanisms responsible for bacterial inactivation cannot be directly compared to the CAPP-based inactivation of bacterial spores. The used plasma generation system, operation conditions, process gas as well as the treatment conditions (e.g. direct or indirect) influence the spore inactivation. Different target microorganisms, matrix effects, as well as methodic differences, complicate the comparability. Especially the influence of the food matrix surface, the spores are attached to, on the inactivation efficiency of spores cannot be neglected. Nevertheless, it is known that the spore inactivation depends on the different generated components of the CAPP, as reactive oxygen and nitrogen species (ROS/RNS) and (V)UV photons. However, the weighting of those components with respect to their role in the inactivation of spores on different structured surfaces has not been truly understood yet. The often described biphasic inactivation kinetics of various *Bacillus* spores on dry surfaces, fast inactivation within the first phase, followed by a slower inactivation in the second phase, probably indicate the involvement of different inactivation effects (Brandenburg et al. 2009; Hertwig et

al. 2015b; Moisan et al. 2001; Moreau et al. 2000; Reineke et al. 2015). Often an inactivation is proposed that depends on mechanisms as the inactivation by DNA damage due to emitted (V)UV photons and/or the decomposition of the spore through intrinsic photodesorption and etching (Figure 2—8) (Moreau et al. 2000; Moisan et al. 2001). The fast inactivation within the first phase is attributed to the emitted (V)UV photons and the slower inactivation of the second phase is attributed to the decomposition of the spore through photodesorption and etching as well as to the emitted (V)UV photons. VUV and UV photons are known to induce strain breaks and other damages in the spore DNA (Setlow 2007). Furthermore, UV photons with wavelength below 275 nm can break C–C or C–H bonds (Brandenburg et al. 2009) and affect protein and other macromolecules structures and functioning.

Some studies claim that under atmospheric conditions (V)UV photons play a minor role in the inactivation process. These authors stated that the inactivation is caused by the action of ROS and RNS (Lim et al. 2007; Deng et al. 2006; Laroussi & Leipold 2004; Hong et al. 2009; van Bokhorst-van de Veen et al. 2015; Matsui et al. 2015; Yoshino et al. 2015), since major quantities of (V)UV photons are only emitted in low pressure or vacuum plasma systems. Park et al. (2004) treated *Bacillus subtilis* spores inoculated on filter paper using a microwave induced plasma jet with argon and reported damaged and ruptured spores. The authors claimed that the strong etching process, due to oxygen atoms and radicals, is responsible for the inactivation. Similar results were reported by Deng et al. (2006), these authors observed slightly shrunken und membrane-ruptured *Bacillus subtilis* spores. The observed damage was maybe caused by the generated ROS of the used helium/oxygen plasma plume. Van Bokhorst-van de Veen et al. (2015) treated *Bacillus cereus* spores using a plasma jet driven with nitrogen and reported etching effects and the appearance of a rough spore surface, which were related to generated RNS. The shown decomposition of the spores using SEM does not have to be the main inactivation mechanism, since decomposition processes as etching and intrinsic photodesorption can also affect already inactivated spores.

On the contrary, studies showed that UV photons can dominate the inactivation process of bacterial spores (Trompeter et al. 2002; Boudam et al. 2006; Hertwig et al. 2015b; Reineke et al. 2015). Boudam et al. (2006) treated *Bacillus subtilis* spores using a DBD plasma system with nitrogen and nitrous oxide mixtures and showed decreasing D-values with increasing UV emission. Reineke et al. (2015) treated *Bacillus subtilis* and *Bacillus atrophaeu*s spores using a plasma jet and showed an extension of the initial fast inactivation phase of the biphasic inactivation kinetic with increasing UV emission. In addition, the authors showed the significant role

of UV photons in the inactivation process using UV sensitive *Bacillus subtilis* mutant strains. Moreover, Wang et al. (2016) studied the germination behavior of cold plasma treated *Bacillus subtilis* spores. Their results suggested that the CAPP treatment damages the spores' inner membrane and key germination proteins.

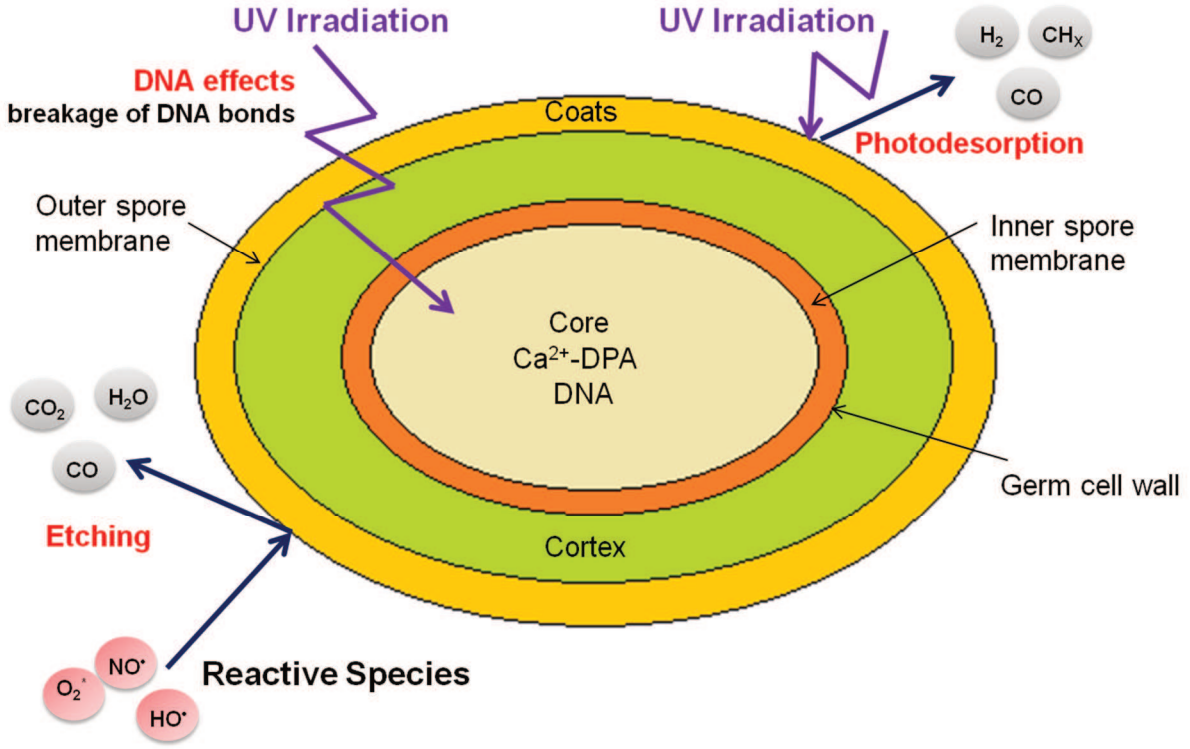

Figure 2—8: Scheme of Bacillus subtilis spore and plasma-based inactivation mechanisms.

In case of using an indirect CAPP application the role of emitted (V)UV photons in the inactivation process can often be neglected, as shown by Schnabel et al. (2013) and Hertwig et al. (2015a). The authors inactivated *Bacillus atrophaeus* und *Bacillus subtilis* spores using PPA generated by a microwave-driven plasma torch, whereby the plasma has no contact with the treated matrix and the antimicrobial effect is related to long living RNS in the PPA. The role of the humidity of the process gas is not yet clear. Muranyi et al. (2008) reported a decreased inactivation with increased process gas humidity for *Bacillus subtilis* spores, this effect was more pronounced for short treatment times. In contrast Patil et al. (2014) and Jeon et al. (2014) showed an increased inactivation with increasing process gas humidity for *Bacillus atrophaeus* and *Geobacillus stearothermophilus* spores, probably due to a higher generation of $OH^{\bullet}$ during the CAPP treatment.

Besides the generated reactive components, such as (V)UV photons, ROS and NOS, in the plasma and process gas, the structure of the surface, to which the spores are attached, can also

influence the inactivation of endospores (Schnabel, Niquet & Krohmann 2012; Hertwig et al. 2015b). Hertwig et al. (2015b) showed that a surface with a complex structure, like black peppercorns, affected the inactivation of *Bacillus subtilis* spores negatively, independent of the used process gas. Likewise, different obtained inactivation for various spore strains (*Geobacillus stearothermophilus*, *Bacillus subtilis*, *pumilus*, *atrophaeus* and *cereus*) were reported, whereby *G. stearothermophilus* and *B. atrophaeus* spores showed often a higher resistance towards CAPP as the other investigated spore strains (Kelly-Wintenberg et al. 1998; Kelly-Wintenberg et al. 1999; Morris et al. 2007; Venezia et al. 2008; Klämpfl et al. 2012; van Bokhorst-van de Veen et al. 2015). However, these studies showed no clear trend towards a possible indicator spore strain for cold atmospheric pressure plasma treatment.

Due to the quite complex interactions of the plasma with the endospores, which are influenced by many parameters, such as plasma system, process gas and treated surface structure; it is difficult to compare results obtained by different plasma applications. Nevertheless, mechanisms responsible for the inactivation of spores, depending on different structured surfaces the spores are attached to, different kinds of plasma sources and process gases will be discussed for recent data on *Bacillus subtilis* in chapter 7 “Conclusion and perspectives”.

3. The impact of different process gas compositions on the inactivation effect of an atmospheric pressure plasma jet on *Bacillus* spores

In: Innovative Food Science and Emerging Technologies, 30, p. 112–118, 2015

Cite as:

Reineke, K., Langer, K., Hertwig, C., Ehlbeck, J., Schlüter, O., 2015. The impact of different process gas compositions on the inactivation effect of an atmospheric pressure plasma jet on *Bacillus* spores. Innovative Food Science & Emerging Technologies. 30: 112–118.

doi:http://dx.doi.org/10.1016/j.ifset.2015.03.019

Innovative Food Science and Emerging Technologies 30 (2015) 112–118

Contents lists available at ScienceDirect

Innovative Food Science and Emerging Technologies

journal homepage: www.elsevier.com/locate/ifset

The impact of different process gas compositions on the inactivation effect of an atmospheric pressure plasma jet on *Bacillus* spores

Kai Reineke [a], Katharina Langer [a], Christian Hertwig [a], Jörg Ehlbeck [b], Oliver Schlüter [a,*]

[a] Quality and Safety of Food and Feed, Leibniz Institute for Agricultural Engineering (ATB), Potsdam, Germany
[b] Leibniz Institute for Plasma Science and Technology (INP), Greifswald, Germany

ARTICLE INFO

Article history:
Received 4 January 2015
Received in revised form 27 February 2015
Accepted 31 March 2015
Available online 17 April 2015

Keywords:
Cold atmospheric pressure plasma
Endospore
Sporicidal effects
Inactivation mechanisms

ABSTRACT

Atmospheric plasma provides the advantages of high microbial inactivation that can be performed under ambient conditions. It is consequently regarded as potential alternative to traditional food preservation methods. In this study we systematically tested the influence of argon as plasma carrier gas with admixtures of oxygen (0–0.34 vol.%) and nitrogen (0–0.3 vol.%) towards its emission intensity of UV-C light, excited OH and N_2-species and atomic oxygen. A mixture of argon, 0.135 vol.% oxygen and 0.2 vol.% nitrogen emitted four fold more UV photons than pure argon. However, sporicidal effects on *Bacillus atrophaeus* (3.1 $\log_{10}$) and *Bacillus subtilis* spores (2.4 $\log_{10}$) were found for pure argon plasma, which were similar as compared to the sporicidal effect of the plasma with highest UV-emission. To distinguish lethal effects caused by emitted UV-light and reactive species, UV-sensitive mutant spore strains (PS578 and FB122) were exposed to plasmas with different UV-emission intensities and a significant impact of UV-light on the first phase of spore inactivation was confirmed. *Industrial relevance:* As an efficient method for the inactivation of microorganisms at low temperatures and atmospheric pressure, plasma is already commercially used for the sterilization of medical devices. The results presented in this study could be useful for a process optimization regardless if the plasma is applied for food preservation or surface decontamination. Especially the impact of emitted UV photons from the plasma on the first inactivation phase of endospores attached to surfaces, depicts a high potential of such plasmas for a rapid spore inactivation.

1. Introduction

The formation of highly resistant endospores by stressed vegetative cells belonging to class *Bacilli* or *Clostridia* results in perfect vehicles for the spoilage of food and/or infection of humans. Spores alone are not hazardous in stored food or during food consumption, but they can cause foodborne diseases after outgrowth. After the sporulation, the matured spore has a well-structured multilayer morphology with several mechanisms to withstand multiple environmental stress conditions, like wet and dry heat, desiccation, irradiation and chemical agents (P. Setlow, 2007). Consequently, spores are perfectly adapted to survive on the surface of dry food products like herbs and spices (Sagoo et al., 2009; Vij, Ailes, Wolyniak, Angulo, & Klontz, 2006) or in a food production line (Faille et al., 2013).

Several pasteurization and sterilization methods are applied to increase the microbial safety of herbs and spices, which include the treatment with wet steam, fumigation with ethylene-oxide or γ-irradiation (Mckee, 1995). However, all of these methods have disadvantages with regard to sensorial properties, consumer safety or acceptance. Consequently, there is a need for alternative low-temperature pasteurization and sterilization processes for the surface of dry foods. A promising process with the potential to fulfill these requirements is a cold atmospheric pressure plasma treatment.

In general, plasma is a gas containing free electrons, ions and neutral particles, which can be further categorized by its thermodynamic properties into thermal and non-thermal plasmas (Schlüter et al., 2013). Thermal plasmas are characterized by the existence of a thermodynamic equilibrium between neutral particles, ions and electrons. The temperature of these plasmas is usually above 6000 K under atmospheric pressure (Moreau, Orange, & Feuilloley, 2008). In contrast the temperature of nonthermal plasmas is much lower and can be directly applied to thermal sensitive surfaces. In nonthermal plasmas the electron temperature can reach several 10,000 K, whereas the gas temperature can be close to ambient temperature. The term "cold plasma" is defined for treatment temperatures below 70 °C (Schlüter et al., 2013).

Nonthermal plasmas at atmospheric pressure can be generated by different plasma setups, whereas one of the most common is a plasma

* Corresponding author.
E-mail address: o.schlueter@atb-potsdam.de (O. Schlüter).

http://dx.doi.org/10.1016/j.ifset.2015.03.019
1466-8564/

jet. Here the carrier gas (e.g. argon, helium, air or nitrogen) is passed through a nozzle in which an electric field with a high voltage difference is present. This voltage creates a strong force on orbiting electrons, which in turn provides energy for their escape, resulting in the ionization of atoms and/or molecules. The free electrons quickly collide with gas molecules providing excitation energy to create unique, highly reactive products (Keener, 2008) and the emission of UV light (Brandenburg et al., 2009) with antimicrobial effects. The concentrations in which the agents occur in the plasma depend greatly on the device setup, the operating conditions (gas type and power of plasma excitation) and the gas composition (Brandenburg et al., 2009; Roth, Feichtinger, & Hertel, 2010).

The inactivation potential towards bacterial spores of these nonthermal atmospheric plasmas was shown by many authors (Boudam et al., 2006; Brandenburg et al., 2009; Lassen, Nordby, & Grun, 2005; Moreau et al., 2008; Schnabel et al., 2012; van Gils, Hofmann, Boekema, Brandenburg, & Bruggeman, 2013), but the mechanisms leading to spore inactivation are still under investigation. The often described biphasic inactivation kinetics of various *Bacillus* spore strains on dry surfaces are presumably due to combined inactivation effects of the nonthermal plasma. Of special interest in this regard are UV and VUV photons, since they are known to induce DNA strain breaks (P. Setlow, 2007) or to damage other proteins in the cell (Philip et al., 2002).

UV photons with a wavelength ≤ 275 nm can break C—H and C—C bonds and might be responsible for the initial rapid inactivation (Boudam et al., 2006). However, larger quantities of UV and VUV photons are only emitted in low-pressure or vacuum plasma systems, which are in most cases not suitable for food treatments (Knorr et al., 2011). Further, most researchers claim that UV emission plays a minor role in the inactivation of microorganisms at atmospheric pressure, and the inactivation process is controlled by chemically reactive species (Knorr et al., 2011; Laroussi, 2005; Laroussi & Leipold, 2004; Pointu et al., 2005). The mechanisms involved are the intrinsic photodesorption and etching (Moisan, Barbeau, & Pelletier, 2001), which describe the degradation and erosion of outer structures of microorganisms, leading to cell death.

This study investigates the inactivation behavior of *Bacillus subtilis* spores and isogenic mutant strains, with increased sensitivity towards UV light, on glass surfaces to clarify the impact of UV emission from an atmospheric plasma jet on spore inactivation. Further a systematic modification of the plasma carrier gas composition towards a maximum amount of emitted UV photons was done to enhance spore inactivation and to optimize the process.

2. Material and methods

2.1. Nonthermal radio-frequency-driven plasma jet

The atmospheric pressure plasma jet used in this study was described in detail by Brandenburg et al. (2009). The jet consists of ceramic nozzle with an inner diameter of 7 mm. The radio frequency (RF, frequency 27.12 MHz and system power 30 W) is coupled via a matching network to the wolfram-needle-electrode, which is mounted in the center of the nozzle. A grounded ring electrode is placed at the nozzle outlet and a gas flow of 10 slm of argon was used to generate plasma from the tip of the needle electrode to the inner wall of the nozzle. The generated plasma expanded to the outside of the nozzle with a length of 15 mm. The plasma is found to be filamentary and a mixing of the argon gas with the surrounding air could be determined by optical emission spectroscopy for the pure argon plasma. To increase the emission of UV photons in the plasma, 0.1, 0.2 and 0.3 vol.% of nitrogen and 0 to 0.34 vol.% (increase in 0.01% steps) of oxygen were added to the argon gas until an unstable plasma ignition was visible.

2.2. Optical emission spectroscopy

For optical emission spectroscopy a Black-Comet-UV–vis spectrometer (StellarNet Inc., Tempa, USA), equipped with a F400-UV–vis-SR fiber optic and a quartz lens in the range from 190 to 900 nm, was used. This setup enabled the measurement of UV-C (190–280 nm), UV-B (280–320 nm) and UV-A (320–400 nm) irradiation, as well as the spectral bands of OH radicals (309 nm) and atomic oxygen (777.5 nm). The distance between the detection lens and the nozzle outlet was 15 mm in axial and 10 mm in vertical direction. The spectrum was measured 10 times with an integration time of 100 ms. The average spectrum was base-line corrected and normalized using a self-written LabVIEW routine.

2.3. Measurement of UV dosage

The intensity of the emitted UV dosage for certain carrier gas compositions (Table 1) was further quantified with UV-Tec control strips (UV-Tec Messtechnik GmbH, Bergisch Gladbach, Germany). The strips were placed at different distances in axial direction to the nozzle outlet (Table 1) for different exposure times. After exposure the UV-dosage is directly shown by means of coloration of the UV-control-strips (sensitivity in the range λ: 250–420 nm). After measuring the affected area (Table 1) and quantifying the UV-dosage related to a defined exposure time, the UV irradiance in W cm^{-2} was calculated.

2.4. B. subtilis strains, spore preparation and purification

In this study we used a *Bacillus athropheus* strain (WIS 396/3), a *B. subtilis* strain PS832 (wild-type) (Paidhungat & Setlow, 2000) and two isogenic derivatives of the *B. subtilis* strain, namely FB122 (Douki, Setlow, & Setlow, 2005) and PS578 (Genest, Setlow, Melly, & Setlow, 2002). Spores of *B. athropheus* strain (WIS 396/3) are used as surrogates for *Bacillus anthracis* during chemical and UV- and γ-irradiation sterilization (personal communication Dr. Marshall Bundeswehr Research Institute for Protective Technologies and NBC Protection (WIS)). The strain FB122 (*sleB spo VF*) lacks the gene for encoding the cortex lytic enzyme sleB and is not able to synthesize dipicolinic acid (DPA) during sporulation. The strain PS578 ($\alpha^-\beta^-$), lacks the genes encoding the spore's two major α/β-type small acid soluble proteins (SASP), such that the α/β-type SASP level in PS578 spores is only ~25% of that in PS832 wild-type spores.

All spore strains were prepared at 37 °C on 2xSG agar plates without antibiotics, according to a method described elsewhere (Nicholson & Setlow, 1990; Paidhungat & Setlow, 2000). After sporulation the spores were harvested and cleaned by repeated centrifugation (3-fold at 5000 *g*), washed with cold distilled water (4 °C), and sonicated for 1 min. The purified spore suspensions contained ≥95% phase-bright spores and nearly no spore agglomerates, as was verified by a particle image analysis system (FPIA 3000, Malvern Instruments, Worcestershire, UK). The spores were then stored in distilled water in the dark at 4 °C.

Table 1
Experimental settings for UV-dosage determination with UV-control strips.

Carrier gas composition	Distance between nozzle and surface [mm]	Exposure time [min]	Irradiated area [cm^2]
Argon	10	1.5	0.2
	15	5	0.80
	20	15	1.77
Argon + 0.135% vol oxygen	10	1.5	0.2
	15	5	0.80
	20	15	1.77
Argon + 0.135% vol oxygen + 0.2% vol nitrogen	10	1.5	0.2
	15	5	0.80
	20	15	1.77

2.5. Plasma treatment of inoculated glass petri-dishes

Aliquots of each stock spore suspension were diluted 1:10 with deionized water and 25 μL was transferred into sterile glass petri-dishes (diameter 3 cm). The droplets of spore solution covered an area of ~2.25 cm^2 and were allowed to dry under aseptic conditions in a laminar air flow for at least 1 h, resulting in a final spore density of ~1.44×10^6 to 4.44×10^5 spores/cm^2.

The inoculated petri-dishes were exposed to the plasma afterglow (distance 15 mm) for various treatment times. A direct contact between the plasma and the glass surface was avoided to prevent the spore layer from abrasion by the plasma filaments. The pure gas flow had no effect on the inactivation of attached spores. The petri-dishes reached a maximum temperature of 81 °C during a 5 min plasma exposure, which had no effect no spore viability. For the measurements an infrared camera (ThermaCam 500, Flir, Frankfurt am Main, Germany) was used. The emissivity of glass-petri dishes was set at 0.94. The camera was installed from above at a distance of 1 m to the sample and infrared images were taken at a frequency of 60 min^{-1}.

After plasma exposure, the glass petri-dishes were filled with 1 mL cold phosphate buffer solution (PBS) (pH 7, 0.05 M) and 4 sterile glass beads were added. The spores were resuspended by continuously shaking (250 rpm) for 20 min. The obtained spore suspensions were serially diluted in PBS and plated on nutrient agar plates (Carl Roth GmbH, Karlsruhe, Germany). The plates were incubated at 37 °C and the colony forming units (cfu) were counted after 24 and 48 h.

All treatments were done at least in triplicates.

2.6. Modelling of spore inactivation

The mean values of the inactivation data were fitted with GInaFiT (Geeraerd and Van Impe Inactivation Model Fitting Tool), a freeware Add-Inn for Microsoft ® Excel by using a biphasic inactivation model (Cerf, 1977). In this model, the relation between survival and exposure time is given by the equation:

$$\frac{N(t)}{N_0} = \varphi \cdot e^{k_1 \cdot t} + (1-\varphi) \cdot e^{k_2 \cdot t}$$

where $N(t)$ is the number of surviving spores after a certain time (t) and N_0 is the initial number of spores. φ is a constant designating the transition from the first inactivation phase to the second where k_1 and k_2 represent corresponding rate constants.

3. Results and discussion

3.1. Optimization of the plasma process gas composition

To identify the effect of gas composition on the emitted amount of UV-light and reactive species, a stepwise addition of nitrogen (up to 0.3 vol.%) and oxygen (up to 0.34 vol.%) to argon gas was conducted. The increasing admixture of oxygen was stopped, until the filamentary plasma discharge was unstable. The plasma afterglow was measured 15 mm in axial distance from the nozzle outlet, at the same position where the inoculated spore glass petri-dishes were treated later on. After a baseline normalization of the measured spectra (between $\lambda =$ 337.5 and 360 nm) the area below the emission spectra was calculated in wavelength range from 190 to 280 nm (UV-C-light emission), from 280 to 400 nm (UV-A, UV-B and OH-radical emission) and from 772 to 783 nm (atomic oxygen emission band at 777.5 nm). The results are shown in Fig. 1 and clearly depict significant variations in the emission spectra, caused by the addition of oxygen and nitrogen. The stepwise increase of oxygen in the carrier gas, mainly affected the amount of emitted UV-C light (Fig. 1A). The highest emission was measured for an addition of 0.2 vol.% of nitrogen and 0.135 vol.% of oxygen. This gas composition emitted a 2.5 fold higher amount of UV photons compared to the other tested nitrogen concentrations (0, 0.1 and 0.3 vol.%). In general argon is the main single gas emitting UV-light in a plasma discharge at atmospheric pressure, but it is not the only one. Nitrogen as well as mixtures of argon and nitrogen has also been reported to emit UV-light (Heise, Neff, Franken, Muranyi, & Wunderlich, 2004).

The detected UV-C emission of the plasma jet afterglow in this study is mainly due to molecular bands nitric oxide (NO_γ-system) and molecular nitrogen (second positive system) (Brandenburg et al., 2009). Consequently, an increase in the nitrogen and oxygen content in the carrier gas increases the amount of NO_γ and N_2 emissions. However, high concentrations of oxygen and nitrogen, caused instabilities of the plasma discharge and a shift to a weaker and more filamentous plasma. This is due to electron attachment and the quenching of argon metastable states (Brandenburg et al., 2009) as well as quenching of UV-C photons by the added nitrogen and oxygen itself.

Contrary to the measured UV-C emission for this plasma jet source, Surowsky, Frohling, Gottschalk, Schluter, and Knorr (2014) reported for a similar device no relevant UV-C emission for argon as carrier gas with a stepwise addition of oxygen up to 0.1 vol.%. This finding correlates only partially with our results. For admixtures up to 0.1 vol.% oxygen to the different gas compositions, highest emission of photons in the UV-C emission band was found for argon with 0.2 vol.% nitrogen, but also pure argon emitted UV-C photons (Fig. 1A). This contradictory finding could have many reasons and might attributed to the used plasma device, the optical emission measurement setup or the data analysis. Surowsky et al. (2014) compared the emission spectra in the UV-C emission band but the relative irradiance intensity was not calculated.

The admixture of nitrogen and oxygen had nearly no impact on the emission intensity of UV-A and UV-B light (Fig. 1B) (280 to 400 nm). The addition of 0.05 vol.% of oxygen increased the amount of emitted photons in this wavelength range for all tested nitrogen concentration with a further slight increase up to 0.3 vol.%, whereas the highest emission intensity was found for pure argon with 0.135 vol.% oxygen. The emission spectrum from 280 to 400 nm is dominated by the so-called NO_β molecular stemming, respectively from the NO(B) upper excited levels of the NO molecule (Boudam et al., 2006) and OH radicals (Surowsky et al., 2014). The nitrogen molecules needed to produce NO molecules in an excited state (NO_β) are presumably from the plasma expansion into the surrounding air atmosphere and to a minor extend from impurities in the used gases. Significant changes in the emission intensity of $OH^\bullet$ radicals at 309 nm were not observed by admixture of oxygen and nitrogen, which was also reported by Brandenburg et al. (2009) for the admixture of 50 sccm of air to 20 slm argon for the same plasma jet.

Fig. 1C shows the relative emission intensity from 772 to 783 nm. In this wavelength range the O I line at 777 nm (metastable singlet state of oxygen) emission was measured. The pure argon carrier gas with an admixture of oxygen emitted the highest photon intensity. The emission intensity was up to 6-fold higher compared to a mixture of argon and nitrogen. With increased nitrogen content in the carrier gas, the relative emission intensity decreased. For pure argon a pronounced increase of singlet state oxygen was observed above oxygen concentrations of 0.05 vol.%. These reactive oxygen species (ROS) are reported to be the dominant reactive species regarding the erosion of bacterial spores through etching (Knorr et al., 2011; Philip et al., 2002). Philip et al. (2002) further attributed an enhanced etching to the emission of UV photons, which break chemical bonds and, therefore, provide sites for ROS to adsorb. To prove this assumption and to further characterize the used plasma system in this study, we decided to test three different plasma gas compositions for a further measurement of the emitted UV light by UV-test strips and its antimicrobial effect on *B. subtilis* spores and isogenic mutant strains with reported higher UV sensitivity.

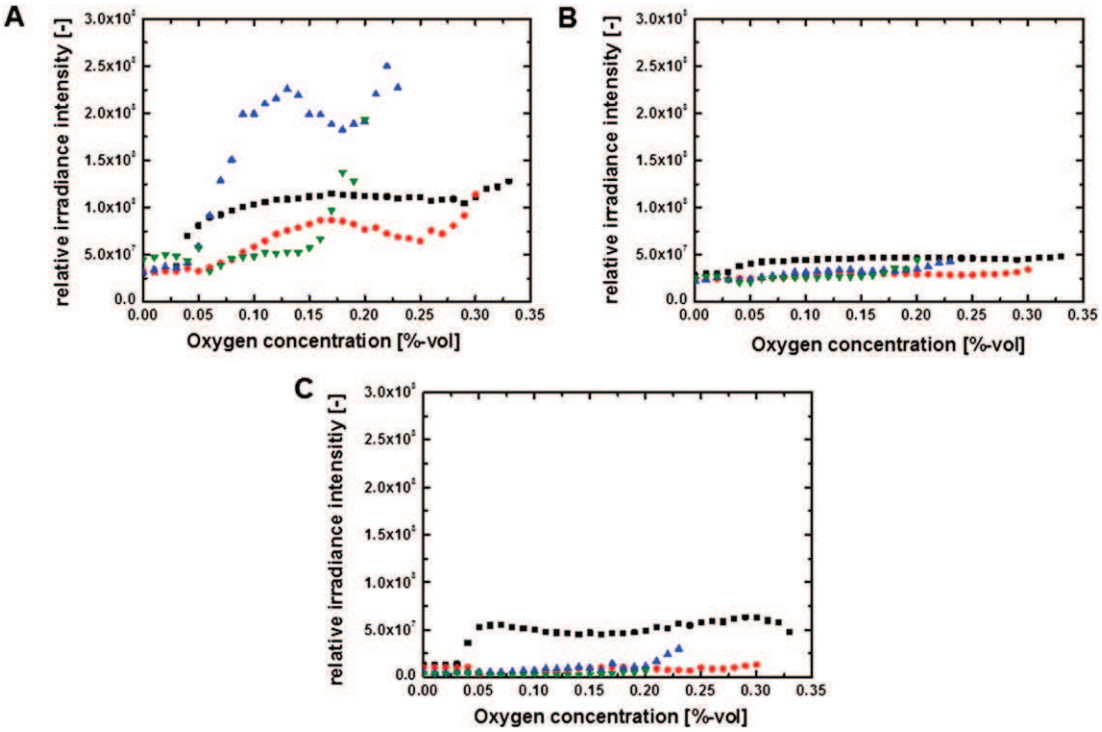

Fig. 1. Normalized relative irradiation intensity in dependence of different oxygen concentrations, measured at a distance of 15 mm from the nozzle outlet. Added amount of nitrogen: ■ 0% vol., ● 0.1% vol., ▲ 0.2% vol. and ▼ 0.3% vol. Relative irradiation intensity for wavelengths from A) 180 to 280 nm (UV-C-light), B) 280 to 400 nm (excited OH and N_2-species) and C) 773 to 783 nm (atomic oxygen emission).

3.2. Quantification of emitted UV light by test strips

Based on the optical emission spectroscopy three different process gas compositions namely: I) pure argon; II) argon + 0.135 vol.% oxygen and III) argon + 0.135 vol.% oxygen and 0.2% vol. nitrogen were used for a further evaluation of its antimicrobial potential and UV emission intensity. The emission spectra of these three gas compositions in the UV-C range and for the metastable singlet state of oxygen are shown in Fig. 2 for a distance of 15 mm from the nozzle tip.

Fig. 2A depicts, that the highest UV-C spectral intensity was emitted by a process gas composition of argon + 0.135 vol.% oxygen and 0.2 vol.% nitrogen. The pure argon radiated nearly no UV-C photons. This was also confirmed by the UV-test strips. The dosage of UV light was determined by coloration of the strips and enabled a calculation of the UV irradiance in mW cm^{-2} (Fig. 3). The UV irradiance intensity decreased exponentially with higher distance to the plasma nozzle outlet, similar to the measurements from Brandenburg et al. (2009). Further, the significant difference in the quantity of emitted UV-light between the three different gas compositions was confirmed. Argon with an admixture of 0.135 vol.% oxygen and 0.2 vol.% nitrogen irradiated 0.44 mW cm^{-2} in comparison to 0.11 mW cm^{-2} for pure argon at an axial distance of 10 mm to the nozzle outlet. The measured UV irradiance is in the same magnitude as reported by Brandenburg et al. (2009), who measured 0.08 mW cm^{-2} (10 mm axial distance) for argon with an admixture of 0.1 vol.% air, but in comparison 5.5 fold lower to our optimized plasma carrier gas composition. The plasma containing all three gases emitted 40 mJ cm^{-2} after 1.5 min at an axial distance of 10 mm or after 10 min at an axial distance of 15 mm, which exceeds the lethal

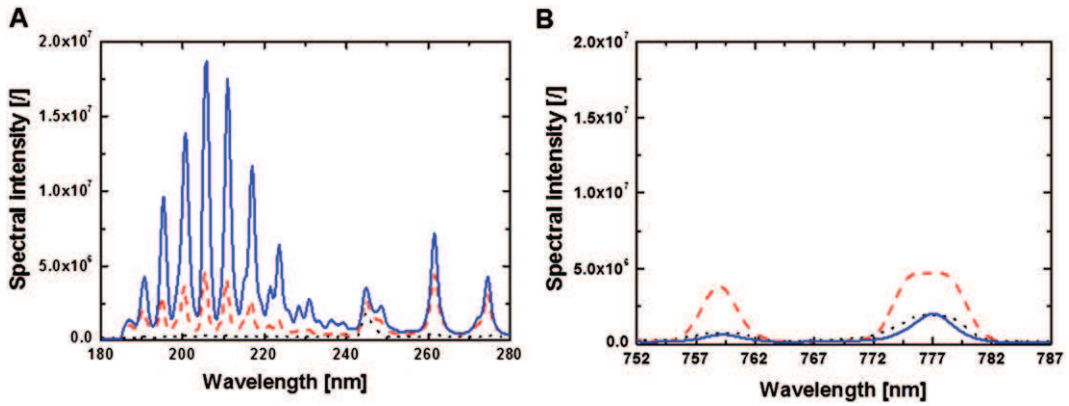

Fig. 2. Emission spectra measured at 15 mm distance from the jet tip for pure argon (dotted black line), argon + 0.135% vol. oxygen, (dashed red line) and argon + 0.135% vol. oxygen + 0.2% vol. nitrogen (solid blue line) for wavelengths from A) 180 to 280 nm (UV-C-light), B) 772 to 783 nm (atomic oxygen emission).

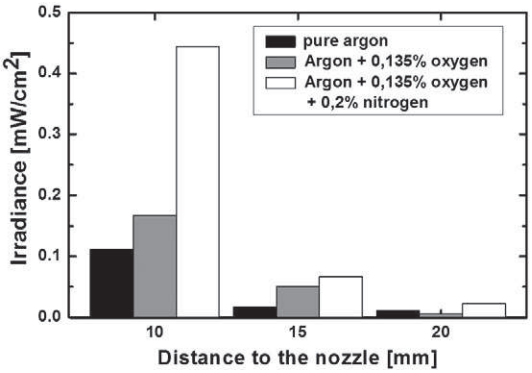

Fig. 3. UV irradiance measured with UV control strips at different distances to the nozzle outlet and process gas compositions.

dose of 36 mJ cm^{-2} needed for a 1 $\log_{10}$ *B. subtilis* spore inactivation (P. Setlow, 2007). However, the admixture of nitrogen and oxygen causes also slight instabilities in plasma discharge, resulting in weaker discharge filaments due to the quenching of argon metastable states and electron attachment (Brandenburg et al., 2009).

3.3. Effect of different carrier gas compositions on endospore inactivation

To investigate the effects of the three plasma carrier gas compositions glass petri-dishes were inoculated with *B. atrophaeus* and *B. subtilis* endospores and were exposed to the plasma at an axial distance of 15 mm to the nozzle, which was the closest distance without plasma induced spore abrasion. The results are shown in Fig. 4 and depict a higher resistance of the *B. subtilis* PS832 (wild-type) strain compared to *B. atrophaeus*. The highest inactivation efficiency showed pure argon as carrier gas with a 3.1 $\log_{10}$ reduction for *B. atrophaeus* and 2.4 $\log_{10}$ for *B. subtilis* after 5 min plasma exposure followed by argon + 0.135% vol. oxygen + 0.2% vol. nitrogen with 2.3 $\log_{10}$ reduction for *B. atrophaeus* and 2.2 $\log_{10}$ for *B. subtilis*. Hence, a 5 min treatment was sufficient for nearly all gas composition to reduce the total spore count close the statistical detection limit.

Further, all inactivation kinetics showed an accelerated initial inactivation, which leveled off in a tailing for longer treatment times. This inactivation behavior could be adequately described for all inactivation kinetics with a biphasic inactivation model.

The root mean sum of squared error (RMSE) values for each fit (Table 2) were in the ranges of the coefficients of variations of the spore counts, indicating that the biphasic model was well suited to represent the experimental data (Geeraerd, Valdramidis, & Van Impe, 2005). In most cases the total spore inactivation was close or even below the statistical reliable detection limit, which is also one explanation for a k_2 value of 0. The relatively small detection limits are attributed to the low initial inoculum, which was used to avoid the formation of several multilayers of spores or huge agglomerates. The k_1 values for *B. athropheus* and *B. subtilis* (Table 2), confirmed that the highest inactivation rate was archived by using pure argon and that *B. athropheus* showed a higher sensitivity towards the plasma treatment. This was not expected, due to the fact that this strain is a surrogate strain for chemical sterilization and sterilization by irradiation. However, variations in spore resistance could be attributed to several different factors and can vary tremendously between individual strains and species (Pedraza-Reyes, Ramírez-Ramírez, Vidales-Rodríguez, & Robleto, 2012).

The decreasing k_1 values for *B. atrophaeus* and *B. subtilis* also depict a change in the inactivation mechanism, which is also visible in Fig. 4. Whereas for pure argon as process gas, the first inactivation phase (described with k_1) lasts for 1 to 1.5 min this first phase is extended to 2 to 3 min for the process gas mixture argon + oxygen + nitrogen. Moisan, Barbeau, Moreau, Pelletier, Tabrizian and Yahia (2001) and Moisan, Barbeau and Pelletier (2001) proposed three main factors contributing to spore inactivation during a plasma exposure: I) UV irradiation of the DNA; II) intrinsic photodesorption and III) etching of organic molecules. Whereas the first rapid inactivation phase is attributed to the emitted UV-light in the plasma, the second (and some cases third) slower inactivation phase is caused by a combination of photodesorption and etching (Knorr et al., 2011). The pure argon

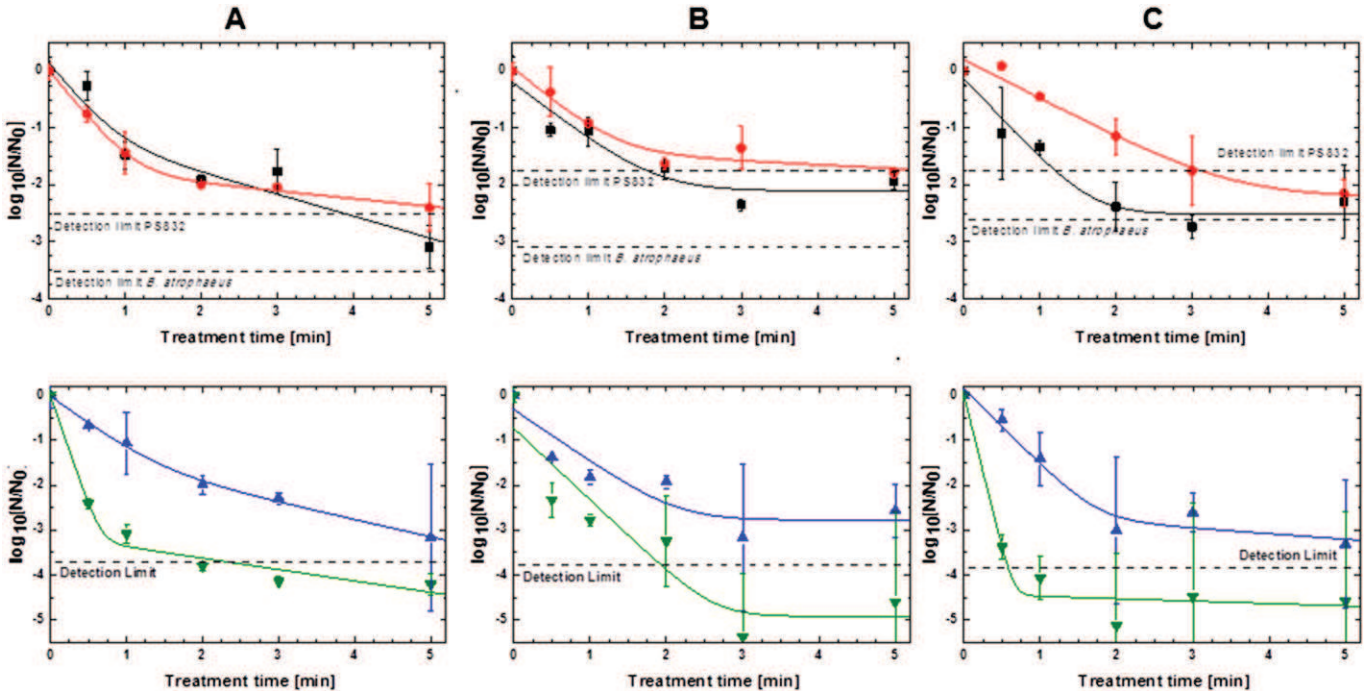

Fig. 4. Inactivation data for *Bacillus atrophaeus* endospores (■) and *Bacillus subtilis* PS832 (●), FB122 (▲) and PS578 (▼) endospores on glass discs at an axial distance of 15 mm from the nozzle in dependence of different carrier gas compositions: A) pure argon; B) argon + 0.135% vol. oxygen; and C) argon + 0.135% vol. oxygen + 0.2% vol. nitrogen. Dashed lines represent the statistical detection limit of each spore strain.

Table 2
Inactivation rate constants k_1 and k_2 for a biphasic fit of *Bacillus atrophaeus*, *Bacillus subtilis* (PS832—wild-type), FB122 and PS578 endospore inactivation and parameters for the goodness of fit (R^2 and RSME) for different carrier gas compositions.

Strain		Argon	Carrier gas composition	
			Argon + 0.135% vol. oxygen	Argon + 0.135% vol. oxygen + 0.2% vol. nitrogen
Bacillus atrophaeus	k_1 [−]	3.88	2.35	3.26
	k_2 [−]	0.89	0.00	0.00
	R^2	0.93	0.92	0.96
	RSME	0.47	0.38	0.33
Bacillus subtilis	k_1 [−]	3.81	2.63	1.58
PS832	k_2 [−]	0.31	0.16	0.00
	R^2	1.00	0.96	0.98
	RSME	0.06	0.23	0.22
Bacillus subtilis	k_1 [−]	2.96	2.78	3.91
FB122	k_2 [−]	0.89	0.00	0.29
	R^2	1.00	0.88	0.97
	RSME	0.11	0.61	0.38
Bacillus subtilis	k_1 [−]	11.29	3.67	15.67
PS578	k_2 [−]	0.58	0.00	0.12
	R^2	0.98	0.88	0.97
	RSME	0.33	1.04	0.52

plasma emitted the lowest amount of UV photons (Figs. 1– 3) in our study. Hence, the first period of inactivation was relatively short (Fig. 4a) and the second phase was prolonged. The higher total inactivation compared to the other two gas compositions tested, might be caused by higher amount of reactive nitrogen species (RNS) and ROS, especially hydroxyl radicals ($OH^{\bullet}$), in the pure argon plasma, which were quenched in the other process gas compositions.

However, some research groups claim that UV-light plays a minor role in the inactivation of microorganisms at atmospheric pressure (Laroussi, 2002, 2005; Laroussi & Leipold, 2004; Moisan, Barbeau, Moreau, Pelletier, Tabrizian et al., 2001; Pointu et al., 2005). To assess the impact of UV-light on spore inactivation in the first inactivation phase, we tested the sporicidal effect of all three gas combinations on isogenic mutant strains of *B. subtilis* PS832 with reduced UV-resistance.

3.4. Effect of different process gas compositions on UV sensitive isogenic mutant spore strains

The tested spore strain FB122 is unable to synthesize DPA during the sporulation and the strain PS578 lacks the genes encoding the spore's two major SASPs of which both DPA and SASP contribute to spore UV resistance (P. Setlow, 2007). Accordingly, the strain PS578 showed a higher sensitivity to all plasma carrier gases compared to the wild-type *B. subtilis* strain (Fig. 4). After 2 min more than 4 $\log_{10}$ were inactivated, whereas the highest sporicidal effect had the gas composition argon + 0.135% vol. oxygen + 0.2% vol. nitrogen (Fig. 4c), which is the one with the highest UV-light emission. Further, for all gas compositions the inactivation of the strain PS578 was higher compared to the FB122 strain. This spore strain showed a similar inactivation behavior as the wild-type spore strain PS832, but an up to 0.9 $\log_{10}$ higher total inactivation for the gas composition with highest UV-C-light emission.

Again nearly all inactivation kinetics showed a biphasic inactivation behavior, which was adequately described to be the inactivation model proposed by Cerf (1977). The parameters for the goodness of fit as well as the inactivation rate constants are given in Table 2. The nearly similar resistance towards the different plasma exposures of the strains FB122 and PS832 is also visible in the rate constants k_1 and k_2 (Table 2). However, a significant difference for k_1 was found for the process gas composition with the highest UV emission (Fig. 4c), pointing towards a sporicidal effect of the emitted UV-light. Nicholson, Munakata, Horneck, Melosh, and Setlow (2000) and Douki et al. (2005) reported a protective effect of DPA as a part of the spore photoproduct formation in the spore core and the protection of the DNA from UV damage. However, Setlow, Atluri, Kitchel, Koziol-Dube, and Setlow (2006) tested the UV resistance of the strain FB122 and compared it to the behavior of wild-type *B. subtilis* spores and concluded that DPA-less FB122 spores exhibited similar UV resistance but had lower resistance to wet heat, dry heat, hydrogen peroxide, and desiccation.

The inactivation of the strain PS578 differed significantly from the two other tested *B. subtilis* strains. Whereas the k_2 values for all strains are similar, the k_1 values are much higher. For all tested process gases more than 2 $\log_{10}$ were inactivated in 0.5 min with the highest inactivation rate for the argon with an admixture of oxygen and nitrogen (3.3 $\log_{10}$ after 0.5 min). The admixture of 0.135% oxygen to the argon gas (Fig. 4b) showed the lowest inactivation capacity. Whereas the amount of emitted UV-light is higher (shift from phase one to phase two of the inactivation after 2.5 min) for this gas composition compared to pure argon, ROS, RNS and other metastable species in the plasma gas might be quenched, resulting in a lower total sporicidal effect. However, the impact of emitted UV-light from the plasma is clearly visible. The strain PS578, in which α/β-type SASPs are absent, are especially sensitive towards UV-light exposure (Pedraza-Reyes et al., 2012). These proteins bind to and saturate the spore DNA (P. Setlow, 2007) and cause structural changes in the DNA and altering the DNA's photochemistry (Lee, Bumbaca, Kosman, Setlow, & Jedrzejas, 2008). Similar findings were also reported by Roth et al. (2010) who tested the resistance of a similar strain towards a vacuum dielectric barrier discharge (DBD) plasma exposure with nitrogen (80%) and oxygen (20%) as plasma gas and a high emission of vacuum UV (VUV) light. The highest resistance in this study showed the tested wild-type *B. subtilis* strain and the strongest inactivation was found for the α^- β^- mutant strain. The reason for this lower resistance was clearly attributed to lack of SASPs and its inability to protect the DNA, which denotes that the DNA is the primary target for spore inactivation by emitted VUV and UV-light from a plasma source.

Boudam et al. (2006) proposed for a DBD atmospheric pressure plasma source with nitrogen and nitrous oxide as process gas, that if the UV intensity is high enough spore inactivation is dominated by action of UV photons. In the absence of UV, the inactivation is controlled be the action of reactive species. However, in our study we showed that for an atmospheric pressure plasma jet, it is possible to adjust operating conditions in such a way to have plasma with high UV-light emission (argon + oxygen + nitrogen), high amounts of ROS and RNS (pure argon) or a plasma with medium amounts of UV-light and ROS and RNS (argon + oxygen). Moreover, we could show that in dependence of the used process gas composition, the pathway of spore inactivation and the inactivation rate can be influenced.

4. Conclusion

The systematic testing of argon as process gas with admixtures of oxygen (0 to 0.34 vol.%) and nitrogen (0 to 0.3 vol.%) enabled us to significantly enhance the amount of emitted UV-light from an atmospheric pressure plasma jet. For the selected system and under the tested conditions we identified that a process gas composition of argon, 0.135 vol.% oxygen and 0.2 vol.% nitrogen emitted four fold more UV photons than pure argon and more than all other tested gas compositions. The measured UV dosage of 0.44 mW cm^{-2} respectively 40 mJ cm^{-2} after 1.5 min at an axial distance of 10 mm exceeds the lethal dose needed for a rapid endospore spore inactivation.

The potential sporicidal effect of this plasma was confirmed by determining inactivation kinetics of *B. atrophaeus* and *B. subtilis* spores at a distance of 15 mm. All assessed inactivation kinetics showed a biphasic inactivation with extended initial inactivation phase with increasing UV emission from the plasma. However, compared to pure argon the process gas with the highest UV emission showed a similar sporicidal effect, presumably due to higher amount of ROS, RNS and metastable species in the pure argon plasma expanding into the surrounding atmosphere.

To distinguish lethal effects of UV-light and reactive species the *B. subtilis* spore strain FB122, which is unable to synthesize DPA during the sporulation and the strain PS578, which lacks the genes encoding the spore's two major SASPs, were exposed to plasmas with different UV-emission intensity. Both DPA and SASPs contribute to spore UV resistance, whereas the protective effect of DPA against UV photons from the tested plasma jet was less compared to the SASPs. The strain PS578 was inactivated by more than 2 $\log_{10}$ in 0.5 min for all tested process gases with the highest inactivation (3.3 $\log_{10}$) for the argon with an admixture of oxygen (0.135% vol.) and nitrogen (0.2% vol.). Hence, a significant impact of UV-light on spore inactivation was confirmed for a direct plasma treatment with an atmospheric plasma jet.

In conclusion, based on the process gas composition for an atmospheric pressure plasma jet the mode of inactivation of bacterial spores can be influenced. If the UV intensity is high enough spore inactivation is dominated by action of UV photons, in the absence of UV, the inactivation is controlled by the action of reactive and metastable species.

These findings could be useful for a potential application in the food industry, regardless if plasma should be used for the sanitization of a food surface or the cleaning of processing equipment. The biphasic nature of spore inactivation kinetics and the shown impact of UV-light on the progress of this kinetics suggest a two-step inactivation process. In a first step, a plasma with high UV-emission can inactivate spores on the top layer of aggregates or biofilms. In a second step the process gas composition used to run the plasma source is changed, to obtain a plasma with high contents of reactive and metastable species to enhance photodesorption and etching effects.

Acknowledgments

This research was funded by the research project “development of novel and advanced decontamination sustainable technologies for the production of high quality dried herbs and spices (GreenFooDec)”, which was financially supported by the European Commission within the 7th Framework Program (FP7-SME-2011-285838).

References

Boudam, M. K., Moisan, M., Saoudi, B., Popovici, C., Gherardi, N., & Massines, F. (2006). Bacterial spore inactivation by atmospheric-pressure plasmas in the presence or absence of UV photons as obtained with the same gas mixture. *Journal of Physics D: Applied Physics*, *39*, 3494–3507.

Brandenburg, R., Lange, H., von Woedtke, T., Stieber, M., Kindel, E., Ehlbeck, J., et al. (2009). Antimicrobial effects of UV and VUV radiation of nonthermal plasma jets. *Ieee Transactions on Plasma Science*, *37*(6), 877–883.

Cerf, O. (1977). Tailing of survival curves of bacterial spores. *Journal of Applied Bacteriology*, *42*, 1–19.

Douki, T., Setlow, B., & Setlow, P. (2005). Photosensitization of DNA by dipicolinic acid, a major component of spores of *Bacillus* species. *Photochemical & Photobiological Sciences*, *4*(8), 591–597.

Faille, C., Benezech, T., Blel, W., Ronse, A., Ronse, G., Clarisse, M., et al. (2013). Role of mechanical vs. chemical action in the removal of adherent Bacillus spores during CIP procedures. *Food Microbiology*, *33*(2), 149–157.

Geeraerd, A. H., Valdramidis, V., & Van Impe, J. F. (2005). GInaFiT, a freeware tool to assess non-log-linear microbial survivor curves. *International Journal of Food Microbiology*, *102*(1), 95–105.

Genest, P. C., Setlow, B., Melly, E., & Setlow, P. (2002). Killing of spores of *Bacillus subtilis* by peroxynitrite appears to be caused by membrane damage. *Microbiology-Sgm*, *148*, 307–314.

Heise, M., Neff, W., Franken, O., Muranyi, P., & Wunderlich, J. (2004). Sterilization of polymer foils with dielectric barrier discharges at atmospheric pressure. *Plasmas and Polymers*, *9*(1), 23–33.

Keener, K. M. (2008). Atmospheric non-equilibrium plasma. *Encyclopedia of agricultural, food, and biological engineering*, *1–5*.

Knorr, D., Froehling, A., Jaeger, H., Reineke, K., Schlueter, O., & Schoessler, K. (2011). Emerging technologies in food processing. *Annual Review of Food Science and Technology*, *2*, 203–235.

Laroussi, M. (2002). Nonthermal decontamination of biological media by atmospheric-pressure plasmas: Review, analysis, and prospects. *Ieee Transactions on Plasma Science*, *30*(4), 1409–1415.

Laroussi, M. (2005). Low temperature plasma-based sterilization: Overview and state-of-the-art. *Plasma Processes and Polymers*, *2*(5), 391–400.

Laroussi, M., & Leipold, F. (2004). Evaluation of the roles of reactive species, heat, and UV radiation in the inactivation of bacterial cells by air plasmas at atmospheric pressure. *International Journal of Mass Spectrometry*, *233*(1–3), 81–86.

Lassen, K. S., Nordby, B., & Grun, R. (2005). The dependence of the sporicidal effects on the power and pressure of RF-generated plasma processes. *Journal of Biomedical Materials Research Part B: Applied Biomaterials*, *74B*(1), 553–559.

Lee, K. S., Bumbaca, D., Kosman, J., Setlow, P., & Jedrzejas, M. J. (2008). Structure of a protein–DNA complex essential for DNA protection in spores of *Bacillus* species. *Proceedings of the National Academy of Sciences of the United States of America*, *105*(8), 2806–2811.

Mckee, L. H. (1995). Microbial-contamination of spices and herbs—A review. *LWT - Food Science and Technology*, *28*(1), 1–11.

Moisan, M., Barbeau, J., Moreau, S., Pelletier, J., Tabrizian, M., & Yahia, L. H. (2001a). Low-temperature sterilization using gas plasmas: A review of the experiments and an analysis of the inactivation mechanisms. *International Journal of Pharmaceutics*, *226*(1–2), 1–21.

Moisan, M., Barbeau, J., & Pelletier, J. (2001b). Plasma sterilization—Methods and mechanisms. *Vide-Science Technique Et Applications*, *56*(299), 15–28.

Moreau, M., Orange, N., & Feuilloley, M. G. J. (2008). Non-thermal plasma technologies: New tools for bio-decontamination. *Biotechnology Advances*, *26*(6), 610–617.

Nicholson, W. L., Munakata, L., Horneck, G., Melosh, H. J., & Setlow, P. (2000). Resistance of *Bacillus* endospores to extreme terrestrial and extraterrestrial environments. *Microbiology and Molecular Biology Reviews*, *64*, 549–560.

Nicholson, W. L., & Setlow, P. (1990). Sporulation, germination and outgrowth. In C. R. Harwood, & S. M. Cutting (Eds.), *Molecular biological methods for Bacillus* (pp. 391–450). John Wiley & Sons.

Paidhungat, M., & Setlow, P. (2000). Role of Ger-proteins in nutrient and non-nutrient triggering of spore germination in *Bacillus subtilis*. *Journal of Bacteriology*, *182*(2513–2519).

Pedraza-Reyes, M., Ramírez-Ramírez, N., Vidales-Rodríguez, L. E., & Robleto, E. A. (2012). Mechanisms of bacterial spore survival. In E. Abel-Santos (Ed.), *Bacterial spores* (pp. 73–88). Norfolk, UK: Caister Academic Press.

Philip, N., Saoudi, B., Crevier, M. C., Moisan, M., Barbeau, J., & Pelletier, J. (2002). The respective roles of UV photons and oxygen atoms in plasma sterilization at reduced gas pressure: The case of N-2-O-2 mixtures. *Ieee Transactions on Plasma Science*, *30*(4), 1429–1436.

Pointu, A. M., Ricard, A., Dodet, N., Odic, E., Larbre, J., & Ganciu, M. (2005). Production of active species in N-2-O-2 flowing post-discharges at atmospheric pressure for sterilization. *Journal of Physics D: Applied Physics*, *38*(12), 1905–1909.

Roth, S., Feichtinger, J., & Hertel, C. (2010). Characterization of *Bacillus subtilis* spore inactivation in low-pressure, low-temperature gas plasma sterilization processes. *Journal of Applied Microbiology*, *108*(2), 521–531.

Sagoo, S. K., Little, C. L., Greenwood, M., Mithani, V., Grant, K. A., McLauchlin, J., et al. (2009). Assessment of the microbiological safety of dried spices and herbs from production and retail premises in the United Kingdom. *Food Microbiology*, *26*(1), 39–43.

Schlüter, O., Ehlbeck, J., Hertel, C., Habermeyer, M., Roth, A., Engel, K. H., et al. (2013). Opinion on the use of plasma processes for treatment of foods*. *Molecular Nutrition & Food Research*, *57*(5), 920–927.

Schnabel, U., Niquet, R., Krohmann, U., Winter, J., Schlueter, O., Weltmann, K. -D., et al. (2012). Decontamination of microbiologically contaminated specimen by direct and indirect plasma treatment. *Plasma Processes and Polymers*, *9*, 569–575.

Setlow, P. (2007). I will survive: DNA protection in bacterial spores. *Trends in Microbiology*, *15*, 172–180.

Setlow, B., Atluri, S., Kitchel, R., Koziol-Dube, K., & Setlow, P. (2006). Role of dipicolinic acid in resistance and stability of spores of *Bacillus subtilis* with or without DNA-protective alpha/beta-type small acid-soluble proteins. *Journal of Bacteriology*, *188*(11), 3740–3747.

Surowsky, B., Frohling, A., Gottschalk, N., Schluter, O., & Knorr, D. (2014). Impact of cold plasma on *Citrobacter freundii* in apple juice: Inactivation kinetics and mechanisms. *International Journal of Food Microbiology*, *174*, 63–71.

van Gils, C. A. J., Hofmann, S., Boekema, B. K. H. L., Brandenburg, R., & Bruggeman, P. J. (2013). Mechanisms of bacterial inactivation in the liquid phase induced by a remote RF cold atmospheric pressure plasma jet. *Journal of Physics D: Applied Physics*, *46*(17).

Vij, V., Ailes, E., Wolyniak, C., Angulo, F. J., & Klontz, K. C. (2006). Recalls of spices due to bacterial contamination monitored by the US Food and Drug Administration: The predominance of salmonellae. *Journal of Food Protection*, *69*(1), 233–237.

4. Impact of surface structure and feed gas composition on *Bacillus subtilis* endospore inactivation during direct plasma treatment

In: Frontiers in Microbiology: Microbial decontamination by novel technologies - Analytic approaches and mechanistic insights, 2015

Cite as:

Hertwig, C., Steins, V., Reineke, K., Rademacher, A., Klocke, M., Rauh, C., Schlüter, O., 2015. Impact of surface structure and feed gas composition on *Bacillus subtilis* endospore inactivation during direct plasma treatment. Front. Microbiol. 6:774.

doi: https://doi.org/10.3389/fmicb.2015.00774

frontiers in Microbiology

ORIGINAL RESEARCH
published: 06 August 2015
doi: 10.3389/fmicb.2015.00774

Impact of surface structure and feed gas composition on *Bacillus subtilis* endospore inactivation during direct plasma treatment

Christian Hertwig[1], Veronika Steins[2], Kai Reineke[1], Antje Rademacher[1], Michael Klocke[1], Cornelia Rauh[2] and Oliver Schlüter[1]**

[1] Leibniz Institute for Agricultural Engineering, Potsdam-Bornim, Germany, [2] Department of Food Biotechnology and Food Process Engineering, Berlin University of Technology, Berlin, Germany

OPEN ACCESS

Edited by:
Michael Gänzle, University of Alberta, Canada

Reviewed by:
Eva-Guadalupe Lizárraga-Paulín, Instituto Tecnológico y de Estudios Superiores de Monterrey Campus Estado de México, Mexico
Peter Setlow, University of Connecticut Health Center, USA

***Correspondence:**
Oliver Schlüter and Christian Hertwig, Leibniz Institute for Agricultural Engineering, Max-Eyth-Allee 100, 14469 Potsdam-Bornim, Germany
oschlueter@atb-potsdam.de; chertwig@atb-potsdam.de

Specialty section:
This article was submitted to Food Microbiology, a section of the journal Frontiers in Microbiology

Received: *17 April 2015*
Accepted: *14 July 2015*
Published: *06 August 2015*

Citation:
Hertwig C, Steins V, Reineke K, Rademacher A, Klocke M, Rauh C and Schlüter O (2015) Impact of surface structure and feed gas composition on Bacillus subtilis endospore inactivation during direct plasma treatment. Front. Microbiol. 6:774. doi: 10.3389/fmicb.2015.00774

This study investigated the inactivation efficiency of cold atmospheric pressure plasma treatment on *Bacillus subtilis* endospores dependent on the used feed gas composition and on the surface, the endospores were attached on. Glass petri-dishes, glass beads, and peppercorns were inoculated with the same endospore density and treated with a radio frequency plasma jet. Generated reactive species were detected using optical emission spectroscopy. A quantitative polymerase chain reaction (qPCR) based ratio detection system was established to monitor the DNA damage during the plasma treatment. Argon + 0.135% vol. oxygen + 0.2% vol. nitrogen as feed gas emitted the highest amounts of UV-C photons and considerable amount of reactive oxygen and nitrogen species. Plasma generated with argon + 0.135% vol. oxygen was characterized by the highest emission of reactive oxygen species (ROS), whereas the UV-C emission was negligible. The use of pure argon showed a negligible emission of UV photons and atomic oxygen, however, the emission of vacuum (V)UV photons was assumed. Similar maximum inactivation results were achieved for the three feed gas compositions. The surface structure had a significant impact on the inactivation efficiency of the plasma treatment. The maximum inactivation achieved was between 2.4 and 2.8 $\log_{10}$ on glass petri-dishes and 3.9 to 4.6 $\log_{10}$ on glass beads. The treatment of peppercorns resulted in an inactivation lower than 1.0 $\log_{10}$. qPCR results showed a significant DNA damage for all gas compositions. Pure argon showed the highest results for the DNA damage ratio values, followed by argon + 0.135% vol. oxygen + 0.2% vol. nitrogen. In case of argon + 0.135% vol. oxygen the inactivation seems to be dominated by the action of ROS. These findings indicate the significant role of VUV and UV photons in the inactivation process of *B. subtilis* endospores.

Keywords: cold plasma, spore inactivation, inactivation mechanism, DNA damage, qPCR

Introduction

In recent years, the application of cold atmospheric pressure plasma (CAPP) for the decontamination of food products, food packing material and/or food contact surfaces raised in attention (Pankaj et al., 2014; Schlüter and Fröhling, 2014). Plasma is in general an at least partially ionized gas, which contains charged particles such as ions and electrons as well as neutral

species such as atoms, molecules, and radicals, furthermore also UV photons. Depending on their thermodynamic properties plasmas can be classified as thermal and non-thermal plasmas (Schlüter et al., 2013).

Thermal plasmas are characterized by a local thermodynamic equilibrium between the electrons, ions and neutral species, whereby the temperature of the plasma can reach several 1000 kelvins under atmospheric pressure (Moreau et al., 2008). In non-thermal plasma, there is a significant difference between the electron temperature and the temperature of the charged particles and bulk gas. The electron temperature can reach several 1000 kelvins, whereas the bulk gas temperature can be closed to ambient. These so called "cold" plasmas can be directly applied also to thermal sensitive surfaces (Ehlbeck et al., 2011).

Under atmospheric condition cold plasmas can be generated using different set-ups, such as dielectric barrier discharges or plasma jet systems (Surowsky et al., 2014). Various studies showed already the antimicrobial potential of different CAPP applications (Niemira, 2012), whereby the different reactive species inside the plasma, neutral and charges particles, UV photons and also irradiated heat, are responsible for the antimicrobial effect of the plasma application (Laroussi, 2002; Moisan et al., 2002). The obtained composition of the generated plasma depends on the plasma source, feed gas and also on operation conditions, e.g., energy input (Weltmann et al., 2008; Ehlbeck et al., 2011; Reineke et al., 2015).

The potential of several cold plasma applications to inactivate different endospores on various matrices was shown in other studies already (Lassen et al., 2005; Boudam et al., 2006; Deng et al., 2006; Brandenburg et al., 2009; Kim et al., 2014; Hertwig et al., 2015a,b; Reineke et al., 2015). Nevertheless, the mechanisms leading to the inactivation of endospores are not clear and are still under investigations. The inactivation behavior of endospores by plasma treatment is often described by biphasic inactivation kinetics (Moreau et al., 2000; Brandenburg et al., 2009; Reineke et al., 2015). These biphasic inactivation kinetics probably indicate the involvement of different inactivation effects of the cold plasma, like the inactivation by DNA damage due to emitted UV photons and the decomposition of microorganisms through photodesorption and etching. Whereas photodesorption is a UV-induced erosion of the cell, where UV photons break chemical bonds and lead to the formation of volatile compounds. Etching, however, is the adsorption of reactive species on microorganisms, leading to chemical reaction and the formation of volatile compounds (Moisan et al., 2002).

The main subject of the ongoing controversy regarding the CAPP based inactivation of microorganisms is the role of the generated UV and vacuum (V)UV photons. UV and VUV photons are known to induce strand breaks and other damages in DNA in the cell. Furthermore UV photons with wavelength below 275 nm can break C–C or C–H bonds (Brandenburg et al., 2009) and hence affect protein and other macromolecules structures and functioning. Most of the published studies claim that under atmospheric conditions UV photons play only a minor role in the inactivation process (Laroussi and Leipold, 2004; Perni et al., 2007; Lu et al., 2008; Knorr et al., 2011), since major quantities of (V)UV photons are only emitted in low-pressure or vacuum plasma systems. Nevertheless, some groups showed that UV photons can dominate the inactivation process (Boudam et al., 2006; Reineke et al., 2015).

The structure of the contaminated surface has also a certain impact on the spore inactivation efficiency of the CAPP treatment, as rough surfaces with pits and cracks can hinder the inactivation of microorganisms (Surowsky et al., 2014). In most cases endospores were inoculated and plasma treated on smooth surfaces such as glass, polyethylene strips, polycarbonate membranes, or polymer foils (Heise et al., 2004; Deng et al., 2006; Brandenburg et al., 2009; Reineke et al., 2015). However, studies investigating the inactivation of endospores on different surfaces are scarce.

In this study the effect of different structured surfaces (glass petri-dishes, glass beads and peppercorns) concerning the inactivation of *Bacillus subtillis* endospores during CAPP treatment using a radio frequency plasma jet was investigated and to ensure comparable results all samples were inoculated with a similar endospore density. The selection of different surfaces, from a simple even glass surface via a spherical model (glass beads) to a real food matrix (peppercorns), in combination with an inoculation of comparable spore density enable a closer insight into the surface-related inactivation effect of *B. subtilis* endospores. The samples were treated using three different feed gas compositions, in order to vary the composition of the generated plasma and also the focus between the different involved mechanisms in endospore inactivation. Considering that the DNA play likely a considerable role during the inactivation process by CAPP, the quantification of DNA damage during the plasma exposure may help to closer understand the plasma based mechanisms responsible for the inactivation of endospores. Therefore a quantitative polymerase chain reaction (qPCR) based ratio detection system was established, which detected the degree of *B. subtilis* DNA damage during the CAPP treatment.

Materials and Methods

Bacillus subtilis Endospore Preparation

The endospore forming *B. subtilis* strain PS832 was used in this study. *B. subtilis* was sporulated using the method previously published by Nicholson and Setlow (1990). Sporulation was induced on 2x SG medium agar plates at 37°C without addition of antibiotics. After sporulation, the endospores were harvested with distilled water. The obtained suspension was washed and cleaned with cold distilled water by repeated centrifugation (threefold at 5000 *g*) and intermittently treated with ultrasonic (1 min). The cleaned endospore suspension contained ≥95% phase bright endospores and nearly no endospore agglomerates. The endospores were stored in the dark at 4°C, until needed.

Sample Preparation

In this study three different surfaces, such as glass petri-dishes (30 mm diameter), glass beads and whole black peppercorns

(*Piper nigrum*), were used. Peppercorns were purchased from JJ Albaracin (Murcia, Spain). To ensure comparable results between the different surfaces, all samples were inoculated with an endospore density of about $4*10^6$ endospores cm^{-2}, which is comparable to the native microbial load of black peppercorns (Hertwig et al., 2015a). Therefore, the surface of the peppercorns was measured using a particle analyzer PartAn 3001L (AnaTec GmbH, Duisburg, Germany). 1 g of peppercorns had a surface of 18.4 cm^2. The glass beads had a diameter of 5 mm. For the inoculation with *B. subtilis* endospores, 3.5 g of sterile peppercorns and 82 sterile glass beads, which had a similar surface of 64.4 cm^2, were placed into a sterile beaker and 175 µL stock endospore suspension was added. The beaker was placed on an automatic stirrer and shaken for 4 min at 400 rpm to obtain a homogenous coating of the microorganisms on the samples surface. The inoculated samples were placed under a clean bench for drying at room temperature for 30 min. Regarding the inoculation of the glass petri-dishes the stock endospore suspension was diluted 1:5 with ACES-buffer (pH 7). An aliquot of 300 µL diluted endospore suspension was mixed with 700 µL ethanol (96%). 35 µL of the ethanolic endospore suspension were spread on an area of 1.5 cm^2 of the glass petri-dishes.

Plasma Source and Plasma Treatment

The radio frequency (rf) plasma jet equipment used in this study was described elsewhere in detail (Brandenburg et al., 2007). The apparatus consists of a ceramic nozzle (nozzle tip diameter ∼7 mm) with a needle electrode inside, a grounded ring electrode at the nozzle outlet, an rf-generator and a gas supply system. The rf-voltage is coupled with the needle electrode. The plasma is generated at the tip of this electrode and expands into the air outside the nozzle with a length of up to 15 mm. Prior to plasma treatment, the atmospheric pressure plasma jet was let run at experimental conditions for 15 min to allow preheating and passivation of the electrodes. Argon with additional mixing of 0.2% vol. nitrogen and/or 0.135% vol. oxygen was used as feed gas with a gas flow of 10 standard liter per minute and an operation power of 30 W. 1 g inoculated peppercorns and 23 inoculated glass beads were placed in individual sterile glass petri-dishes (30 mm diameter) and placed on an automatic stirrer below the collimated plasma beam with a distance of 12 mm to the nozzle outlet. The peppercorns were treated up to 15 min, glass beads up to 10 min, respectively. The inoculated glass petri-dishes were also plasma treated with a distance of 12 mm to the nozzle outlet, up to 5 min. A direct contact between the plasma and the surface of the glass petri-dishes was avoided, to prevent the endospores from abrasion by the plasma filaments. All treatments were done at least in quadruplicate.

Optical Emission Spectroscopy

A Black Comet UV-VIS Spectrometer (StellarNet, Inc., Tampa, FL, USA) equipped with a F400 UV-VIS-SR fiber optic and a quartz lens was used to measure the emission spectrum of the direct CAPP set-up. The spectrum was measured in the range from 190 to 850 nm. The distance from the middle of the nozzle outlet to the middle of the lens was 10 mm in vertical and 12 mm in the horizontal axis. The spectrum was measured 10 times with an integration time of 100 ms. The average spectrum was baseline corrected and normalized (between $\lambda = 450$–470 nm) using a self-written LabVIEW routine.

Viable Cell Counts

After the plasma treatment, the viable cell count was determined by standard cell culture methods. Therefore, the glass petri-dishes were filled with 1 ml ACES-buffer and four sterile glass beads were added. The *B. subtilis* endospores were resuspended by continuously shaking (250 rpm) for 30 min. The recovery of the endospores from the peppercorns and glass beads was carried out by shaking the samples in 4 ml ACES-buffer for 3 min at 400 rpm. The obtained suspensions were serially diluted in ACES-buffer and every dilution was plated on nutrient agar plates (Carl Roth GmbH, Karlsruhe, Germany) in duplicates. The plates were incubated at 37°C and the colony forming units (cfu) were counted after 24 and 48 h. The obtained inactivation kinetics were modeled with GInaFiT (Geeraerd and Van Impe Inactivation Model Fitting Tool), a freeware applet for Microsoft Excel, using a biphasic inactivation model (Cerf, 1977). In this model, the relation between the survival and exposure time is given by following equation:

$$\log_{10} S(t) = \varphi \cdot e^{k_1 \cdot t} + (1 - \varphi) \cdot e^{k_2 \cdot t}$$

where S(t) is N(t)/N0, with N(t) as the number of colony forming units at the time t and N0 as the initial number of colony forming units. φ is the fraction of the initial population in a major population and (1-φ) is the fraction of the initial population in a minor population; k_1 and k_2 are the specific inactivation rates of the two populations.

Infrared Temperature Imaging

During the plasma treatments, the surface temperature of the glass petri-dishes, glass beads and peppercorns was recorded by an infrared camera (ThermaCam 500, Flir, Frankfurt am Main, Germany) in triplicates. The emissivity of the glass petri-dishes and glass beads was set to 0.94 and 0.96 for peppercorns (BARTEC Messtechnik und Sensorik, 2001). The camera was installed from above at a distance of 1 m to the plasma treated sample; infrared images were taken at a frequency of 1 Hz. To exclude thermal inactivation effect, *B. subtilis* endospores inoculated on the three used material were thermal treated at the highest peak temperature measured during the plasma treatment, according to the corresponding plasma treatment time. The samples were placed in a heating and drying oven UT 20 (Heareus Instruments GmbH, Hanau, Germany) and the surface temperatures of the samples were measured using fiberglass-encased K-type thermocouples connected with a USB data acquisition system (Personal Daq/56, SynoTECH, Hückelhofen, Germany) and DASYLab 13.0 software.

Determination of Endospore DNA Damage

A qPCR based ratio detection system (Bauer et al., 2004; Roth et al., 2010) was used to determine the degree of DNA

damage of the *B. subtilis* endospores after plasma treatment. The recovered endospore suspensions were pooled and collected by centrifugation (10 min; 10,000 *g*; 4°C). In case of the glass petri-dishes recovered endospore suspension of four replicates were pooled together. For chemical decoating, the pellet was suspended in 200 µL of 50 mmol L^{-1} Tris-HCl (pH 8.0), which contains 8 mol L^{-1} urea, 1% sodium dodecyl sulfate, 10 mmol L^{-1} EDTA and 50 mmol L^{-1} dithiothreitol. After 90 min incubation at 37°C, the decoated endospores were washed three times by repeated centrifugation (10 min; 10,000 *g*; 4°C) with cold, sterile water (Fairheadt et al., 1993). By suspending the endospores in 200 µL STE-buffer (150 mmol L^{-1} NaCl, 10 mmol L^{-1} Tris-HCl, pH 8.0; 10 mmol L^{-1} EDTA) containing 2 mg mL^{-1} lysozyme and incubating at 37°C for 60 min, the disruption of the endospores was accomplished. From the disrupted endospores, chromosomal DNA was purified using the High Pure PCR Template Preparation Kit (Roche, Penzberg, Germany). The concentration of the DNA was determined using a NanoDrop 3300 fluorospectrometer (Thermo Fisher Scientific, Inc., Waltham, MA, USA) applying the PicoGreen® dsDNA assay (Life Technologies GmbH, Darmstadt, Germany). The method used for the DNA damage determination was established by Roth et al. (2010) and optimized for the qPCR system used in this study. It can be assumed, that the plasma treatment causes randomly distributed defects along the DNA double strands, accordingly increases the probability of the detecting such defects with increasing length of the examined DNA fragment. Two PCR primer pairs Bs_dnaK855f (5′-CACAATGGGTCCTGTCCGTC-3′)/Bs_dnaK1254r (5′-AGACATTGGGCGCTCACCT-3′) and Bs_dnaK1154f (5′-ACACGACGATCCCAACAAGC-3′)/Bs_dna K1254r were used to amplify a 400 bp reporter and an internal 101 bp fragment from the *dna*K locus. The 101 bp fragment was used as an internal standard. Both fragments were amplified on a CFX96 Touch™ real-time PCR detection system (Bio-Rad Laboratories GmbH, München, Germany) in separate 20 µL volume reactions, each in triplicates. Per reaction 10 µL SYBR Green reagent (Quiagen, Hilden, Germany), 0.2 µmol L^{-1} of each primer and 0.10–0.15 ng templates DNA was used.

A 10-fold dilution series of a *B. subtilis* PS832 plasmid including the target fragment were used as an external standard and to determine the absolute copy number. The plasma treatment may cause cross-links between the DNA and other endospore components, thus influencing the quality and efficiency of DNA extraction and also unpredictably affecting the detection of the target fragments by PCR (Roth et al., 2010). The applied qPCR based ratio detection system (Roth et al., 2010) take this into account, whereby the target fragment copy numbers cn_{400} were normalized to those of the internal 101 bp fragment cn_{101}. Thus, the degree of DNA damage was expressed as a ratio (CN) between the detected 400 and 101 bp fragment copy numbers. For non-degraded DNA is the resulting ratio equal to 1 and decreases with increasing degrees of DNA damage. This ratio detection system can only be used for qualitative evaluation, because the correlation between actual degree of DNA damage and the ratio is unknown. This method allows the detection of various DNA damages like double or single strand breaks and thymidine dimers (Roth et al., 2010).

Results

Surface Temperature during CAPP Treatment

The average surface temperatures measured during the CAPP treatment are shown in **Table 1**. The CAPP treatment of glass beads leads to maximum local temperatures up to 90.1°C, the ones for the glass petri-dishes and peppercorns were slightly lower. The average surface temperature measured directly after the treatment was in the range of 56.9–75.2°C. Considering the measured surface temperatures, this CAPP application cannot be classified as a non-thermal treatment. To exclude thermal inactivation effects *B. subtilis* endospores inoculated on the three different sample types were thermal treated at 90°C in a heat and drying oven, according to the maximum CAPP treatment time. The thermal treatment resulted in no considerable inactivation; only for glass beads an inactivation of 0.2 $\log_{10}$ was obtained. However, the temperatures during the CAPP treatment may support the inactivation; nevertheless this effect should be comparable on the different treated surfaces due to the similar maximum local temperatures.

Characterization of Reactive Plasma Species

Three different feed gas compositions (1. pure argon, 2. argon + 0.135% vol. oxygen and 3. argon + 0.135% vol. oxygen + 0.2% vol. nitrogen) were used for detailed investigation of the involved inactivation mechanisms. Reineke et al. (2015) systematically investigated the emission intensity of argon plasma with the admixture of different oxygen and nitrogen concentration and showed that plasma running with argon + 0.135% vol. oxygen emitted a high amount of reactive oxygen species (ROS), whereas plasma running with argon + 0.135% vol. oxygen + 0.2% vol. nitrogen was characterized by the highest emission of UV-C photons. The emission spectra of the used plasmas, generated with the chosen gas compositions, are shown in **Figure 1**. The addition of oxygen and nitrogen causes significant changes in the emission spectra. In case of pure argon, molecular bands of oxygen, nitrogen, and other species were also detected due to interactions of the argon plasma with the surrounding air. The use of argon + 0.135% vol. oxygen + 0.2% vol. nitrogen resulted in considerable emission in the UV-C range (**Figure 1A**), whereas

TABLE 1 | Mean surface temperatures (±SD) before and after CAPP treatment.

	Starting temperature [°C]	Temperature after CAPP treatment [°C]	Maximum temperature during CAPP treatment [°C]
Glass petri-dishes	29.8 (±3.5)	56.9 (±1.0)	82.3 (±2.3)
Glass beads	27.7 (±0.4)	75.2 (±1.3)	90.1 (±0.2)
Peppercorns	28.3 (±1.7)	63.8 (±4.2)	88.3 (±0.6)

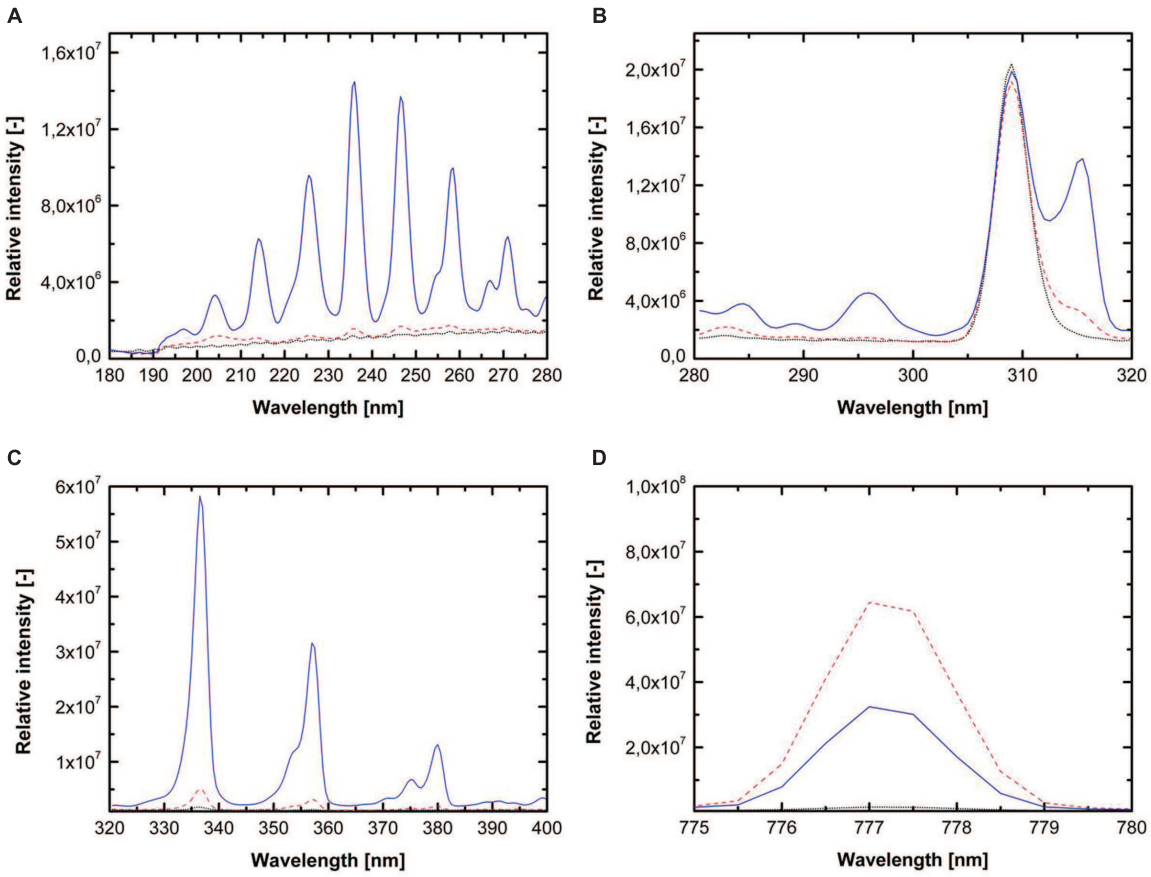

FIGURE 1 | Emission spectra for pure argon (dotted black line), argon + 0.135% vol. oxygen (dashed red line) and argon + 0.135% vol. oxygen + 0.2% vol. nitrogen (solid blue line) for wavelength from (A) 180–280 nm (UV-C light), (B) 280–320 nm (UV-B light), (C) 320–400 nm (UV-A light), and (D) 775–780 nm (atomic oxygen emission).

the emission of UV-C photons was negligible for the two other feed gas compositions. **Figure 1B** shows the emission intensity of the UV-B range, which was dominated by the signal of OH radicals with the maximum of 309 nm. The addition of oxygen and nitrogen resulted in no significant changes in the emission intensity of OH radicals. The emission spectrum from 320 to 400 nm (UV-A, **Figure 1C**) is dominated by molecular bands of the second positive system of N_2. The emissions for pure argon and argon + 0.135% vol. oxygen were negligible comparing to the use of argon + 0.135% vol. oxygen + 0.2% vol. nitrogen. **Figure 1D** shows the emission intensity from 775 to 780 nm, this wavelength range is characterized by the atomic oxygen band at 777 nm, and depicts considerable variations depending on the gas composition. The feed gas composition argon + 0.135% vol. oxygen emitted the highest photon intensity.

Effect of Feed Gas Composition and Surface Structure on the Inactivation of *B. subtilis* Endospores

To ensure comparable results between the three surfaces, all samples were inoculated with equal endospore densities of *B. subtilis* endospores. The obtained inactivation data were modeled using a biphasic inactivation model, which adequately described the inactivation behavior (**Table 2**). The resulting inactivation kinetics are shown in **Figure 2**. All inactivation kinetics showed an accelerated initial followed by a retarded inactivation for longer plasma exposure times, which can be also seen by inactivation rate constants (k). In general the k_1 (first inactivation phase) were higher than the k_2 (second inactivation phase) values. For each treated surface, the achieved maximum inactivation levels were relatively close together independent of the used feed gas composition. Nevertheless, the use of pure argon as feed gas for all three different surfaces resulted in the highest inactivation level, whereas the lowest inactivation was achieved by CAPP running with argon + 0.135% vol. oxygen in all cases.

In contrast to the feed gas composition, the treated surface had a tremendous impact on the inactivation efficiency of the CAPP plasma treatment. On the glass petri-dishes, the use of pure argon as feed gas for 5 min inactivated (**Figure 2A**) 2.7 $\log_{10}$ *B. subtilis* endospores, whereas the use of the second and third gas composition resulted in an inactivation of 2.2 and 2.5 $\log_{10}$, respectively. In contrast, the CAPP treatment of glass beads resulted in significantly higher maximum inactivation levels of

about 2 $\log_{10}$ (**Figure 2B**). CAPP generated by pure argon achieved an inactivation after 10 min treatment of 4.7 $\log_{10}$, followed by argon + 0.135% vol. oxygen + 0.2% vol. nitrogen with 4.5 $\log_{10}$ and argon + 0.135% vol. oxygen with 4.2 $\log_{10}$. The higher endospore inactivation after the CAPP treatment of glass beads cannot only be explained with the longer treatment time compared to the glass petri-dishes, because the inactivation obtained after a 4 min treatment were already higher than the maximum inactivation of the glass petri-dishes, i.e., 3.7, 3.5, and 4.0 $\log_{10}$ for the three feed gas compositions. The CAPP treatment of peppercorns resulted for all three used gas compositions in an inactivation less than 1.0 $\log_{10}$ after 15 min.

Endospore DNA Damage caused by Different Feed Gas Compositions

In case of CAPP treated peppercorns no assessment of DNA damage was conducted. Peppercorns are often highly spoiled with microorganisms. Even though they can be sterilized, the DNA material of the native microbial load is still present on the peppercorns surface and would falsify the results. For a better comparison between the inactivation and DNA damage ratio, only inactivation data of samples, which were also used for the analyzing of the DNA damage, were considered for the depiction of the inactivation behavior. Thus the inactivation kinetics shown in **Figures 3** and **4** may differ slightly from those shown in **Figure 2**. The DNA damage ratio values were also modeled using the biphasic equation (Cerf, 1977) to investigate if the damage of the *B. subtilis* DNA during the CAPP showed a similar course as the corresponding inactivation kinetics. Furthermore, the point of inflection (PI) of the biphasic kinetics (inactivation and DNA damage) was calculated, which describe the transition between the first and the second phase and can be calculated as the point of intersection between the two linear phases.

The results for the DNA damage of *B. subtilis* endospores on glass petri-dishes are depicted in **Table 3** and **Figure 3**. The maximum DNA damage ratio correlates with the corresponding maximum inactivation level. Comparing to the inactivation kinetics not all DNA damage kinetics could be adequately described using the biphasic model, with an accelerated initial DNA damage followed by a retarded damage of DNA. The use of pure argon resulted in the highest inactivation of 2.8 $\log_{10}$ and also in the highest DNA damage with a ratio of 0.51. The shift from the accelerated first inactivation phase to the second one was at 1.9 min, whereas the shift between these phases was already at 0.1 min for DNA damage kinetic. Plasma running with argon + 0.135% vol. oxygen + 0.2% vol. nitrogen achieved after 5 min treatment an inactivation and DNA damage ratio value of 2.5 $\log_{10}$ and 0.57, respectively. The DNA damage showed a linear behavior, because k_1 and k_2 had the same value. The shift to the second inactivation phase was after 0.4 min. Argon + 0.135% vol. oxygen as a feed gas composition inactivated up to 2.4 $\log_{10}$ endospores and the resulting DNA damage ratio was the highest with 0.63. For DNA damage kinetic no point of inflection could be calculated, since φ was smaller than 0.5. The shift between the two inactivation phases was at about 1.0 min.

TABLE 2 | Statistical parameters and the corresponding standard error (in brackets) of the biphasic model obtained from GInaFit.

	Pure argon				Argon + 0.135% vol. oxygen				Argon + 0.135% vol. oxygen + 0.2% vol. nitrogen			
	Adj. R^2	φ [–]	k_1 [min^{-1}]	k_2 [min^{-1}]	Adj. R^2	φ [–]	k_1 [min^{-1}]	k_2 [min^{-1}]	Adj. R^2	φ [–]	k_1 [min^{-1}]	k_2 [min^{-1}]
Glass petri-dishes	1.00	0.93 (0.03)	2.54 (0.34)	0.71 (0.11)	0.98	0.86 (0.07)	3.28 (0.94)	0.62 (0.12)	0.99	0.77 (0.08)	3.85 (1.24)	0.87 (0.09)
Glass beads	0.99	1.00 (0.00)	4.15 (0.51)	0.42 (0.07)	0.99	1.00 (0.00)	4.04 (0.55)	0.32 (0.09)	1.00	1.00 (0.00)	4.48 (0.29)	0.19 (0.06)
Peppercorns	0.93	0.68 (0.12)	0.82 (0.43)	0.06 (0.03	0.96	0.76 (0.27)	0.29 (0.16)	0.01 (0.07)	0.98	0.76 (0.04)	0.64 (0.12)	0.02 (0.02)

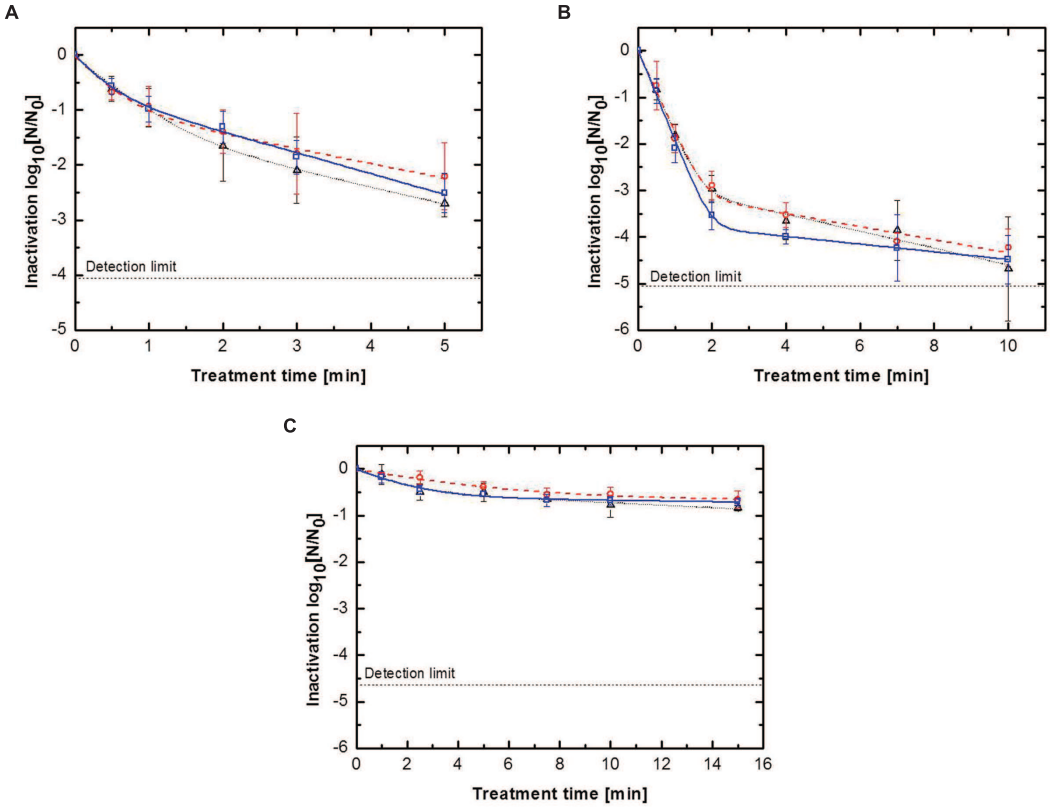

FIGURE 2 | Inactivation kinetics for *Bacillus subtilis* endospores for (△) pure argon, (◯) argon + 0.135% vol. oxygen, (□) argon + 0.135% vol. oxygen + 0.2% vol. nitrogen inoculated on: (A) glass petri-dishes, (B) glass beads and (C) peppercorns, with biphasic fit.

As above mentioned, the inactivation efficiency of CAPP for the treatment of *B. subtilis* endospores on glass beads was significant higher than on the glass petri-dishes. The maximum DNA damage was also significant higher, indicated by ratio values between 0.46 and 0.25 (**Figure 4**). All DNA damage kinetics could be adequately described using the biphasic model (**Table 4**). CAPP generated with pure argon achieved again the highest inactivation level after 10 min with 4.6 $\log_{10}$, followed by the third and second gas composition with 4.0 and 3.9 $\log_{10}$ (**Figure 4**), respectively. The points of inflection for the biphasic inactivation kinetics of pure argon and argon + 0.135% vol. oxygen were relatively close together at 1.2 and 1.3 min. The accelerated first inactivation phase of argon + 0.135% vol. oxygen + 0.2% vol. nitrogen lasted until 1.9 min. The maximum values for the DNA damage showed the same trend as the maximum inactivation values. Pure argon had a ratio value of 0.25. The ones for the other two feed gas composition were considerably higher, 0.46 for argon + 0.135% vol. oxygen and 0.41 for argon + 0.135% vol. oxygen + 0.2% vol. nitrogen. No point of inflection could be calculated for the use of argon + 0.135% vol. oxygen, because φ was again smaller than 0.5. For pure argon, the shift of the two phases was already at 0.2 min, whereas the shift for the third gas composition was at 1.0 min.

Discussion

To study the inactivation mechanisms of CAPP on endospores, *B. subtilis* endospores inoculated on different surfaces were plasma treated using three different feed gas compositions. CAPP treatment is usually described as a non-thermal process, however, during the experiment in this study peak temperatures up to 90°C were reached (**Table 1**). However, a strong thermal inactivation effect on the *B. subtilis* endospores during the CAPP treatment could not be detected in this study. The three different used gas compositions were characterized by their different emission spectra. Plasma generated by pure argon showed less emission in the UV range and of atomic oxygen than the other used feed gas compositions. The use of argon + 0.135% vol. oxygen leads to a strong emission of atomic oxygen; however, the emission in the UV range was also negligible. Plasma running with argon + 0.135% vol. oxygen + 0.2% vol. nitrogen showed a significant emission in the UV-C range, furthermore it emitted also an significant amount of reactive oxygen and nitrogen species (RNS). The emission of OH radicals reached for all three gas compositions the same range. Reineke et al. (2015) showed similar results for the emission intensities of the three used gas composition. They reported a fourfold higher UV emission by plasma running with argon + 0.135% vol. oxygen + 0.2% vol. nitrogen compared

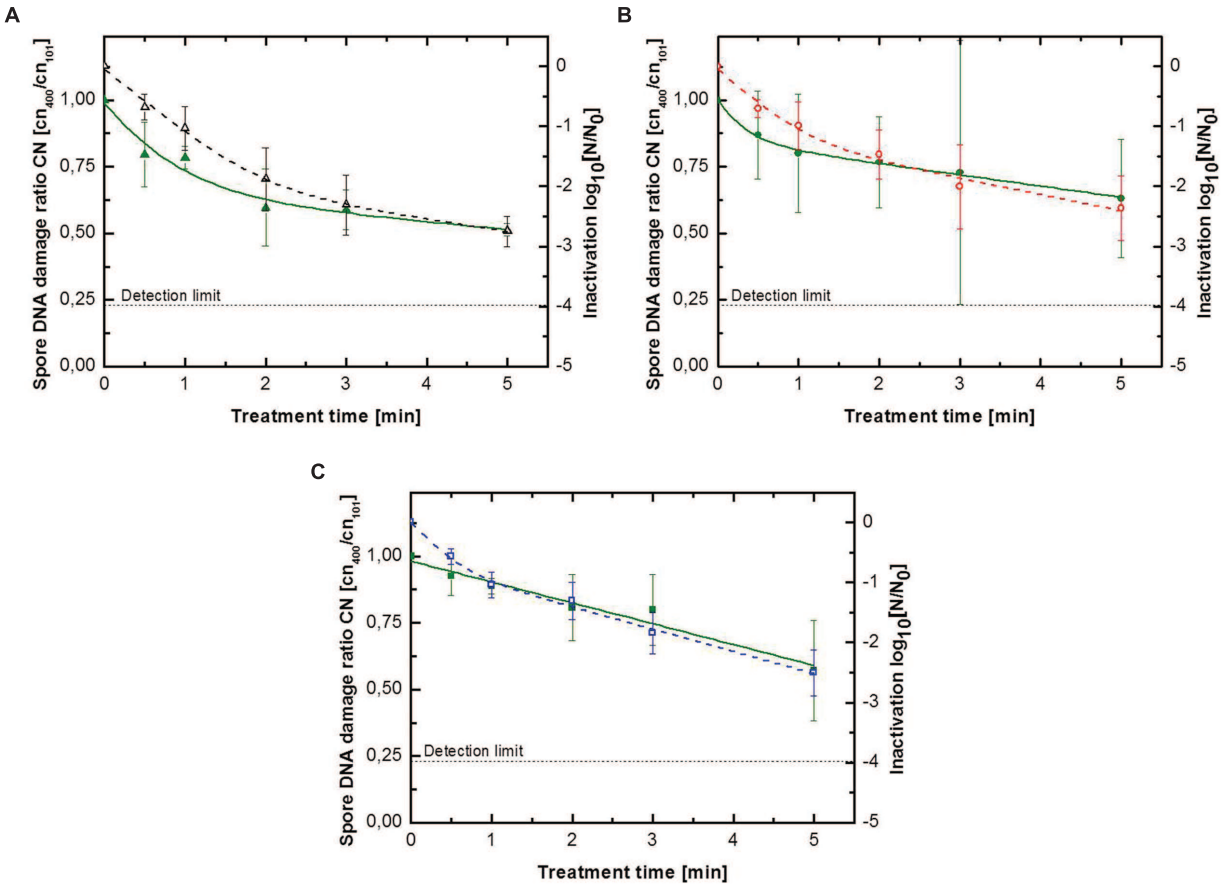

FIGURE 3 | Kinetics for *B. subtilis* endospores inoculated on glass petri-dishes for (A) pure argon with (△) inactivation and (▲)endospore DNA damage ratio, (B) argon + 0.135% vol. oxygen with (○) inactivation and (●)endospore DNA damage ratio, (C) argon + 0.135% vol. oxygen + 0.2% vol. nitrogen with (□) inactivation and (■) endospore DNA damage ratio. Solid lines represent the biphasic fit for the DNA damage and the dashed lines for endospore inactivation.

to the use of pure argon. Furthermore they also showed that the admixture of oxygen leads to an enhanced atomic oxygen emission. Regarding their different spectral intensities (**Figure 1**), different inactivation efficiencies could be expected and also different inactivation mechanisms.

In general the inactivation of endospores by CAPP treatment can be attributed to three different main mechanisms: (1) DNA damage due to UV photons, (2) intrinsic photodesorption, and (3) etching of organic molecules (Moisan et al., 2001). In case of plasma generated with argon + 0.135% vol. oxygen, which emitted the highest amount of ROS, the inactivation process should be dominated by the oxidation potential of the different ROS, namely OH radicals and atomic oxygen. In comparison, using plasma generated by argon + 0.135% vol. oxygen + 0.2% vol. nitrogen the inactivation process should be dominated by the damage of endospores DNA. A factor, which could contribute to the inactivation process are VUV photons, which can effectively inactivate *B. subtilis* endospores (Munakata et al., 1991). Argon driven plasma jets are well known to emit a certain amount of VUV light, dominated by argon excimer Ar^*_2 with an intensity maximum at $\lambda = 126$ nm (Brandenburg et al., 2009; Ehlbeck et al., 2011). Brandenburg et al. (2009) characterized the VUV emission of an identically constructed argon driven plasma jet and showed that the absolute radiance in the VUV range (115–200 nm) did not change substantially up to a distance of 10 mm to the nozzle outlet and the irradiance at that distance can be estimated with about 2 Mw cm^{-2}. However, the emission of VUV photons could not be measured with the spectrometer used in this study.

The results depicted in **Figure 2** indicated that the inactivation efficiency is almost independent of the used feed gas composition. On all three CAPP treated surfaces the maximum achieved inactivation of the different gas compositions was relatively similar. In contrast, the treated surface had a significant impact on the inactivation efficiency of the CAPP treatment. All different surfaces were inoculated with a similar endospore density of about $4*10^6$ endospores cm^{-2} to ensure comparable results. Nevertheless, the distribution of the endospores on the surface can be different and can influence the inactivation efficiency of the plasma treatment. The significant lower inactivation of endospores on peppercorns can be explained by the structured and uneven surface. The surface of peppercorns is characterized

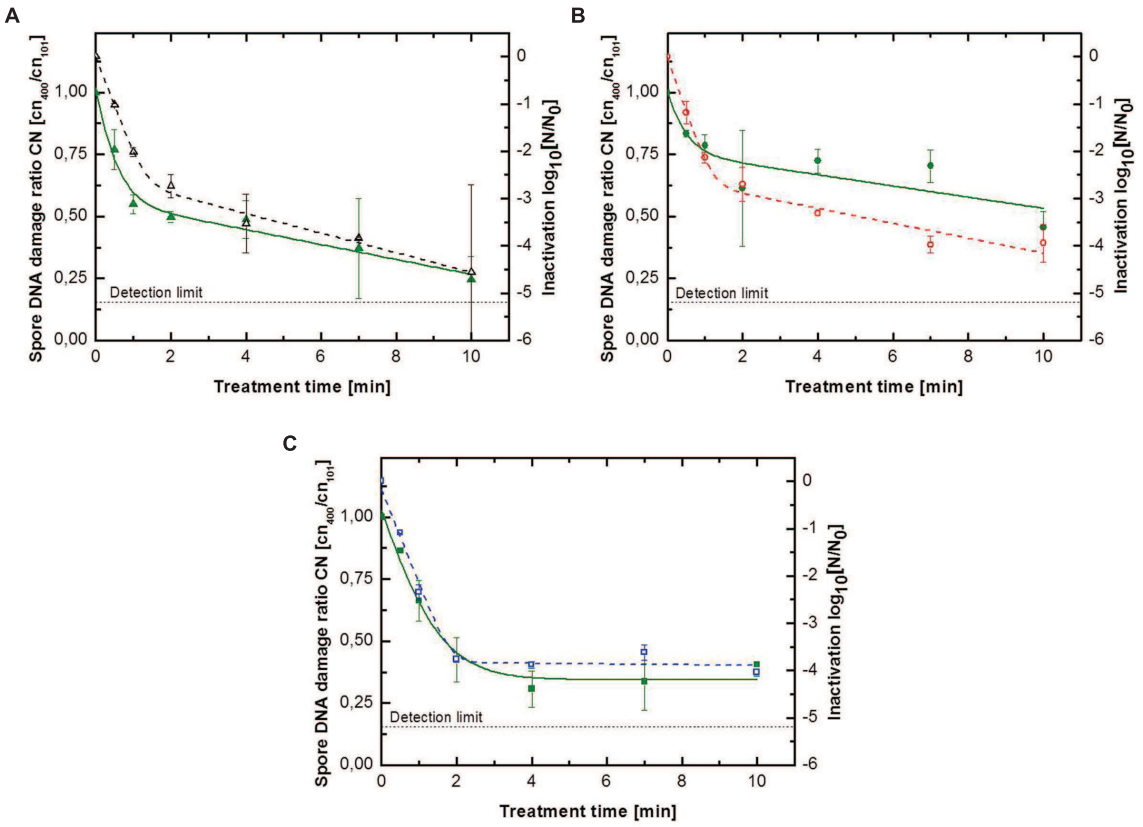

FIGURE 4 | Kinetics for *B. subtilis* endospores inoculated on glass beads for (A) pure argon with (△) inactivation and (▲)endospore DNA damage ratio, (B) argon + 0.135% vol. oxygen with (○) inactivation and (●)endospore DNA damage ratio, (C) argon + 0.135% vol. oxygen + 0.2% vol. nitrogen with (□) inactivation and (■) endospore DNA damage ratio. Solid lines represent the biphasic fit for the DNA damage and the dashed lines for endospore inactivation.

by cracks, grooves, and pits (Hertwig et al., 2015b) and cause probably shadow effects, for the emitted (V)UV photons, reactive species and charged particles, which reduce the efficiency of the CAPP treatment.

As described above, the higher endospore inactivation for the treatment of glass beads compared to the maximum achieved inactivation on glass petri-dishes cannot only be explained with the longer treatment time. The distribution of the inoculated *B. subtilis* endospores is presumably more homogenous on glass beads than on glass petri-dishes. The endospore inoculation on the petri-dishes causes probably the formation of agglomerates on the outer edge of the endospore suspension drop. Since the penetration depth of the (V)UV photons and reactive species is restricted to a few nm, the CAPP treatment would only effect the top layer of aggregated endospores (Hertwig et al., 2015b). Noticeable is that plasma generated by pure argon, which had the lowest emission of UV photons and other reactive species, achieved on all three treated surfaces the highest inactivation. The feed gas composition argon + 0.135% vol. oxygen + 0.2% vol. nitrogen, which emitted the highest amount of UV-C photons and considerable amounts of ROS and RNS, showed on all surfaces the second highest inactivation.

Reineke et al. (2015) reported similar results for the inactivation of *B. subtilis* endospores on glass petri-dishes and showed that the use of pure argon and argon + 0.135% vol. oxygen + 0.2% vol. nitrogen for the generation of plasma resulted in a similar inactivation efficiency after a treatment of 5 min. All inactivation kinetics showed a biphasic behavior, with an accelerated first inactivation phase and a slower second one, k_1 values were always higher than the k_2 values (**Table 2**). The biphasic inactivation curves pointed toward different inactivation mechanisms which may be involved during the treatment. Whereas the fast inactivation during the first phase can be attributed to the emitted (V)UV photons, which cause DNA damage, the slower inactivation during the second phase is presumably caused by a combination of DNA damage, photodesorption and etching (Knorr et al., 2011).

Reineke et al. (2015) treated UV-sensitive *B. subtilis* endospore mutant strains, FB122 and PS578, using plasmas with different UV-emission intensities and showed the significant impact of UV photons on the first inactivation phase. The strain FB122 is unable to synthesize DPA during the sporulation; whereas the strain PS578 lacks the genes encoding the spore's two major SASPs. Both DPA and SASPs contribute to the UV resistance

TABLE 3 | Statistical parameters and the corresponding standard error (in brackets) of biphasic model obtained regarding the inactivation and DNA damage of *B. subtilis* endospores inoculated on glass petri-dishes.

	Pure argon					Argon + 0.135% vol. oxygen					Argon + 0.135% vol. oxygen + 0.2% vol. nitrogen				
	Adj. R^2	φ [–]	k_1 [min^{-1}]	k_2 [min^{-1}]	PI [min]	Adj. R^2	φ [–]	k_1 [min^{-1}]	k_2 [min^{-1}]	PI [min]	Adj. R^2	φ [–]	k_1 [min^{-1}]	k_2 [min^{-1}]	PI [min]
Inactivation kinetic	0.99	0.98 (0.01)	2.52 (0.32)	0.48 (0.16)	1.9	0.97	0.90 (0.07)	2.92 (0.99)	0.62 (0.19)	1.0	0.99	0.79 (0.09)	4.02 (1.41)	0.85 (0.10)	0.4
DNA damage ratio kinetic	0.92	0.54 (0.16)	1.46 (0.92)	0.06 (0.09)	0.1	0.99	0.30 (0.04)	3.18 (1.05)	0.10 (0.01)	–	0.91	0.97 (8.0E+14)	0.18 (–)	0.18 (–)	–

Table 4 | Statistical parameters and the corresponding standard error in brackets of biphasic model obtained regarding the inactivation and DNA damage of *B. subtilis* endospores inoculated on glass beads.

	Pure argon					Argon + 0.135% vol. oxygen					Argon + 0.135% vol. oxygen + 0.2% vol. nitrogen				
	Adj. R^2	φ [–]	k_1 [min^{-1}]	k_2 min^{-1}]	PI [min]	Adj. R^2	φ [–]	k_1 [min^{-1}]	k_2 [min^{-1}]	PI [min]	Adj. R^2	φ [–]	k_1 [min^{-1}]	k_2 [min^{-1}]	PI [min]
Inactivation kinetic	0.99	1.00 (0.00)	4.81 (0.59)	0.48 (0.06)	1.3	0.97	1.00 (0.00)	5.20 (0.95)	0.36 (0.09)	1.2	0.98	1.00 (0.00)	4.59 (0.69)	0.02 (0.11)	1.9
DNA damage ratio kinetic	0.97	0.64 (0.05)	2.55 (0.73)	0.07 (0.02)	0.2	0.65	0.43 (0.19	2.43 (3.08)	0.05 (0.04)	–	0.96	0.79 (0.05)	1.29 (0.32)	0.00 (0.03)	1.0

of *B. subtilis* endospores (Reineke et al., 2015). The different weighting between the involved inactivation mechanisms can be seen in the different shift between the two inactivation phases (**Tables 3** and **4**). To further investigate the inactivation mechanisms, a qPCR based ratio detection system (Bauer et al., 2004; Roth et al., 2010) was established to monitor the damage of endospore's DNA during the CAPP treatment. DNA is the primary target of emitted (V)UV photons during the CAPP treatment. ROS, namely atomic oxygen and OH radicals, are well known for their oxidation potential and can react with almost all cell components (Surowsky et al., 2014). Whereas OH radicals have the highest oxidation potential of all ROS, they are able to oxidize unsaturated fatty acids, proteins and to initiate DNA damage (Laroussi, 2002; Surowsky et al., 2014). However, the saturation of *B. subtilis* endospores DNA with α/β-type small acid soluble proteins (SASP) protects the DNA against damage caused by OH radicals (Setlow and Setlow, 1993). Hence, the measured DNA damage can be attributed to the emitted (V)UV photons. The DNA damage ratio values showed the same dependence on the used feed gas composition like the maximum achieved inactivation. The fact that plasma running with pure argon obtained on both surfaces the highest DNA damage showed that VUV photons can play a significant role in the inactivation of endospores at atmospheric pressure. All DNA damage kinetics, except the one of argon + 0.135% vol. oxygen + 0.2% vol. nitrogen on glass beads, showed a continuous increase of DNA damage during the entire inactivation process. The DNA damage kinetic for the treatment on glass beads using plasma running with argon + 0.135% vol. oxygen + 0.2% vol. nitrogen merge into a tailing after 3 min (**Figure 4C**). However, the corresponding inactivation curve showed the same tailing, this behavior support the finding, that the damage of DNA due to (V)UV photons is one of the main inactivation mechanisms.

The point of inflection between the two inactivation phases was achieved always significantly earlier for the DNA damage kinetics than for the corresponding inactivation kinetics (**Tables 3** and **4**). The accelerated first inactivation phase is often attributed to the damage of DNA by (V)UV photons (Moisan et al., 2002), however, the different shift between the two phases for the inactivation and DNA damage showed that the (V)UV based inactivation is presumably not the only mechanism contributing to the first fast inactivation phase. The linear behavior for the DNA damage kinetic of argon + 0.135% vol. oxygen + 0.2% vol. nitrogen (**Figure 3C**) can be explained by the high amount of emitted ROS and RNS. High amounts of reactive species are necessary for the decomposition of endospores due to etching, which lead to exposure of former covered endospores in, e.g., agglomerates and consequently to a further DNA damage. The early shift in the inactivation kinetic at 0.4 min may indicate the point, where the inactivation based on UV photons change to an inactivation process based on UV photons and supported by etching and photodesorption. For both DNA damage kinetics of argon + 0.135% vol. oxygen (glass beads and glass petri-dishes) the shift between the two phases could not be calculated, because both φ were under 0.5 and the treatment

resulted in the highest DNA damage ratio value for both surfaces. Plasma generated with argon + 0.135% vol. oxygen emitted the highest amount of ROS, furthermore the admixture of air to argon decreases the VUV emission due to an increase of atomic oxygen emission (Brandenburg et al., 2009). Considering this, the inactivation process seems to be dominated by the action of ROS.

Conclusion

It can be stated that (V)UV photons emitted by CAPP play presumably a considerable role during the inactivation process of *B. subtilis* endospores, if the (V)UV intensity is high enough. Furthermore, the structure of the plasma treated surface as well as the distribution of the endospores on it affects the inactivation efficiency of CAPP treatment.

Acknowledgments

This study was funded by the research project "Plasma-based decontamination of dried plant related products for an enhancement of food safety (^{3}Plas)," which was financially supported by the German Federal Ministry of Food and Agriculture (2819102713).

References

BARTEC Messtechnik und Sensorik. (2001). *Emissionsfaktor-Tabelle*. Gotteszell: BARTEC Messtechnik und Sensorik. Available at: http://www.bartec.de/homepage/deu/downloads/produkte/19_temperatur/Ti_Tabelle_Emission_d.pdf (accessed September 14, 2014).

Bauer, T., Hammes, W. P., Haase, N. U., and Hertel, C. (2004). Effect of food components and processing parameters on DNA degradation in food. *Eur. Food Res. Technol.* 3, 215–223. doi: 10.1051/ebr:2005005

Boudam, M. K., Moisan, M., Saoudi, B., Popovici, C., Gherardi, N., and Massines, F. (2006). Bacterial spore inactivation by atmospheric-pressure plasmas in the presence or absence of UV photons as obtained with the same gas mixture. *J. Phys. D Appl. Phys.* 39, 3494–3507. doi: 10.1088/0022-3727/39/16/S07

Brandenburg, R., Ehlbeck, J., Stieber, M., Woedtke, T. V., Zeymer, J. S., and Schlüter, O. (2007). Antimicrobial treatment of heat sensitive materials by means of atmospheric pressure Rf-driven plasma jet. *Contribut. Plasma Phys.* 47, 72–79. doi: 10.1002/ctpp.200710011

Brandenburg, R., Lange, H., von Woedtke, T., Stieber, M., Kindel, E., and Ehlbeck, J. (2009). Antimicrobial Effects of UV and VUV Radiation of Nonthermal Plasma Jets. *IEEE Trans. Plasma Sci.* 37, 877–883. doi: 10.1109/TPS.2009.2019657

Cerf, O. (1977). Tailing of survival curves of bacterial spores. *J. Appl. Bacteriol.* 42, 1–19. doi: 10.1111/j.1365-2672.1977.tb00665.x

Deng, X., Shi, J., and Kong, M. (2006). Physical mechanisms of inactivation of *Bacillus subtilis* spores using cold atmospheric plasmas. *IEEE Trans. Plasma Sci.* 34, 1310–1316 doi: 10.1128/AEM.00583-12

Ehlbeck, J., Schnabel, U., Polak, M., Winter, J., Von Woedtke, T., Brandenburg, R., et al. (2011). Low temperature atmospheric pressure plasma sources for microbial decontamination. *J. Phys. D Appl. Phys.* 44, 1–18. doi: 10.1016/j.jhin.2012.02.012

Fairheadt, H., Setlow, B., and Setlow, P. (1993). Prevention of DNA damage in spores and in vitro by small, acid-soluble proteins from *Bacillus* species. *J. Bacteriol.* 175, 1367–1374.

Heise, M., Neff, W., Franken, O., Muranyi, P., and Wunderlich, J. (2004). Sterilization of polymer foils with dielectric barrier discharges at atmospheric pressure. *Plasmas Polym.* 9, 23–33. doi: 10.1023/B:PAPO.0000039814.70172.c0

Hertwig, C., Reineke, K., Ehlbeck, J., Knorr, D., and Schlüter, O. (2015a). Impact of remote plasma treatment on natural microbial load and quality parameters of selected herbs and spices. *J. Food Eng.* (in press). doi: 10.1016/j.jfoodeng.2014.12.017

Hertwig, C., Reineke, K., Ehlbeck, J., Knorr, D., and Schlüter, O. (2015b). Decontamination of whole black pepper using different cold atmospheric pressure plasma applications. *Food Control* 55, 221–229. doi: 10.1016/j.foodcont.2015.03.003

Kim, J. E., Lee, D.-U., and Min, S. C. (2014). Microbial decontamination of red pepper powder by cold plasma. *Food Microbiol.* 38, 128–136. doi: 10.1016/j.fm.2013.08.019

Knorr, D., Froehling, A., Jaeger, H., Reineke, K., and Schlueter, O. (2011). Emerging technologies in food processing. *Annu. Rev. Food Sci. Technol.* 2, 203–235. doi: 10.1146/annurev.food.102308.124129

Laroussi, M. (2002). Nonthermal decontamination of biological media by atmospheric-pressure plasmas: review, analysis, and prospects. *IEEE Trans. Plasma Sci.* 30, 1409–1415. doi: 10.1109/TPS.2002.804220

Laroussi, M., and Leipold, F. (2004). Evaluation of the roles of reactive species, heat, and UV radiation in the inactivation of bacterial cells by air plasmas at atmospheric pressure. *Int. J. Mass Spectrom.* 233, 81–86. doi: 10.1016/j.ijms.2003.11.016

Lassen, K. S., Nordby, B., and Grün, R. (2005). The dependence of the sporicidal effects on the power and pressure of RF-generated plasma processes. *J. Biomed. Mater. Res. Part B Appl. Biomater.* 74, 553–559. doi: 10.1002/jbm.b.30239

Lu, X., Ye, T., Cao, Y., Sun, Z., Xiong, Q., Tang, Z., et al. (2008). The roles of the various plasma agents in the inactivation of bacteria. *J. Appl. Phys.* 104, 1–5. doi: 10.1063/1.2977674

Moisan, M., Barbeau, J., Moreau, S., Pelletier, J., Tabrizian, M., and Yahia, L. H. (2001). Low-temperature sterilization using gas plasmas: a review of the experiments and an analysis of the inactivation mechanisms. *Int. J. Pharm.* 226, 1–21. doi: 10.1016/S0378-5173(01)00752-9

Moisan, M., Sakudo, A., Burke, P., and Mcdonnell, G. (2002). Plasma sterilization. Methods and mechanisms. *Pure Appl. Chem.* 74, 349–358. doi: 10.1016/S0378-5173(01)00752-9

Moreau, M., Orange, N., and Feuilloley, M. G. J. (2008). Non-thermal plasma technologies: new tools for bio-decontamination. *Biotechnol. Adv.* 26, 610–617. doi: 10.1016/j.biotechadv.2008.08.001

Moreau, S., Moisan, M., Tabrizian, M., Barbeau, J., Pelletier, J., Ricard, A., et al. (2000). Using the flowing afterglow of a plasma to inactivate *Bacillus subtilis* spores: influence of the operating conditions. *J. Appl. Phys.* 88, 1166–1174. doi: 10.1063/1.373792

Munakata, N., Saito, M., and Hieda, K. (1991). Inactivation action spectra of *Bacillus subtlis* spores in extended ultraviolet wavelengths(50–300nm) obtained with snchrotron radiation. *Photochem. Photobiol.* 54, 761–768. doi: 10.1111/j.1751-1097.1991.tb02087.x

Nicholson, W. L., and Setlow, P. (1990). "Sporulation, germination and outgrowth," in *Molecular Biological Methods for Bacillus*, eds C. R. Harwood, S. M. Cutting, and R. Chambert (Chichester: Wiley), 391–450. doi: 10.1111/j.1751-1097.1991.tb02087.x

Niemira, B. (2012). Cold plasma decontamination of foods. *Annu. Rev. Food Sci. Technol.* 3, 125–142. doi: 10.1146/annurev-food-022811-101132

Pankaj, S. K., Bueno-Ferrera, N. N., Misraa, V., Milosavljevića, B., O'Donnellb, C. P., Bourkea, P., et al. (2014). Applications of cold plasma technology in food packaging. *Trends. Food Sci. Technol.* 35, 5–17. doi: 10.1016/j.tifs.2013.10.009

Perni, S., Shama, G., Hobman, J. L., Lund, P. A., Kershaw, C. J., Hidalgo-Arroyo, G. A., et al. (2007). Probing bactericidal mechanisms induced by cold atmospheric plasmas with *Escherichia coli* mutants. *Appl. Phys. Lett.* 90:073902. doi: 10.1063/1.2458162

Reineke, K., Langera, K., Hertwig, C., Ehlbeck, J., and Schlüteret, O. (2015). The impact of different process gas compositions on the inactivation effect of an atmospheric pressure plasma jet on *Bacillus spores*. *Innov. Food Sci. Emerg. Technol.* 30, 112–118. doi: 10.1016/j.ifset.2015.03.019

Roth, S., Feichtinger, J., and Hertel, C. (2010). Characterization of *Bacillus subtilis* spore inactivation in low-pressure, low-temperature gas plasma sterilization processes. *J. Appl. Microbiol.* 108, 521–531. doi: 10.1111/j.1365-2672.2009.04453.x

Schlüter, O., Ehlbeck, J., Hertel, C., Habermeyer, M., Roth, A., Engel, K. H., et al. (2013). Opinion on the use of plasma processes for treatment of foods. *Mol. Nutr. Food Res.* 57, 920–927. doi: 10.1002/mnfr.201300039

Schlüter, O., and Fröhling, A. (2014). *Encyclopedia of Food Microbiology*. Oxford: Elsevier.

Setlow, B., and Setlow, P. (1993). Binding of small, acid-soluble spore proteins to DNA plays a significant role in the resistance of *Bacillus subtilis* spores to hydrogen peroxide. *Appl. Environ. Microbiol.* 59, 3418–3423.

Surowsky, B., Schlüter, O., and Knorr, D. (2014). Interactions of non-thermal atmospheric pressure plasma with solid and liquid food systems: a review. *Food Eng.* 7, 82–108. doi: 10.1007/s12393-014-9088-5

Weltmann, K.-D., Brandenburg, R., von Woedtke, T., Ehlbeck, J., Foest., R., Stieber, M., et al. (2008). Antimicrobial treatment of heat sensitive products by miniaturized atmospheric pressure plasma jets (APPJs). *J. Phys. D Appl. Phys.* 41, 1–6. doi: 10.1088/0022-3727/41/19/194008

Conflict of Interest Statement: The authors declare that the research was conducted in the absence of any commercial or financial relationships that could be construed as a potential conflict of interest.

5. Factors involved in *Bacillus* spores' resistance to cold atmospheric pressure plasma

In: Innovative Food Science & Emerging Technologies. (submitted)

Cite as:

Hertwig, C., Reineke, K., Rauh, C., Schlüter, O., 2017. Factors involved in *Bacillus* spores' resistance to cold atmospheric pressure plasma. Innovative Food Science & Emerging Technologies. (submitted).

Factors involved in *Bacillus* spore's resistance to cold atmospheric pressure plasma

Christian Hertwig [a, b], Kai Reineke [a], Cornelia Rauh [b], Oliver Schlüter [a,*]

[a] Leibniz Institute for Agricultural Engineering and Bioeconomy (ATB), Quality and Safety of Food and Feed, Max-Eyth-Allee 100, 14469 Potsdam-Bornim, Germany

[b] Department of Food Biotechnology and Food Process Engineering, Berlin University of Technology, Königin-Luise-Straße 22, 14195 Berlin, Germany

[*] Corresponding author:
Oliver Schlüter
Tel.: +49 331 5699 613
E-mail address: oschlueter@atb-potsdam.de

Keywords: *Bacillus subtilis*, spore inactivation, plasma treatment, surface decontamination, mutant strains, postharvest processing

Abstract

In this study factors involved in spore resistance to cold atmospheric pressure plasma (CAPP) were investigated. Therefore, *Bacillus subtilis* spores and isogenic mutant strains, PS578 lacking the genes encoding the spore's two major SASPs, FB122 being unable to synthesize DPA during sporulation and PS3328 lacking the outer spore coat, were CAPP treated using different process gases (air, N_2, O_2, CO_2). Obtained inactivation depended on the process gas; highest inactivation efficiency was obtained with N_2-plasma. The results indicated the different factors involved in *Bacillus subtilis* spores' resistance to CAPP. SASPs contribute in general to spores' CAPP resistance. DPA and outer spore coat are also important in the protection against UV photons, however the protective effect is not so pronounced as for SASPs. Furthermore, they contribute in resistance against generated ozone. *Bacillus atrophaeus* spores, the surrogate for chemical and irradiation sterilization, showed over all a lower resistance to all tested CAPPs.

Industrial relevance

The application of cold atmospheric pressure plasma (CAPP) is an emerging low temperature technology for the inactivation of bacterial spores on different surfaces, such as food products as well as food contact surfaces and packing material. The results presented in this study help to understand the inactivation mechanisms and also the factors involved in the high resistance of bacterial spores to CAPP. This knowledge could be useful to optimize the plasma process for the decontamination of various surfaces in the food industry.

1 Introduction

The application of plasma at industrial scale to generate ozone and ultraviolet (UV) light has been used for decades in the food industry (Knorr et al., 2011). In 1857 Werner von Siemens designed a dielectric barrier discharge (DBD) plasma system to generated ozone, the so-called ozone tube was used to sanitize tap water (Siemens, 1857). Recently, cold atmospheric pressure plasma (CAPP) has gained importance as an emerging low temperature process for the inactivation of microorganism on food products and packing material as well as other food contact surfaces (Misra, Segat, & Cullen, 2015; Pankaj et al., 2014), especially for the decontamination of dry plant products like herbs and spices (Hertwig et al. 2015a), wheat grains (Butscher et al., 2015) or almonds (Deng et al., 2007). CAPP can be generated using different set-ups, like DBD or plasma jet systems (Surowsky, Schlüter, & Knorr, 2014). In general, CAPP is a partially ionized gas, which contains different components; like neutral particles such as atoms, molecules; charged particles as ions and electrons; furthermore, radical, UV photons and also irradiated heat. Whereby, the different generated reactive components and their synergetic combinations are responsible for the antimicrobial effect of the CAPP treatment. Furthermore, the composition of the generated plasma depends on the used plasma source, process gas, kind of application (direct or indirect) and also on the operation conditions, e.g., energy input (Ehlbeck et al., 2011; Weltmann et al., 2008).

Bacterial spores belonging to class *Bacilli* or *Clostridia* are extremely resistant towards multiple environmental stress conditions, like wet and dry heat, irradiation, UV, high pressure and chemicals (Peter Setlow, 2014). Consequently, bacterial spores are perfectly adapted to survive on surfaces like dry food products or food production lines, thus being the major vector causing food spoilage, foodborne diseases and other human illnesses (Logan, 2012; Mallozzi, Viswanathan, & Vedantam, 2010). Various studies have already showed the potential of different CAPP applications to inactivate *Bacillus* spores on different surfaces

(Butscher et al., 2015; Hertwig, Reineke, Ehlbeck, Knorr, & Schlüter, 2015b; Hertwig, Steins, et al., 2015c; Kim, Lee, & Min, 2014; Reineke, Langer, Hertwig, Ehlbeck, & Schlüter, 2015). However, the mechanisms responsible for *Bacillus* spores' inactivation have not been fully understood yet and still under investigation. It is known that mechanisms, like etching, photodesorption or the action of UV photons are involved in the inactivation process (Moisan et al., 2002). Whereby, the UV photons can have a significant impact on the inactivation process due to DNA damage (Hertwig, Steins, et al., 2015c; Reineke et al., 2015). Wang et al. (2016) suggested that their cold atmospheric plasma treatment damages spores' inner membrane and also key germination proteins, causing spore inactivation.

Although a lot of work has been done investigating the *Bacillus* spores' inactivation mechanisms during plasma treatment, the knowledge about the involved spores' resistance properties towards CAPP is limited. As already mentioned *Bacillus* spores are extremely resistant towards various environmental stresses, whereby several factors, such as their multilayer morphology, are involved in their resistance. The spore o, which contains a huge amount of total spore protein, is a permeability barrier, thus restricting the access of large molecule like enzymes to the spore (Driks 1999; Setlow 2014). Furthermore, the coat protects the spore also against biocidal chemicals, probably due to detoxifying them (Setlow, 2006). The inner spore membrane acts also as a permeability barrier, limiting the access of toxic chemicals to the spore core. The core of the spore has quite a low water content, which is important in the wet heat resistance. It also contains a spore unique acid, the dipicolinic acid (DPA), which protects spores' DNA against some damaging agents (Setlow 2014). The DNA is saturated with α/β-type small acid soluble proteins (SASP), which protect the DNA against different kinds of damages, caused by various chemicals, wet and dry heat, UV photons and γ-irradiation (Fairheadt et al. 1993; Setlow & Setlow 1993; Setlow 2014). Further on, the *Bacillus* spore is able to repair certain DNA damage during spore outgrowth (Peter Setlow, 2014). Reineke et al. (2015) have already showed the contribution of the SASPs and the DPA

98 to Bacillus spore's UV resistance, whereby the SASPs seem to play a more important role as
99 the DPA.

100 This study investigated the inactivation behavior of *B. subtilis* spores to CAPP treatment.
101 Further on, isogenic mutant strains were used to determine the spores's properties involved in
102 the resistance to CAPP treatment, focusing on spores' outer coat, DPA and SASP. To
103 distinguish between the different generated reactive species of the CAPP, regarding the
104 inactivation process and resistant properties, different process gases, as dry air, N_2, O_2 and
105 CO_2 were used to control the generation of these species during the CAPP treatment. The
106 obtained inactivation data were compared with *Bacillus atrophaeus* spores, which is a
107 surrogate strain for *Bacillus anthracis* spores during chemical, UV- and γ-irradiation
108 sterilization processes.

109

110 ## 2 Material and Methods

111 ### 2.1 *Bacillus* strains and spore preparation

112 In this study spores of *B. atrophaeus* strain WIS 396/3, *B. subtilis* strain PS832 (wild type)
113 and three isogenic derivates of this *B. subtilis* strain, namely FB122 (Douki, Setlow, &
114 Setlow, 2005), PS578 (Genest, Setlow, Melly, & Setlow, 2002) and PS3328 (Paidhungat,
115 Ragkousi, & Setlow, 2001) were used. The spores of *B. atrophaeus* strain WIS 396/3 are used
116 as surrogates for *B. anthracis* spores during chemical, UV- and γ-irradiation sterilization
117 (Reineke et al., 2015). The strain FB122 (*sleB spo VF*) lacks the gene encoding the cortex
118 lytic enzyme sleB and is not able to synthesize DPA during the sporulation. The strain PS578
119 (α^- β^-) lacks the genes encoding the spore's two major α/β-type SASPs, thus the α/β-type
120 SASP level in the PS578 spores is only ~25 % of that in the wild types spores PS832. The
121 strains PS3328 (*cotE*) lack the CotE protein, which is essential for the spore's coat

morphology (Henriques & Moran, 2007), especially for the structure of the outer spore coat (Driks, 1999). All spore strains were sporulated using a method previously published (Nicholson & Setlow, 1990). The sporulation was induced on 2x SG medium agar plates at 37 °C without adding antibiotics. However, for the strain PS3328 tetracycline (Sigma Aldrich) was added with a concentration of 20 $\mu g*L^{-1}$. After sporulation, the spores were harvested using distilled water. The obtained spore suspensions were washed and cleaned with cold distilled water by repeated centrifugation (threefold at 5000 g) and intermittently treated with ultrasonic for 1 min. The cleaned spore suspensions contained ≥95 % phase bright spores and nearly no agglomerates. The spore suspensions were stored in the dark at 4 °C, until needed.

2.2 Sample preparation

In this study glass beads were used as a spherical model to investigate the inactivation of the different spore strains. The samples were inoculated with a spore density of about $5*10^5$ to $6*10^6$ spore cm^{-2}. Therefore, 82 sterile glass beads were placed into a sterile beaker and 175 µL stock spore suspension was added. The beaker was placed on an automatic stirrer and shaken for 4 min at 400 rpm to obtain a homogenous coating of the microorganisms on the samples surface. The inoculated samples were placed under a clean bench for drying at room temperature for 30 min.

2.3 Plasma source and plasma treatment

For the CAPP treatment a diffuse coplanar surface barrier discharge 400 (DCSBD) plasma plate (CEPLANT, R&D Centre for Low-Cost Plasma and Nanotechnology Surface Modifications, Masaryk University, Brno, Czech Republic) was used, which is shown in

Figure 1 and described in detail by Černák et al. (2011). The plasma generated with the DCSBD plate consists of a high number of various microdischarges and creates an approximately 0.3 mm thick and homogeneous plasma layer. The plasma was generated by applying a sinusoidal high voltage (20 kV peak to peak and a frequency of 15 kHz) on the upper side of an Al_2O_3 ceramic and has no contact with the electrodes on the bottom side of the ceramic. A dielectric insulating oil circulation system is used for the electric insolation of the electrodes. The circulating oil is tempered using a plate heat exchanger and worked as a cooling system for the generated plasma. The application area of the plasma was 200 mm x 80 mm. For the experiments two different treatment chambers were used. The first reactor (Figure 2A) consisted of one DCSBD plate and a glass cover with connections for the temperature and the emission spectrum measurements; and in- and outlet for the process gas. The second reactor (Figure 2B) was used for the treatment of the inoculated glass beads and had one bottom and one top DCSBD plate. The gap between the DCSBD plates was adjustable in the range from 0 two 40 mm. The reactor was covered to work in a static atmosphere and had in- and outlets for the process gas and connectors to analyze the atmosphere in the reactor. For the spore inactivation the gap between the two plates was 20 mm, 46 inoculated glass beads were placed on the bottom DCSBD plate, which was used for the CAPP treatment with a power input of 350 W. For the plasma treatment four different process gases were chosen, dry air, N_2, O_2 and CO_2. The treatment chamber was flushed with the process gas and the inoculated glass beads were treated up to 7 min. However, the treatment time was adapted to the used spore strain and process gas, to compare the inactivation behavior of the different used spore strains. During the treatment the chamber was continuously shaken to obtain a homogenous plasma treatment of the glass beads. A mechanical cleaning effect on the surface of the glass beads due to shaking could be excluded. The experiments were performed at least in triplicate.

2.4 Characterization of generated plasma

A Black Comet UV-VIS Spectrometer (StellarNet Inc., Tampa, USA) equipped with an F400 UV-VIS-SR fiber optic and a quartz lens was used to measure the emission spectrum of the different generated plasmas. The spectrum was measured in the range from 190 to 850 nm, with a distance of 1 mm from the plasma to the quartz lens. The spectrum was measured 20 times with an integration time of 1000 ms. The plasma temperature was measured using a fiber-optic temperature sensor TS4 (OPTOCON AG, Dresden, Germany). The sensor is completely PTFE coated and resistant to electromagnetic interferences and high aggressive chemicals. Furthermore, the generated ozone in the treatment chamber was measured using an OZONE ANALYZER BMT 964 (BMT Messtechnik GmbH, Stahnsdorf, Germany) with a measuring range of up to 25,000 ppm ozone. The ozone analyzer was connected with FEP tubes to the treatment chamber and the ozone concentration was measured with a constant gas flow of 0.8 L/min during the measurements.

2.5 Viable cell counts

After the CAPP treatment the viable cell count was determined by standard cell culture methods. Therefore, the 46 glass beads were divided into two groups of 23 glass beads, which were transferred into sterile glass flaks. The spores were resuspended by shaking the 23 glass beads in 4 mL ACES-buffer for 3 min at 400 rpm. The obtained suspensions were serially diluted in ACES-buffer (pH 7, 0.05 M) and every dilution was plated on nutrient agar plates (Carl Roth GmbH, Karlsruhe, Germany) in duplicates. The plates were incubated at 37 °C and the colony forming units (cfu) were counted after 24 and 48 h. The obtained inactivation kinetics were modeled using OriginPro (Version 8.0724; OriginLab Corporation, Northampton, USA) with the Weibullian power law:

196 $$log_{10}S(t) = -b \cdot t^n$$

197 where S(t) is N(t)/N_0 , with N(t) as the number of colony forming units at the time t and N_0 as
198 the initial number of colony forming units and with *b* as the scale and *n* as the shape
199 parameter. The shape parameter *n* describes the progression of the inactivation curve. For
200 values n < 1 the curve is upward concave, indicating that the remaining spores are more
201 resistant to the CAPP treatment as the already inactivated ones. If n > 1 the curve is
202 downward concave, implying that the remaining spores have increasing sensitivity against the
203 treatment as the already inactivated ones. For n = 1 the inactivation curve is linear as a first
204 order inactivation, meaning that all spores have the same, time independent resistance to the
205 CAPP treatment.

206

207 # 3 Results and Discussion

208 ## 3.1 Characterization of generated plasmas

209 Four different process gases (dry air, N_2, O_2 and CO_2) were used to investigate the resistance
210 factors involved of *B. subtilis* spores' resistance to CAPP. Optical emission spectroscopy was
211 used to obtain an overview about their different compositions. The emission spectra of the
212 used plasma are shown in Figure 3A. The use of dry air generated a plasma with emission
213 intensities in the entire UV range (200-400 nm) and also some in the visible light range.
214 However, comparing the individual UV ranges, it can be stated that intensities in the UV-C
215 range were significant lower as those in the UV-A and UV-B range. Compared to the short
216 wave UV-C light, the antimicrobial efficiency of UV light with longer wavelength is much
217 lower. In the UV-B range (280-320 nm) the spectrum was dominated by the third (296.5 nm)
218 and fourth (315.5 nm) positive system of N_2. No $OH^{\bullet}$ radicals could be detected, probably due
219 to the use of dry air. The high intensities in the UV-A range (320-400 nm) were dominated by

the molecular bands of the second positive system of N_2 (337, 353.5, 357.5, 375 and 380 nm) (Brandenburg et al. 2007). The measured emission spectra of the CAPPs generated with O_2 and CO_2 (Figure 3B) showed very low intensities in entire UV range, O_2-plasma also at around 777 nm for the atomic oxygen band. However, compared to air-plasma the emission intensities in the entire measured range were negligible The use of N_2 as a process gas resulted in plasma, which had, compared to the other used three process gases, the highest emission intensities (Figure 3A). N_2-plasma had also significant intensities in the UV-C range, compared to the other used process gases. The UV-C emission was 4.5fold higher as for plasma generated with air, the emission in the UV-A and UV-B range were twofold higher (Figure 4). The atmosphere inside the treatment chamber was also analyzed regarding the generated ozone concentration, which is a long living reactive oxygen specie with a strong oxidation potential. For the use of air-plasma no ozone could be detected in the treatment chamber, probably due to the presence of reactive nitrogen species, which would react with the generated ozone (Surowsky et al., 2014). CAPP generated with O_2 generated a high ozone concentration inside the treatment chamber of about 24,000 ppm during the treatment (Figure 5A). In the case of CO_2-plasma the ozone concentration was lower and increased continuously during the treatment to a maximum concentration of about 2150 ppm. Moreover, the temperature profile of the different plasmas was measured (Figure 5B), for all used process gases the temperature was below 70 °C during the entire treatment. For air-plasma the temperature increased with increasing treatment time to a maximum of 63 °C, in case of N_2-plasma the maximum temperature was 69°C. For the use of O_2 the plasma temperature increased until 1.5 min to a maximum of 63 °C and then decreased to around 60 °C. For CO_2-plasma the temperature was below 60 °C during the entire treatment. Considering the maximum temperature-time profile of the tested plasmas a thermal inactivation effect is negligible, also for the used *Bacillus* mutant strains (Setlow & Setlow 1995; Setlow et al. 2006; Setlow 2014).

The characterization of the CAPP showed their different composition and temperature depending on the used process gas. N_2-plasma was characterized by high emission of UV photons, especially a significant amount of UV-C photons. O_2-plasma and CO_2-plasma were characterized by negligible emission of UV photons, however those plasmas generated a high amount of reactive oxygen species (ROS), as ozone. Regarding the different composition of the CAPP different inactivation efficiencies of the used *Bacillus* spore strains can be expected. Furthermore, the different composition will be used to closer investigate the role of certain spore resistance properties towards the different plasma components, as UV photons and ROS.

3.2 Effect of process gas on the inactivation of *Bacillus subtilis* wild type spores

To investigate the effect of the different process gases on the inactivation of *B. subtilis* wild type spores, glass beads were inoculated and CAPP treated up to 7 min. The results are shown in Figure 6. The obtained inactivation data were modeled using the weibullian power law model, which adequately describes the inactivation behavior (Table 1). All used CAPPs were able to inactivate the *B. subtilis* wild type spores; however the inactivation depended on the used process gas. For N_2-plasma after a 3 min treatment an inactivation below the detection limit of 5.3 $\log_{10}$ was achieved. The use of the other process gases resulted after a 7 min treatment in a maximum inactivation between 3.5 to 4.0 $\log_{10}$, whereas the use of air-plasma inactivated 3.5 $\log_{10}$. The use of O_2 and CO_2 resulted in a maximum inactivation of 4.0 $\log_{10}$. The shape parameter n of the all inactivation kinetics is smaller as 1, meaning a higher inactivation rate during the beginning of the CAPP treatment. This progress of the inactivation curves indicates that the remaining spores are probably more resistant to the plasma treatment. Furthermore, agglomerated spores can also lower the inactivation, due to limited penetration depth of CAPP (Hertwig, Reineke, Ehlbeck, Knorr, et al., 2015b),

271 resulting in an inactivation tailing. The D-values, which represent in our case the time
272 necessary for the first decimal reduction at a power input of 350 W, were calculated. N_2-
273 plasma had a D-value of 0.06 for the inactivation of *B. subtilis* wild type spores, whereas the
274 D-values of the other used CAPPs were significant higher and between 1.10 and 1.52. The D-
275 value of N_2-plasma underlines the significant role of the UV photons, especially UV-C
276 photons, in spores' inactivation, within 0.06 min 1.0 $\log_{10}$ *B. subtilis* wild type spores were
277 inactivated with treatment temperatures below 52 °C. The penetration depth of UV photons is
278 limited, depending on the material and wavelength it can exceed 1 µm (Lerouge et al. 2000)
279 and is in the order of spore dimension of 1 to 3 µm (Moisan et al. 2001). However, if the
280 spores are stacked and aggregated and not homogeneously distributed on the surface the
281 inactivation by UV photons becomes less important (Hertwig et al. 2015c). Air-plasma, which
282 had also high emission intensities in the UV-A and UV-B range, but negligible in the UV-C
283 range, needed 1.21 min to inactivate 1.0 $\log_{10}$. The significant role of UV-C photons in
284 bacterial spore inactivation was also shown for different plasma systems by Boudam et al.
285 (2006); C Hertwig, Steins, et al. (2015c) and Reineke et al. (2015). Plasma generated with O_2
286 had a D-value of 1.52 and CO_2-plasma of 1.10, although O_2-plasma had a 14fold higher ozone
287 concentration within the first 1.5 min. CO_2-plasma may have generated also other reactive
288 components, which could not be detected using optical emission spectroscopy and may
289 support the inactivation process. Gaseous ozone is known to inactivate various *Bacillus* spores
290 (Akbas & Ozdemir, 2008; Aydogan & Gurol, 2006). Aydogan & Gurol (2006) treated
291 *B. subtilis* spores with an ozone concentration of 1500 ppm and inactivated about 3-log within
292 4 hr. CO_2-plasma inactivated after 5 min with a maximum ozone concentration of about
293 2000 ppm more than 3.15 $\log_{10}$. Probably has the direct contact between inoculated glass
294 beads and generated plasma during the treatment a supporting effect on the inactivation.

295

3.2 Effect of process gas on the inactivation of *Bacillus subtilis* isogenic mutant spores

The role of specific spores' resistance properties towards CAPP was investigated using isogenic mutant spore strains: PS578 lacks the genes encoding the spores' two major SASPs, FB122 is unable to synthesize DPA during sporulation and PS3328 lacks the outer spore coat protein layer. The obtained inactivation data and kinetics for the CAPP treatment of the strain PS578 are shown in Figure 7A and the statistical parameter of the Weibullian power law model as well as D-values in Table 2. The PS578 spores were more sensitive towards the plasma treatment as the wild type spores; all used plasmas inactivated the PS578 spores below the detection limit within a 6 min treatment. Of particular note are the obtained inactivation results for the treatment with N_2-plasma, which had a high emission of UV-C photons. The inactivation was immediately below the detection limit with 5.0 $\log_{10}$ after the shortest treatment time of 10 sec. This shows the essential function of the α/β-type SASPs in the resistance of *B. subtilis* spores against damage induced by UV-C photons, which was also shown by Setlow (2001). Air- plasma, which just had a negligible emission of UV-C photons, besides the emission in the other UV range, needed 2 min to inactivate the PS578 spores by 5.1 $\log_{10}$, below the detection limit. The use of CO_2 as a process gas resulted in a maximum inactivation of 5.0 $\log_{10}$ after a 5 min CAPP treatment. For the treatment with O_2-plasma a 6 min treatment was necessary to obtain an inactivation below the detection limit of 4.8 $\log_{10}$. The results for the two plasmas with negligible emission of UV photons showed also the importance of the spores' α/β-type SASPs in the protection against reactive oxygen species, like ozone. The higher sensitivity of PS578 spores towards the different tested plasmas is also reflected in the D-values (Table 2). For N_2-plasma no D-value could be calculated due to the obtained inactivation below the detections limit already after a 10 sec treatment. The other three used plasmas had lower D-values, between 0.20 and 0.96, as the corresponding ones of the wild type *B. subtilis* spores; showing the faster inactivation of the PS578 spores for the first 1.0 $\log_{10}$. Reineke et al. (2015) used a plasma jet system driven with argon and

admixtures of O_2 and N_2 and reported also a higher inactivation rate for PS578 spores compared to the *B. subtilis* wild type (PS832) spores. Roth et al. (2010) treated a similar *Bacillus* mutant spore strain using a vacuum DBD plasma system with process gases 80 % N_2 and 20 % O_2. In this experiment the mutant spore strain without α/β-type SASPs had in this experiment also a significant higher inactivation as the treated wild type strain. The binding of the SASPs to the spores' DNA causes changes in the DNA UV photochemistry resulting in a unique spore photoproduct, which can be repaired relatively error-free during the spore outgrowth using spore specific enzymes (Peter Setlow, 2014). Setlow (2014) also mentioned the importance of SASPs in DNA protection against oxidizing agents such as H_2O_2.

The results for the CAPP treatment of the FB122 (DPA less) spores are shown in Figure 7B. All inactivation kinetics could be adequately described using the Weibullian power law model Table 2. The use of N_2-plasma resulted again in the highest inactivation efficiency. After 1 min of CAPP treatment an inactivation of 4.8 $\log_{10}$ was obtained. The results for the treatment with air- and CO_2-plasma are comparable to those of the wild type ones. The inactivation was 3.8 and 3.5 $\log_{10}$, respectively after 7 min CAPP treatment. The course of the inactivation kinetic within the first 3 min treatment with O_2-plasma showed a similar behavior as for the use of air- and CO_2-plasma. With a prolonged treatment the FB122 spores become more sensitive towards the O_2-plasma, compared to the use of air- and CO_2-plasma, visible in an inactivation of 4.6 $\log_{10}$ below the detection limit after a 6 min treatment. The calculated D-values of the testes CAPP are shown in Table 2. CAPP generated with N_2 had a D-value of 0.14 and needed, compared to the wild type spores, more as twofold more time for the inactivation of the first 1.0 $\log_{10}$. Although the maximum inactivation below the detection limit was already achieved after 1 min, whereas for the wild type spores a 3 min treatment was necessary. The D-value of CO_2-plasma 1.47 was also higher as the one of the wild type strain, whereas the maximum inactivation after a 7 min CAPP treatment was also slightly lower as the corresponding inactivation of the wild type strain. The other two used process

gases (air, O_2) resulted in lower D-values, indicating the faster inactivation of the FB122 spores. The DPA less FB122 strain has compared to DPA replete spores a 20 % higher level of water content in the spore (B. Setlow, Atluri, Kitchel, Koziol-Dube, & Setlow, 2006). The low water content and the high level of DPA inside the spores' core contribute to the unique spore DNA UV photochemistry (P Setlow, 2006), maybe due to the fact that a low core water content ensures the binding of α/β-type SASPs to the DNA of dormant spore even though the affinity of these proteins for DNA is not extremely high (Peter Setlow, 2014). *B. subtilis* spores without DPA are less resistant toward UV-C light at 254 nm, however this sensitivity is not so pronounced as for *B. subtilis* spores without α/β-type SASPs (Peter Setlow, 2014). The FB122 spores in our experiments were more sensitive towards the N_2-plasma, with the significant UV-C emission, as the PS832 wild type spores, however not as sensitive as the PS578 spores (Figure 7A). Reineke et al. (2015) reported a higher inactivation rate for the FB122 spores compared to the PS832 wild type spores using a plasma jet with high UV emission, whereas the FB122 strain had a similar resistance as the PS832 wild type strain towards plasma with negligible UV emission. The FB122 spores showed a faster inactivation and slightly higher maximum inactivation after a 7 min air-plasma (high emission intensities in UV-A and –B range) treatment as the PS832 wild type spores. Moeller et al. (2009) reported that *B. subtilis* spores which had elevated water content were more sensitive towards environmental UV light of above 280 nm. Slieman & Nicholson (2001) treated the wild type PS832 and DPA less spores with different UV wavelengths, showing that the DPA less spores were less resistant, however this effect was most pronounced for the exposure to artificial UV-B light. Furthermore, Paidhungat et al. (2000) reported a higher sensitivity of *B. subtilis* lacking DPA to the strong oxidizing agent hydrogen peroxide, which correlated with a decrease of spore resistance to hydrogen peroxide with increasing core hydration (Popham, Sengupta, & Setlow, 1995). Probably the high concentration of generated ozone using O_2-

plasma has a similar effect on the DPA lacking FB122 spores, whereas for CO_2 with a 11fold less ozone concentration a similar effect on the inactivation could not be observed.

The last tested isogenic mutant *B. subtilis* spore strain was PS3328, which lacks the outer spore coat protein layer. The results for the obtained inactivation are shown in Figure 7C, which could be adequately fitted with the Weibullian power law model (Table 2). Again the highest inactivation efficiency was obtained using N_2-plasma, after a 2 min treatment an inactivation of 4.9 $\log_{10}$ below the detection limit was obtained. The PS3328 spores were also more sensitive as the wild type spores towards the treatment with air-plasma, after a 7 min treatment the inactivation was 4.4 $\log_{10}$. The maximum inactivation achieved of 4.1 $\log_{10}$ with CO_2-plasma was comparable to those of the wild type spores. The use of O_2 as process gas resulted in a significant higher inactivation as for the wild type spores. The treatment of 6 min with O_2-plasma inactivated up to 4.6 $\log_{10}$ PS3328 spores. Of particular note is the shape parameter n of the corresponding Weibull model. For all other tested CAPPs and *B. subtilis* spores the shape parameter was $n < 1$, as already mentioned above this indicated a slower inactivation rate for longer treatment time, probably due to agglomerated spores or more resistant ones. However, in the case of PS3328 spores treated with O_2-plasma the shape parameter n was 1.01 showing a linear inactivation behavior, with the same time independent resistance of the spores towards this CAPP treatment. The calculated D-values were between 0.05 and 1.27 and for all tested plasma below those of the corresponding wild type PS832 spores, showing the faster inactivation for the first 1.0 $\log_{10}$. In general, the spore coat is an important factor in the resistance against many toxic chemical, larger oxidizing agents (Peter Setlow, 2014), like ozone (Young & Setlow, 2004) and has just a minor role in the resistance towards hydrogen peroxide (Riesenman & Nicholson, 2000). Riesenman & Nicholson (2000) reported a higher UV resistance of *cotE B. subtilis* mutant spores without the outer spore coat compared to *B. subtilis* wild type spores, similar results were shown by Setlow (2014). However, *B. subtilis* spores lacking the outer spore coat were significantly more sensitive as

399 the corresponding wild type spores towards different low-pressure plasma generated with Ar,
400 O_2, H_2 with and without admixtures (Raguse et al., 2016). Roth et al. (2010) reported using
401 low-pressure plasma (80 % N_2 and 20 % O_2) a higher inactivation for directly treated PS3328
402 spores as for wild type ones, however when they were shielded from the generated UV
403 photons using optical long pass filter plates their inactivation was comparable to that of the
404 wild type spores. Further, on Fiebrandt et al. (2017) showed a significantly contribution of the
405 inner and outer *B. subtilis* spore coat to the absorption of UV-C and VUV photons, thus
406 protecting the spore against radiation based damage. The D-value 0.05 of the PS3328 spores
407 treated with N_2-plasma was just slightly lower as the corresponding one for the wild type
408 spores with 0.06. However, the use of N_2-plasma for a 2 min treatment inactivated the PS3328
409 spores below the detection limit, whereas for the wild type spores a 3 min treatment was
410 necessary, showing the higher sensitivity of the PS3328 spores to the emitted UV photons.
411 The PS3328 spores were also more sensitive towards the air-plasma treatment, which had just
412 a negligible emission of UV-C photons compared to N_2-plasma. The high ozone concentration
413 of the O_2-plasma is probably the reason for the higher inactivation compared to the wild type
414 spores, indicating the protective effect of the outer spore coat against oxidizing agents like
415 ozone. Yet, for the use of CO_2-plasma a similar effect could not be observed, whereas the
416 11fold less generated ozone concentration could be an explanation.

417

418 **3.4 Effect of process gas on the inactivation of *Bacillus atrophaeus* spores**

419 *B. atropahaeus* were treated to compare the inactivation of the *B. subtilis* wild type PS832
420 spores with those of a relevant surrogate for chemical, UV- and γ-irradiation sterilization
421 processes. The results are shown in Figure 8. The obtained inactivation data could be
422 adequately fitted using the Weibullian power law model (Table 3). The inactivation of the
423 *B. atrophaeus* spores depended also on the used process gas. The treatment with N_2-plasma

resulted in the fastest inactivation; after 2 min with 5.1 $\log_{10}$ already below the detection limit. The treatment with air- and CO_2-plasma had a similar maximum inactivation after a 7 min treatment with 4.7 and 4.8 $\log_{10}$, respectively. The use of O_2 as a process gas resulted in an inactivation below the detection limit after 6 min with 4.9 $\log_{10}$. Taking into account the maximum achieved inactivation and the corresponding treatment time, *B. atrophaeus* spores were less resistant as the *B. subtilis* wild type spores. However, the calculated D-values and the shape parameter of the Weibullian power law model (Table 3) showed a differentiated perspective. The D-values for air- and N_2-plasma were 1.22 and 0.05 and close to those of the *B. subtilis* wild type spores with 1.21 and 0.06, respectively; showing that a similar time is necessary to inactivate the first 1.0 $\log_{10}$ spores. The D-values for O_2- and CO_2-plasma were 1.80 and 1.28 and higher as those of *B. subtilis* spores, which pointed towards a higher resistance of the *B. atrophaeus* spores at the beginning of the CAPP treatment. Furthermore, the shape parameter for the O_2-plasma is with 1.38 higher as 1, showing that the *B. atrophaeus* spores are more resistant at the beginning of the treatment as the remaining spores. Hertwig, Reineke, et al. (2015b) and Reineke et al. (2015) reported also a higher sensitivity of *B. atrophaeus* spores compared to *B. subtilis* spores, they used different plasma systems for a direct and indirect treatment and different process gases, like air and pure argon as well as with admixtures of N_2 and O_2. However, the resistance of *Bacillus* spores can be attributed to several different factors and can differ tremendously between different spore strains (Pedraza-Reyes, Ramírez-Ramírez, Vidales-Rodríguez, & Robleto, 2012).

4 Conclusions

The effect of different CAPP generated using various process gases (dry air, N_2, O_2 and CO_2) on the inactivation of *B. subtilis* wild type PS832 spores was investigated. The tested plasmas were characterized by their different composition. Air-plasma had emission intensities in the

449 UV-A and UV-B range, due to generated reactive nitrogen species. N_2-plasma had about
450 twofold higher emission intensities in the UV-A and –B range, furthermore also significant
451 emission in the UV-C range. CAPP generated with O_2 and CO_2 had nearly no emission
452 intensities, however these plasmas generated a high concentration of reactive oxygen species
453 like ozone, with about 24,000 ppm and 2150 ppm, respectively. The obtained inactivation was
454 depending on the used process gas. N_2-plasma had the highest inactivation efficiency and a D-
455 value of 0.06. The other three tested plasmas had a similar maximum inactivation after a
456 7 min treatment and D-values between 1.10 and 1.52.

457 Different *B. subtilis* isogenic mutant strains; PS578 lacking the genes encoding the spores'
458 two major SASPs, FB122 being unable to synthesize DPA during sporulation and PS3328
459 lacking the outer spore coat protein layer; were CAPP treated to investigate the role of those
460 spore properties in the resistance to CAPP. SASPs contribute in general to the spores' CAPP
461 resistance. *Bacillus* spores without α/β-type SASPs were sensitive towards all tested plasmas,
462 but especially to the N_2-plasma with the highest UV intensity. These results showed the
463 importance of α/β-type SASPs in the protection against UV photons. The DPA inside the
464 spore core contributes also to the spore UV resistance but to a lower extent. Further on, DPA
465 less FB122 spores were more sensitive towards O_2-plasma with prolonged treatment time,
466 indicating a presumed protective effect of the DPA against the generated ozone or possible
467 oxidative reaction in the hydrated core. A similar effect could not be observed for CO_2-plasma
468 with 11fold less ozone concentration. The spore strain PS3328 was sensitive towards the
469 treatment with air- and N_2-plasma, indicating a presumed protective effect of the outer spore
470 coat protein layer against emitted UV photons. The PS3328 spores showed a similar
471 inactivation behavior as the FB122 spore using O_2- and CO_2-plasma, which may indicate the
472 importance of the outer protein layer in the resistance towards the generated ozone.

B. atrophaeus spores, which are used as the surrogate for chemical and irradiation sterilization processes showed over all a lower resistance to the all tested plasmas as the used *B. subtilis* wild type spores. However for the use of O_2- and CO_2-plasma *B. atrophaeus* spores had higher D-values as the corresponding on of the *B. subtilis* spores, which showed a higher resistance to these plasmas within the beginning of the CAPP treatment.

The results of this work provide new insight to better understand the resistance of bacterial spores to cold atmospheric pressure plasma treatment and the mechanisms responsible for bacterial spores' inactivation by cold atmospheric pressure plasma. This knowledge will support the development of more efficient CAPP applications in the food industry for the decontamination of various surfaces, like food products, packing material or food contact surfaces.

Acknowledgments

This study was funded by the research project "Plasma-based decontamination of dried plant related products for an enhancement of food safety (^{3}Plas)", which was financially supported by the German Federal Ministry of Food and Agriculture (2819102713).

References

Akbas, M., & Ozdemir, M. (2008). Application of gaseous ozone to control populations of Escherichia coli, Bacillus cereus and Bacillus cereus spores in dried figs. *Food Microbiology*, *25*(2), 386–391. doi:10.1016/j.fm.2007.09.007

Aydogan, A., & Gurol, M. (2006). Application of gaseous ozone for inactivation of Bacillus subtilis spores. *Journal of the Air & Waste Management Association (1995)*, *56*(2), 179–

85. doi:10.1080/10473289.2006.10464443

Boudam, M. K., Moisan, M., Saoudi, B., Popovici, C., Gherardi, N., & Massines, F. (2006). Bacterial spore inactivation by atmospheric-pressure plasmas in the presence or absence of UV photons as obtained with the same gas mixture. *Journal of Physics D: Applied Physics*, *39*(16), 3494–3507. doi:10.1088/0022-3727/39/16/S07

Brandenburg, R. et al., 2007. Antimicrobial Treatment of Heat Sensitive Materials by Means of Atmospheric Pressure Rf-Driven Plasma Jet. Contributions to Plasma Physics, 47(1–2), pp.72–79.

Butscher, D., Schlup, T., Roth, C., Müller-Fischer, N., Gantenbein-Demarchi, C., & Rudolf Von Rohr, P. (2015). Inactivation of microorganisms on granular materials: Reduction of Bacillus amyloliquefaciens endospores on wheat grains in a low pressure plasma circulating fluidized bed reactor. *Journal of Food Engineering*, *159*, 48–56. doi:10.1016/j.jfoodeng.2015.03.009

Černák, M., Kováčik, D., Ráhel', J., St'ahel, P., Zahoranová, A., Kubincová, J., … Černáková, L. (2011). Generation of a high-density highly non-equilibrium air plasma for high-speed large-area flat surface processing. *Plasma Physics and Controlled Fusion*, *53*(12), 124031.

Deng, S., Ruan, R., Mok, C. K., Huang, G., Lin, X., & Chen, P. (2007). Inactivation of Escherichia coli on almonds using nonthermal plasma. *Journal of Food Science*, *72*(2), M62–66. doi:10.1111/j.1750-3841.2007.00275.x

Douki, T., Setlow, B., & Setlow, P. (2005). Photosensitization of DNA by dipicolinic acid, a major component of spores of Bacillus species. *Photochemical & Photobiological Sciences*, *4*(8), 591–597.

519 Driks, A. (1999). Bacillus subtilis Spore Coat. *MICROBIOLOGY AND MOLECULAR*
520 *BIOLOGY REVIEWS*, *63*(1), 1–20.

521 Ehlbeck, J., Schnabel, U., Polak, M., Winter, J., von Woedtke, T., Brandenburg, R., …
522 Weltmann, K.-D. (2011). Low temperature atmospheric pressure plasma sources for
523 microbial decontamination. *Journal of Physics D: Applied Physics*, *44*(1), 1–18.
524 doi:10.1088/0022-3727/44/1/013002

525 Fairheadt, H., Setlow, B. & Setlow, P., 1993. Prevention of DNA Damage in Spores and In
526 Vitro by Small , Acid-Soluble Proteins from Bacillus Species. JOURNAL OF
527 BACTERIOLOGY, 175(5), pp.1367–1374.

528 Fiebrandt, M. et al., 2017. VUV absorption spectroscopy of bacterial spores and DNA
529 components. Plasma Physics and Controlled Fusion, 59(1).

530 Genest, P., Setlow, B., Melly, E., & Setlow, P. (2002). Killing of spores of Bacillus subtilis by
531 peroxynitrite appears to be caused by membrane damage. *Microbiology*, *148*(1), 307–
532 314. doi:10.1099/00221287-148-1-307

533 Henriques, A. O., & Moran, C. P. (2007). Structure, assembly, and function of the spore
534 surface layers. *Annual Review of Microbiology*, *61*, 555–588.
535 doi:10.1146/annurev.micro.61.080706.093224

536 Hertwig, C., Reineke, K., Ehlbeck, J., Erdoğdu, B., Rauh, C., & Schlüter, O. (2015a). Impact
537 of remote plasma treatment on natural microbial load and color of selected herbs and
538 spices. *Journal of Food Engineering*. doi:10.1016/j.jfoodeng.2014.12.017

539 Hertwig, C., Reineke, K., Ehlbeck, J., Knorr, D., & Schlüter, O. (2015b). Decontamination of
540 whole black pepper using different cold atmospheric pressure plasma applications. *Food*
541 *Control*, *55*, 221–229. doi:10.1016/j.foodcont.2015.03.003

Hertwig, C., Steins, V., Reineke, K., Rademacher, A., Klocke, M., Rauh, C., & Schlüter, O. (2015c). Impact of surface structure and feed gas composition on Bacillus subtilis endospore inactivation during direct plasma treatment. *Frontiers in Microbiology*, *6*(August), 1–12. doi:10.3389/fmicb.2015.00774

Kim, J. E., Lee, D.-U., & Min, S. C. (2014). Microbial decontamination of red pepper powder by cold plasma. *Food Microbiology*, *38*, 128–36. doi:10.1016/j.fm.2013.08.019

Knorr, D., Froehling, A., Jaeger, H., Reineke, K., Schlueter, O., & Schoessler, K. (2011). Emerging technologies in food processing. *Annual Review of Food Science and Technology*, *2*, 203–235. doi:10.1146/annurev.food.102308.124129

Lerouge, S. et al., 2000. Sterilization by Low-Pressure Plasma : The Role of Vacuum-Ultraviolet Radiation. , 5(1), pp.31–46.

Logan, N. A. (2012). Bacillus and relatives in foodborne illness. *Journal of Applied Microbiology*, *112*(3), 417–429. doi:10.1111/j.1365-2672.2011.05204.x

Mallozzi, M., Viswanathan, V. K., & Vedantam, G. (2010). Spore-forming Bacilli and Clostridia in human disease. *Future Microbiology*, *5*(7), 1109–23. doi:10.2217/fmb.10.60

Misra, N. N., Segat, A., & Cullen, P. J. (2015). Atmospheric-Pressure Non-Thermal Plasma Decontamination of Foods. In R. V Ravishankar (Ed.), *Advances in Food Biotechnology* (1. Edition., pp. 565–574). John Wiley & Sons.

Moeller, R., Setlow, P., Reitz, G., & Nicholson, W. (2009). Roles of small, acid-soluble spore proteins and core water content in survival of Bacillus subtilis spores exposed to environmental solar UV radiation. *Applied and Environmental Microbiology*, *75*(16), 5202–5208. doi:10.1128/AEM.00789-09

565 Moisan, M. et al., 2001. Low-temperature sterilization using gas plasmas: a review of the
566 experiments and an analysis of the inactivation mechanisms. *International journal of*
567 *pharmaceutics*, 226(1–2), pp.1–21.

568 Moisan, M., Barbeau, J., Crevier, M.-C., Pelletier, J., Philip, N., & Saoudi, B. (2002). Plasma
569 sterilization. Methods and mechanisms. *Pure and Applied Chemistry*, *74*(3), 349–358.
570 doi:10.1351/pac200274030349

571 Nicholson, W. L., & Setlow, P. (1990). Sporulation, germination and outgrowth. In C. R.
572 Harwood, S. m Cutting, & R. Chambert (Eds.), *Molecular biological methods for*
573 *Bacillus* (pp. 391–450). Chichester Wiley.

574 Paidhungat, M., Ragkousi, K., & Setlow, P. (2001). Genetic Requirements for Induction of
575 Germination of Spores of Bacillus subtilis by Ca 2 + -Dipicolinate Genetic Requirements
576 for Induction of Germination of Spores of Bacillus subtilis by Ca 2 ☒-Dipicolinate.
577 *JOURNAL OF BACTERIOLOGY*, *183*(16), 4886–4893. doi:10.1128/JB.183.16.4886

578 Paidhungat, M., Setlow, B., & Driks, A. (2000). Characterization of Spores of Bacillus
579 subtilis Which Lack Dipicolinic Acid Characterization of Spores of Bacillus subtilis
580 Which Lack Dipicolinic Acid. *JOURNAL OF BACTERIOLOGY*, *182*(19), 5505–5512.
581 doi:10.1128/JB.182.19.5505-5512.2000.Updated

582 Pankaj, S. K., Bueno-Ferrer, C., Misra, N. N., Milosavljević, V., O'Donnell, C. P., Bourke,
583 P., … Cullen, P. J. (2014). Applications of cold plasma technology in food packaging.
584 *Trends in Food Science & Technology*, *35*(1), 5–17. doi:10.1016/j.tifs.2013.10.009

585 Pedraza-Reyes, M., Ramírez-Ramírez, N., Vidales-Rodríguez, L., & Robleto, E. (2012).
586 Mechanisms of bacterial spore survival. In E. Abel-Santos (Ed.), *Bacterial spores:*
587 *current research and applications* (pp. 73–87). Caister Academic Press.

588 Popham, D. L., Sengupta, S., & Setlow, P. (1995). Heat, hydrogen-peroxide, and UV
589 resistance of Bacillus subtilis spores with increased core water-content and with or
590 without major DNA-binding proteins. *Applied and Environmental Microbiology*, *61*(10),
591 3633–3638. Retrieved from <Go to ISI>://WOS:A1995RY07100020

592 Raguse, M., Fiebrandt, M., Denis, B., Stapelmann, K., Eichenberger, P., Driks, A., …
593 Moeller, R. (2016). Understanding of the importance of the spore coat structure and
594 pigmentation in the Bacillus subtilis spore resistance to low-pressure plasma sterilization.
595 *Journal of Physics D: Applied Physics*, *49*(28), 285401. doi:10.1088/0022-
596 3727/49/28/285401

597 Reineke, K., Langer, K., Hertwig, C., Ehlbeck, J., & Schlüter, O. (2015). The impact of
598 different process gas compositions on the inactivation effect of an atmospheric pressure
599 plasma jet on Bacillus spores. *Innovative Food Science and Emerging Technologies*.

600 Riesenman, P. J., & Nicholson, W. L. (2000). Role of the spore coat layers in Bacillus subtilis
601 spore resistance to hydrogen peroxide, artificial UV-C, UV-B, and solar UV radiation.
602 *Applied and Environmental Microbiology*, *66*(2), 620–626. doi:10.1128/AEM.66.2.620-
603 626.2000

604 Roth, S., Feichtinger, J., & Hertel, C. (2010). Characterization of Bacillus subtilis spore
605 inactivation in low-pressure, low-temperature gas plasma sterilization processes. *Journal*
606 *of Applied Microbiology*, *108*(2), 521–31. doi:10.1111/j.1365-2672.2009.04453.x

607 Setlow, B. & Setlow, P., 1993. Binding of small, acid-soluble spore proteins to DNA plays a
608 significant role in the resistance of Bacillus subtilis spores to hydrogen peroxide. Applied
609 and Environmental Microbiology, 59(10), pp.3418–3423.

610 Setlow, B. & Setlow, P., 1995. Small , acid-soluble proteins bound to DNA protect Bacillus
611 subtilis spores from killing by dry heat . Applied and environmental microbiology, 61(7),

612 pp.2787–2790.

613 Setlow, P., 2001. Resistance of spores of Bacillus species to ultraviolet light. Environmental
614 and molecular mutagenesis, 38(2–3), pp.97–104.

615 Setlow, B. et al., 2006. Role of dipicolinic acid in resistance and stability of spores of Bacillus
616 subtilis with or without DNA-protective α/β-type small acid-soluble proteins. *Journal of*
617 *Bacteriology*, 188(11), pp.3740–3747.

618 Setlow, P. (2006). Spores of Bacillus subtilis: their resistance to and killing by radiation, heat
619 and chemicals. *Journal of Applied Microbiology*, *101*(3), 514–525. doi:10.1111/j.1365-
620 2672.2005.02736.x

621 Setlow, P. (2014). Spore Resistance Properties. *Microbiology Spectrum*, *2*(5), 1–14.
622 doi:10.1128/microbiolspec.TBS-0003-2012

623 Siemens, W. (1857). Ueber die elektrostatische Induction und die Verzögerung des Stroms in
624 Flaschendrähten. *Annalen Der Physik*, *178*(9), 66–122.

625 Slieman, T., & Nicholson, W. (2001). Role of Dipicolinic Acid in Survival of Bacillus subtilis
626 Spores Exposed to Artificial and Solar UV Radiation Role of Dipicolinic Acid in
627 Survival of Bacillus subtilis Spores Exposed to Artificial and Solar UV Radiation.
628 *Society*, *67*(3), 1274–1279. doi:10.1128/AEM.67.3.1274

629 Surowsky, B., Schlüter, O., & Knorr, D. (2014). Interactions of Non-Thermal Atmospheric
630 Pressure Plasma with Solid and Liquid Food Systems: A Review. *Food Engineering*
631 *Reviews*. doi:10.1007/s12393-014-9088-5

632 Wang, S., Doona, C., Setlow, P., & Li, Y. (2016). Use of Raman Spectroscopy and Phase-
633 Contrast Microscopy To Characterize Cold Atmospheric Plasma Inactivation of
634 Individual. *Applied and Environmental Microbiology*, *82*(19), 5775–5784.

635 doi:10.1128/AEM.01669-16.Editor

636 Weltmann, K.-D., Brandenburg, R., von Woedtke, T., Ehlbeck, J., Foest, R., Stieber, M., &
637 Kindel, E. (2008). Antimicrobial treatment of heat sensitive products by miniaturized
638 atmospheric pressure plasma jets (APPJs). *Journal of Physics D: Applied Physics*,
639 *41*(19). doi:10.1088/0022-3727/41/19/194008

640 Young, S. B., & Setlow, P. (2004). Mechanisms of Bacillus subtilis spore resistance to and
641 killing by aqueous ozone. *Journal of Applied Microbiology*, *96*(5), 1133–1142.
642 doi:10.1111/j.1365-2672.2004.02236.x

643

Figure captions:

Figure 1: Scheme of the DCSBD plate (Hertwig et al. 2016).

Figure 2: Treatment chamber: A) consisting of one DCSBD plate and B) of two DCSBD plates (Hertwig et al. 2016).

Figure 3: Emission spectra measured with a distance of 1 mm to the DCSBD plate for the used process gases: A) dry air (blue line) and N_2 (red dashed line), B) O_2 (green dashed dotted line) and CO_2 (purple short dashed line).

Figure 4: Relative intensities for plasma generated with the process gases air and N_2 in the UV-A (320-400 nm), UV-B (280-320 nm) and UV-C range (200-280 nm).

Figure 5: A) generated concentration of ozone inside the treatment chamber for the process gases: O_2 (▲) and CO_2 (▼). B) Temperature profile of the plasma for the used process gases: dry air (blue line), N_2 (red dashed line), O_2 (green dashed dotted line) and CO_2 (purple short dashed line).

Figure 6: Inactivation kinetics for *Bacillus subtilis* wild type spores for the process gases: Air (■), N_2 (●) O_2 (▲) and CO_2 (▼).

Figure 7: Inactivation kinetics for *Bacillus subtilis* isogenic mutant spores; A) PS578, B) FB122 and C) PS3328, for the process gases: Air (■), N_2 (●) O_2 (▲) and CO_2 (▼).

Figure 8: Inactivation kinetics for *Bacillus atrophaeus* spores for the process gases: Air (■), N_2 (●) O_2 (▲) and CO_2 (▼).

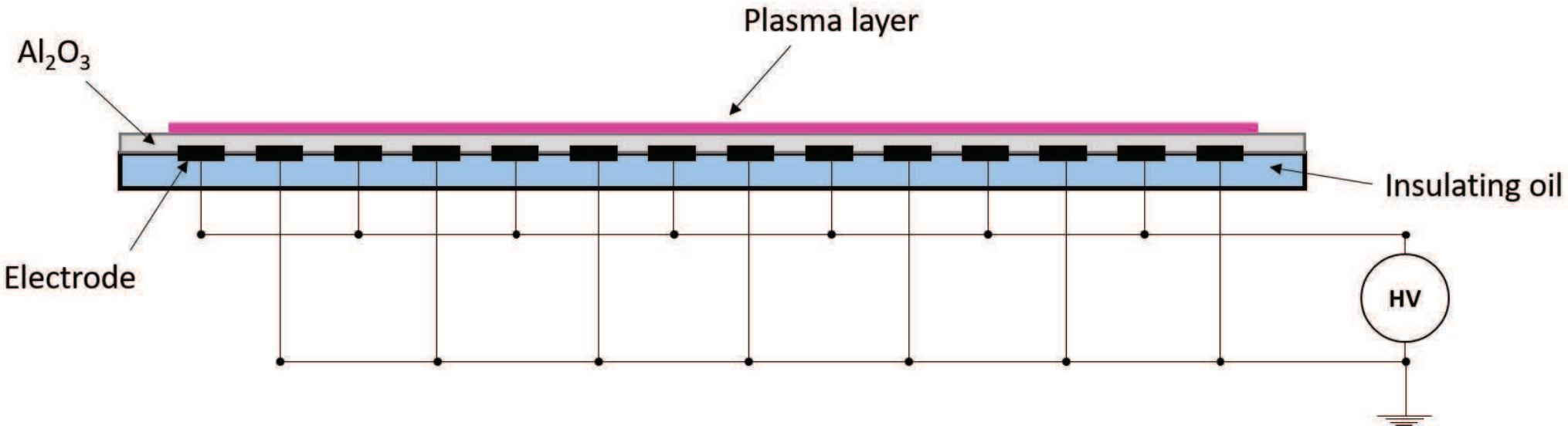
Plasma layer
Al_2O_3
Insulating oil
Electrode
HV

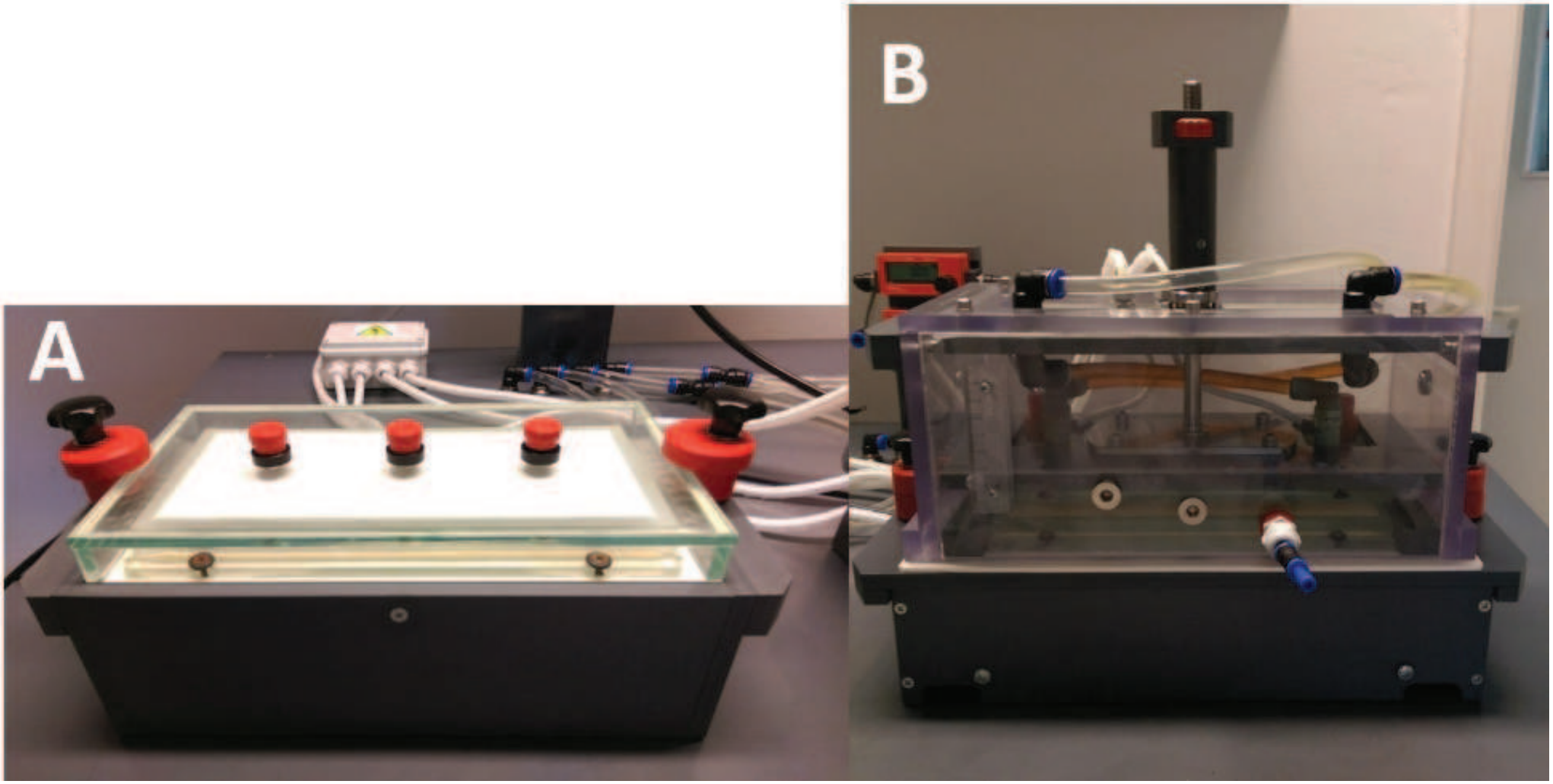
A
B

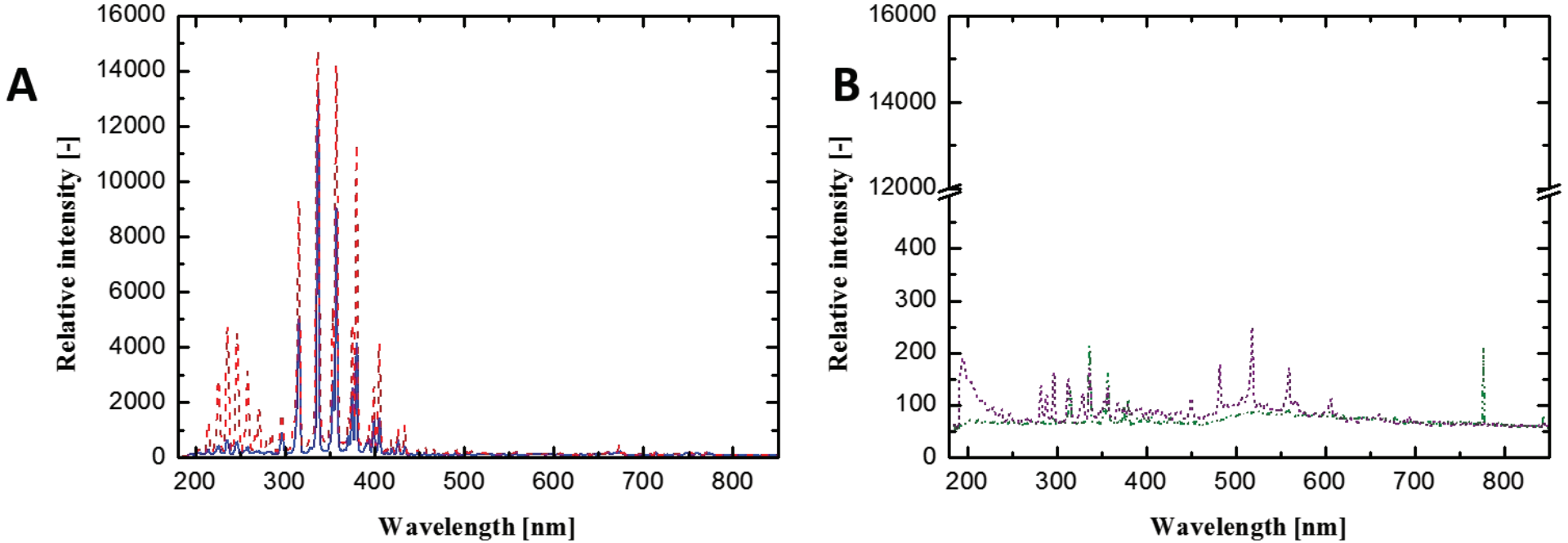
A
Relative intensity [-]
16000
14000
12000
10000
8000
6000
4000
2000
0
200
300
400
500
600
700
800
Wavelength [nm]
B
Relative intensity [-]
16000
14000
12000
400
300
200
100
0
200
300
400
500
600
700
800
Wavelength [nm]

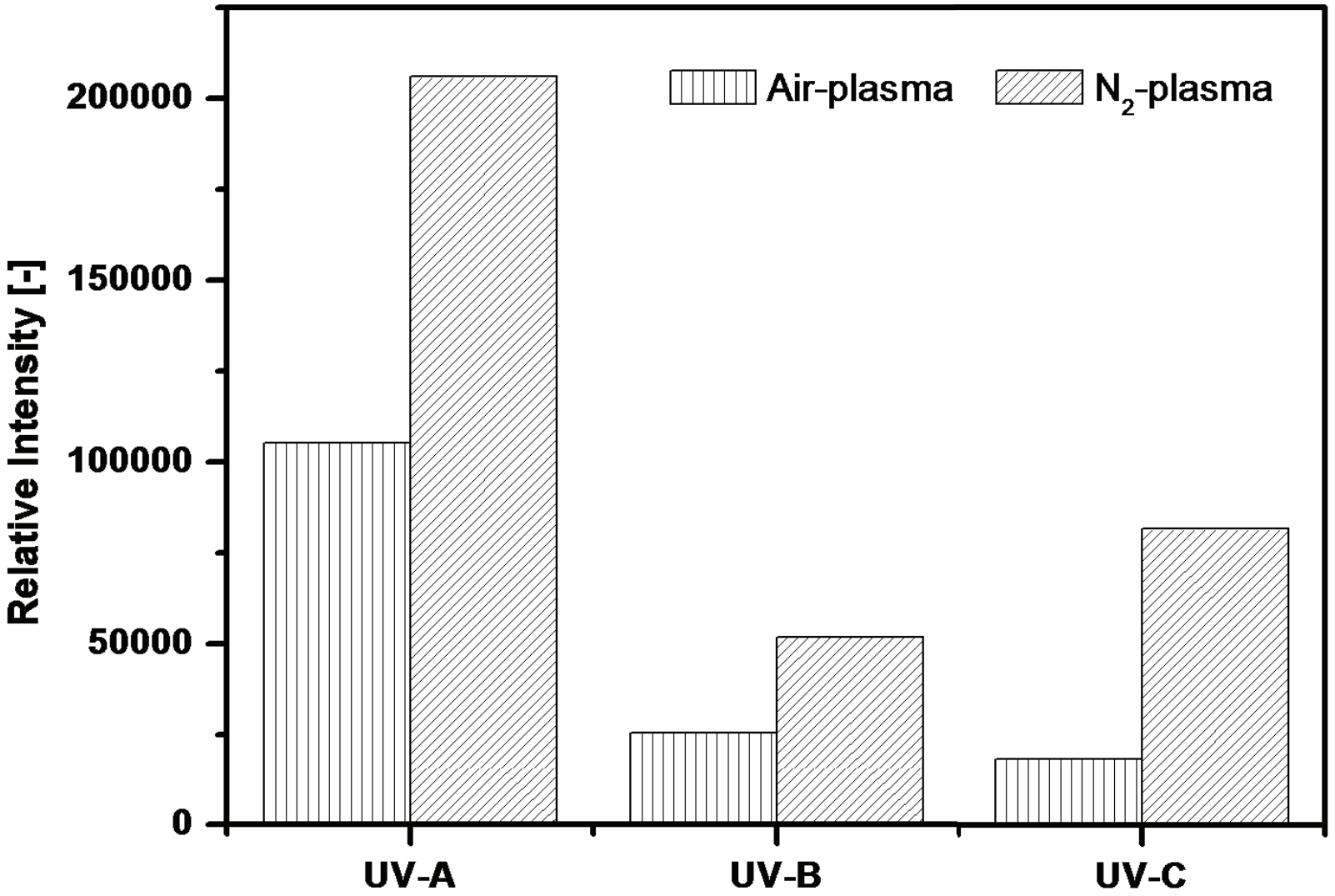
Air-plasma
N2-plasma
Relative Intensity [-]
200000
150000
100000
50000
0
UV-A
UV-B
UV-C

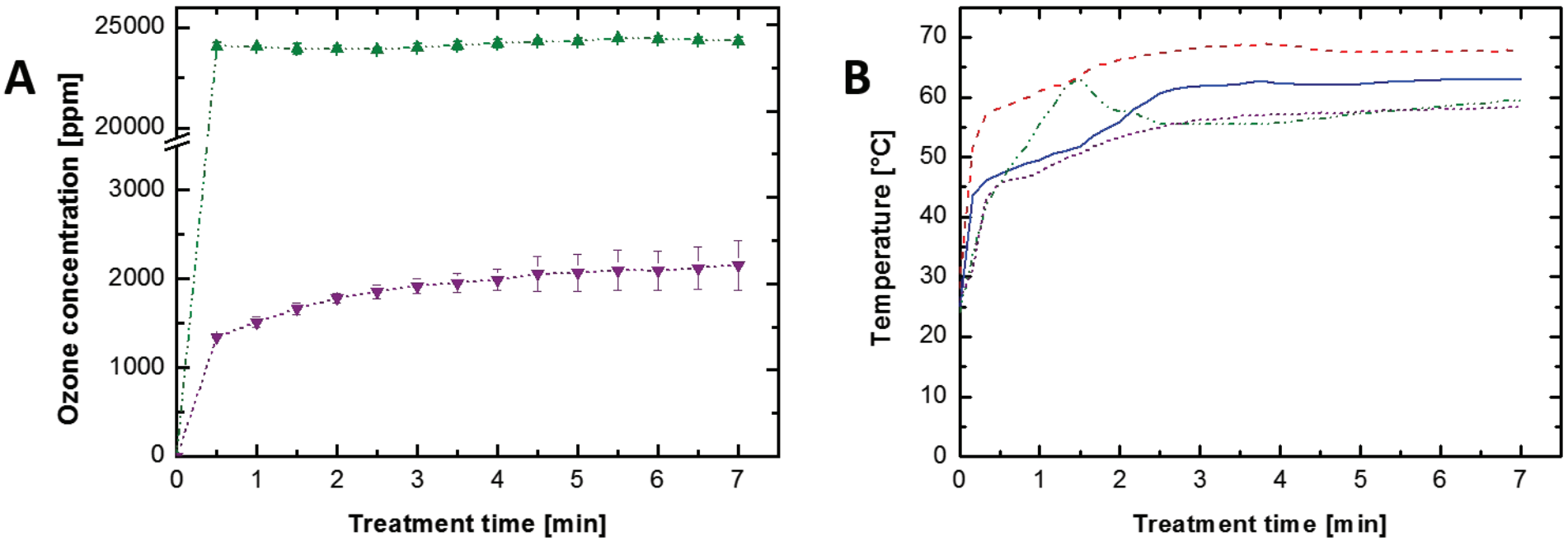
A
Ozone concentration [ppm]
25000
20000
3000
2000
1000
0
0
1
2
3
4
5
6
7
Treatment time [min]
B
Temperature [°C]
70
60
50
40
30
20
10
0
0
1
2
3
4
5
6
7
Treatment time [min]

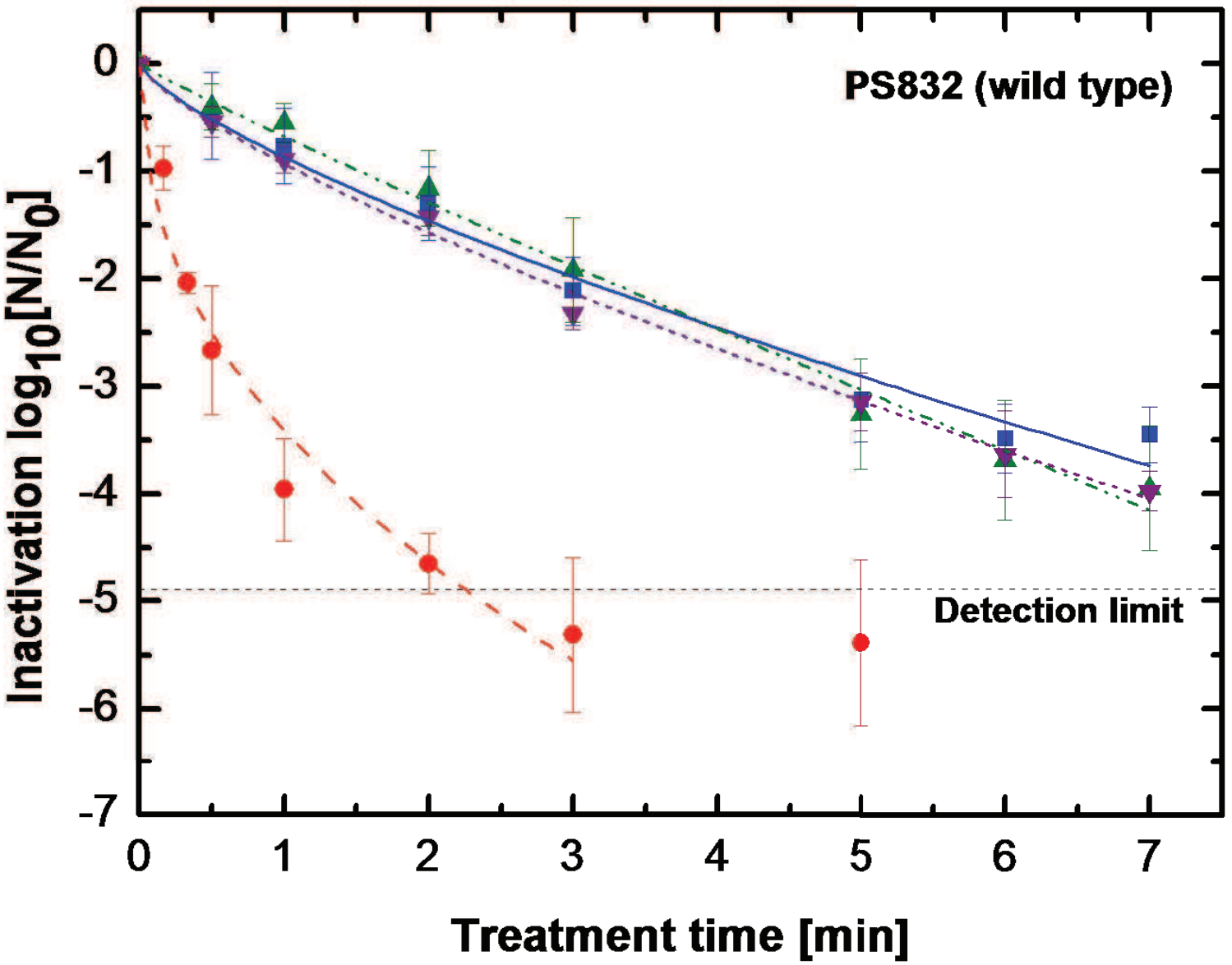
PS832 (wild type)
Detection limit
Inactivation log10[N/N0]
Treatment time [min]
0
-1
-2
-3
-4
-5
-6
-7
0
1
2
3
4
5
6
7

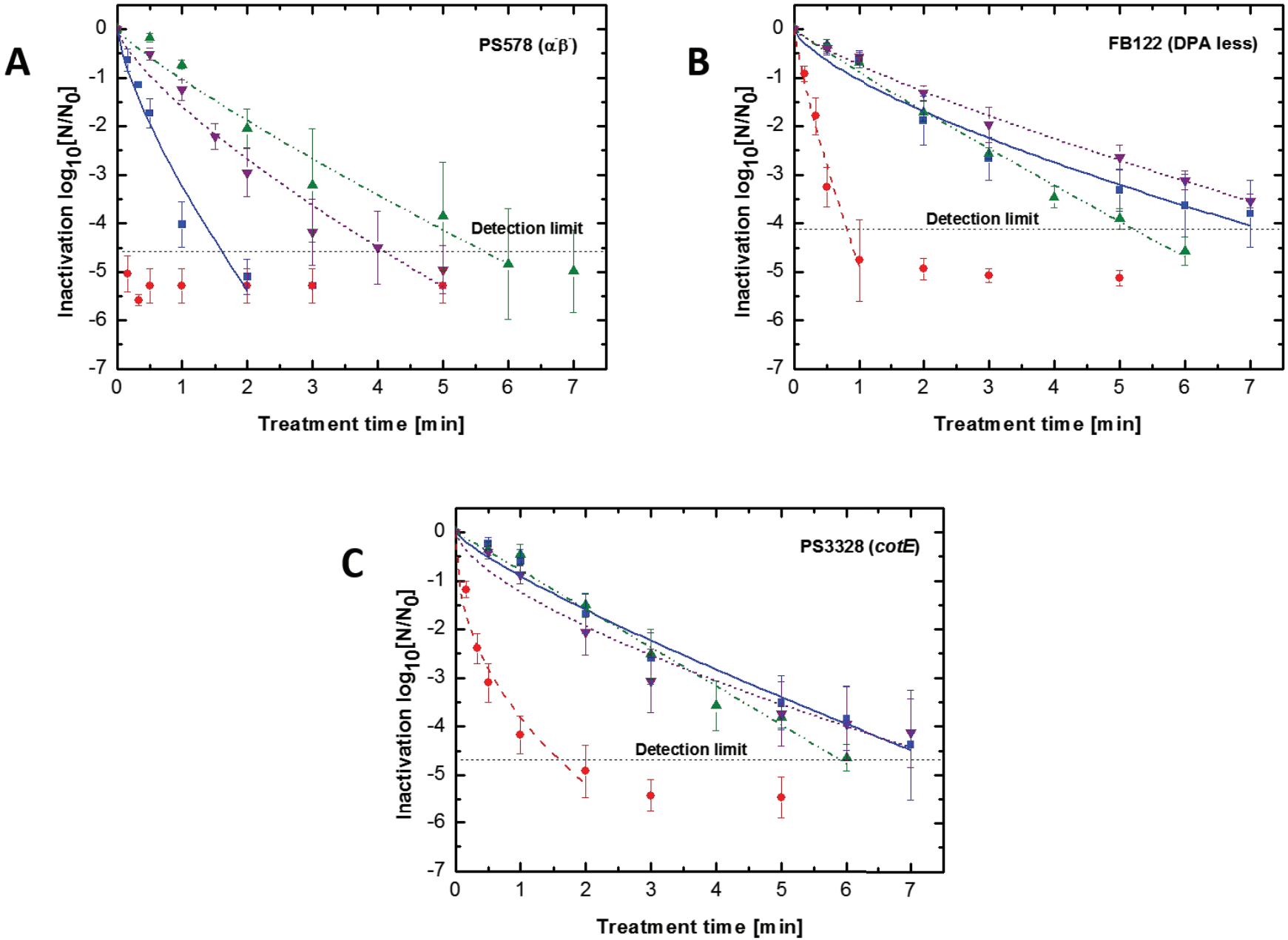
A
PS578 (α⁻β⁻)
Inactivation log10[N/N0]
Detection limit
Treatment time [min]
B
FB122 (DPA less)
Inactivation log10[N/N0]
Detection limit
Treatment time [min]
C
PS3328 (cotE)
Inactivation log10[N/N0]
Detection limit
Treatment time [min]

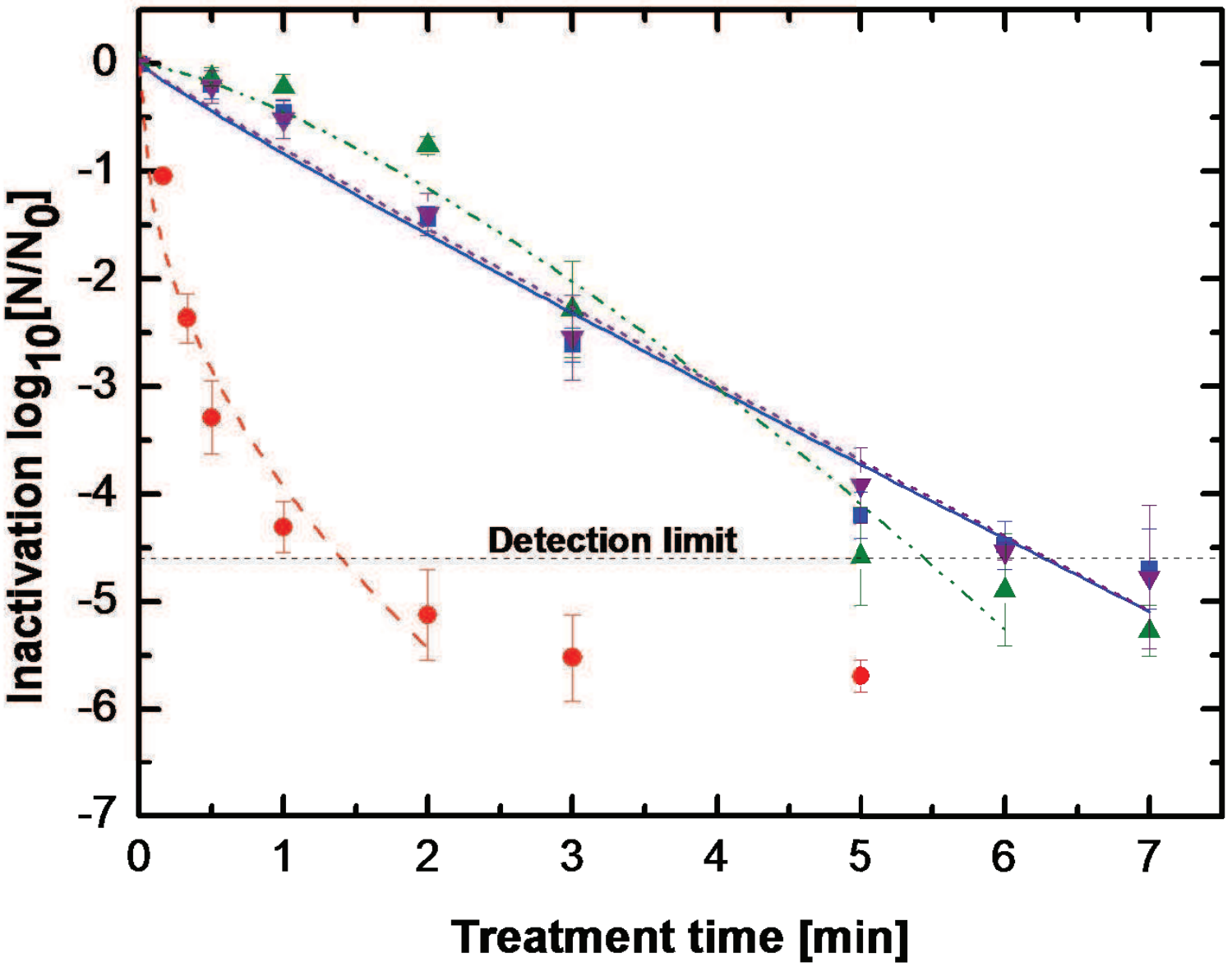
Inactivation log10[N/N0]
0
-1
-2
-3
-4
-5
-6
-7
Detection limit
0
1
2
3
4
5
6
7
Treatment time [min]

Table 1: Statistical parameters of Weibullian power law model and D-values for *Bacillus subtilis* wild type spores.

	b	n	D-value [min]	Adj. R^2	RMSE
Air-plasma	0.87	0.75	1.21	0.98	0.19
N_2-plasma	3.41	0.44	0.06	0.96	0.38
O_2-plasma	0.68	0.93	1.52	0.99	0.15
CO_2-plasma	0.93	0.76	1.10	1.00	0.10

Table 2: Statistical parameters of Weibullian power law model and D-values for *Bacillus subtilis* isogenic mutant spores.

PS578					
	b	n	D-value [min]	Adj. R^2	RMSE
Air-plasma	3.23	0.74	0.20	0.95	0.47
N_2-plasma	-	-	-	-	-
O_2-plasma	1.04	0.86	0.96	0.96	0.36
CO_2-plasma	1.60	0.75	0.53	0.96	0.37
FB122					
	b	n	D-value [min]	Adj. R^2	RMSE
Air-plasma	1.05	0.70	0.94	0.96	0.30
N_2-plasma	4.89	0.81	0.14	0.97	0.34
O_2-plasma	0.88	0.93	1.14	0.99	0.15
CO_2-plasma	0.73	0.81	1.47	0.99	0.10
PS3328					
	b	n	D-value [min]	Adj. R^2	RMSE
Air-plasma	0.90	0.82	1.13	0.98	0.24
N_2-plasma	3.82	0.44	0.05	0.96	0.38
O_2-plasma	0.79	1.01	1.27	0.98	0.24
CO_2-plasma	1.23	0.66	0.73	0.96	0.33

Table 3: Statistical parameters of Weibullian power law model and the time for the first decimal reduction for *Bacillus atrophaeus* wild type spores.

	b	n	D-value [min]	Adj. R^2	RMSE
Air-plasma	0.83	0.93	1.22	0.97	0.34
N_2-plasma	3.93	0.47	0.05	0.94	0.47
O_2-plasma	0.45	1.38	1.80	0.97	0.36
CO_2-plasma	0.79	0.96	1.28	0.98	0.25

Highlights

- CAPP treatment of *Bacillus subtilis* spores, *Bacillus subtilis* mutant spore strains and *Bacillus atrophaeus* spores
- Characterization of the different generated plasma
- Characterization of *Bacillus subtilis* spore properties involved in resistance towards CAPP

6. Decontamination of whole black pepper using different cold atmospheric pressure plasma applications

In: Food Control, 55, p. 221-229, 2015

Cite as:

Hertwig, C., Reineke, K., Ehlbeck, J., Knorr, D., Schlüter, O., 2015. Decontamination of whole black pepper using different cold atmospheric pressure plasma applications. Food Control. 50: 221–229.

doi: http://dx.doi.org/10.1016/j.foodcont.2015.03.003

Food Control 55 (2015) 221–229

Contents lists available at ScienceDirect

Food Control

journal homepage: www.elsevier.com/locate/foodcont

Decontamination of whole black pepper using different cold atmospheric pressure plasma applications

Christian Hertwig [a], Kai Reineke [a], Jörg Ehlbeck [b], Dietrich Knorr [c], Oliver Schlüter [a, *]

[a] Leibniz Institute for Agricultural Engineering, Max-Eyth-Allee 100, 14469, Potsdam-Bornim, Germany
[b] Leibniz Institute for Plasma Science and Technology, Felix-Hausdorff-Straße 2, 17489, Greifswald, Germany
[c] Department of Food Biotechnology and Food Process Engineering, Berlin University of Technology, Königin-Luise-Straße 22, 14195, Berlin, Germany

ARTICLE INFO

Article history:
Received 11 January 2015
Received in revised form
2 March 2015
Accepted 3 March 2015
Available online 11 March 2015

Keywords:
Bacterial endospores
Salmonella
Atmospheric pressure plasma jet
Spices
Decontamination
Quality

ABSTRACT

Whole black pepper is a dry product, which is often naturally contaminated with bacterial endospores and sometimes also with human pathogens like Salmonella. Dry pepper itself is a shelf-stable product, but if it is incorporated into high moisture minimally processed food, the microorganisms can reduce the shelf-life of the final product and/or can cause foodborne diseases. In this study the antimicrobial effect of two different atmospheric pressure plasma applications for the decontamination of whole black pepper was investigated. Naturally contaminated peppercorns and with *Bacillus subtilis* spores, *Bacillus atrophaeus* spores and *Salmonella enterica* inoculated ones were treated using a plasma jet or a microwave-driven remote plasma. Surface color and the content of essential oils and piperine was measured. *S. enterica*, *B. subtilis* spores and *B. atrophaeus* spores were reduced by 4.1, 2.4 and 2.8 log, respectively, after 30 min remote plasma treatment. Direct plasma jet treatment did not result in equivalent inactivation levels. However, both plasma applications did not considerable affect the quality parameters.

1. Introduction

Pepper is one of the most frequently used and imported spices in the EU (CBI., 2010). In general pepper can have a high microbial load with viable counts greater than 10^7 cfu/g and most of them are spore-forming bacteria (Boer, Spiegelenberg, & Janssen, 1985; Piggott & Othman, 1993). Further, black peppercorns can also be spoiled with human pathogens like the spore-forming *Bacillus cereus* and *Clostridium perfringens*; and Salmonella (Boer et al., 1985). The hygienic handling conditions of herbs and spices, during harvest and following processes like drying, in their country of origins determines the initial level of bacterial contamination. Due to the low water activity on the seed surface the present microorganism cannot grow and multiply. However, dry stress resistant microorganisms, like bacterial spores or some types of Salmonella, are still viable and have the ability to multiply if the product is rehydrated and a sufficient amount of nutrients is available. Though contaminated pepper can cause foodborne diseases, besides being responsible for a drastical reduction of the product's shelf-life. Of special concern are ready-to-eat food products, because they are not subjected to further heat treatments (Little, Omotoye, & Mitchell, 2003). In 2010 contaminated red and black pepper, which was incorporated in salami, was the reason for a Salmonella outbreak in 44 states of the United States (Gieraltowski et al., 2013).

The current decontamination technologies for herbs and spices are thermal or chemical treatments, like steam treatments and fumigation, besides the irradiation with gamma rays (Schweiggert, Carle, & Schieber, 2007). The fumigation with ethylene oxide and the gamma irradiation are quite efficient. However the use of ethylene oxide can lead to carcinogenic byproducts and is banned by law in the European Union (Schweiggert et al., 2007; Tateo & Bononi, 2006). Irradiation can be applied only in authorized facilities and in controlled doses in order to be safe and harmless; moreover it has a poor consumer acceptance. Steam treatment is extensively used in the European herbs and spices industry. For spices with an high microbial load, like pepper, this method is not recommended due to its low reduction effect and the possible alterations in aroma and odor (Schweiggert et al., 2007; Tainter & Grenis, 2001). Therefore the development of alternative processes becomes necessary; a potential technology could be the application of cold plasma.

* Corresponding author. Tel.: +49 331 5699 613.
E-mail address: oschlueter@atb-potsdam.de (O. Schlüter).

http://dx.doi.org/10.1016/j.foodcont.2015.03.003
0956-7135/

Cold atmospheric pressure plasma (CAPP) is a non-thermal technology, which enables a microbial multi target inactivation on food surface. Plasma is either a partially or complete ionized gas and is the fourth state of matter. Cold plasma can be generated under atmospheric and low-pressure conditions, using radio frequency or microwave sources. Plasma applications working under atmospheric pressure have already antimicrobial effects at temperatures below 40 °C (Fröhling, Baier, Ehlbeck, Knorr, & Schlüter, 2012; Knorr et al., 2011). The generated plasma contains different reactive species, like free radicals and charged particles, furthermore heat and UV light, being responsible for the antimicrobial plasma effects (Laroussi, 2002; Moisan et al., 2002). The working gas used and other process parameters determine the concentration of these different reagents (Ehlbeck et al., 2011; Weltmann et al., 2008). Various studies showed the potential of non-thermal atmospheric plasmas to inactivate vegetative bacteria, molds and bacterial endospores on almonds (Deng et al., 2007), fresh pork meat (Fröhling, Durek, et al., 2012) or on different herbs and spices (Hertwig et al., 2015). Furthermore, the emitted reactive reagents may react with lipids, protein, carbohydrates or other food components (Schlüter et al., 2013). A detailed review about the interaction of CAPP with various food systems was given by Surowsky, Schlüter and Knorr (2014). Hertwig et al. (2015) showed a product-specific alteration of the color after non-thermal remote plasma treatment, the plasma treatment had no impact on the color of black peppercorns. In food microbiology models of inactivation kinetics are useful to describe the destruction of microbial populations, since the knowledge about the quantity of surviving microorganisms is essential to guarantee food quality. Various studies on the inactivation of *Bacillus* spores by direct plasma treatment reported biphasic inactivation kinetics (Moisan et al., 2002; Moreau et al., 2000). They assume an inactivation process depending on different mechanisms, like the inactivation due to UV light and the decomposition of the microorganism through photodesorption and etching.

The objective of this study was to investigate the antimicrobial effect of two different plasma sources for the decontamination of whole black pepper. A microbial characterization of the used whole black peppercorns was done, to determine the main spoiling microorganisms. Naturally contaminated peppercorns and with *Bacillus subtilis*, *Bacillus atrophaeus* spores and *Salmonella enterica* inoculated samples were treated. *B. atrophaeus* was chosen as the surrogate microorganism for chemical and physical inactivation processes. Furthermore the surface color, the content of volatile oils and the main aroma compound of pepper, piperine, were measured, to estimate the impact of the plasma treatment on the product quality.

2. Materials and methods

2.1. Growth of bacteria and spore preparation

S. enterica DSM 17058 was stored on cryo beads (Carl Roth GmbH, Karlsruhe, Germany) at −80 °C. One cryo bead was added to 5 ml sterile nutrient broth (Carl Roth GmbH, Karlsruhe, Germany) and incubated at 37 °C for 24 h under continuous shaking (125 rpm). Afterwards, the optical density of the pre-culture was measured at 620 nm (OD_{620}) and 25 ml of nutrient broth was inoculated with *S. enterica* cell suspension, corresponding to a start OD of 0.07. The cell culture was incubated for 24 h at 37 °C under continuous shaking (125 rpm) to achieve *S. enterica* cell cultures in the stationary phase. Each day, a fresh prepared *S. enterica* culture was used.

Bacillus spore strains used in this study, *B. subtilis* (PS 832) and *B. atrophaeus* (WIS 39 6/3), were sporulated using a method described elsewhere (Nicholson & Setlow, 1990). Sporulation was induced at 37 °C on solid 2x SG medium agar plates without antibiotics. The spore suspension was cleaned by repeated centrifugation (3-fold at 5000 *g*), washed with cold distilled water (4 °C), and was treated intermittently with sonication for 1 min. The clean spore suspensions contained ≥95% phase bright spores and nearly no spore agglomerates. The spore suspension was stored in the dark at 4 °C.

2.2. Sample preparation

Whole Black peppercorns (*Piper nigrum*) were purchased from JJ Albarracin (Murcia, Spain). 3.5 g of sterile peppercorns were placed into a sterile beaker and 175 μL (*Bacillus* spores) or 350 μL (*S. enterica*) cell suspension was added. The beaker was placed on an automatic shaker and shaken for 4 min at 400 rpm to obtain a homogenous coating of the microorganisms on the seed surface. The seeds inoculated with *Bacillus* spores were placed under a clean bench and allowed to dry for 30 min at room temperature. Salmonella inoculated samples were dried for 16 h to obtain a natural selection towards drought stress resistant one. The initial contamination of the inoculated microorganisms on peppercorns was approximately 10^7 cfu/g.

2.3. Plasma sources and plasma treatment

Two different types of plasma devices were used. A direct plasma treatment with a radio frequency (rf) plasma jet and an remote treatment with a microwave generated plasma. The rf-plasma jet equipment is described elsewhere in detail (Brandenburg et al., 2007). The apparatus consists of a ceramic nozzle (nozzle tip diameter approx. 7 mm) with a needle electrode inside, a grounded ring electrode at the nozzle outlet, an rf-generator and a gas supply system. The rf-voltage is coupled with the needle electrode. The plasma is generated at the tip of this electrode and expands into the air outside the nozzle. Depending on the gas flow rate and the application power the plasma had a length of up to 30 mm and a diameter of about 8 mm. Before the plasma treatment, the atmospheric pressure plasma jet was let run at experimental conditions for 15 min to allow preheating and passivation of the electrodes. For the treatment argon was used as working gas with a gas flow of 10 standard liter per minute (slm) and an operation power of 30 W. 1 g non-inoculated and inoculated black peppercorns were place in individual sterile petri dishes (30 mm diameter) and placed on an automatic shaker below the collimated plasma beam with a distance of 12 mm to the nozzle outlet. During the treatment the seeds were shaken continuously (at 250 rpm) to obtain a homogenous distribution of plasma on the surface layer of the seeds. The samples were treated up to 15 min.

For the remote CAPP treatment plasma processed air (PPA) was used. The PPA was generated by a microwave-driven plasma torch (PLexc®, INP, Greifswald, Germany). The microwaves had a frequency of 2.45 GHz and a power consumption of 1.2 kW. The process gas was air with a gas flow of 18 slm (standard liter per minute, 30.3975 $(Pa*m^3)/s$). The generated microwave plasma had a peak temperature of about 3700 °C. An optical emission spectrum of the used microwave plasma torch is shown by Pipa, Andrasch, Rackow, Ehlbeck, and Weltmann (2012). The plasma generating device (Fig. 1) was connected with a 25 cm long metal tube to a concentration bottle, which was connected to the reaction chamber (250 ml sterile glass bottle). During the way in the concentration bottle the PPA cooled down to 120 °C and inside further to 22 °C. 3.5 g of non-inoculated and inoculated pepper, respectively, was transferred into the reaction chamber. After filling the reaction chamber with the PPA, the bottles were shaken to obtain a

Fig. 1. Experimental set-up of the remote plasma treatment, (1) microwave torch, (2) cooling system, (3) gas reservoir, (4) filling system.

homogenous treatment. The peppercorns were treated up to 30 min. After the treatment the remaining PPA was removed. Trials were carried out at least in duplicate.

2.4. Optical emission spectroscopy

A Black Comet UV-VIS Spectrometer (StellarNet Inc., Tampa, USA) equipped with an F400 UV-VIS-SR fibre optic was used to measure the emission spectrum of the direct CAPP set-up. The spectrum was measured in the range from 190 to 850 nm. The distance from the middle of the nozzle outlet to the middle of the detector was 10 mm in vertical and 12 mm in the horizontal axis. The spectrum was measured 10 times with an integration time of 100 ms. The average spectrum was base-line corrected and normalized (between $\lambda = 450–470$ nm) using a self-written LabVIEW routine.

2.5. Viable cell counts

The viable cell count after the CAPP treatment was determined by cell culture methods in duplicate. The recovery of the microorganisms was carried out by shaking the seeds in ACES-buffer solution with pH 7 (0.05 M) for 3 min at 400 rpm. The obtained suspensions were serially diluted in ACES-buffer solution. *B. subtilis*, *B. atrophaeus* and *S. enterica* solutions were plated on nutrient-agar plates (Carl Roth GmbH, Karlsruhe, Germany). The plates were incubated at 37 °C for 24 h and the colony forming units (cfu) were counted. For native contaminated peppercorns bacterial spores and total mesophilic aerobic count were analyzed. For total mesophilic aerobic count plate-count-agar plates (Carl Roth GmbH, Karlsruhe, Germany) and for bacterial spores nutrient-agar plates were used. The agar plates of the native contaminated samples were incubated for 72 h at either 30 °C (total mesophilic aerobic count) or 37 °C (bacterial spores) and counted each day. The obtained inactivation kinetics were modeled with GInaFiT (Geeraerd and Van Impe Inactivation Model Fitting Tool), Add-Inn for Microsoft ® Excel. The inactivation kinetics obtained by the direct CAPP treatment were modeled using a biphasic inactivation model (Eq. (1)) (Cerf, 1977):

$$log_{10}S(t) = \varphi \cdot e^{k_1 \cdot t} + (1 - \varphi) \cdot e^{k_2 \cdot t} \quad (1)$$

where S(t) is $N(t)/N_0$, with N(t) as the number of colony forming units at the time t and N_0 as the initial number of colony forming units, φ is a constant designating the transition from the first inactivation phase to the second were k_1 and k_2 represent corresponding rate constants.

The inactivation kinetics obtained by the remote CAPP treatment were modeled using the Weibull model (Eq. (2)):

$$log_{10}S(t) = -(t/\delta)^p \quad (2)$$

where S(t) is also $N(t)/N_0$, with N(t) as the number of colony forming units at the time t and N_0 as the initial number of colony forming units, δ is the scale parameter and p is the shape parameter.

2.6. Microbial characterization

The full microbial characterization of the used peppercorns was done according the respective ISO standards (Table 1) on selective agar plates.

2.7. Scanning electron microscopy

Zeiss DSM 982 GEMINI SEM was used to take micrographs of inoculated *B. atrophaeus* spores on the surface of black peppercorns. The samples were dehydrated, critical point dried and sputtered with carbon. The samples were critical point dried using a method described elsewhere (Reineke et al., 2013). The following vaporization with carbon made the sample conductive.

2.8. Determination of quality parameters

The sample color appearance was measured using a colorimeter (Konica Minolta) based on the CIE L*a*b* colorimetric system. Each color sample was measured in triplicate and the average values were calculated. For the determination of piperine a high performance liquid chromatography method according to the DIN ISO 10235 standard was used. Whole peppercorns were finely ground, so that the sample could pass through a 500 μm sieve. 50 ml ethanol was added to 1 g pepper powder inside a rotary evaporator connected to a condenser. The mix was cooked under reflux for 3 h and filtrated. The filtrate was stored in the dark until analyzing. The content of volatile oils was measured in accordance with DIN ISO 6571 using a steam distillation process. Therefore an aqueous suspension of finely grounded pepper was distilled for 4 h. The

Table 1
Overview of analytical methods.

Microorganism	Analytical method of reference
Salmonella	ISO 6579:2002
Presumptive *B. cereus*	ISO 7932:2004
Escherichia coli	ISO 16649-2:2001
Coagulase-positive Staphylococcus	ISO 6888-1:1999
Clostridium perfringens	ISO 7937:2004
Molds and yeasts	European Pharmacopeia 6.7. Apt. 2.6.12
Sulf-red anaerobes	ISO 15213:2003
Enterobacteriaceae	ISO 21528-2:2004

distillate was collected and a defined volume of xylene was added to bind the volatile oils. The volume of the organic phase was measured and the content of volatile oils calculated. The volatile oil and piperine content was measured in duplicate for longest direct and remote plasma treatment.

3. Results and discussion

3.1. Microbial characterization

The results of the microbial characterization are shown in Table 2 and point out the high contamination level of whole black pepper corn with up to $1.0*10^8$ cfu/g. The detected contamination level is comparable to other studies (McKee, 1995). The main spoiling microorganisms on pepper are aerobic endospores with a concentration of $5.6*10^7$ cfu/g, with $5.6*10^7$ cfu/g presumptive *B. cereus* spores. Besides those human pathogens like *C. perfringens*, *Staphylococcus* and Salmonella were detected. The microbial characterization showed that for the industrial target of a total plate count below $1.0*10^4$ cfu/g (personal communication Gerhard Weber Association of the German Spice Industry) of whole black pepper, the focus will be on the inactivation of the highly resistant bacterial spores. Furthermore the inactivation of Salmonella is of special interest, since industry requires herbs and spices free of Salmonella for addition in dairy products.

3.2. Direct CAPP treatment of inoculated and naturally contaminated pepper

The emission spectra from the used radio frequency argon driven plasma jet is shown in Fig. 2A. Besides the spectral lines of the different excited argon states spectral lines of various impurities were also measured. Due to interaction of the argon plasma with the surrounding air molecular bands of oxygen, nitrogen and other species were detected. The intensity of the signal in the UV-C range from 200 to 280 nm was negligible. In the UV-B spectrum (Fig. 2B) the signal for OH radicals with the maximum at 309 nm was significant. These radicals can be produced by electronic dissociation and excitation or by collisions with long lived species, like the argon 4s metastable state (Brandenburg et al., 2007). The UV-A spectrum (Fig. 2C) was dominated by molecular bands of the second positive system of N_2 at 336 nm. Compared to the short wave UV-C light, the antimicrobial efficiency of longer wavelength UV light is much lower. The upper wavelength range from 650 to 850 nm was dominated mainly by argons atoms excited in the 4p state and by the metastable single state of oxygen (Fig. 2D) at around 777.5 nm (Surowsky, Fröhling, Gottschalk, Schlüter, & Knorr, 2014). Furthermore it is well known that argon driven plasma jets emit a certain amount of vacuum ultraviolet (VUV) light, dominated by argon excimer Ar^*_2 with an intensity maximum at $\lambda = 126$ nm (Brandenburg et al., 2009; Ehlbeck et al., 2011). Brandenburg et al. (2009) characterized the VUV emission of the same argon driven plasma jet, they showed that the absolute radiance in the VUV range (110–200 nm) did not change substantially up to a distance of 10 mm to the nozzle outlet. This wavelength range is known to effectively inactivate *B. subtilis* spores (Munakata, Saito, & Hieda, 1991). Considering this, it can be assumed that the emitted VUV light could be relevant regarding the inactivation process.

Table 2
Microbial characterization of whole black peppercorns and the corresponding standard deviation in brackets.

Microorganism	Results [cfu/g]
Total mesophilic aerobic count	$1.0*10^8$ ($\pm 9.6*10^6$)
Spores of mesophilic aerobes	$5.6*10^7$ ($\pm 8.5*10^6$)
Presumptive *B. cereus*	$5.6*10^7$ ($\pm 8.5*10^6$)
Clostridium perfringens	$2.7*10^3$ ($\pm 7.1*10^1$)
Enterobacteriaceae	$1.5*10^2$ ($\pm 7.1*10^1$)
Sulf-red anaerobes	$4.7*10^6$ ($\pm 1.7*10^6$)
Escherichia coli	$1.0*10^3$ ($\pm 4.2*10^2$)
Coagulase-positive Staphylococcus	$4.9*10^4$ ($\pm 6.4*10^3$)
Molds and yeasts	$6.0*10^3$ ($\pm 1.4*10^3$)
Salmonella (in 25 g)	Detected

To investigate the impact of the direct CAPP treatment for the decontamination of whole black peppercorns, naturally contaminated peppercorns and also with *B. atrophaeus* spores, *B. subtilis* spores and *S. enterica* inoculated ones were treated using the rf-plasma jet. The inactivation kinetics displayed in (Fig. 3) were described using a biphasic fit (Table 3). After 15 min of direct CAPP exposure an inactivation of 0.7 $\log_{10}$ for the total mesophilic aerobic count and 0.6 $\log_{10}$ for the total spore count was achieved. The native microbial flora was more resistant towards the CAPP treatment then the inoculated spores. Whereby *B. atrophaeus* spores were more sensitive towards the treatment than *B. subtilis* spores. After 15 min exposure to direct CAPP 0.8 $\log_{10}$ of *B. subtilis* and 1.3 $\log_{10}$ of *B. atrophaeus* spores were inactivated. As expected, the highest inactivation of 2.7 $\log_{10}$ after 15 min of direct CAPP treatment was achieved for *S. enterica*, because vegetative bacteria are generally more sensitive towards decontamination techniques (M. Moreau, Orange, & Feuilloley, 2008).The way of interaction between cold plasma and microorganisms is quite complex, depending on the used working gas, plasma generator, nature of application and investigated microorganism, like bacterial specie (Gram positive or negative) or spores. Thus, it is difficult to compare results obtained by different plasma applications. Studies using a similar plasma system are scarce. Brandenburg et al. (2007) showed the antimicrobial efficiency of the same direct CAPP system. They treated *B. atrophaeus* spores and *Escherichia coli* inoculated on polyethylene strips, with an inactivation of about 4 $\log_{10}$ for the spores after 7 min and for the vegetative bacteria after 2 min treatment, respectively. Fröhling, Baier, Ehlbeck, Knorr, and Schlüter (2012), Fröhling, Durek, et al. (2012) investigated the inactivation of *Listeria innocua* and *E. coli* at polysaccharides surfaces using the same direct CAPP system. They achieved already after 4 min plasma exposure an inactivation of more than 6 $\log_{10}$. However, these studies were done on smooth surfaces and in the case of Fröhling, Baier, Ehlbeck, Knorr, and Schlüter (2012), Fröhling, Durek, et al. (2012) on a sample with a high water content, between such a model and a real food system there is a significant difference due to the complex surface structure of a food product, which can also affect the efficiency of the plasma treatment. The structured peppercorn surface (Fig. 4A) with cracks, grooves, pits might cause shadow effects for the emitted (V)UV photons and other reactive species. Hence the efficiency of the direct plasma treatment is reduced.

The application of CAPP for microbial inactivation resulted in different shaped survivor curves, depending on the method of plasma exposure, direct or remote, respectively (Laroussi, 2002). The obtained biphasic inactivation curves for the direct CAPP inactivation pointed towards different inactivation mechanisms which may be involved during the treatment. The fast inactivation during the first phase points to the fact that (V)UV light plays a dominant role in the inactivation process (Laroussi, 2005). Nevertheless, the signals of the measured spectrum in the (V)UV-C range were negligible, so that an inactivation due to DNA damage by (V) UV light in those wavelengths is not predominate. Slieman and Nicholson (2000) reported that UV-B and UV-A light is also capable to induce single-strand and double-strand breaks, as well as the formation of cyclobutane pyrimidine dimers in *B. subtilis*

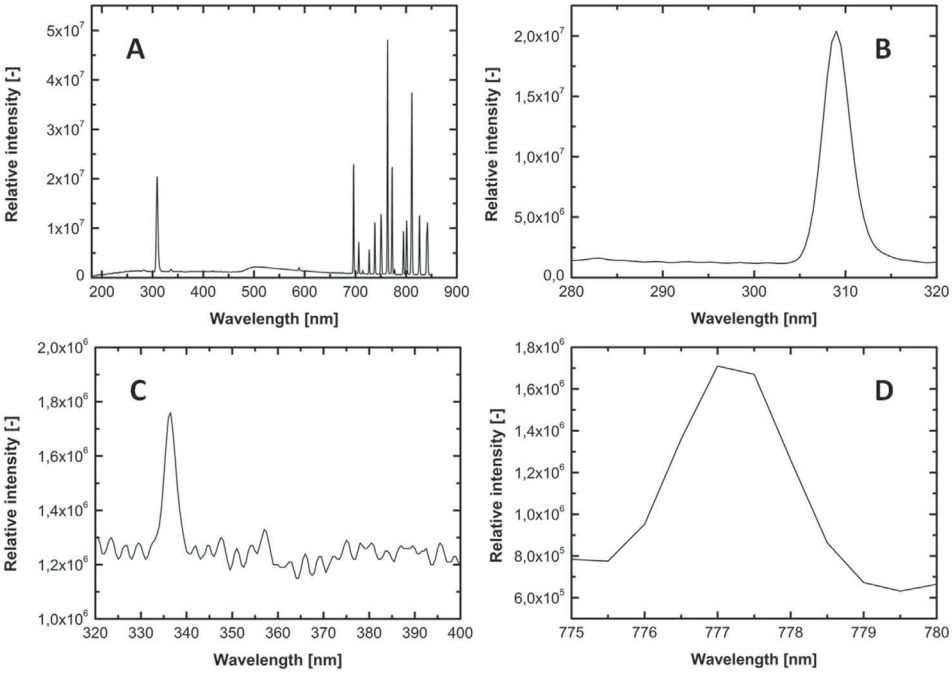

Fig. 2. (A) Emission spectrum of the direct plasma set-up, (B–D) selected parts of the spectrum more precisely.

spores DNA. The emitted reactive oxygen and nitrogen species in wavelength range from 280 to 400 nm (Fig. 2) have strong oxidative effects and can cause irreversible oxidative damage to protein, genetic material and fatty acids due to diffusion inside the microorganisms (Boudam et al., 2006; Laroussi & Leipold, 2004). However, the penetration depth of the (V)UV light and reactive species is restricted, so they could only effect single bacteria and spores, or if they are stacked or aggregated only the ones in the top layer. The slower inactivation during the second phase points to other involved inactivation mechanisms. The SEM micrograph (Fig. 4C) shows clearly a modification of the spore surface of the direct CAPP treated *B. atrophaeus* spores, compared to the untreated spores (Fig. 4B). This modification of the external shape could be attributed to the decomposition of organic material by etching and

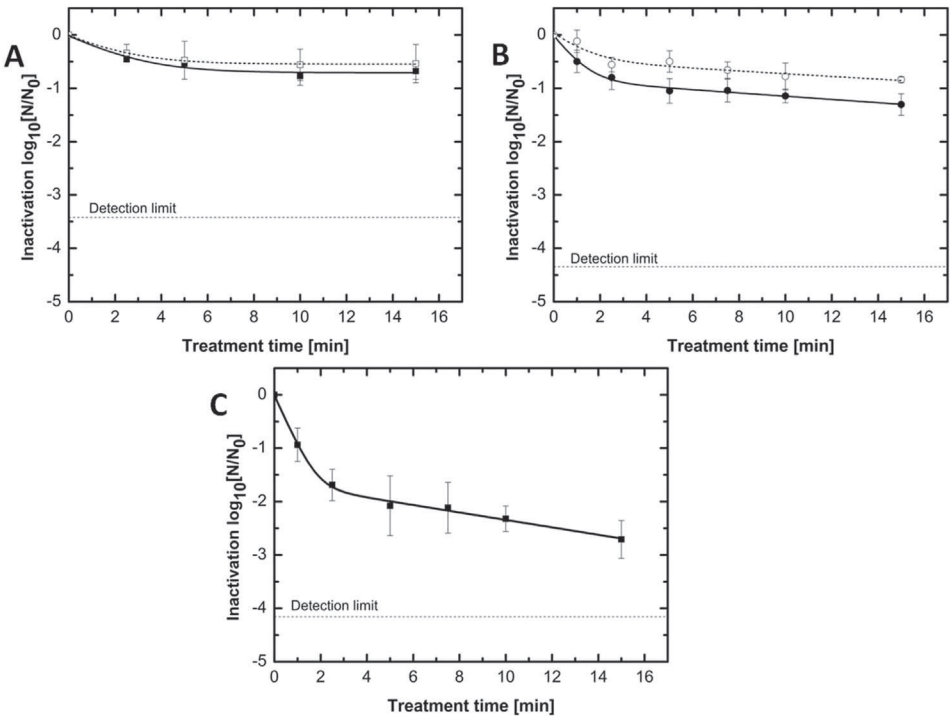

Fig. 3. Effect of direct plasma treatment on the inactivation of (A) naturally contaminated whole black peppercorns, total mesophilic aerobic count (■) and total spore count (□), (B) inoculated *Bacillus atrophaeus* (●) and *Bacillus subtilis* (○) and (C) inoculated *Salmonella enterica* on the surface of whole black peppercorns. Depicted are means (±sd).

Table 3
Statistical parameters and the corresponding standard error in brackets of biphasic model obtained from GInaFit for direct plasma treatment.

Microorganisms	Adj. R^2	RMSE	φ [-]	k_1 [-]	k_2 [-]
Total mesophilic aerobic count	0.85	0.12	0.80 (0.19)	0.55 (0.38)	0.00 (0.07)
Total spore count	0.99	0.02	0.72 (0.05)	0.55 (0.10)	0.00 (0.01)
B. atrophaeus	0.99	0.05	0.85 (0.02)	1.40 (0.21)	0.07 (0.01)
B. subtilis	0.89	0.11	0.69 (0.13)	0.94 (0.58)	0.06 (0.04)
S. enterica	0.99	0.06	0.98 (0.00)	2.23 (0.22)	0.16 (0.02)

photodesorption. Photodesorption is an (V)UV-induced erosion of the cell, where (V)UV photons break chemical bonds and lead to the formation of volatile compounds (Moisan et al., 2002). Whereas etching is the adsorption of generated reactive species inside the plasma on the microorganisms, then they undergo chemical reaction to form volatile compounds (Moisan et al., 2002). So the whole inactivation process could be attributed to an interaction of different components inside the plasma. First the initial fast inactivation could be attributed to (V)UV light, inactivating single microorganisms or the top layer of stacked or aggregated spores. In the second step the combination of (V)UV light and reactive species in the plasma decompose already inactivated microorganisms, so that reactive particles from the plasma can reach the next layer of stacked or aggregated microorganisms.

3.3. Remote CAPP treatment of inoculated and naturally contaminated pepper

To compare both CAPP systems, naturally contaminated peppercorns and also with *B. atrophaeus* spores, *B. subtilis* spores and *S. enterica* inoculated ones were also treated with a remote plasma application. The results of the remote CAPP treatment (Fig. 5) were all fitted using the Weibull model. Because for the remote CAPP treatment only PPA was used, which is characterized by the absence of (V)UV light. This model based on reliability engineering and can be used as a universal tool to fit various inactivation curves of different decontaminating processes with great accuracy (Van Boekel, 2002). The Weibull model is well suitable to describe the inactivation kinetics of remote plasma treatment (Table 4). Within the first 15 min of treatment a fast reduction of 1.7 $\log_{10}$ for the total mesophilic aerobic count and of 1.4 $\log_{10}$ for the total spore count was observed. The final inactivation of 2.0 $\log_{10}$ respectively 1.7 $\log_{10}$ was achieved after 30 min of CAPP treatment. The inoculated *Bacillus* spores were more sensitive towards the remote CAPP, compared to the naturally flora. However *B. subtilis* showed a higher resistance towards the remote treatment, compared with *B. atrophaeus*. After 30 min a final inactivation of 2.4 $\log_{10}$ for *B. subtilis* and of 2.8 $\log_{10}$ for *B. atrophaeus* was achieved. The remote CAPP is quite efficient to inactivate *S. enterica* on the surface of whole black pepper. After 15 min treatment 3.2 $\log_{10}$ Salmonella were inactivated. The final inactivation achieved by the remote CAPP treatment after 30 min was 4.1 $\log_{10}$. As already mentioned above it is difficult to compare results obtained by different plasma systems and furthermore studies dealing with plasma application on dry products are rare. Hertwig et al. (2015) used the same CAPP system for the treatment of different herbs and spices. They successfully inactivated the native microbial flora of peppercorns, crushed oregano and paprika powder. Schnabel, Niquet, and Krohmann (2012) treated various seeds inoculated with *B. atrophaeus* spores using the same CAPP system as in this study, but without mixing the sample during the exposure to the PPA.

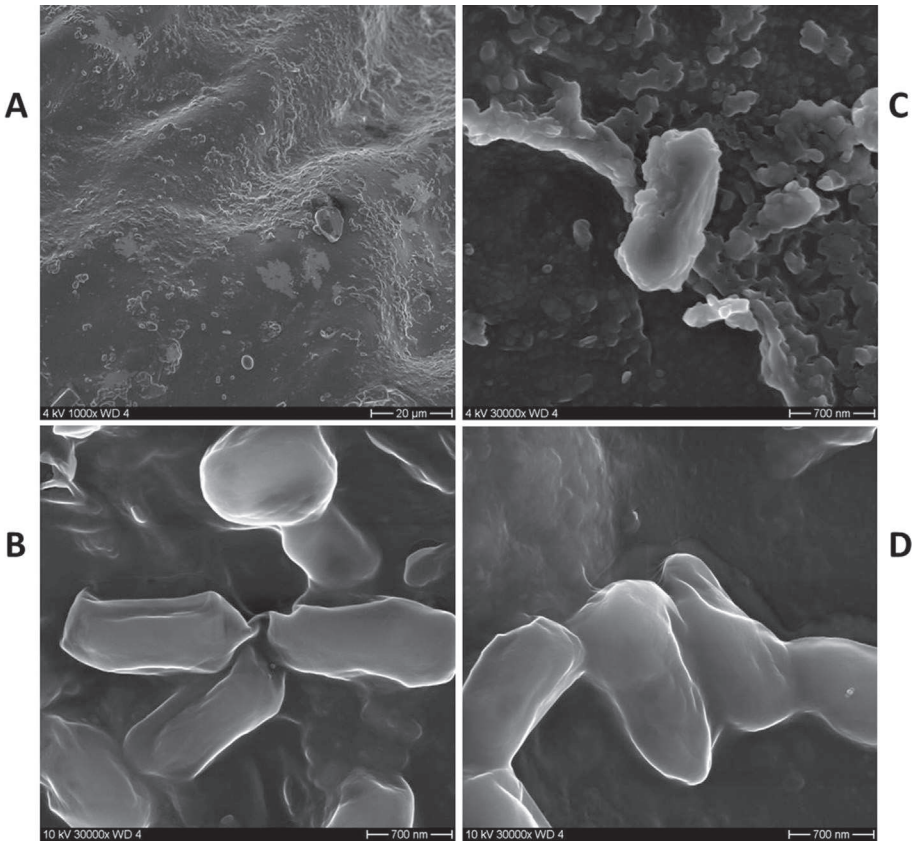

Fig. 4. SEM pictures of inoculated *Bacillus atrophaeus* spores on the surface of black peppercorns, (A and B) untreated, (C) 15 min direct plasma treatment and (D) 30 min remote plasma treatment.

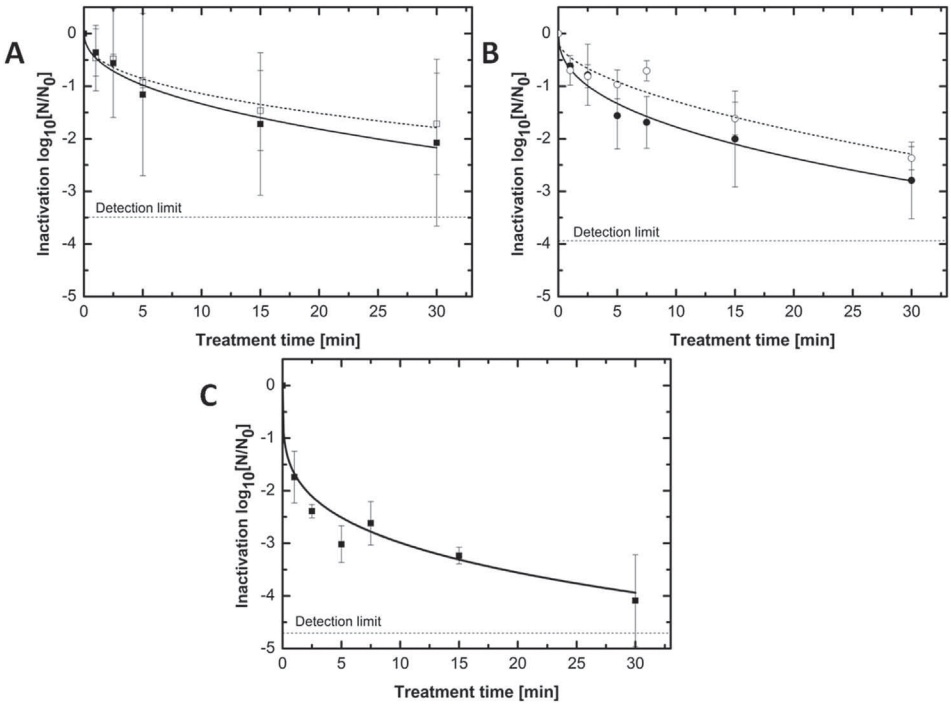

Fig. 5. Effect of remote plasma treatment on the inactivation of (A) naturally contaminated whole black peppercorns, total mesophilic aerobic count (■) and total spore count (□), (B) inoculated *Bacillus atrophaeus* (●) and *Bacillus subtilis* (○) and (C) inoculated *Salmonella enterica* on the surface of whole blackcorns. Depicted are means (±sd).

Treatment resulted in an inactivation of up to 5.6 $\log_{10}$ after 15 min for carrot seeds. Nevertheless for peppercorns only 1.7 $\log_{10}$ after 5 min treatment time was achieved with no further inactivation with increasing treatment time, which they attributed to the complex structure of peppercorns surface compared to the other used seeds.

The used remote CAPP system is working with dry air. In air plasmas different reactive species, like reactive nitrogen and oxygen species are generated, they have direct impact on microorganisms and can lead to their inactivation (Laroussi & Leipold, 2004). Fröhling, Durek, et al. (2012b) measured in the PPA gas generated by the same CAPP system concentrations of 0.6% NO•, 1.8% NO_2•, 0.007% CO_2, 0.04% HNO_3, 0.08% HNO_2 and 0.03% H_2O by using FT-IR spectroscopy. Based on these data it can be assumed that probably only the reactive nitrogen species can cause the observed inactivation. In this regard, it is necessary to distinguish between vegetative microorganisms and bacterial spores. In vegetative microorganisms, like Salmonella, reactive nitrogen species can accumulate on the surface and easily diffuse through cell membranes, causing a decrease of intracellular pH. The intracellular pH plays a major role in cell function and affects enzyme activity, reaction rates, protein stability and structure of nucleic acids (Slonczewski, Fujisawa, Dopson, & Krulwich, 2009). Exceeding a critical gradient between external and intracellular pH, the pH homeostasis cannot be maintained any longer, resulting in the inactivation of the bacterial cell (Booth, 1985; Padan & Schuldiner, 1987).

Due to their multilayer structure and the low water content in the spore's core, spores are extremely resistant to various chemicals, like acids, bases, oxidizing agents or aldehydes (P. Setlow, 2006). However, treatment with nitrous acid kills spores by DNA damage (Tennen, Setlow, Davis, Loshon, & Setlow, 2000). Further Setlow et al. (2002) reported a rupture of the spore's inner membrane by a strong acid treatment in aqueous solutions, causing inactivation.

The reactive nitrogen species in the PPA might have the same effect. After diffusion through the various spore's layer, they might react with the little amount of free water in the spore's core and react to nitric and nitrous acid. SEM pictures (Fig. 4D) of *B. atrophaeus* after 30 min treatment showed no damage or alteration of the spore's outer structure. It would be reasonable, that the reactive nitrogen species destroy the inner spore membrane and hence inactivate the spore without affecting their outer structure.

Table 4
Statistical parameters and the corresponding standard error in brackets of Weibull model obtained from GInaFit for remote plasma treatment.

Microorganisms	Adj. R^2	RMSE	δ [min]	p [-]
Total mesophilic aerobic count	0.95	0.18	4.67 (2.28)	0.43 (0.09)
Total spore count	0.96	0.13	6.97 (2.71)	0.40 (0.08)
B. atrophaeus	0.97	0.18	2.35 (1.10)	0.41 (0.06)
B. subtilis	0.88	0.26	7.90 (4.27)	0.57 (0.18)
S. enterica	0.94	0.31	0.13 (0.16)	0.25 (0.05)

3.4. CAPP impact on quality parameters

To estimate the impact of both CAPP systems on the quality of the peppercorns, the surface color, the piperine and volatile oil content was measured. The results of the color measurement are summarized in Fig. 6. Neither the remote nor the direct treatment had a major impact on the surface color of the peppercorns. The color of the pepper is an important factor determining the commercial quality of the product, another major quality attribute of pepper is the content of piperine. The measured amount of piperine after 15 min of direct CAPP treatment and 30 min of remote treatment was only slightly lower than the amount determined in the untreated black pepper (Fig. 7). The results of the volatile oil content showed similar results compared to the determination of the piperine content. Both CAPP applications had only a minimal

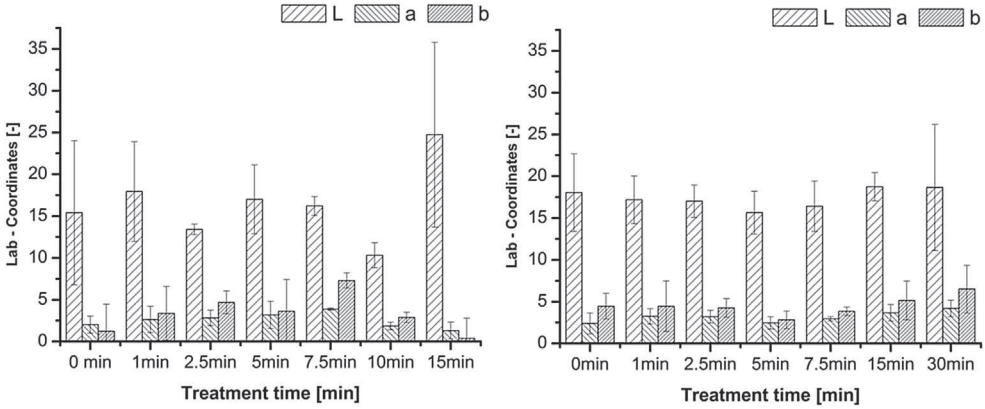

Fig. 6. Effect of cold atmospheric pressure plasma treatment on the surface color of black peppercorns, left direct treatment and right remote treatment. Depicted are means (±sd).

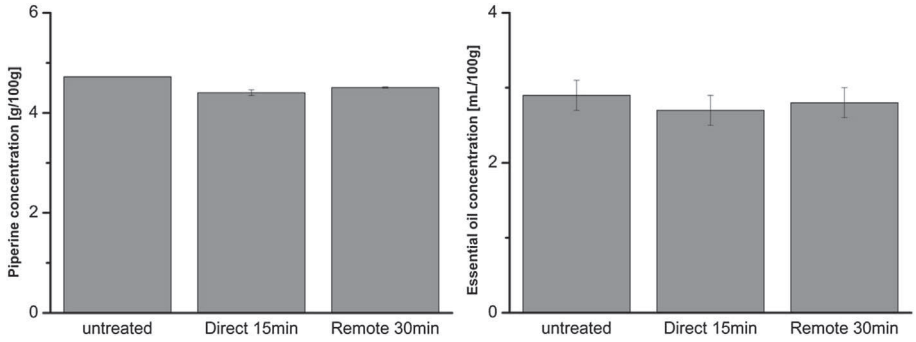

Fig. 7. Effect of cold atmospheric pressure plasma treatment on piperine content (left) and essential oil content (right) of black peppercorns. Depicted are means (±sd).

impact, the content in the CAPP treated samples was slightly lower compared to the untreated one (Fig. 7). The results of both CAPP applications did not have a noticeably impact on the examined quality parameters, pointing towards a high sensorial quality of the decontaminated pepper.

4. Conclusions

This study shows the difference in the antimicrobial efficiency between different cold atmospheric pressure plasma applications. The remote treatment with PPA inactivates *S. enterica* and showed promising results for the inactivation of both *Bacillus* spores on the surface of black peppercorns. The results of the direct CAPP treatment showed a much lower inactivation, probably due to different involved inactivation mechanisms and the complex surface structure of the peppercorns. Nevertheless both CAPP applications did not significantly alter the quality parameters, like color, piperine and volatile oil content of the treated peppercorns. Furthermore *B. subtilis* spores showed a higher resistance towards both CAPP systems, compared with *B. atrophaeus* spores, which is the surrogate microorganism for irradiation with γ-rays and chemical inactivation processes.

The results of this work demonstrate the potential of certain cold atmospheric pressure plasma applications for the decontamination of dry and heat sensitive food products, like whole black peppercorns, even though more research is needed to fully understand and further improve the application of cold atmospheric pressure plasma and the product–plasma interactions.

Acknowledgments

This study was funded by the research project "Development of novel and advanced decontamination sustainable technologies for the production of high quality dried herbs and spices (GREENFOODEC)", which was financially supported by the European Commission within the 7th Framework Program (FP7-SME-2011-285838).

References

Boer, E. De, Spiegelenberg, W., & Janssen, F. (1985). Microbiology of spices and herbs. *Antonie van Leeuwenhoek, 51*, 435–438.
Booth, I. R. (1985). Regulation of cytoplasmic pH in bacteria. *Microbiological Reviews, 49*(4), 359–378.
Boudam, M. K., Moisan, M., Saoudi, B., Popovici, C., Gherardi, N., & Massines, F. (2006). Bacterial spore inactivation by atmospheric-pressure plasmas in the presence or absence of UV photons as obtained with the same gas mixture. *Journal of Physics D: Applied Physics, 39*(16), 3494–3507.
Brandenburg, R., Ehlbeck, J., Stieber, M., Woedtke, T. V., Zeymer, J., Schlüter, O., et al. (2007). Antimicrobial treatment of heat sensitive materials by means of atmospheric pressure Rf-driven plasma jet. *Contributions to Plasma Physics, 47*(1–2), 72–79.
Brandenburg, R., Lange, H., von Woedtke, T., Stieber, M., Kindel, E., Ehlbeck, J., et al. (2009). Antimicrobial effects of UV and VUV radiation of nonthermal plasma jets. *IEEE Transactions on Plasma Science, 37*(6), 877–883.
CBI.. (2010). *The spice and herbs market in the EU*.
Cerf, O. (1977). Tailing of survival curves of bacterial spores. *Journal of Applied Bacteriology, 42*, 1–19.
Deng, S., Ruan, R., Mok, C. K., Huang, G., Lin, X., & Chen, P. (2007). Inactivation of Escherichia coli on almonds using nonthermal plasma. *Journal of Food Science, 72*(2), 62–66.
Ehlbeck, J., Schnabel, U., Polak, M., Winter, J., von Woedtke, T., Brandenburg, R., et al. (2011). Low temperature atmospheric pressure plasma sources for microbial decontamination. *Journal of Physics D: Applied Physics, 44*(1), 1–18.
Fröhling, A., Baier, M., Ehlbeck, J., Knorr, D., & Schlüter, O. (2012). Atmospheric pressure plasma treatment of Listeria innocua and Escherichia coli at polysaccharide surfaces: Inactivation kinetics and flow cytometric characterization. *Innovative Food Science & Emerging Technologies, 13*, 142–150.
Fröhling, A., Durek, J., Schnabel, U., Ehlbeck, J., Bolling, J., & Schlüter, O. (2012). Indirect plasma treatment of fresh pork: decontamination efficiency and effects on quality attributes. *Innovative Food Science & Emerging Technologies, 16*, 381–390.

Gieraltowski, L., Julian, E., Pringle, J., Macdonald, K., Quilliam, D., Marsden-Haug, N., et al. (2013). Nationwide outbreak of Salmonella Montevideo infections associated with contaminated imported black and red pepper: warehouse membership cards provide critical clues to identify the source. *Epidemiology & Infection, 141*(6), 1244–1252.

Hertwig, C., Reineke, K., Ehlbeck, J., Erdoğdu, B., Rauh, C., & Schlüter, O. (2015). Impact of remote plasma treatment on natural microbial load and color of selected herbs and spices. *Journal of Food Engineering*. http://dx.doi.org/10.1016/j.jfoodeng.2014.12.017.

Knorr, D., Froehling, A., Jaeger, H., Reineke, K., Schlueter, O., & Schoessler, K. (2011). Emerging technologies in food processing. *Annual Review of Food Science and Technology, 2*, 203–235.

Laroussi, M. (2002). Nonthermal decontamination of biological media by atmospheric-pressure plasmas: review, analysis, and prospects. *IEEE Transactions on Plasma Science, 30*(4), 1409–1415.

Laroussi, M. (2005). Low temperature plasma-based sterilization: overview and state-of-the-art. *Plasma Processes and Polymers, 2*(5), 391–400.

Laroussi, M., & Leipold, F. (2004). Evaluation of the roles of reactive species, heat, and UV radiation in the inactivation of bacterial cells by air plasmas at atmospheric pressure. *International Journal of Mass Spectrometry, 233*(1–3), 81–86.

Little, C., Omotoye, R., & Mitchell, R. (2003). The microbiological quality of ready-to-eat foods with added spices. *International Journal of Environmental Health Research, 13*(1), 31–42.

McKee, L. H. (1995). Microbial contamination of spices and herbs: a review. *LWT - Food Science and Technology, 28*(1), 1–11.

Moisan, M., Barbeau, J., Crevier, M.-C., Pelletier, J., Philip, N., & Saoudi, B. (2002). Plasma sterilization. Methods and mechanisms. *Pure and Applied Chemistry, 74*(3), 349–358.

Moreau, S., Moisan, M., Tabrizian, M., Barbeau, J., Pelletier, J., Ricard, A., et al. (2000). Using the flowing afterglow of a plasma to inactivate Bacillus subtilis spores: Influence of the operating conditions. *Journal of Applied Physics, 88*(2), 1166–1174.

Moreau, M., Orange, N., & Feuilloley, M. G. J. (2008). Non-thermal plasma technologies: new tools for bio-decontamination. *Biotechnology Advances, 26*(6), 610–617.

Munakata, N., Saito, M., & Hieda, K. (1991). Inactivation action spectra of *Bacillus subtilis* spores in extended ultraviolet wavelengths (50-300nm) obtained with snchrotron radiation. *Photochemistry and Photobiology, 54*(5), 761–768.

Nicholson, W. L., & Setlow, P. (1990). Sporulation, germination and outgrowth. In C. R. Harwood, S. M. Cutting, & R. Chambert (Eds.), *Molecular biological methods for Bacillus* (pp. 391–450). Chichester Wiley.

Padan, E., & Schuldiner, S. (1987). Intracellular pH and membrane potential as regulators in the prokaryotic cell. *Journal of Membrane Biology, 198*, 189–198.

Piggott, J., & Othman, Z. (1993). Effect of irradiation on volatile oils of black pepper. *Food Chemistry, 46*(2), 115–119.

Pipa, A. V., Andrasch, M., Rackow, K., Ehlbeck, J., & Weltmann, K.-D. (2012). Observation of microwave volume plasma ignition in ambient air. *Plasma Sources Science and Technology, 21*(3).

Reineke, K., Ellinger, N., Berger, D., Baier, D., Mathys, A., Setlow, P., et al. (2013). Structural analysis of high pressure treated Bacillus subtilis spores. *Innovative Food Science & Emerging Technologies, 17*, 43–53.

Schlüter, O., Ehlbeck, J., Hertel, C., Habermeyer, M., Roth, A., Engel, K., et al. (2013). Opinion on the use of plasma processes for treatment of foods. *Molecular Nutrition & Food Research, 57*(5), 920–927.

Schnabel, U., Niquet, R., & Krohmann, U. (2012). Decontamination of microbiologically contaminated seeds by microwave driven discharge processed gas. *Journal of Agricultural Science and Applications, 1*(4), 100–106.

Schweiggert, U., Carle, R., & Schieber, A. (2007). Conventional and alternative processes for spice production – a review. *Trends in Food Science & Technology, 18*(5), 260–268.

Setlow, P. (2006). Spores of Bacillus subtilis: their resistance to and killing by radiation, heat and chemicals. *Journal of Applied Microbiology, 101*(3), 514–525.

Setlow, B., Loshon, C. A., Genest, P. C., Cowan, A. E., Setlow, C., & Setlow, P. (2002). Mechanisms of killing spores of Bacillus subtilis by acid, alkali and ethanol. *Journal of Applied Microbiology, 92*(2), 362–375.

Slieman, T. A., & Nicholson, W. L. (2000). Artificial and solar UV radiation induces strand breaks and cyclobutane pyrimidine dimers in *Bacillus subtilis* spore DNA artificial and solar UV radiation induces strand breaks and cyclobutane pyrimidine dimers in *Bacillus subtilis* spore DNA. *Applied and Environmental Microbiology, 66*(1), 199–205.

Slonczewski, J. L., Fujisawa, M., Dopson, M., & Krulwich, T. A. (2009). Cytoplasmic pH measurement and homeostasis in bacteria and archaea. *Advances in Microbial Physiology, 55*, 1–79, 317.

Surowsky, B., Fröhling, A., Gottschalk, N., Schlüter, O., & Knorr, D. (2014). Impact of cold plasma on Citrobacter freundii in apple juice: Inactivation kinetics and mechanisms. *International Journal of Food Microbiology, 174*, 63–71.

Surowsky, B., Schlüter, O., & Knorr, D. (2014). Interactions of Non-Thermal atmospheric pressure plasma with solid and liquid food systems: a review. *Food Engineering Reviews*.

Tainter, D., & Grenis, A. (2001). In D. Tainter, & A. Grenis (Eds.), *Spices and seasonings: A food technology handbook* (2nd ed.). New York: Wiley.

Tateo, F., & Bononi, M. (2006). Determination of ethylene chlorohydrin as marker of spices fumigation with ethylene oxide. *Journal of Food Composition and Analysis, 19*(1), 83–87.

Tennen, R., Setlow, B., Davis, K. L., Loshon, C. A., & Setlow, P. (2000). Mechanisms of killing of spores of Bacillus subtilis by iodine, glutaraldehyde and nitrous acid. *Journal of Applied Microbiology, 89*(2), 330–338.

Van Boekel, M. A. J. S. (2002). On the use of the Weibull model to describe thermal inactivation of microbial vegetative cells. *International Journal of Food Microbiology, 74*(1–2), 139–159.

Weltmann, K.-D., Brandenburg, R., von Woedtke, T., Ehlbeck, J., Foest, R., Stieber, M., et al. (2008). Antimicrobial treatment of heat sensitive products by miniaturized atmospheric pressure plasma jets (APPJs). *Journal of Physics D: Applied Physics, 41*(19).

7. Conclusion and perspectives

The mechanistic background of bacterial spore inactivation by cold atmospheric pressure plasma is still part of ongoing discussions (Boudam et al. 2006; Muranyi et al. 2010; van Bokhorst-van de Veen et al. 2015; Wang et al. 2016). The various plasma sources, used process gases or mixtures and form of applications lead to numerous factors that can influence the spore inactivation. Moreover, different target spore strains, matrix effects, spore density and distribution on the treated surface as well as methodic differences limit the comparability of the results. It is well known that spore inactivation by CAPP is caused by the different generated reactive components, such as VUV and UV photons; neutral and charged particles and free radicals, of the CAPP. The plasma-spore interactions are complex, as those reactive components can act individually and/or synergistically. The CAPP-based inactivation of endospores is often described using biphasic inactivation kinetics, with a fast-initial inactivation followed a slower inactivation within the second phase (tailing). Whereby the inactivation is ascribed to DNA damage due to emitted UV photons and the decomposition of organic material by photodesorption and etching processes (Moreau et al. 2000; Moisan et al. 2001). However, it is also reported that CAPP can damage the inner spore membrane and key germination proteins (Wang et al. 2016). Further on, the knowledge about the spores' properties involved in the resistance to the application of cold atmospheric pressure plasma is scarce. Up until now, no official reference spore strain for CAPP-based inactivation processes has been identified, probably due to the numerous involved parameters and variations of CAPP treatments. Therefore, this study chose to investigate the inactivation behavior of *Bacillus subtilis* spores, since this is one of the best explored prokaryotes in terms of molecular and cell biology. The inactivation behavior of *Bacillus subtilis* (PS832) spores was investigated using different CAPP setups (plasma jet, DCSBD system and PPA), a broad spectrum of process gases, air, N_2, O_2, CO_2, Ar and Ar with admixtures of N_2 and O_2 as well as different surfaces the spores were attached to. Scanning electron microscopy was used to investigate the distribution of the spores on the different surfaces and to observe potential morphological changes of the treated spores. A quantitative real-time polymerase chain reaction (qPCR) assay was established and modified to monitor the plasma effect on the spores' DNA during the treatment, which helps to further understand the CAPP inactivation of bacterial spores. To identify possible factors involved in spores' resistance towards a cold plasma treatment the inactivation behavior of isogenic mutant strains of *Bacillus subtilis*, lacking the outer spore coat, DPA and α/β-type SASPs inside the core was

also investigated. Likewise, the inactivation behavior of *Bacillus subtilis* spores was compared with *Bacillus atrophaeus* (WIS 39 6/3) spores, the surrogate for *Bacillus anthracis* during chemical, UV- and γ-irradiation sterilization. Since the composition of the generated plasma affects the inactivation process tremendously, the different generated plasmas were described in detail using optical emission spectroscopy, determining the emitted UV dosage, the generated ozone concentration and the process temperature.

Combining the use of different plasma systems, process gases, the detailed description of the tested plasmas and the applied analysis methods, unique insights in the inactivation of *Bacillus* spores by cold atmospheric pressure plasma were possible. This helped to understand underlying mechanisms of spore inactivation during CAPP treatments and to identify properties of *Bacillus* spores responsible for their resistance to CAPP.

It is well known that the used process gas or process gas composition determines the composition of the generated plasma and influences the inactivation efficiency of the CAPP treatment (Trompeter et al. 2002; Laroussi & Leipold 2004; Lim et al. 2007; Reineke et al. 2015; Hertwig et al. 2015a; Hertwig et al. 2017). Thus, within this work the effect of the process gas composition using a RF-driven plasma jet system on the emitted amount of UV photons, reactive oxygen and nitrogen species was analyzed. The amount of N_2 (up to 0.3 vol.%) and O_2 (up to 0.34 vol.%) to the carrier gas argon was increased gradually and the optical emission spectra of the generated plasma was measured. The addition of N_2 and O_2 caused significant variations in the emission spectra. The highest amount of emitted UV-C photons was measured for the use of argon with the addition of 0.2 vol.% N_2 and 0.135 vol.% O_2. Mainly molecular bands of nitric oxide (NO_γ-system) are responsible for the detected UV-C emission of the plasma jet afterglow (Brandenburg et al. 2009). Consequently, an increased addition of N_2 and O_2 to the carrier gas increases the amount of emitted UV-C photons, due to higher emission of NO_γ. However, high concentrations of N_2 and O_2 to the carrier gas causes instabilities of the plasma jet discharge, resulting in a weaker and more filamentous plasma. This is probably due to the quenching of argon metastable states and electron attachment as well as the quenching of UV-C photons by the added N_2 and O_2 itself (Brandenburg et al. 2009). The emission intensities in the UV-B range were dominated by the signal of $OH^\bullet$ radicals with the maximum of 309 nm. Significant changes in the emission intensity of $OH^\bullet$ radicals by the addition of N_2 and O_2 were not observed. ROS as atomic oxygen are important regarding the erosion of bacterial spores through etching (Deng et al. 2006; Lim et al. 2007; Shen et al. 2012), the emission intensities from 772 to 783 nm (atomic oxygen emission band at around 777.5 nm) were measured. Pure

argon with the addition of O_2 emitted the highest intensities, up to sixfold higher as for argon with the addition of N_2. With increasing N_2 addition to argon and O_2 the emission intensities decreased. Based on the optical emission spectroscopy three different gas compositions were chosen to investigate the impact on the *Bacillus* spore inactivation:

1. Pure argon
2. Argon + 0.135 vol.% O_2
3. Argon + 0.135 vol.% O_2 + 0.2 vol.% N_2

In plasma generated with pure argon, molecular bands of ROS and RNS were detected, such as $OH^{\bullet}$ radicals, due to interactions of the plasma with the surrounding air. The process gas composition argon + 0.135 vol.% O_2 generated a plasma with a high amount of ROS, e.g. $OH^{\bullet}$ radicals and atomic oxygen. Plasma generated with argon + 0.135 vol.% O_2 + 0.2 vol.% N_2 emitted the highest amount of UV-C photons, as well as ROS and RNS. The UV-C emission for the other two process gas composition was negligible. The *Bacillus* spores were inoculated on a flat glass surface and exposed to the different plasmas. *Bacillus atrophaeus* spores were more sensitive towards all three tested gas compositions as the *Bacillus subtilis* spores. Furthermore, all inactivation kinetics showed biphasic inactivation behavior, with an accelerated initial inactivation, which level off in a tailing for longer treatments. This biphasic inactivation behavior was reported in various studies (Lee et al. 2006; Boudam et al. 2006; Muranyi et al. 2008; Brandenburg et al. 2009; Muranyi et al. 2010; Reineke et al. 2015; Hertwig et al. 2015a; Hertwig et al. 2015b). Moreau et al. (2000) and Moisan et al. (2001) proposed three main mechanisms contributing to the spore inactivation:

1. DNA damage due to UV photons
2. Intrinsic photodesorption
3. Etching of organic material

The fast initial inactivation in the first phase is attributed to the emitted UV photons, whereas the following slower inactivation of the second phase is attributed to a combination process of all three mechanisms. For the treatment with plasma generated with pure argon the first inactivation phase lasted until 1 and 1.5 min, respectively. For the use of plasma generated with argon and the addition of N_2 and O_2, which had the significant emission of UV-C photons, the first inactivation phase lasts until 2 to 3 min, respectively. These results suggested that the emitted UV-C photons of the CAPP can play a major role in *Bacillus* spore inactivation. To access the impact of UV-C photons in the spore inactivation, the same trials were carried out with isogenic

mutant strains of *Bacillus subtilis* (PS832) with reduced resistance to UV light. The spore strain FB122 is not able to synthesize DPA during the sporulation. The spore strain PS578 lacks the genes encoding the spore's two major α/β-type SASPs. Again, the spores showed a biphasic inactivation behavior for tested plasmas. However, the strain PS578 had a higher sensitivity to all plasmas than the wild-type strain PS832. The strain FB122 had a similar inactivation behavior as the wild-type strain PS832 but a higher maximum inactivation for the process gas composition with the highest UV-C photon emission. These results showed the impact of emitted UV photons on the inactivation by CAPP.

The structure of the surface the microorganisms are attached to has a certain impact on the inactivation efficiency of the CAPP treatment, as rough surfaces with pits and cracks can hinder the inactivation of microorganisms (Surowsky et al. 2014; Hertwig et al. 2015a). In most cases endospores were inoculated and plasma treated on smooth surfaces, such as glass polyethylene strips, polycarbonate membranes or polymer foils (Heise et al. 2004; Deng et al. 2006; Brandenburg et al. 2009; Reineke et al. 2015; Wang et al. 2016). Studies investigating the inactivation of endospores on different surfaces are scarce or have methodic differences in the inoculated spore density on the surfaces (Butscher et al. 2016). Based on the results for the *Bacillus* spore inactivation on the flat glass surfaces, the next step was to investigate the inactivation behavior on different structured surfaces. Therefore, a dry food product was chosen with a high native load of bacterial spores: black peppercorn. Different surfaces were selected, from a simple flat glass surface via a spherical model (glass beads) to a real food matrix (peppercorns), and inoculated with a similar spore density of about $4*10^6$ *Bacillus subtilis* spores cm^{-2}, which is comparable to the native microbial load of black peppercorns (Hertwig et al. 2015a). The combination of the different surfaces and the comparable spore density enable a closer insight into the surface-related inactivation of *Bacillus* spores. The samples were treated using the same RF-driven plasma jet system and the three already described process gas compositions. The maximum obtained inactivation for the three process gas compositions were similar on each surface and all inactivation kinetics showed a biphasic inactivation behavior. In contrast to the process gas composition, the treated surface had a tremendous impact on the inactivation efficiency of the CAPP treatment. The fastest and highest inactivation was achieved for the treatment of glass beads, followed by the flat glass surface and black peppercorns (Hertwig et al. 2015b). Figure 7—1 shows the distribution of *Bacillus subtilis* spores on the flat glass surface. In the center of the inoculated area the spores are distributed homogeneously almost without aggregation. However, on the edge of the inoculated areas spore agglomerates are clearly visible.

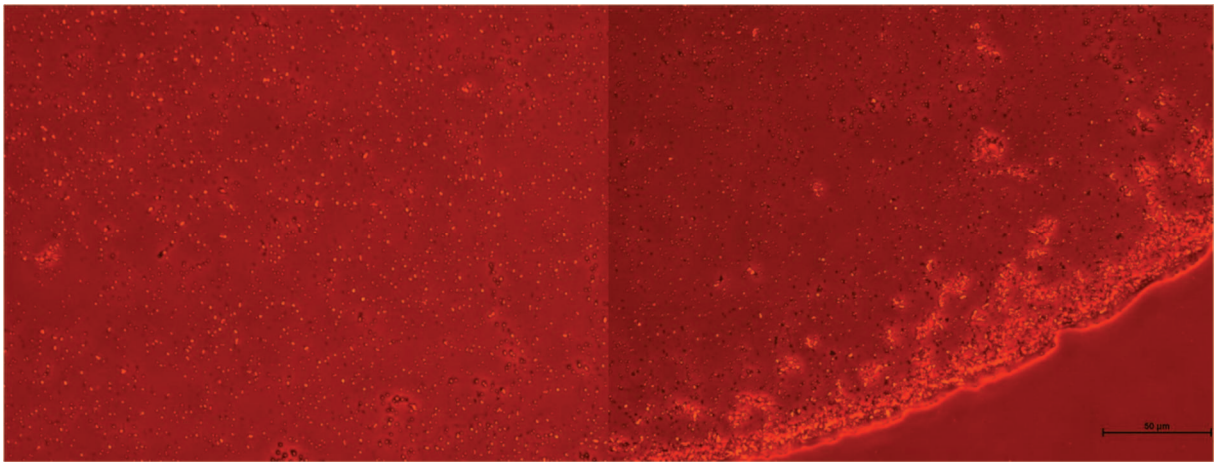

Figure 7—1: Phase contrast micrographs of Bacillus subtilis spores inoculated on flat glass surface, on the left in the center and on the right side on the edge of the inoculated area.

The structure of the glass beads and peppercorns and the distribution of the inoculated *Bacillus subtilis* spores are shown in Figure 7—2. The glass beads have a smooth surface with micro irregularities. The spores are scattered on the surface and spore agglomerates are rarely visible. In contrast, black peppercorns have a well-structured surface with elevations, cracks, pits and grooves. The *Bacillus subtilis* spores are distributed inhomogeneously on the surface, gathering in cracks and grooves and stacking together in agglomerates. Besides the structure of the treated surface, also the distribution of the spores on the surface has a major impact on the inactivation efficiency of the plasma treatment. Spore agglomerates are more difficult to inactivate by CAPP due to the limited penetration depth of the generated components. The penetration depth of UV photons depends on the material and wavelength and can exceed 1 µm (Lerouge et al. 2000) and is in the order of spore dimension 1 to 3 µm (Moisan et al. 2001). If spores are aggregated, just the top layer of the spores is affected by the emitted UV photons. The spores inside the agglomerated will only be affected by the CAPP when the top layer of spores is decomposed by photodesorption and etching processes. However, in the case of black peppercorns the structured surface causes shadow effects, which means that generated components of the plasma, as UV photons, ROS and RNS, cannot interact with the spores located in cracks and grooves, hence reducing the antimicrobial efficiency of the CAPP treatment (Hertwig et al. 2015a; Hertwig et al. 2015b).

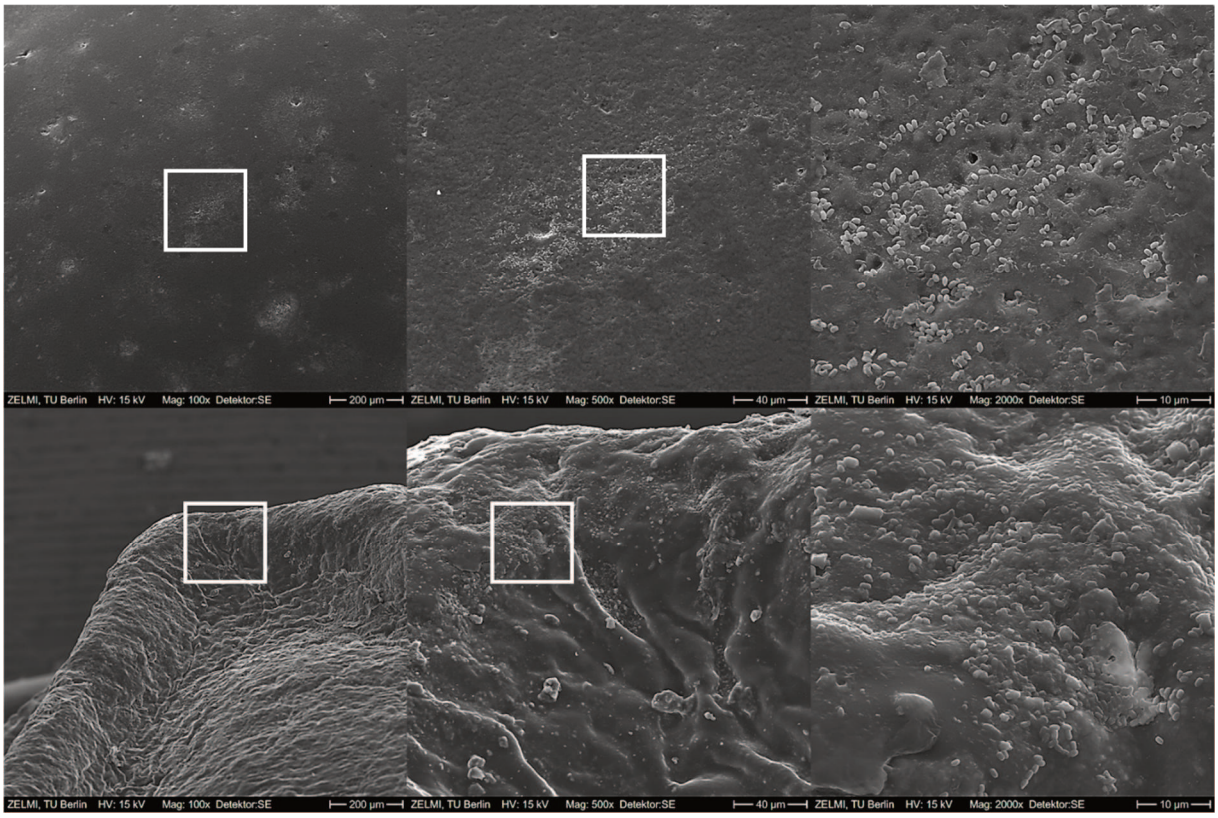

Figure 7—2: Scanning electron micrographs of Bacillus subtilis spores on: top row glass beads and bottom row black peppercorns. The white frame represents the section of the following pictures.

Besides the effect of the treated surface structure on the inactivation of bacterial spores, also detailed knowledge about the mechanisms involved in the plasma-based spore inactivation is necessary. Muranyi et al. (2010) reported DNA damage of *Bacillus atrophaeus* spores because of CAPP treatment. In this study a qPCR based ratio detection system was used to detect the degree of *Bacillus subtilis* DNA damage during the three different CAPP treatments. The results showed that the three different applied CAPPs caused a relevant DNA damage of the treated *Bacillus subtilis* spores (Hertwig et al. 2015b). The maximum DNA damage values depended on the used process gas composition and corresponded in maximum inactivation levels. CAPP generated with pure argon caused the highest DNA damage values followed by the process gas composition with the highest intensity of emitted UV-C photons. Brandenburg et al. (2009) showed for an identically constructed plasma jet system driven with pure argon, that this system generated a significant amount of VUV photons and the absolute radiance in the VUV range (115-200 nm) did not change significantly up to a distance of 10 mm from the plasma jet nozzle. Whereas the addition of oxygen decreased the emission of VUV photons. The emitted VUV photons of the CAPP generated with pure argon can effectively inactivate *Bacillus subtilis* spores (Munakata et al. 1991) and can induce DNA damage of *Bacillus subtilis* spores (Munakata et al. 1986).

The composition of the used process gas for CAPP generation had just a minor impact on the maximum obtained spore inactivation on the different treated surfaces. However, it has been shown how the process gas composition can influence the inactivation process of *Bacillus subtilis* spores. In case of a process gas compositions, which generates plasma with a certain amount of (V)UV photons, the inactivation of *Bacillus* spores is presumably dominated by the interaction of (V)UV photons with the spores, causing DNA damage. Otherwise, the inactivation of the spores is more driven by the action and interaction of the different generated reactive components inside the plasma, such as ROS and RNS.

The release of DPA can be used to detect damage of the inner spore membrane. However, in case of a CAPP treatment it can be assumed that the generated reactive components of the CAPP can also interact with the DPA and disintegrate it. Figure 7—3 shows the disintegration of DPA, dried on a glass petri-dish and treated with the same distance as the samples inoculated with *Bacillus* spores using a RF-driven plasma jet system and pure argon as a process gas. Due to the fact that CAPP is also able to disintegrate DPA, the release of DPA after CAPP treatment cannot be used as a reliable tool to detect possible damage of the inner spore membrane caused by the plasma treatment.

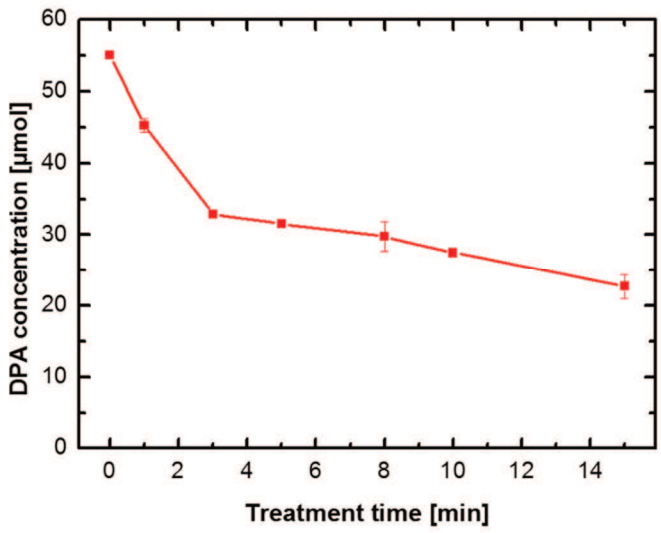

Figure 7—3: Disintegration of DPA exposed to a RF-driven plasma jet with pure argon as process gas.

Igniting cold plasma in the surrounding ambient air the plasma, independently of the used plasma source or process gas, interacts with the ambient air. These interactions cause the generation of ROS and RNS, even though the plasma is generated with a noble gas (e.g. argon) (Brandenburg et al. 2007; Brandenburg et al. 2009; Hertwig et al. 2015b; Reineke et al. 2015). These interactions hamper studies investigating the role and importance of certain reactive components of the CAPP in the spore inactivation. To overcome such problems *Bacillus* spores were plasma treated under a static atmosphere inside a treatment chamber using the DCSBD plasma system (Hertwig et al. 2017). *Bacillus* spores inoculated on glass beads were treated using dry air, N_2, O_2 and CO_2 as a process gas, whereas the different CAPPs generated different reactive components in different concentrations. CAPP generated with air had emission intensities in the UV-B and -A range, indicating the generation of RNS, and lower ones in the UV-C range. N_2-plasma had higher intensities in the entire UV range compared to air-plasma and a 4.5-fold higher intensity in the UV-C range. CO_2-plasma showed negligible emission intensities but generated a significant amount of ozone. O_2-plasma had also just negligible emission intensities, but generated a low concentration of atomic oxygen and a 11-fold higher ozone concentration as CO_2-plasma. For a better comparison of the obtained inactivation, the D-values of the different CAPP treatments were calculated. The important role of the generated UV-C photons in plasma-based *Bacillus subtilis* spore inactivation is shown for the treatment with N_2-plasma, which had a D-value of 0.06 min. The other three used plasmas had a similar inactivation behavior and D-values between 1.10 (CO_2), 1.21 (air) and 1.52 min (O_2). The inactivation of the *Bacillus subtilis* spores was also compared with *Bacillus atrophaeus* spores. In general, the *Bacillus atrophaeus* spores were more sensitive towards all tested plasmas. However, at the beginning of the treatment these spores exhibit a higher resistance towards the CAPPs with the high concentration of ROS, O_2- and CO_2-plasma, indicated by D-values of 1.80 and 1.28 min, respectively. The four different CAPPs generated with the DCSBD system were also used to investigate certain *Bacillus subtilis* spore properties involved in the resistance toward CAPP. Therefore, *Bacillus subtilis* isogenic mutant strains were used:

- PS578, lacks the genes encoding the spore's two major α/β-type SASPs, thus the α/β-type SASP level in the PS578 spores is only ~25 % of that in the wild types spores PS832
- FB122, lacks the gene encoding the cortex lytic enzyme *sleB* and is not able to synthesize DPA during the sporulation
- PS3328, lacks the *CotE* protein, which is essential for the spore's coat morphology, especially for the structure of the outer spore coat.

The strain PS578 was less resistant to all tested plasmas as the wild-type PS832. The results showed the contribution of the α/β-type SASP in general to the spores' CAPP resistance. The inactivation achieved with the N_2-plasma is especially notable, since not even a D-value could be calculated, showing the importance of the α/β-type SASPs in the resistance towards UV-C photons (Setlow 2001; Reineke et al. 2015). The DPA inside the spore core also contributes to the spores' UV resistance, but to a lower extent than the α/β-type SASPs (Setlow 2014; Reineke et al. 2015). The low water content and the DPA inside the spores' core contribute to the unique spore DNA UV photochemistry (Setlow 2006). With prolonged CAPP treatment, the FB122 spores were also more sensitive towards the O_2-plasma, showing a presumed protective effect of the DPA against ROS, e.g. ozone. A similar effect for CO_2-plasma was not observed, maybe due to the 11-fold lower generation of ozone. Compared to DPA replete spores the strain FB122 has a water content in the core that is 20 % higher (Setlow et al. 2006), hence the generated ROS can cause possible oxidative reactions in the hydrated core. A higher sensitivity of *Bacillus subtilis* spores lacking DPA to hydrogen peroxide was reported by Paidhungat et al. (2000). In addition, Popham et al. (1995) showed a decrease of spore resistance to hydrogen peroxide with an increasing core water content. The strain PS3328 without the outer spore coat had a similar inactivation behavior as the FB122 spores towards O_2- and CO_2-plasma, showing the importance of the outer coat in the resistance towards ROS. The spore coat is an important factor in the resistance towards larger oxidizing agents, as ozone (Setlow 2014; Young & Setlow 2004). The outer coat is also involved in the protection of the spores against UV photons (Fiebrandt et al. 2017), indicated by the higher sensitivity of the PS3328 spores to air- and N_2-plasma compared with the wild-type spores PS832. All tested spore strains showed a comparable distribution on the glass beads (Figure 7—4) as the *Bacillus subtilis* wild-type spores (Figure 7—2). The spores are scattered on the surface of the glass beads and bigger spore agglomerates are rarely visible, hence a lower antimicrobial efficiency of the CAPP treatment due to spore agglomeration can be excluded.

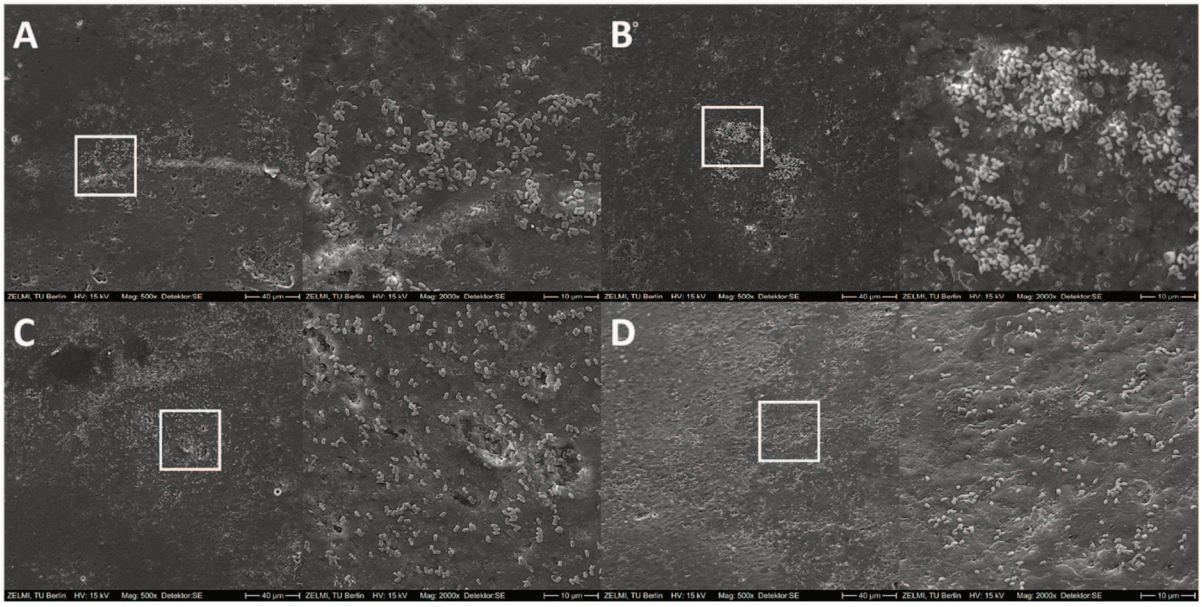

Figure 7—4: Scanning electron micrographs of Bacillus spores' distribution on glass beads. A) Bacillus atrophaeus, B) PS578, C) FB122 and D) PS3328. The white frame represents the section of the following pictures.

In this study the antimicrobial efficiency of the CAPP applications was also investigated on a real food matrix. Therefore, black peppercorns were chosen as a usually highly contaminated matrix with spore-forming bacteria as main spoilage microorganisms (Hertwig et al. 2015a). Besides of the peppercorns with native microbial load, also decontaminated peppercorns inoculated with *Bacillus subtilis* and *Bacillus atrophaeus* spores as well as the vegetative bacteria *Salmonella enterica* (DSM 17058) were treated. The DCSBD plasma system could not be used for the peppercorn treatment. Due to electrostatic charges the peppercorns could not be moved on the DCSBD plate for a homogeneous CAPP treatment. The black peppercorns were directly plasma treated using the RF-driven plasma jet system and indirectly with PPA using a microwave plasma torch. After 15 min the direct CAPP treatment resulted in an inactivation of the native microbial load below 1.0 $\log_{10}$, similar results were obtained for both inoculated *Bacillus* spore strains, whereas *Salmonella enterica* had a higher inactivation of 2.7 $\log_{10}$, as expected. The indirect CAPP treatment with PPA resulted in a slightly higher inactivation for all investigated microorganisms. Scanning electron microscopy was used to investigate the impact of both CAPP applications on the *Bacillus atrophaeus* spores' morphology. The direct plasma treatment resulted in a clear modification and rupture of the spore surface, whereas the indirect plasma treatment caused no alteration or damage of the spore outer structure. However, both applied CAPP treatments did not result in the sufficient reduction of the native microbial flora.

Furthermore, the impact of the different CAPP applications on quality parameters of the black peppercorns was investigated. Both CAPP applications had no impact on the quality of the peppercorns, as surface color, the main aroma compound piperine and the essential oil content. Nevertheless, the treatment of crushed oregano and paprika powder with PPA resulted in significant color changes (Hertwig et al. 2015c). The treatment of unpeeled almonds using the DCSBD plasma system lead to a significant browning of the almond surface. The color changes were attributed to generated RNS, since the browning just occurred for the treatment with air- and N_2-plasma, whereas the treatment with O_2- and CO_2-plasma did not cause any changes in the surface color (Hertwig et al. 2016). These results for the CAPP treatment of dry products point out how complex the plasma-product interactions can be. Therefore, possible applications of CAPP need to be product-specifically optimized to obtain the desired goal and reduce unwanted plasma-product interactions.

Besides the CAPP treatment solid surfaces, CAPP can also be used to inactivate bacterial spores in liquid media. However, the involved inactivation mechanisms are different to those of the CAPP treatment on dry surfaces. A liquid matrix represents a quite reactive environment for the different generated reactive components of the plasma. The reaction of ROS and RNS resulted often in a pH change of the media (Oehmigen et al. 2010). Furthermore, the reactive components of the plasma first react with the liquid, so that the spores are not directly affected by the reactive component of the plasma but by their succeeding reaction products. The different reactive components of the plasma, e.g. ROS and RNS, can interact with the water and other molecules resulting in multiple chain reactions in the liquid media, which produce a great variety of different reactive species. Figure 7—5A shows the pH of different liquids exposed to PPA and the resulting rapid pH decrease. PPA contains a high amount of RNS (Fröhling, Durek, et al. 2012; Hertwig et al. 2015a), which probably react to nitric and nitrous acid in the liquid media.

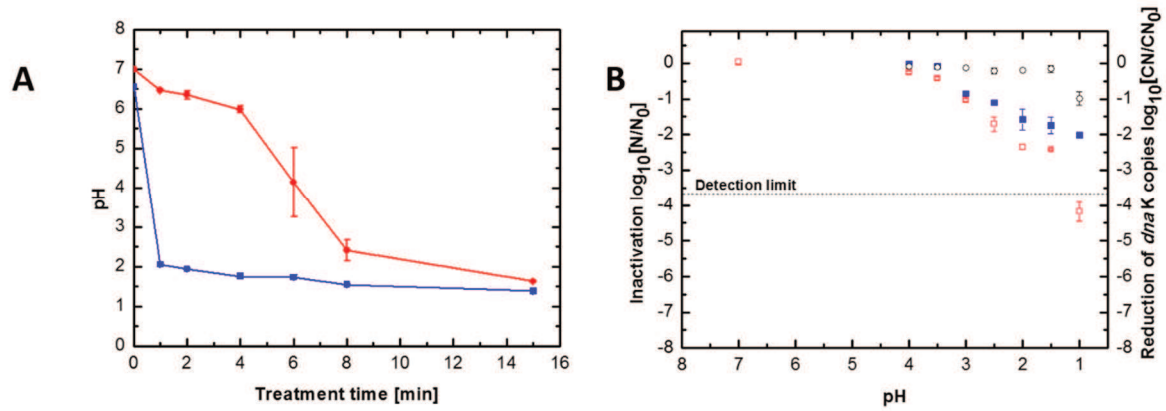

Figure 7—5: A) Plasma-induced pH change in the spore suspensions in water (■) and ACES (●). B) Impact of nitric acid on the inactivation (■) and DNA damage (○) of Bacillus subtilis spores and the inactivation after a mild heat treatment (80 °C for 20 min) (□).

The inactivation of *Bacillus subtilis* is shown in Figure 7—6A, whereby the inactivation was plotted versus the plasma-induced pH changes. All *Bacillus subtilis* spores were sensitive to a mild heat treatment (80 °C for 20 min) below a plasma-induced pH of 4.8, which might indicate a damage of the inner spore membrane. The release of DPA could not be detected due to possible interactions of the DPA with the acidic liquid and succeeding reaction products, which influence the detection using HPLC. However, scanning electron micrographs showed collapsed *Bacillus subtilis* spores, presumably due to DPA release, at a plasma-induced pH of 2.1 (water) and 1.7 (ACES) (Figure 7—7B and C). Moreover, the treatment with PPA caused a damage of the spores' DNA (Figure 7—6B).

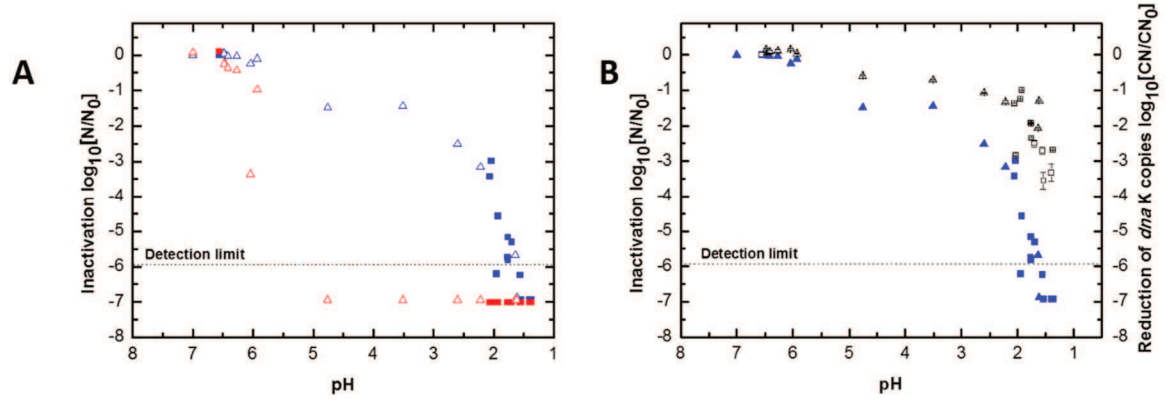

Figure 7—6: A) Inactivation of Bacillus subtilis spores in water (■) and ACES (Δ) plotted versus the plasma-induced pH change and after mild heat treatment (80 °C for 20 min) in water (■) and ACES (Δ). B) Comparison of inactivation (■) and DNA damage (□) in water and inactivation (▲) and DNA (Δ) damage in ACES.

The incubation of *Bacillus subtilis* spores in nitric acid solutions with different pH values for 30 min did not result in comparable findings regarding the inactivation and DNA damage (Figure 7—5B) as well as effects on the spores' morphology (Figure 7—7D), indicating that the

plasma-induced acidification of the liquid media is not the main factor responsible for the inactivation of *Bacillus subtilis* spores. The great variety of different produced reactive species in the liquid media is presumably affecting the inactivation process of the spores.

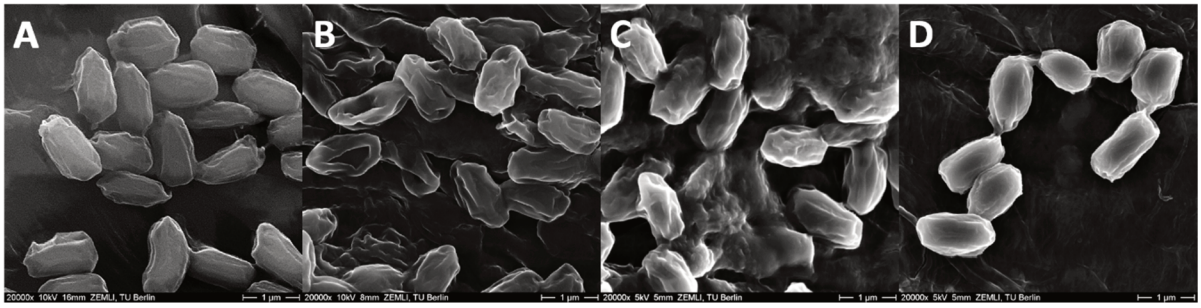

Figure 7—7: Scanning electron micrographs of dried Bacillus subtilis, A) untreated, B) in water at a plasma induced pH of 2.1, C) in ACES at a plasma induced pH of 1.7 and D) in nitric acid solution at pH 2.0.

This work gives a comprehensive insight into the inactivation of *Bacillus* spores by cold atmospheric pressure plasma and helps to understand the underlying mechanisms of spore inactivation during CAPP treatment.

Properties of *Bacillus subtilis* spores responsible for the resistance towards CAPP have been identified (Table 7-1). CAPP is composed, depending on the used process gas and form of application, of different reactive components, which are involved in the inactivation process of bacterial spores. Thus, various spore properties are responsible for the spores' resistance towards CAPP, such as the outer coat, saturation of the DNA with α/β-type SASP, as well as the DPA level inside the core and presumably the low water content. For the use of a plasma with high emission of (V)UV photons, the same spore properties are involved in the resistance as for the treatment with UV radiation. The binding of the α/β-type SASPs to the DNA of the spore resulted in a different DNA UV photochemistry, when the spores were exposed to UV radiation. The formed unique spore photoproduct allows a relatively error-free repair during the spore outgrowth (Setlow 2014). In the case of a plasma, which generated a high amount of ROS, such as ozone, similar resistance mechanisms are involved as for the treatment of spores with oxidizing agents. Again the saturation of the spore's DNA with α/β-type SASPs is a major factor. Furthermore, the outer spore coat also contributes substantially to the resistance of the spores (Setlow 2014). In contrast to the application of UV radiation or other inactivation treatments, such as the application of oxidizing agents, CAPP consists of different reactive components. These components, like (V)UV photons, ROS and RNS, allow a multi-target inactivation of bacterial spores. Moreover, these components cannot only act individually, they can also act

synergistically in the inactivation process, being a major advantage of plasma-based spore inactivation.

Table 7-1: Factors involved in endospore resistance towards different physical and chemical treatments, adapted from Reineke 2012.

Sporicidal treatment	Defense mechanism/ factor influencing the resistance	Reference
Wet heat	• Sporulation temperature	(Melly et al. 2002; Raso et al. 1995)
	• Core's level of DPA and Ca^{2+}	(Setlow et al. 2006)
	• α/β-type SASP	(Setlow 2007)
	• Core's low water content	(Gerhardt & Marquis 1989)
Dry heat	• DNA protection by α/β-type SASP	(Huesca Espitia et al. 2002; Setlow et al. 2006)
	• DNA repair enzymes ExoA and Nfo (active during germination)	(Salas-pacheco et al. 2005; Barraza-Salas et al. 2010)
Desiccation	• DNA protection by α/β-type SASP	(Setlow 1995)
Hydrogen peroxide	• DNA protection by α/β-type SASP	(Setlow 2006)
Ionizing radiation	• DNA repair enzymes ExoA and Nfo (active during germination)	(Salas-pacheco et al. 2005; Barraza-Salas et al. 2010)
	• Core's low water content	(Nicholson et al. 2000)
	• Sulphur-rich spore coat proteins and DPA	(Nicastro et al. 2002)
	• Increased levels of Mn2+ and other divalent cations	(Granger et al. 2011)
UV radiation	• UV-Photochemistry of DPA - DNA – formation of "spore photoproduct"	(Nicholson et al. 2000; Douki et al. 2005a)
	• Error free repair "spore photoproducts"	(Douki et al. 2005b)
	• DNA protection by α- and β- type SASP	(Setlow 2006)
	• DNA repair enzymes ExoA (active during germination)	(Nicholson et al. 2000)
	• Specific DNA repair system for "spore photoproduct"	(Nicholson et al. 2000)
High pressure	• Sporulation temperature	(Raso et al. 1998)
	• Demineralization of the core	(Igura et al. 2003)
	• Ability to retain DPA	(Margosch et al. 2004; Reineke et al. 2013)
Cold atmospheric pressure plasma	•α/β-type SASP	(Hertwig et al. 2017)
	• Core's level of DPA	
	• Outer spore coat	

The inactivation of bacterial spores is a quite complex process, which is influenced by process related factors and by factors related to the treated surface. Additionally, the inactivation depends also on the used spore strain. An overview about the factors is given in Figure 7—8. All of these factors need to be taken into account to understand the CAPP-based inactivation of bacterial spores.

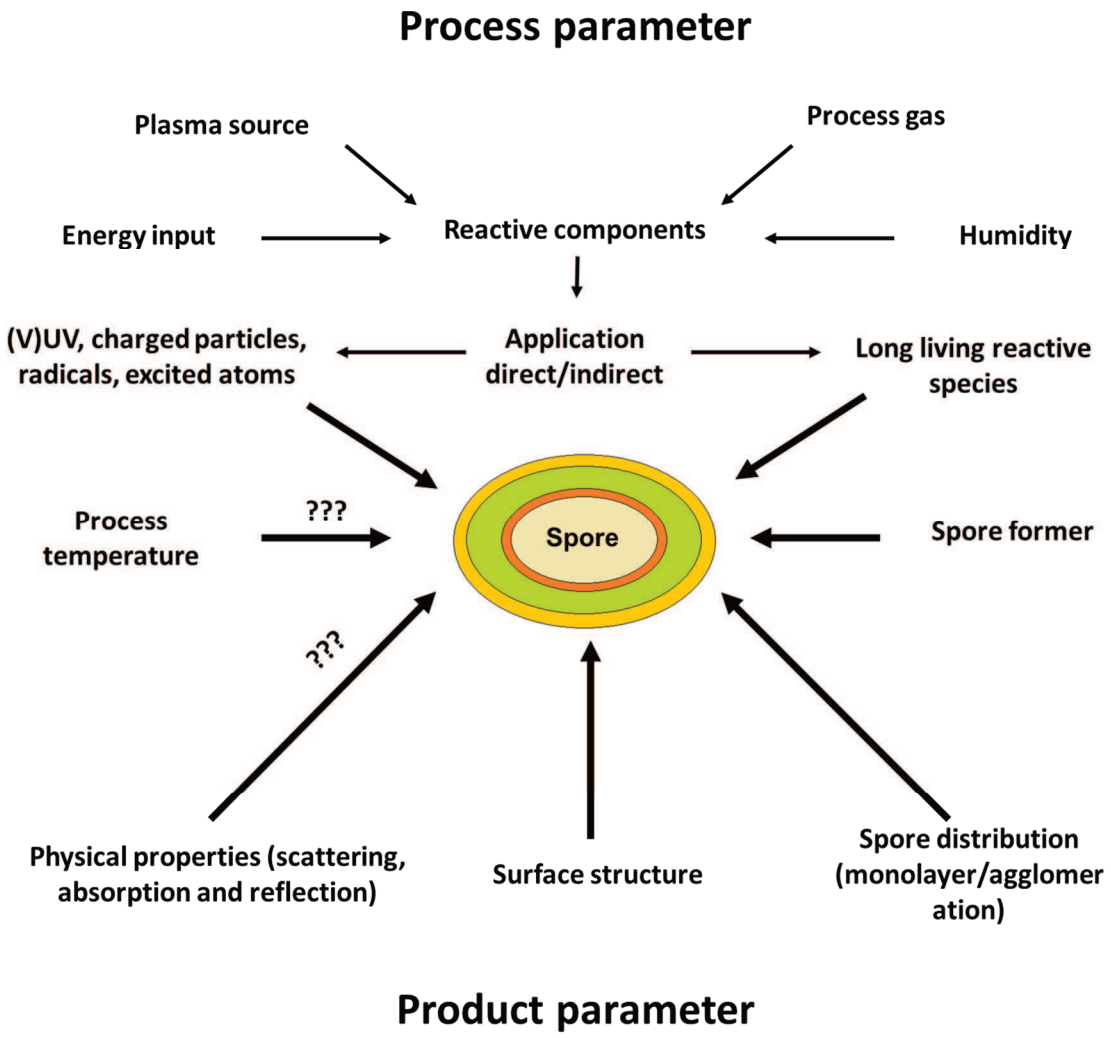

Figure 7—8: Relevant factors of spore inactivation by cold atmospheric pressure plasma.

The inactivation depends basically on the different generated reactive components of the CAPP. However, the generation of these components and their concentration depends for instance on the used plasma source and process gas. The results of this work show the importance of the (V)UV photons emitted by the plasma with reference to the inactivation process of the spores. The use of N_2 as a process gas or the admixture of N_2 and O_2 to a noble gas increase the amount of emitted UV photons. This results in a considerably faster inactivation of the spores, compared to plasma with a lower amount of UV photons (Hertwig et al. 2015b; Hertwig et al. 2017).

Moreover, the composition of the different generated components of the CAPP influence the process of spore inactivation. CAPP with a high amount of emitted (V)UV photons caused a high degree of DNA damage of the spores, compared to a considerable lower degree of DNA damage for CAPP with a lower amount of (V)UV photons (Hertwig et al. 2015b). Furthermore, the kinds of CAPP application, direct or indirect treatment, also influences the inactivation. Because in case of an indirect treatment, for example with PPA, the role of (V)UV photons can be neglected and the inactivation is driven by long living reactive components (Hertwig et al. 2015a). The surface related parameters can also affect the inactivation of bacterial spores tremendously. A complex surface structure as found on black peppercorn, with cracks, pits and grooves, lowers the antimicrobial efficiency of a CAPP treatment significantly, either for plasma with a high amount of (V)UV photons or for a plasma with a high amount of ROS and RNS (Hertwig et al. 2015b). Structured surfaces can cause shadow effects, thus the plasma components cannot interact with the spores on the surface. Moreover, the physical properties of the treated material should also be taken into consideration, as electromagnetic waves, e.g. UV photons, are influenced by the scattering, absorption and reflection of the treated material. Therefore, these material properties may also influence the antimicrobial efficiency of a CAPP treatment. Another factor, which influences the inactivation process, is the distribution of the spores on the surface. If the spores on the treated surface are present in a monolayer, they can be fast inactivated using CAPP with a high emission of (V)UV photons (Hertwig et al. 2015b; Hertwig et al. 2017). On the other hand, spore agglomerates hamper the inactivation by CAPP treatment. The penetration depth of UV photons is limited, so that just the top layer of spore agglomerates is affect by the UV photons. However, using a plasma with a high amount of ROS and RNS can support the decomposition of spores by etching effects and allows a further inactivation of agglomerated spores. The use of different spore strains can also lead to different inactivation results. For all in this study investigated CAPPs, *Bacillus atrophaeus* spores, which are most commonly used as a surrogate strain for *Bacillus anthracis* spores for various inactivation technologies, were more sensitive as the used *Bacillus subtilis* spores. Yet, the results may differ for other sub-species or for different sporulation conditions, since variations in spore resistance can be attributed to several factors and can vary tremendously between individual strains and species (Pedraza-Reyes et al. 2012).

The application of CAPP is a promising technology for the nonthermal decontamination of various surfaces in the food industry. In this work, it could be shown, that CAPP is able to successfully inactivate *Bacillus* spores on different kinds of surfaces. However, the limitations of current CAPP applications for the spore inactivation on surfaces with a complex structure,

such as whole black peppercorns, were shown. In contrast to CAPP the application of low energy electron beam (< 300 keV) offers the possibility to inactivate 5 $\log_{10}$ of bacterial spores on dry plant products, such as herbs and spices, within a treatment time of less than one second and is already available at pilot scale level (Conde-Petit 2016). Nevertheless, CAPP can rapidly inactivate on even surfaces *Bacillus* spores, showing the potential for the decontamination of food packaging materials or contact surfaces. The DCSBD plasma technology is already used at industrial scale in the textile industry to modify animal fibers (Cernak et al. 2014). The modular construction of this plasma system is an advantage and offers the possibility to easily implement the DCSBD plasma system into industrial processing lines, to decontaminate for instance food packaging material. Furthermore, this process could allow to achieve a decontamination and modification of the treated surface in one processing step.

Besides the interaction of the CAPP with the spores, CAPP also interacts with the surface the spores are attached to and may cause undesirable plasma-product reactions. Therefore, it needs to be taken into account, that optimized process parameters for spore inactivation can also result in the highest rate of plasma-product reactions. For further studies it will be essential to identify an indicator spore strain for CAPP-based inactivation processes and to evaluate the role of the process temperature during the plasma treatment. Temperature and CAPP can have a synergistic effect on the inactivation of spores. The identification of an indicator strain would increase the comparability between different plasma systems. This could lead to a better understanding of the spore inactivation mechanisms and could be useful to optimize future plasma-based inactivation concepts for various surfaces in the food industry.

References

Akitsu, T. et al., 2005. Plasma sterilization using glow discharge at atmospheric pressure. *Surface and Coatings Technology*, 193(1–3 SPEC. ISS.), pp.29–34.

Baier, M. et al., 2014. Non-thermal atmospheric pressure plasma: Screening for gentle process conditions and antibacterial efficiency on perishable fresh produce. *Innovative Food Science & Emerging Technologies*, 22, pp.147–157.

Barraza-Salas, M. et al., 2010. Effects of forespore-specific overexpression of apurinic/apyrimidinic endonuclease Nfo on the DNA-damage resistance properties of *Bacillus subtilis* spores. *FEMS Microbiology Letters*, 302(2), pp.159–165.

Blane, H.W., 1890. Anthrax: The disease of the Egyptian plagues. *New Orleans Med. Surg. J.*, 12, pp.233–236.

van Bokhorst-van de Veen, H. et al., 2015. Inactivation of chemical and heat-resistant spores of *Bacillus* and *Geobacillus* by nitrogen cold atmospheric plasma evokes distinct changes in morphology and integrity of spores. *Food Microbiology*, 45, pp.26–33.

Booth, I.R., 1985. Regulation of cytoplasmic pH in bacteria. *Microbiological reviews*, 49(4), pp.359–78.

Boudam, M.K. et al., 2006. Bacterial spore inactivation by atmospheric-pressure plasmas in the presence or absence of UV photons as obtained with the same gas mixture. *Journal of Physics D: Applied Physics*, 39(16), pp.3494–3507.

Braithwaite, N.S.J., 2000. Introduction to gas discharges. *Plasma Sources Science and Technology*, 9, pp.517–527.

Brandenburg, R. et al., 2009. Antimicrobial Effects of UV and VUV Radiation of Nonthermal Plasma Jets. *IEEE Transactions on Plasma Science*, 37(6), pp.877–883.

Brandenburg, R. et al., 2007. Antimicrobial Treatment of Heat Sensitive Materials by Means of Atmospheric Pressure Rf-Driven Plasma Jet. *Contributions to Plasma Physics*, 47(1–2), pp.72–79.

Bußler, S. et al., 2015. Impact of thermal treatment versus cold atmospheric plasma processing on the techno-functional protein properties from Pisum sativum "Salamanca." *Journal of Food Engineering*, 167, pp.166–174.

Butscher, D. et al., 2016. Plasma inactivation of bacterial endospores on wheat grains and polymeric model substrates in a dielectric barrier discharge. *Food Control*, 60, pp.636–645.

Cano, R.J. & Borucki, M.K., 1995. Revival and identification of bacterial spores in 25-to 40-million-year-old Dominican amber. *Science*, 268(5213), p.1060.

Cernak, M. et al., 2014. METHOD FOR IMPROVING FELTING PROPERTIES OF ANIMAL FIBRES BY PLASMA TREATMENT. European Patent, (EP2488690 B1).

Černák, M. et al., 2009. Diffuse Coplanar Surface Barrier Discharge and its applications for in-line processing of low-added-value materials. *The European Physical Journal Applied Physics*, 47(2), p.22806.

Cheng, C. et al., 2014. Atmospheric pressure plasma jet utilizing Ar and Ar/H 2 O mixtures and its applications to bacteria inactivation. *Chinese Physics B*, 23(7), p.75204.

Claro, T. et al., 2015. Cold-Air Atmospheric Pressure Plasma Against *Clostridium difficile* Spores: A Potential Alternative for the Decontamination of Hospital Inanimate Surfaces. *Infection control and hospital epidemiology*, 36(6), pp.742–4.

Cohn, F.J., 1876. Untersuchungen über Bakterien M. Müller, ed. *Beiträge zur Biologie der Pflanzen 2*, pp.249–276.

Conde-Petit, B., 2016. The challenge of pathogenic bacteria in low water activity foods – Technology solutions for today and tomorrow. Oral presentation at: 30th EFFoST Conference 2016, Vienna.

Cortezzo, D.E. & Setlow, P., 2005. Analysis of factors that influence the sensitivity of spores of *Bacillus subtilis* to DNA damaging chemicals. *Journal of Applied Microbiology*, 98(3), pp.606–617.

Deng, X., Shi, J. & Kong, M., 2006. Physical mechanisms of inactivation of *Bacillus subtilis* spores using cold atmospheric plasmas. *IEEE Transactions on Plasma Sciences*, 34(4), pp.1310–1316.

Dobrynin, D. et al., 2010. Cold plasma inactivation of *Bacillus cereus* and *Bacillus anthracis* (anthrax) spores. *IEEE Transactions on Plasma Science*, 38(8 PART 2), pp.1878–1884.

Douki, T., Setlow, B. & Setlow, P., 2005a. Effects of the Binding of α/β-type Small, Acid-soluble Spore Proteins on the Photochemistry of DNA in Spores of *Bacillus subtilis* and In Vitro¶. *Photochemistry and Photobiology*, 81(1), pp.163–169.

Douki, T., Setlow, B. & Setlow, P., 2005b. Photosensitization of DNA by dipicolinic acid, a major component of spores of *Bacillus* species. *Photochemical & Photobiological Sciences*, 4(8), pp.591–597.

Ehlbeck, J. et al., 2008. PLASMOSE - antimicrobial effects of modular atmospheric plasma sources. *GMS Krankenhaushygiene Interdisziplinär*, 3(1).

Ehlbeck, J. et al., 2011. Low temperature atmospheric pressure plasma sources for microbial decontamination. *Journal of Physics D: Applied Physics*, 44(1), pp.1–18.

Eliasson, B. & Kogelschatz, U., 1991. Nonequilibrium Volume Plasma Chemical Processing. *IEEE Transactions on Plasma Science*, 19(6), pp.1063–1077.

Fairheadt, H., Setlow, B. & Setlow, P., 1993. Prevention of DNA Damage in Spores and In Vitro by Small , Acid-Soluble Proteins from Bacillus Species. *Journal of Bacteriology*, 175(5), pp.1367–1374.

Fernández, A. et al., 2012. Effect of microbial loading on the efficiency of cold atmospheric gas plasma inactivation of *Salmonella enterica* serovar Typhimurium. *International Journal of Food Microbiology*, 152(3), pp.175–80.

Fiebrandt, M. et al., 2017. VUV absorption spectroscopy of bacterial spores and DNA components. *Plasma Physics and Controlled Fusion*, 59(1), p.14010.

Fridman, A., 2008. *Plasma Chemistry*, New York: Cambridge University Press.

Fridman, A. & Friedman, G., 2013. *Plasma Medicine*, New York: John Wiley & Sons, Ltd.

Fröhling, A., Baier, M., et al., 2012. Atmospheric pressure plasma treatment of *Listeria innocua* and *Escherichia coli* at polysaccharide surfaces: Inactivation kinetics and flow cytometric characterization. *Innovative Food Science & Emerging Technologies*, 13, pp.142–150.

Fröhling, A., Durek, J., et al., 2012. Indirect plasma treatment of fresh pork: Decontamination efficiency and effects on quality attributes. *Innovative Food Science & Emerging Technologies*, 16, pp.381–390.

GBIF, 2016. Global Biodiversity Information Facility - Deutschland.

Gerhardt, P. & Marquis, R.E., 1989. Spore thermoresistance mechanisms. In I. Smith, R. A. Slepecky, & P. Setlow, eds. *Regulation of Procaryotic Development*. Washington, DC, pp. 43–63.

De Geyter, N. et al., 2007. Treatment of polymer films with a dielectric barrier discharge in air, helium and argon at medium pressure. *Surface and Coatings Technology*, 201(16–17), pp.7066–7075.

Gould, G.W., 2006. History of science - Spores: Lewis B Perry Memorial Lecture 2005. *Journal of Applied Microbiology*, 101(3), pp.507–513.

Granger, A.C. et al., 2011. Effects of Mn and Fe levels on *Bacillus subtilis* spore resistance and effects of Mn2+, other divalent cations, orthophosphate, and dipicolinic acid on protein resistance to ionizing radiation. *Applied and Environmental Microbiology*, 77(1), pp.32–40.

Greenberg, D.L. et al., 2010. Identifying experimental surrogates for *Bacillus anthracis* spores: a review. *Investigative Genetics*, 1(1), p.4.

Grzegorzewski, F., 2010. *Influence of Non-Thermal Plasma Species on the Structure and Functionality of Isolated and Plant-based 1, 4-Benzopyrone Derivatives and Phenolic Acids*. PhD, Technische Universität Berlin.

Heinz, V. & Knorr, D., 2001. Effects of High Pressure on Spores. In M. E. G. Hendrickx et al., eds. *Ultra High Pressure Treatments of Foods*. Boston, MA: Springer US, pp. 77–113.

Heise, M. et al., 2004. Sterilization of Polymer Foils with Dielectric Barrier Discharges at Atmospheric Pressure. *Plasmas and Polymers*, 9(1), pp.23–33.

Henriques, A.O. & Moran, C.P., 2007. Structure, assembly, and function of the spore surface layers. *Annual review of microbiology*, 61, pp.555–588.

Hergelová, B. et al., 2014. Polylactic acid surface activation by atmospheric pressure dielectric barrier discharge plasma. *Open Chemistry*, 13(1), pp.564–569.

Herrmann, H.W. et al., 1999. Decontamination of chemical and biological warfare (CBW) agents using an atmospheric pressure plasma jet (APPJ). *Physics of Plasmas*, 6(5), pp.2284–2289.

Hertwig, C., Reineke, K., Ehlbeck, J., Knorr, D., et al., 2015a. Decontamination of whole black pepper using different cold atmospheric pressure plasma applications. *Food Control*, 55, pp.221–229.

Hertwig, C., Reineke, K., et al., 2017. Factors involved in *Bacillus* spore's resistance to cold atmospheric pressure plasma. *submitted*.

Hertwig, C., Reineke, K., Ehlbeck, J., Erdoğdu, B., et al., 2015c. Impact of remote plasma treatment on natural microbial load and color of selected herbs and spices. *Journal of Food Engineering*, 167, pp.12–17.

Hertwig, C., Steins, V., et al., 2015b. Impact of surface structure and feed gas composition on *Bacillus subtilis* endospore inactivation during direct plasma treatment. *Frontiers in Microbiology*, 6(August), pp.1–12.

Hertwig, C., Leslie, A., et al., 2016. Inactivation of *Salmonella* Enteritidis PT30 on the surface of unpeeled almonds by cold plasma. *submitted.*

Hong, Y.F. et al., 2009. Sterilization effect of atmospheric plasma on *Escherichia coli* and *Bacillus subtilis* endospores. *Letters in Applied Microbiology*, 48(1), pp.33–37.

De Hoon, M.L., Eichenberger, P. & Vitkup, D., 2010. Hierarchical evolution of the bacterial sporulation network. *Current Biology*, 20(17), pp.735–745.

Hort, G., 1958. The plagues of Egypt. *Zeitschrift für die Alttestamentaliche Wissenschaft*, 70, pp.48–59.

Huesca Espitia, L.D.C. et al., 2002. Base-change mutations induced by various treatments of *Bacillus subtilis* spores with and without DNA protective small, acid-soluble spore proteins. *Mutation Research - Fundamental and Molecular Mechanisms of Mutagenesis*, 503(1–2), pp.77–84.

Igura, N. et al., 2003. Effects of Minerals on Resistance of *Bacillus subtilis* Spores to Heat and Hydrostatic Pressure. *Applied and Environmental Microbiology*, 69(10), pp.6307–6310.

Jeon, J. et al., 2014. Sporicidal properties from surface micro-discharge plasma under different plasma conditions at different humidities. *New Journal of Physics*, 16.

Jung, H. et al., 2010. Enhanced inactivation of bacterial spores by atmospheric pressure plasma with catalyst TiO2. *Applied Catalysis B: Environmental*, 93(3–4), pp.212–216.

Keener, K.M. et al., 2012. Decontamination of *Bacillus subtilis* Spores in a Sealed Package Using a Non-thermal Plasma System. In *NATO Science for Peace and Security Series A: Chemistry and Biology*. pp. 417–429.

Kelly-Wintenberg, K. et al., 1998. Room temperature sterilization of surfaces and fabrics with a one atmosphere uniform glow discharge plasma. *Journal of Industrial Microbiology & Biotechnology*, 20(1), pp.69–74.

Kelly-Wintenberg, K. et al., 1999. Use of a one atmosphere uniform glow discharge plasma to kill a broad spectrum of microorganisms. *Journal of Vacuum Science & Technology A*, 17(4), pp.1539–1544.

Kim, J.E., Lee, D.-U. & Min, S.C., 2014. Microbial decontamination of red pepper powder by cold plasma. *Food microbiology*, 38, pp.128–36.

Klämpfl, T.G. et al., 2012. Cold atmospheric air plasma sterilization against spores and other microorganisms of clinical interest. *Applied and Environmental Microbiology*, 78(15), pp.5077–5082.

Klämpfl, T.G., 2014. *Cold atmospheric plasma decontamination against nosocomial bacteria*. PhD, Technische Universität München.

Klobutcher, L., Ragkousi, K. & Setlow, P., 2006. The *Bacillus subtilis* spore coat provides "eat resistance" during phagocytic predation by the protozoan Tetrahymena thermophila. *Proceedings of the National Academy of Sciences of the United States of America*, 103(1), pp.165–70.

Knorr, D. et al., 2011. Emerging technologies in food processing. *Annual review of food science and technology*, 2, pp.203–235.

Koch, A., 1888. Über Morphologie und Entwickelungsgeschichte einiger endosporer Bacterienformen. *Bot Ztg* 46, 277-287.

Kong, M.G. et al., 2009. Plasma medicine: An introductory review. *New Journal of Physics*, 11.

Koval'ová, Z. et al., 2013. Decontamination of Streptococci biofilms and *Bacillus cereus* spores on plastic surfaces with DC and pulsed corona discharges. *The European Physical Journal Applied Physics*, 61(2).

Langmuir, I., 1928. Oscillations in Ionized Gases. *Proceedings of the National Academy of Sciences*, 14(8), pp.627–637.

Laroussi, M., 2002. Nonthermal decontamination of biological media by atmospheric-pressure plasmas: Review, analysis, and prospects. *IEEE Transactions on Plasma Science*, 30(4), pp.1409–1415.

Laroussi, M. & Leipold, F., 2004. Evaluation of the roles of reactive species, heat, and UV radiation in the inactivation of bacterial cells by air plasmas at atmospheric pressure. *International Journal of Mass Spectrometry*, 233(1–3), pp.81–86.

Lee, K. et al., 2006. Sterilization of bacteria, yeast, and bacterial endospores by atmospheric-pressure cold plasma using helium and oxygen. *Journal of Microbiology (Seoul, Korea)*, 44(3), pp.269–75.

Lerouge, S. et al., 2000. Sterilization by low-pressure plasma: the role of vacuum-ultraviolet radiation. *Plasmas and Polymers*, 5(1), pp.31–46.

Li, J. et al., 2013. Study on plasma agent effect of a direct-current atmospheric pressure oxygen-plasma jet on inactivation of *E. coli* using bacterial mutants. *IEEE Transactions on Plasma Science*, 41(4), pp.935–941.

Lim, J.P., Uhm, H.S. & Li, S.Z., 2007. Influence of oxygen in atmospheric-pressure argon plasma jet on sterilization of *Bacillus atrophaeous* spores. *Physics of Plasmas*, 14(9).

Logan, N.A., 2012. *Bacillus* and relatives in foodborne illness. *Journal of Applied Microbiology*, 112(3), pp.417–429.

Lu, P., Cullen, P.J. & Ostrikov, K., 2016. Atmospheric Pressure Nonthermal Plasma Sources. In *Cold Plasma in Food and Agriculture*. pp. 83–116.

Mallozzi, M., Viswanathan, V.K. & Vedantam, G., 2010. Spore-forming Bacilli and Clostridia in human disease. *Future Microbiology*, 5(7), pp.1109–23.

Manos, D.M. & Flamm, D.L., 1989. *Plasma Etching: An Introduction*, Elsevier.

Margosch, D. et al., 2004. Pressure inactivation of *Bacillus* endospores. *Applied and Environmental Microbiology*, 70(12), pp.7321–7328.

Mathys, A., 2008. *Inactivation mechanisms of Geobacillus and Bacillus spores during high pressure thermal sterilization.* PhD, Technische Universität Berlin.

Matsui, K., Ikenaga, N. & Sakudo, N., 2015. Effects of humidity on sterilization of *Geobacillus stearothermophilus* spores with plasma-excited neutral gas. *Japanese Journal of Applied Physics*, 54(6).

Melly, E. et al., 2002. Analysis of the properties of spores of *Bacillus subtilis* prepared at different temperatures. *Journal of Applied Microbiology*, 92(6), pp.1105–1115.

Menashi, P., 1968. Treatment of Surfaces. US patent, (US3383163 A).

Mendis, D.A., Rosenberg, M. & Azam, F., 2000. A Note on the Possible Electrostatic Disruption of Bacteria. *IEEE Transactions on Plasma Science*, 28(4), pp.1304–1306.

Misra, N.N. et al., 2011. Nonthermal Plasma Inactivation of Food-Borne Pathogens. *Food Engineering Reviews*, 3(3–4), pp.159–170.

Misra, N.N., Schlüter, O. & Cullen, P.J., 2016. Plasma in Food and Agriculture. In *Cold Plasma in Food and Agriculture*. pp. 1–16.

Moisan, M. et al., 2001. Low-temperature sterilization using gas plasmas: a review of the experiments and an analysis of the inactivation mechanisms. *International Journal of Pharmaceutics*, 226(1–2), pp.1–21.

Møller, I.M., Jensen, P.E. & Hansson, A., 2007. Oxidative modifications to cellular components in plants. *Annual review of plant biology*, 58, pp.459–81.

Moreau, S. et al., 2000. Using the flowing afterglow of a plasma to inactivate *Bacillus subtilis* spores: Influence of the operating conditions. *Journal of Applied Physics*, 88(2), pp.1166–1174.

Morris, A. et al., 2007. Bactericidal effects of non-equilibrium cold plasma on *Geobacillus stearothermophilis* and *Bacillus cereus*. *28th ICPIG, Prague, Czech Republic*, pp.1301–1303.

Munakata, N. et al., 1986. Action spectra in ultraviolet wavelengths (150-250 nm) for inactivation and mutagenesis of *Bacillus subtilis* spores obtained with synchrotron radiation. *Photochemistry and Photobiology*, 44(3), pp.385–390.

Munakata, N., Saito, M. & Hieda, K., 1991. Inactivation action spectra of *Bacillus subtilis* spores in extended ultraviolet wavelengths(50-300nm) obtained with snchrotron radiation. *Photochemistry and Photobiology*, 54(5), pp.761–768.

Muranyi, P., 2008. *Einsatz eines Atmosphärendruckplasmas zur Entkeimung von lebensmittelrelevanten Verpackungen aus Kunststoff*. PhD, Technische Universität München.

Muranyi, P., Wunderlich, J. & Heise, M., 2008. Influence of relative gas humidity on the inactivation efficiency of a low temperature gas plasma. *Journal of Applied Microbiology*, 104(6), pp.1659–1666.

Muranyi, P., Wunderlich, J. & Heise, M., 2007. Sterilization efficiency of a cascaded dielectric barrier discharge. *Journal of Applied Microbiology*, 103(5), pp.1535–1544.

Muranyi, P., Wunderlich, J. & Langowski, H.C., 2010. Modification of bacterial structures by a low-temperature gas plasma and influence on packaging material. *Journal of Applied Microbiology*, 109(6), pp.1875–1885.

Nicastro, A.J., Vreeland, R.H. & Rosenzweig, W.D., 2002. Limits imposed by ionizing radiation on the long-term survival of trapped bacterial spores: beta radiation. *International Journal of Radiation Biology*, 78(10), pp.891–901.

Nicholson, W.L. et al., 2000. Resistance of *Bacillus* endospores to extreme terrestrial and extraterrestrial environments. *Microbiology and Molecular Biology Reviews*, 64(3), pp.548–72.

Oehmigen, K. et al., 2010. The Role of Acidification for Antimicrobial Activity of Atmospheric Pressure Plasma in Liquids. *Plasma Processes and Polymers*, 7(3–4), pp.250–257.

Padan, E. & Schuldiner, S., 1987. Intracellular pH and membrane potential as regulators in the prokaryotic cell. *Journal of Membrane Biology*, 198, pp.189–198.

Paidhungat, M., Setlow, B. & Driks, A., 2000. Characterization of Spores of *Bacillus subtilis* Which Lack Dipicolinic Acid Characterization of Spores of *Bacillus subtilis* Which Lack Dipicolinic Acid. *Journal of Bacteriology*, 182(19), pp.5505–5512.

Pankaj, S.K. et al., 2014. Applications of cold plasma technology in food packaging. *Trends in Food Science & Technology*, 35(1), pp.5–17.

Pankaj, S.K. et al., 2014. Characterization of polylactic acid films for food packaging as affected by dielectric barrier discharge atmospheric plasma. *Innovative Food Science & Emerging Technologies*, 21, pp.107–113.

Park, J.C. et al., 2004. Fungal sterilization using microwave-induced argon plasma at atmospheric pressure. *Journal of Microbiology and Biotechnology*, 14(1), pp.188–192.

Patil, S. et al., 2014. Influence of high voltage atmospheric cold plasma process parameters and role of relative humidity on inactivation of *Bacillus atrophaeus* spores inside a sealed package. *Journal of Hospital Infection*, 88(3), pp.162–169.

Pedraza-Reyes, M. et al., 2012. Mechanisms of bacterial spore survival. In E. Abel-Santos, ed. *Bacterial Spores: Current Research and Applications*. Norfolk: Caister Academic Press, pp. 73–87.

Phillips, Z.. V & Strauch, M.A., 2002. *Bacillus subtilis* sporulation and stationary phase gene expression. *Cellular and Molecular Life Sciences*, 59(3), pp.392–402.

Pointu, A. et al., 2008. Nitrogen atmospheric pressure post discharges for surface biological decontamination inside small diameter tubes. *Plasma Processes and Polymers*, 5(6), pp.559–568.

Pointu, A. et al., 2005. Production of active species in N2–O2 flowing post-discharges at atmospheric pressure for sterilization. *Journal of Physics D: Applied Physics*, 38, pp.1905–1909.

Polak, M. et al., 2012. Innovative plasma generation in flexible biopsy channels for inner-tube decontamination and medical applications. *Plasma Processes and Polymers*, 9(1), pp.67–76.

Popham, D.L., 2002. Cellular and Molecular Life Sciences Specialized peptidoglycan of the bacterial endospore : the inner wall of the lockbox. *Cellular and Molecular Life Sciences*, 59, pp.426–433.

Popham, D.L., Sengupta, S. & Setlow, P., 1995. Heat, hydrogen-peroxide, and UV resistance of *Bacillus subtilis* spores with increased core water-content and with or without major DNA-binding proteins. *Applied and Environmental Microbiology*, 61(10), pp.3633–3638.

Rahul, R. et al., 2005. Optical and RF electrical characteristics of atmospheric pressure open-air hollow slot microplasmas and application to bacterial inactivation. *Journal of Physics D: Applied Physics*, 38(11), pp.1750–1759.

Ramírez-Guadiana, F.H. et al., 2012. Alternative excision repair of ultraviolet B- and C-Induced DNA damage in dormant and developing spores of *bacillus subtilis*. *Journal of Bacteriology*, 194(22), pp.6096–6104.

Raso, J. et al., 1995. Influence of sporulation temperature on the heat resistance of a strain of *Bacillus licheniformis* (Spanish Type Culture Collection 4523). *Food Microbiology*, 12(C), pp.357–361.

Raso, J., Barbosa-Cánovas, G. & Swanson, B.G., 1998. Sporulation temperature affects initiation of germination and inactivation by high hydrostatic pressure of *Bacillus cereus*. *Journal of Applied Microbiology*, 85, pp.17–24.

Reineke, K., 2012. *Mechanisms of Bacillus spore germination and inactivation during high pressure processing*. PhD, Technische Universität Berlin.

Reineke, K. et al., 2015. The impact of different process gas compositions on the inactivation effect of an atmospheric pressure plasma jet on *Bacillus* spores. *Innovative Food Science and Emerging Technologies*, 30, pp.112–118.

Reineke, K. et al., 2013. The release of dipicolinic acid - The rate-limiting step of *Bacillus* endospore inactivation during the high pressure thermal sterilization process. *International Journal of Food Microbiology*, 162(1), pp.55–63.

Robleto, E.A. et al., 2012. Gene regulations of sporulation in *Bacillus subtilis*. In E. Abel-Santos, ed. *Bacterial Spores: Current Research and Applications*. Norfolk: Caister Academic Press, pp. 9–17.

Salas-pacheco, J.M. et al., 2005. Role of the Nfo (YqfS) and ExoA Apurinic / Apyrimidinic Endonucleases in Protecting *Bacillus subtilis* Spores from DNA Damage. *Journal of Bacteriology*, 187(21), pp.7374–7381.

Scheubert, P., 2001. *Crashkurs "Plasmatechnologie"*. Oral presentation at: Fraunhofer Institut für Verfahrenstechnik und Verpackung, Freising.

Schlegel, J., Köritzer, J. & Boxhammer, V., 2013. Plasma in cancer treatment. *Clinical Plasma Medicine*, 1(2), pp.2–7.

Schlüter, O. et al., 2013. Opinion on the use of plasma processes for treatment of foods. *Molecular Nutrition & Food Research*, 57(5), pp.920–927.

Schlüter, O. & Fröhling, A., 2014. Cold Plasma for Bioefficient Food Processing. *Encyclopedia of Food Microbiology*, pp.948-953.

Schnabel, U. et al., 2014. Decontamination and Sensory Properties of Microbiologically Contaminated Fresh Fruits and Vegetables by Microwave Plasma Processed Air (PPA). *Journal of Food Processing and Preservation*, 39(6), pp.653-662.

Schnabel, U., Niquet, R., Krohmann, U., et al., 2012. Decontamination of Microbiologically Contaminated Specimen by Direct and Indirect Plasma Treatment. *Plasma Processes and Polymers*, 9(6), pp.569–575.

Schnabel, U. et al., 2013. Inactivation of Vegetative Microorganisms and *Bacillus atrophaeus* Endospores by Reactive Nitrogen Species (RNS). *Plasma Processes and Polymers*, 11(2), pp.110-116.

Schnabel, U., Niquet, R. & Krohmann, U., 2012. Decontamination of Microbiologically Contaminated Seeds by Microwave Driven Discharge Processed Gas. *Journal of Agricultural Science and Applications*, 1(4), pp.100–106.

Schweiggert, U., Carle, R. & Schieber, A., 2007. Conventional and alternative processes for spice production – a review. *Trends in Food Science & Technology*, 18(5), pp.260–268.

Setlow, B. et al., 2006. Role of dipicolinic acid in resistance and stability of spores of *Bacillus subtilis* with or without DNA-protective α/β-type small acid-soluble proteins. *Journal of Bacteriology*, 188(11), pp.3740–3747.

Setlow, B. & Setlow, P., 1995. Small , acid-soluble proteins bound to DNA protect *Bacillus subtilis* spores from killing by dry heat . *Applied and environmental microbiology*, 61(7), pp.2787–2790.

Setlow, P., 2012. Dynamics of the assembly of a complex macromolecular structure - the coat of spores of the bacterium *Bacillus subtilis*. *Molecular Microbiology*, 83(2), pp.241–244.

Setlow, P., 2007. I will survive: DNA protection in bacterial spores. *Trends in Microbiology*, 15(4), pp.172–180.

Setlow, P., 1995. Mechanisms for the prevention of damage to DNA in spores of *Bacillus* species. *Annual Review of Microbiology*, 49, pp.29–54.

Setlow, P., 2001. Resistance of spores of *Bacillus* species to ultraviolet light. *Environmental and Molecular Mutagenesis*, 38(2–3), pp.97–104.

Setlow, P., 2014. Spore Resistance Properties. *Microbiology Spectrum*, 2(5), pp.1–14.

Setlow, P., 2006. Spores of *Bacillus subtilis*: their resistance to and killing by radiation, heat and chemicals. *Journal of Applied Microbiology*, 101(3), pp.514–525.

Sevenich, R., 2016. *High pressure processing at ambient and high temperatures and its influence on food processing contaminants, food borne diseases*. PhD, Technische Universität Berlin.

Sharma, V. et al., 2013. Effects of Cold Atmospheric Pressure Plasma Jet on the Viability of *Bacillus subtilis* Endospores. *Advanced Materials Research*, 647, pp.524–531.

Shen, J. et al., 2012. Sterilization of *bacillus subtilis* spores using an atmospheric plasma jet with argon and oxygen mixture gas. *Applied Physics Express*, 5(3), pp.5–8.

Shimizu, S. et al., 2014. Cold atmospheric plasma - A new technology for spacecraft component decontamination. *Planetary and Space Science*, 90, pp.60–71.

Siemens, W., 1857. Ueber die elektrostatische Induction und die Verzögerung des Stroms in Flaschendrähten. *Annalen der Physik*, 178(9), pp.66–122.

Smet, C. et al., 2016. Impact of food model (micro)structure on the microbial inactivation efficacy of cold atmospheric plasma. *International Journal of Food Microbiology*.

Surowsky, B. et al., 2016. Cold Plasma Interactions With Food Constituents in Liquid and Solid Food Matrices. In *Cold plasma in food and agriculture*. pp. 179–203.

Surowsky, B., Schlüter, O. & Knorr, D., 2014. Interactions of Non-Thermal Atmospheric Pressure Plasma with Solid and Liquid Food Systems: A Review. *Food Engineering Reviews*.

Tainter, D. & Grenis, A., 2001. *Spices and Seasonings: A Food Technology Handbook* 2end ed. D. Tainter & A. Grenis, eds., New York: Wiley.

Takemura, Y. et al., 2014. Inactivation treatment of bacterial spores contaminated spices by atmospheric plasma jet. *Plasma Medicine*, 4(1–4), pp.89–100.

Tateo, F. & Bononi, M., 2006. Determination of ethylene chlorohydrin as marker of spices fumigation with ethylene oxide. *Journal of Food Composition and Analysis*, 19(1), pp.83–87.

Torred, M. et al., 2012. Historical Notes and Introduction to Bacterial Spores. In E. Abel-Santos, ed. *Bacterial Spores: Current Research and Applications*. Norfolk: Caister Academic Press, pp. 1–8.

Trompeter, F. et al., 2002. Reduction of *Bacillus Subtilis* and *Aspergillus Niger* Spores Using Nonthermal Atmospheric Gas Discharges. *IEEE Transactions on Plasma Science*, 30(4), pp.1416–1423.

Turner, M., 2016. Physics of Cold Plasma. In *Cold Plasma in Food and Agriculture*. Elsevier Inc., pp. 17–51.

Uhm, H.S., Hong, Y.C. & Shin, D.H., 2006. A microwave plasma torch and its applications. *Plasma Sources Science and Technology*, 15(2), pp.S26–S34.

Venezia, R.A. et al., 2008. Lethal Activity of Nonthermal Plasma Sterilization Against Microorganisms. *Infection Control and Hospital Epidemiology*, 29(5), pp.430–436.

Vreeland, R.H., Rosenzweig, W.D. & Powers, D.W., 2000. Isolation of a 250 million-year-old halotolerant bacterium from a primary salt crystal. *Nature*, 407(6806), pp.897–900.

Wang, S. et al., 2016. Use of Raman Spectroscopy and Phase-Contrast Microscopy To Characterize Cold Atmospheric Plasma Inactivation of Individual. *Applied and Environmental Microbiology*, 82(19), pp.5775–5784.

Weltmann, K.-D. et al., 2008. Antimicrobial treatment of heat sensitive products by miniaturized atmospheric pressure plasma jets (APPJs). *Journal of Physics D: Applied Physics*, 41(19).

Winter, J., Brandenburg, R. & Weltmann, K.-D., 2015. Atmospheric pressure plasma jets: an overview of devices and new directions. *Plasma Sources Science and Technology*, 24(6), p.64001.

Yoshino, D. et al., 2015. Development of low-temperature sterilization device using atmospheric pressure air plasma with circulating flow. *Mechanical Engineering Journal*, 2(5), pp.15-187-15–00187.

Young, S.B. & Setlow, P., 2004. Mechanisms of *Bacillus subtilis* spore resistance to and killing by aqueous ozone. *Journal of Applied Microbiology*, 96(5), pp.1133–1142.

Zahoranová, A. et al., 2016. Effect of Cold Atmospheric Pressure Plasma on the Wheat Seedlings Vigor and on the Inactivation of Microorganisms on the Seeds Surface. *Plasma Chemistry and Plasma Processing*, 36(2), pp.397–414.

Zimmermann, J.L. et al., 2011. Effects of cold atmospheric plasmas on adenoviruses in solution. *Journal of Physics D: Applied Physics*, 44(50), p.505201.

Ziuzina, D. et al., 2014. Atmospheric cold plasma inactivation of *Escherichia coli*, *Salmonella enterica* serovar Typhimurium and *Listeria monocytogenes* inoculated on fresh produce. *Food Microbiology*, 42, pp.109–116.

Annex

1. Analysis of the DPA degradation

For the quantification of the DPA degradation due to the cold atmospheric pressure plasma a Dionex Ultimate 3000 system was used (Dionex Coporation, Sunnyvale, CA, USA), with a reversed phase separating column (RP 18-5 µm LiChroCart 124-4; Merck KGaA, Darmstadt, Germany) that was protected with a guard column (LiChroCart 4-4, Merck KGaA, Darmstadt, Germany). The detection limit of the HPLC setup was 1 µM DPA. Standard solutions of known DPA concentration were used to calculate a calibration curve.

Known DPA concentration of the standard solutions (standard deviation in brackets) and the obtained calibration curve.

DPA conentration [µM]	Area [mAU*min]
1	0.02 (±0.00)
5	1.08 (±0.00)
10	2.36 (±0.00)
20	4.95 (±0.01)
30	7.32 (±0.02)
40	9.46 (±0.01)
50	12.27 (±0.02
100	25.08 (±0.03)

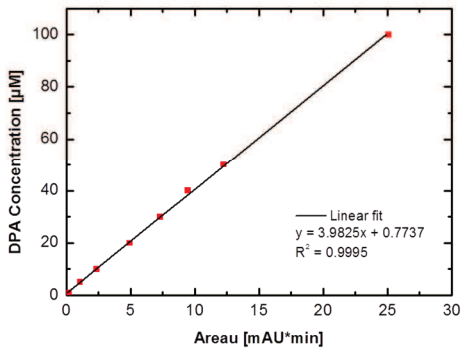

Measured DPA concentration (standard deviation in brackets) after the cold atmospheric pressure plasma treatment.

Treatment time [min]	DPA conentration [µM]
0	55.04 (±0.42)
1	45.27 (±0.96)
3	32.83 (±0.49)
5	31.54 (±0.46)
8	29.74 (±2.08)
10	27.48 (±0.22)
15	22.72 (±1.66)

Chromatogram of DPA standard concentration of 5 µM.

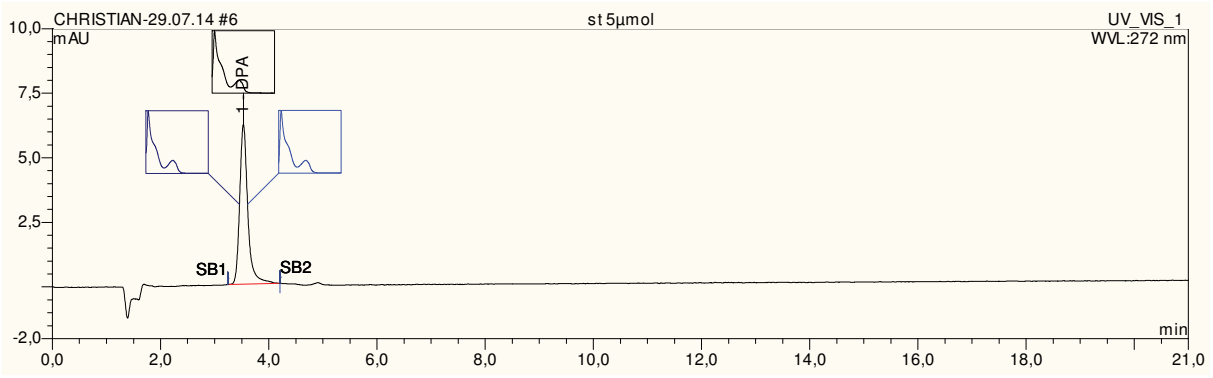

Chromatogram of DPA after 1 min cold atmospheric pressure plasma treatment.

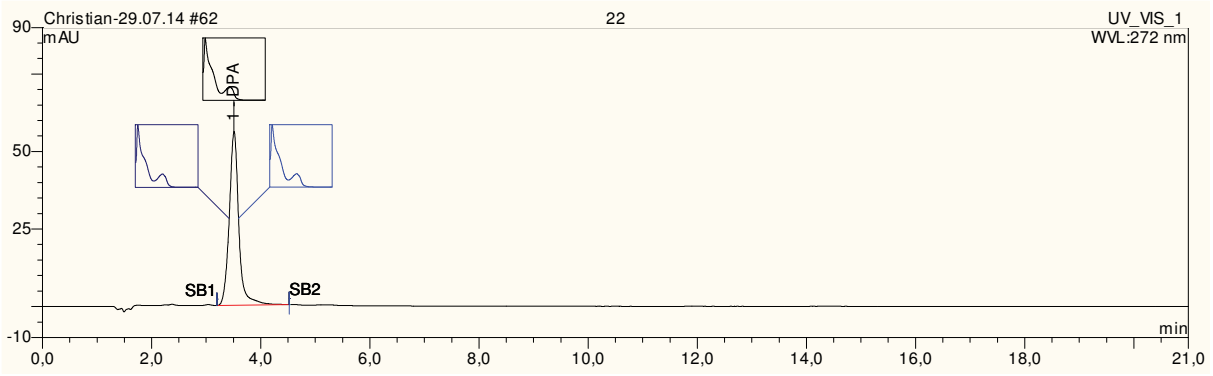

Chromatogram of DPA after 15 min cold atmospheric pressure plasma treatment.

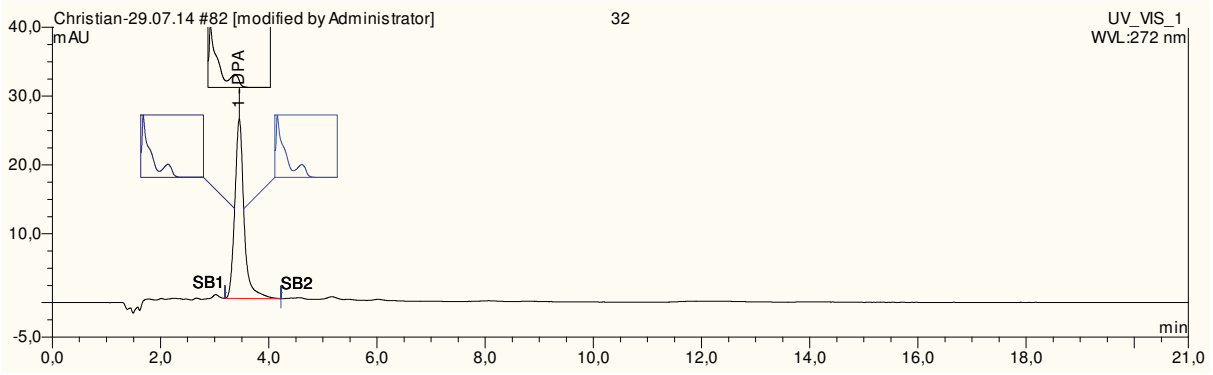

2. *Bacillus subtilis* spores treated in liquid media with plasma processed air

Bacillus subtilis spores were suspended in sterilized water and ACES-buffer (pH 7, 0.05M) solution with a final concentration of about 10^8 CFU*mL^{-1} and then exposed to plasma processed air up to 15 min.

Plasma-induced pH after the treatment with plasma processed air.

Treatment time [min]	pH in water		pH in ACES	
0	6.56		7.00	
1	2.06	2.04	6.46	6.48
2	1.93	1.95	6.27	6.42
4	1.76	1.76	6.04	5.93
6	1.77	1.70	4.76	3.52
8	1.56	1.54	2.60	2.22
15	1.40	1.37	1.64	1.62

Results (standard deviation in brackets) for the incubation of *Bacillus subtilis* spores in nitric acid for 30 min.

pH	Inactivation [$\log_{10}(N/N_0)$]	Reduction of *dna* K 400bp copies [$\log_{10}(CN/CN_0)$]	Inactivation [$\log_{10}(N/N_0)$] after thermal post-treatment (80°C/20min)
7	0	-	0.04 (±0.08)
4	-0.02 (±0.02)	-0.09 (±0.05)	-0.25 (±0.03)
3.5	-0.08 (±0.08)	-0.12 (±0.00)	-0.42 (±0.03)
3	-0.86 (±0.00)	-0.14 (±0.00)	-1.02 (±0.04)
2.5	-1.11 (±0.04)	-0.21 (±0.09)	-1.71 (±0.19)
2	-1.58 (±0.29)	-0.20 (±0.02)	-2.35 (±0.07)
1.5	-1.75 (±0.23)	-0.15 (±0.10)	-2.41 (±0.02)
1	-2.03 (±0.01)	-0.99 (±0.20)	-4.18 (±0.28)

Results (standard deviation in brackets) for the treatment of *Bacillus subtilis* spores suspended in water with plasma processed air.

pH	Inactivation $[\log_{10}(N/N_0)]$	Reduction of *dna* K 400bp copies $[\log_{10}(CN/CN_0)]$	Inactivation $[\log_{10}(N/N_0)]$ after thermal post-treatment (80°C/20min)
6.56	0	-	0.09
2.06	-3.43	-1.38 (±0.03)	-7.02
2.04	-2.99	-2.82 (±0.03)	-7.02
1.95	-6.20	-1.25 (±0.02)	-7.02
1.93	-4.58	-1.01 (±0.02)	-7.02
1.77	-5.74	-1.92 (±0.02)	-7.02
1.76	-5.17	-1.95 (±0.01)	-7.02
1.76	-5.81	-2.35 (±0.04)	-7.02
1.70	-5.30	-2.50 (±0.10)	-7.02
1.56	-6.24	-2.71 (±0.11)	-7.02
1.54	-6.93	-3.55 (±0.24)	-7.02
1.40	-6.93	-3.32 (±0.25)	-7.02
1.37	-6.93	-2.67 (±0.03)	-7.02

Results (standard deviation in brackets) for the treatment of *Bacillus subtilis* spores suspended in ACES-buffer with plasma processed air.

pH	Inactivation $[\log_{10}(N/N_0)]$	Reduction of *dna* K 400bp copies $[\log_{10}(CN/CN_0)]$	Inactivation $[\log_{10}(N/N_0)]$ after thermal post-treatment (80°C/20min)
7.00	0	-	0.07
6.48	0.04	0.16 (±0.02)	-0.25
6.46	-0.02	0.07 (±0.01)	-0.25
6.42	-0.03	0.09 (±0.04)	-0.37
6.27	-0.03	0.12 (±0.04)	-0.43
6.04	-0.24	0.16 (±0.02)	-3.35
5.93	-0.10	0.04 (±0.02)	-0.98
4.76	-1.49	-0.59 (±0.02)	-6.94
3.51	-1.44	-0.70 (±0.02)	-6.94
2.60	-2.50	-1.06 (±0.01)	-6.94
2.22	-3.16	-1.32 (±0.03)	-6.94
1.64	-5.67	-2.07 (±0.02)	-6.94
1.62	-6.88	-1.29 (±0.03)	-6.94

Eidesstattliche Erklärung

Hiermit versichere ich an Eides statt, dass ich die Dissertation selbständig verfasst habe. Alle benutzten Hilfsmittel und Quellen sind aufgeführt. Weiter erkläre ich, dass ich nicht schon anderweitig einmal die Promotionsabsicht angemeldet oder ein Promotions-eröffnungsverfahren beantragt habe. Veröffentlichungen von irgendwelchen Teilen der vorliegenden Dissertation sind von mir, wie in der vorstehenden Publikationsliste aufgeführt, vorgenommen worden.

Berlin, den 09.02.2017

Christian Hertwig